Numerical and Experimental Investigations for Wind Uplift Force on Flat Roofing System

Nima Dayani

A thesis submitted to the
Faculty of Graduate and Postdoctoral Studies
in partial fulfillment of the requirements for the MASc degree
in Civil Engineering

Department of Civil Engineering
Faculty of Engineering
University of Ottawa

Abstract

The development of the construction industry brought the new methods of structural design, which have been introduced to engineers, although overall this phenomenon has increased building costs. A cost-effective construction is one of the major decision points during the definition of any engineering project, therefore, due to the opposing concepts of these two statements, revising design standards and codes are essential in order to provide adequate and cost-effective design requirements.

A single-ply roof system is a relatively new method of roof construction that has been used in the building industry in recent decades, which seems to have undergone dramatic changes due to significant structural failures that have occurred through the years. Wind-induced damage on flat roofs is a common problem for low-rise buildings and much of this damage is initiated when the steel deck roof fails, leading to the overall roofing system collapse. The FM (Factory Mutual) design recommendations, which is a standard that recommends allowable dimensions and wind rating for the roofing products, have provided tabulated steel deck span dimensions and fasteners distance for many years. To update the FM design recommendations extensive experimental and analytical investigations are required. In the current study an experimental program was conducted at the National Research Council of Canada (NRC) on flat roofing systems, for simulating the wind uplift effect on several roofing systems samples, as recommended by FM design recommendations.

A Finite Element Model (FEM) of the same roofing systems as those used in the experimental cases was developed and different loading patterns were analysed for providing a better simulation of the deflection, moments and forces responses, as measured during the

experiments. The FEM was validated with the experimental results and was further employed for applying the FE analysis for more steel deck span dimensions and wind rating cases, as provided in the FM design recommendations tables.

These results were reported to the Single Ply Roof Industry (SPRI) Committee where the updating of the FM design tables is currently under discussion.

Acknowledgements

I would like to express my deepest appreciation to my supervisor, Dr. Elena Dragomirescu, who continuously and convincingly conveyed a spirit of adventure in regard to my research and always supported me during my MSc. program. I am so pleased to have had this great opportunity to study under her supervision and to learn so much from her.

I would like to express my sincere thanks to the thesis examiners, Dr. Beatriz Martin-Pérez and Dr. Heng Aik Khoo, for taking the time to review my thesis and for their valuable comments and feedback. In addition, special thanks to Dr. Bas Baskaran for giving me the opportunity to be part of the team group at the National Research Council (NRC). Also, I would like to express special thanks to the supporting organizations, NRC and Canadian General Tower Ltd.

I would like to dedicate this thesis to my beloved mother, who has continuously motivated and supported me during my studies, and kindly prepared me to be the best I can be in my life to accomplish my goals. Also, I consecrate the thesis to my wife who accompanied me during my study.

Table of Contents

List of Tables

List of Figures

List of Acronyms

ANSI	American National Standard Institute
ASCE	American Association of Civil Engineers
CBC	Canadian Broadcasting Corporation
CSSBI	Canadian Sheet Steel Building Institute
FEM	Finite Element Modelling
FM	Factory Mutual
Ksi	Kilopound per square inches
O.C.	On-Centre
NRC	National Research Council of Canada
SPRI	Single-ply Roofing Industry
CSA123.21-10	Standard test method for the dynamic wind-uplift resistance of membrane-roofing systems

Chapter 1 Introduction

1.1 Background

For many decades, high wind speeds and the pressure they induce on structures were known to be one of the main natural hazards contributing to major disasters. During the last century, many studies have been performed to report on two important features of natural wind: i) the intensity of the wind speed and ii) the wind forces induced on structures. Recent investigations [1] show that most roof collapses are a result of the structural failure of the roofing system subjected to extreme wind forces as opposed to the failure of the building itself, which is more resistant in wind. Moreover, wind-induced natural hazards are not always the main cause of the structural collapse of the roofing system, but sometimes this is associated with insufficient information provided by the design codes or standards, which might allow the system to become vulnerable to structural collapse. Therefore, the key role to control such potential failure mechanisms is to periodically update the design requirements and standards so they reflect the characteristics of the newly developed roofing construction technology.

Highly fluctuating wind forces are a source of vibration and possible aerodynamic instabilities, especially for large and slender structures, such as suspension bridges and high-rise buildings; however, for medium-size low-rise structures, one of the crucial aspects of the wind-induced pressure is its static component, which acts on flexible and inflexible elements of the structural system and thus might cause local failures. Therefore, strains and stress as a result of the deformations can be calculated from wind-tunnel experiments, but can also be collected from site measurements. In a large number of cases, both methods are adopted and

recommendations may be obtained from the appropriate national authority [1]. The fundamental reference to define the response of a structure is an accurate, reliable and statistical determination of wind forces.

Because finding the maximum wind force in any area is almost impossible, scientists stated that "the probability that a particular wind force may not be exceeded can be calculated and this probability can lead to a probable lifetime for the structure. Therefore, it should be notified that any code which accepts or guarantees a maximum wind force is unrealistic" [1].

Over the last decades, major changes in climate change and nature can be related to an increasing number of hurricanes, tornados and floods. For example, several regions in Canada experience high wind pressures as a result of these natural disasters [2]. These extreme wind conditions can have fundamental effects on structures such as uplifting, blowing them off or overturning them. The record shows, between 2004 and 2005, the losses in the US as a result of hurricanes and severe tornados were 45 and 115 billion dollars, respectively [2]. In October 2012, Hurricane Sandy caused multiple damages to building roofs, hydro lines, toppled large trees and most importantly caused the loss of lives in both Canada and the US [3].

In general, the roof of the building is the structural element that is mainly exposed to wind uplift forces, and in order to enhance its resistance various technologies are presently applied. One of these is the Single-ply Roof system (SPRs) composed of different layers and materials, all of which work as one system; hence, any damage in this system could cause a failure of the entire roof system operation. Figure 1.1 [4] shows the links between the different parts of the SPR's roofing system schematically.

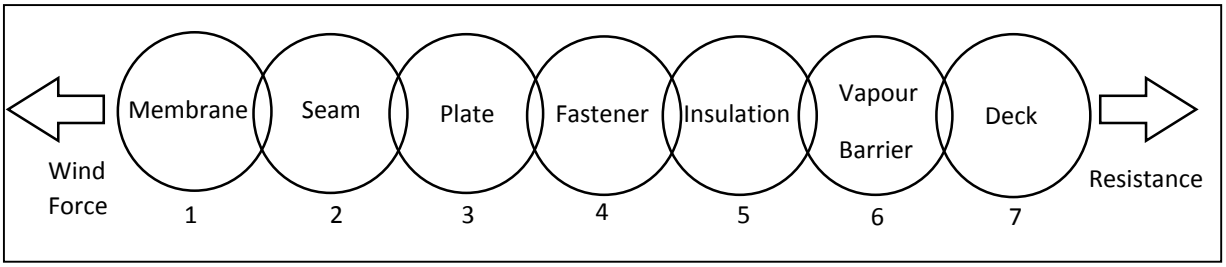

Figure 1.1 Roof system link diagram [4]

Damages to roof components can also result from insufficient information provided by the standards and design codes, errors in attaching different layers of the system or an improper installation of the roofing system. As illustrated in Figure 1.1 [4], the SPR's system is made of an assembly of seven layers, each having a different function: the membrane will ensure the impermeability of the roofing system, while the metal seam and the plate represent the support for the membrane and the resistant element on which fasteners are applied. Furthermore, the fasteners connect thorough the insulation and vapour barrier, which are used for protection and isolation of the inner roofing system, and reach the most resistant structural element, namely the roof steel deck. The entire roofing system is affected by extreme wind actions, however, the direct wind-induced effect is higher on the first layer, and through fasteners it is transferred to the last layer, the steel deck, thus the resistance of the system increases. If any of the links between the chain break, failure of the entire roof system would occur; therefore, if the first layers of the roofing system would collapse, some losses would be registered, but if the bottom layer (steel deck) would collapse, then this might cause the collapse of the entire roofing system.

Each roof component should withstand wind uplift forces; therefore, when all layers are connected properly and remain in place after the load application, the system is resistant against wind-induced pressure and thus no failure would be observed. However if the wind-

induced forces are higher than the prescribed resistance of the layers, failures will occur. Figure 1.2 shows different failures in the first and last components of the roof systems.

Figure 1.2 Roofing system failures: a) Failure in membrane. b) Deck buckling under wind pressure at fasteners row attachment

The roof is the most important component of low-rise buildings, and withstands the strongest wind-induced suction because of the high wind velocity separating the windward edge of the building roof and thus creating intense eddies along the interior region of the flat roof. The wind-flow around a long low-rise building has similar characteristics as the wind acting over a long flat plate. As illustrated in Figure 1.3 [5], due to separation at sharp edges of the building, a small eddy is attached to the lower windward side and a larger eddy remains stationary on the other side.

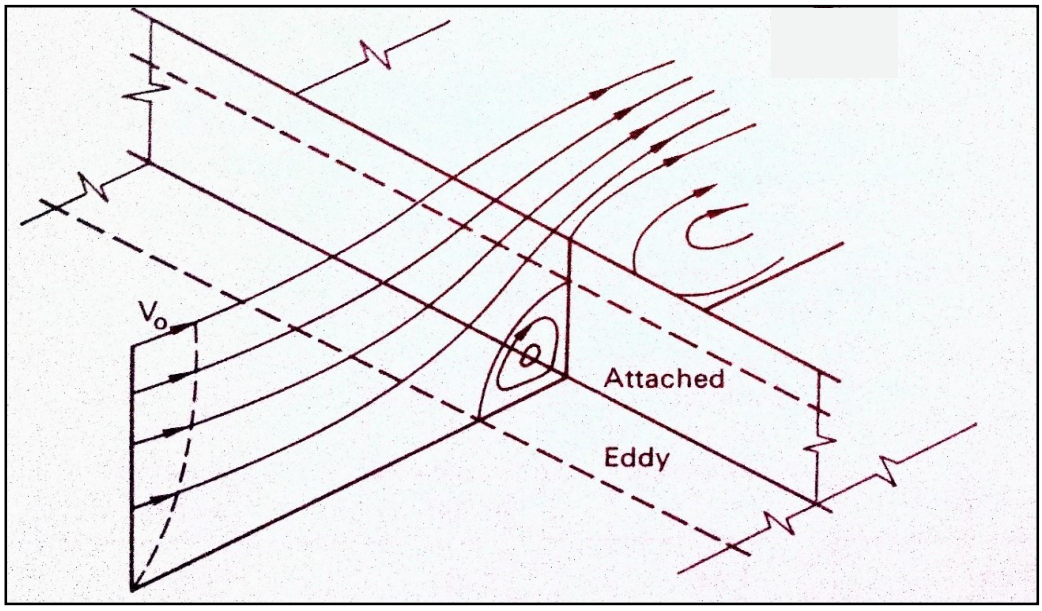

Figure 1.3 Wind flow and pressure distribution for a low-rise building roofing system [5]

When the wind approaches broader and narrower buildings with flat roofs, the high pressure occurs at the windward side of the building, and a very strong suction with pressure coefficients ranging from -0.5 to -0.9 can be registered on the leeward side of the same structure [1]. For flat roofs, higher suctions might occur when the wind approaches the building at an angle, called the angle of attack, and the pressure coefficients can have a value up to -1.0 exactly behind the separation edge, while the side walls could register even higher suctions of up to -1.5 pressure coefficient [1]. The pressure coefficients are very important when designing the roofing system components. To calculate the net pressure on any building roof, the internal pressure must be subtracted from the external pressure [1]. One of the most important factors in calculating wind pressure for this type of building is the ratio between height and depth of the structure [1]. The wind flow over a roof and the calculation of external wind forces depend on various factors such as the roof geometry, the building height and depth, and the characteristics of the approaching wind [5].

To have a better vision of such complex wind flows, a few general rules of fluid mechanics can be applied to help understand wind-structure interaction and the flow behaviour in the vicinity of the roof surface. Figure 1.4 [5] shows the flow stream over roofs of different geometry and slope. As expected, for the situation when the entire flat roof is subjected to suction, a strong fluctuation of negative pressure can be expected at the separation bubble (Fig. 1.4. (a)) [5]. In the case of the roof with a slight slope presented in Figure 1.4 (b), the wind-induced effect on roofing system is considered to be mild because the roof angle θ is smaller than α (the streamline angle) [5].

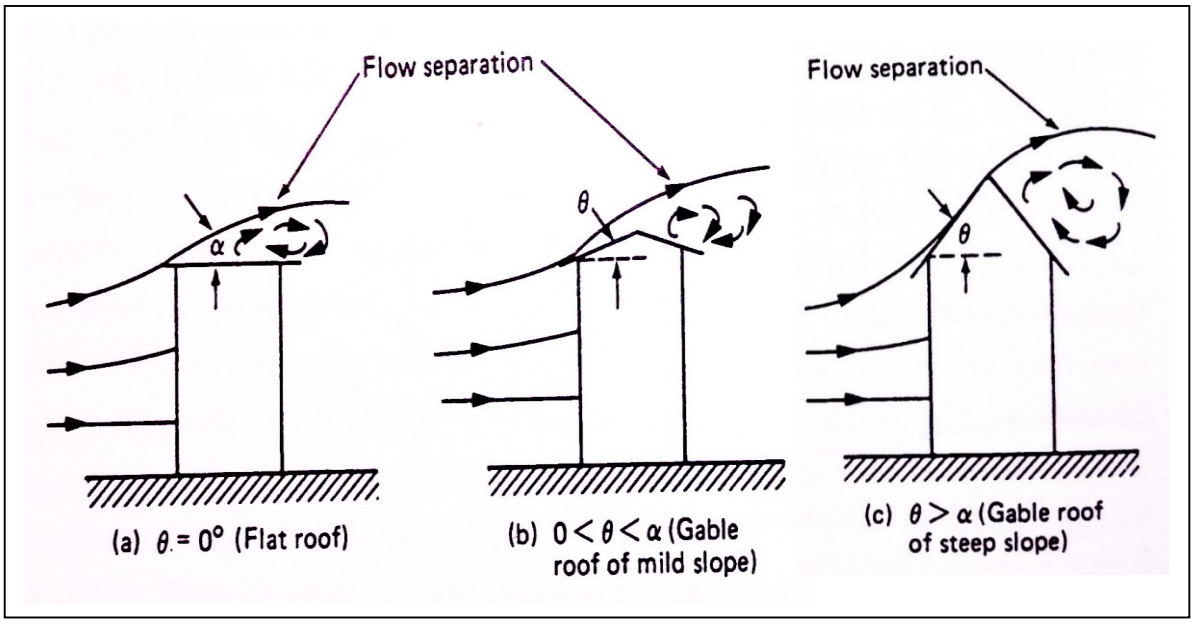

Figure 1.4 Streamlines over roofs with different geometry [5]

For the case when the roof angle θ is much greater than α, as depicted in Figure 1.4 (c), the separation occurs almost at the middle region of the roof, and based on this separation it can be mentioned that the windward part of the roof is under pressure while suction is generated on the leeward side (the other half of the roof) [5].

1.2 Research Motivation

Considering the wind streamlines on different types of roofs, and based on numerous wind-tunnel tests performed for different building shapes, static pressures and forces, was noticed that the biggest part of the exposed roof area is under suction, especially for the flat roofing systems [5]. In recent years, an initiative was undertaken by the major housing insurance companies, such as Factory Mutual (FM) and the roofing design committees, such as Single-ply Roofing Industry (SPRI), to determine the type of wind uplift loading which has the highest impact on the roof assembly failure [6]. Currently the roofing spans dimensions and the fasteners spacing stipulated by the FM tables are the main roof design recommendations adopted by both the insurance companies and the roofing industry. Table 1.1 shows the current FM table used for designing the flat roof spans. As it can be noticed, there are no recommended values for the lower half of the table, where the biggest roof span dimensions and the highest wind ratings should be represented. Also the values in the upper part of the FM table were determined based on a simplified two-dimensional beam calculation with uniform loading as the wind uplift force. This might not reflect the actual allowable values, as the steel deck roof is a flat plate, with punctual wind uplift loading applied at the fasteners of the roof assembly installed on top of the steed deck. Therefore the rest of the FM table should be updated and revised, based on the three-dimensional model of the wind loading distribution on the entire roof plate, which was not considered when the FM tables were developed. The SPRI committee decided to develop and revise the current FM table by converting the applied wind uniform load to a point load system [6, 7]; however this does not consider the three-dimensional configuration of the roof steel deck.

Table 1.1 Current FM table [6]

Fastener Row Spacing (ft.)	Gauge	MAX DECK SPANS (FT) BY WIND RATING (PSF) / FASTENER SPACING, SHEET GAUGE FOR 33 Ksi																		
		330	315	300	285	270	255	240	225	210	195	180	165	150	135	120	105	90	75	60
3.5	18	4.5	5.5	5.5	5.5	5.5	5.5	6	6	6	6	6	6	6	6	6	6	6	6	6
	20	-	4	4	4.5	4.5	4.5	5	5.5	5.5	5.5	6	6	6	6	6	6	6	6	6
	22	-	-	-	-	-	4	4	4.5	4.5	4.5	5.5	5.5	5.5	6	6	6	6	6	6
4	18	4.5	4.5	5	5	5	6	6	6	6	6	6	6	6	6	6	6	6	6	6
	20	-	-	-	-	4	4.5	4.5	5	5	5.5	6	6	6	6	6	6	6	6	6
	22	-	-	-	-	-	-	-	-	4	4.5	5	5	6	6	6	6	6	6	6
4.5	18	-	4	4	4.5	5	5	5.5	6	6	6	6	6	6	6	6	6	6	6	6
	20	-	-	-	-	-	-	4	4	5	5	5.5	6	6	6	6	6	6	6	6
	22	-	-	-	-	-	-	-	-	-	-	4	4.5	5	5.5	6	6	6	6	6
5	18	-	-	-	4	4	4.5	5	5	5.5	6	6	6	6	6	6	6	6	6	6
	20									4	4.5	5	5.5	6	6	6	6	6	6	6
	22	-	-	-	-	-	-	-	-	-	-	-	4	4.5	5	6	6	6	6	6
5.5	18	-	-	-	-	-	-	4	4.5	5	5.5	6	6	6	6	6	6	6	6	6
	20	-	-	-	-	-	-	-	-	-	-	4	4.5	5	6	6	6	6	6	6
	22	-	-	-	-	-	-	-	-	-	-	-	-	-	4.5	5	6	6	6	6
6	18	-	-	-	-	-	-	-	-	4	5	5.5	6	6	6	6	6	6	6	6
	20	-	-	-	-	-	-	-	-	-	-	-	-	4.5	5.5	6	6	6	6	6
	22	-	-	-	-	-	-	-	-	-	-	-	-	-	-	4.5	5.5	6	6	6
6.5	18	-	-	-	-	-	-	-	-	-	4	4.5	5.5	6	6	6	6	6	6	6
	20	-	-	-	-	-	-	-	-	-	-	-	-	-	4.5	5.5	6	6	6	6
	22	-	-	-	-	-	-	-	-	-	-	-	-	-	-	-	4.5	5.5	6	6
7	18	-	-	-	-	-	-	-	-	-	-	-	4	5.5	6	6	6	6	6	6
	20	-	-	-	-	-	-	-	-	-	-	-	-	-	-	4.5	6	6	6	6
	22	-	-	-	-	-	-	-	-	-	-	-	-	-	-	-	-	5	6	6
7.5	18	-	-	-	-	-	-	-	-	-	-	-	-	4	5.5	6	6	6	6	6
	20	-	-	-	-	-	-	-	-	-	-	-	-	-	-	4	5	6	6	6
	22	-	-	-	-	-	-	-	-	-	-	-	-	-	-	-	-	4	6	6
8	18	-	-	-	-	-	-	-	-	-	-	-	-	4	4.5	5.5	6	6	6	6
	20	-	-	-	-	-	-	-	-	-	-	-	-	-	-	-	4	5.5	6	6
	22	-	-	-	-	-	-	-	-	-	-	-	-	-	-	-	-	-	4.5	6

The design recommendations provided by the FM tables specify the allowable values for the deflections at the middle of roof spans, positive moments at supports and negative moments at the middle of spans. To update the FM table, the same three parameters should be considered in the developed FEM for the roofing system, then the results should be compared with the allowable values, recommended by the current FM table.

Apart from the allowable deflection and moment values, the calculation of the FM table results is not simple, because the line load calculations for the three-dimensional spans are solved using statistically indeterminate methods; therefore, using a structural software is necessary to perform the calculations. The Finite Element Model (FEM) and the loading simulation conducted by the aid of the SAP structural software can be controlled by various methods such as the input of the yield stress, the span and location of the point load, employing various boundary conditions, etc. [6].

The output of the FEM developed in the SAP must be validated, therefore, three types of experiments, reproducing different scenarios contained in the FM table should be performed to corroborate the FEM results in regard to the deflection and bending allowable values.

Also based on the SPRI committee's comments, the design recommendations for the flat roof assembly should be provided not only for the standard load case conditions, but also for the worst loading cases scenarios; therefore bigger span dimensions of 6′, 7′6″, 9′6″ for the roof assembly and 6′ for the steel deck alone were considered for the experiments performed at the NRC. The dimensions of the experimental facilities at the NRC were another limitation when selecting the dimensions of the roofing specimens tried in the experimental cases.

1.3 **Research Objectives**

The current study focuses on clarifying and updating the design recommendations for the SPRI's flat roofing assembly, and on simulating the static wind effect on various regions and spans of the roof. The flat roof design should comply with the allowable deflection and allowable moment values recommended by the Factory Mutual insurance agency, which

adopted the design criteria for maximum and average wind loadings from the ASCE 05 [8]. The FM insurance agency provided the FM design recommendations table (Table 1.1), which limits the roof steel deck span dimensions and the distances between the fasteners for the given wind load ratings. However, in the calculation model they recommend that the wind uplift loading be applied as a uniformly distributed loading along the fastener line and thus a conservative structural design of the roof is achieved. When the wind loading uplifts the membrane layer of the roofing system, it has a direct impact on the fasteners that are anchored in the steel deck of the roof assembly. Thus the loading scenarios can be estimated as a punctual loading at the fastener location and not a uniformly distributed loading, as currently considered in the FM tables. Moreover, the three-dimensional effect of the steel deck plate was never taken into consideration when preparing the FM table, and the depth of the steel deck span was ignored in the calculation model.

The last revised version of FM-approved standard class No.4470 was released in June 2012 [9]. The FM 4470 standard is used for single-ply, polymer-modified bitumen sheet, build-up roof (BUR) and liquid-applied roof assemblies evaluation regarding their behaviour under simulated wind uplift, fire from above and below the structural deck, corrosion of metal parts and optionally, puncture resistance and solar reflectance [9]. When the roof assembly meets the FM requirements, it is qualified to be approved by the standard [9]. The revised version of the FM 4470 standard includes numerous updates for the roof assembly heat damage, corrosion, solar reflectance, etc., but for the wind uplift verification the FM 4470 standard specifies only checking the steel deck and steel fasteners' stress calculations under wind uplift pressure to verify if they are overstressed [9]. Therefore, considering the necessity of updating

the calculation methodology and the allowable values recommended by the FM 4470 standards the main research objectives of the current research are defined as follows:

- The first objective is to perform experiments simulating the wind uplift loading on a) the steel deck roof, b) the roof assembly installed at 6′ fasteners spacing, c) the roof assembly installed at 7′6″ fasteners' spacing and d) the roof assembly installed at 9′6″ fastener spacing. These experimental cases were selected based on the steel deck made available by the Canadian General Tower Ltd., and the fasteners spacing for the roofing assemblies were decided in consultancy with the industrial partners considering their vast practical experience.
- The second objective is to develop a Finite Element Model (FEM) of the steel deck and the roof assembly, which simulates the test conditions described above. Also the conversion of the uniform wind uplift loading to the punctual loading applied at the fasteners location must be performed and in order to validate the results obtained under the converted loading, the deflection and the moments obtained from the FEM were compared with the results recorded from the experiments.
- Because for the experiments only the 22 steel deck gauge was available, and the FM table is using 22, 20, 18 steel deck gauges, the experiments and the developed FEM cannot be used directly for updating the entire FM tables, thus the main objective of this research is to provide a validated three-dimensional roof assembly FE model, which can use the point loadings, calibrated with the experiments performed as per the FM tables recommendations. However to demonstrate the application of the FEM developed for the FM tables, additional numerical studies were performed reflecting the 33 ksi steel deck of

22 gauge and fasteners' spacing of 3.5′, 4′, 4.5′, 5′, 5.5′ and 6′ for wind loading cases up to 225 psf. The final target of this research is to deliver a validated three-dimensional FE model of the roof assembly which can be used to update the conservative FM design table based on the allowable stresses and deflections.

1.4 **Research Methodology**

This research consists of two main steps as follows:

a) *Operating step*: experimental and simulation parts of the research were performed at this step. The experimental part comprised of four cases: three cases with insulation and membrane layers (roof assembly), and one case for steel deck only. Moreover, for achieving the objectives stated above, only static analysis was considered for the simulation part involving the FE model of the roof assembly.
b) *Reporting step*: all results from step *a* were interpreted in this step for validating the proposed FEM of the roof assembly with the results measured during the experiments. After the validation was completed the FEM was expanded based on additional numerical studies for updating the FM table. Figure 1.5 shows the overall procedure employed for the research methodology and the final objectives.

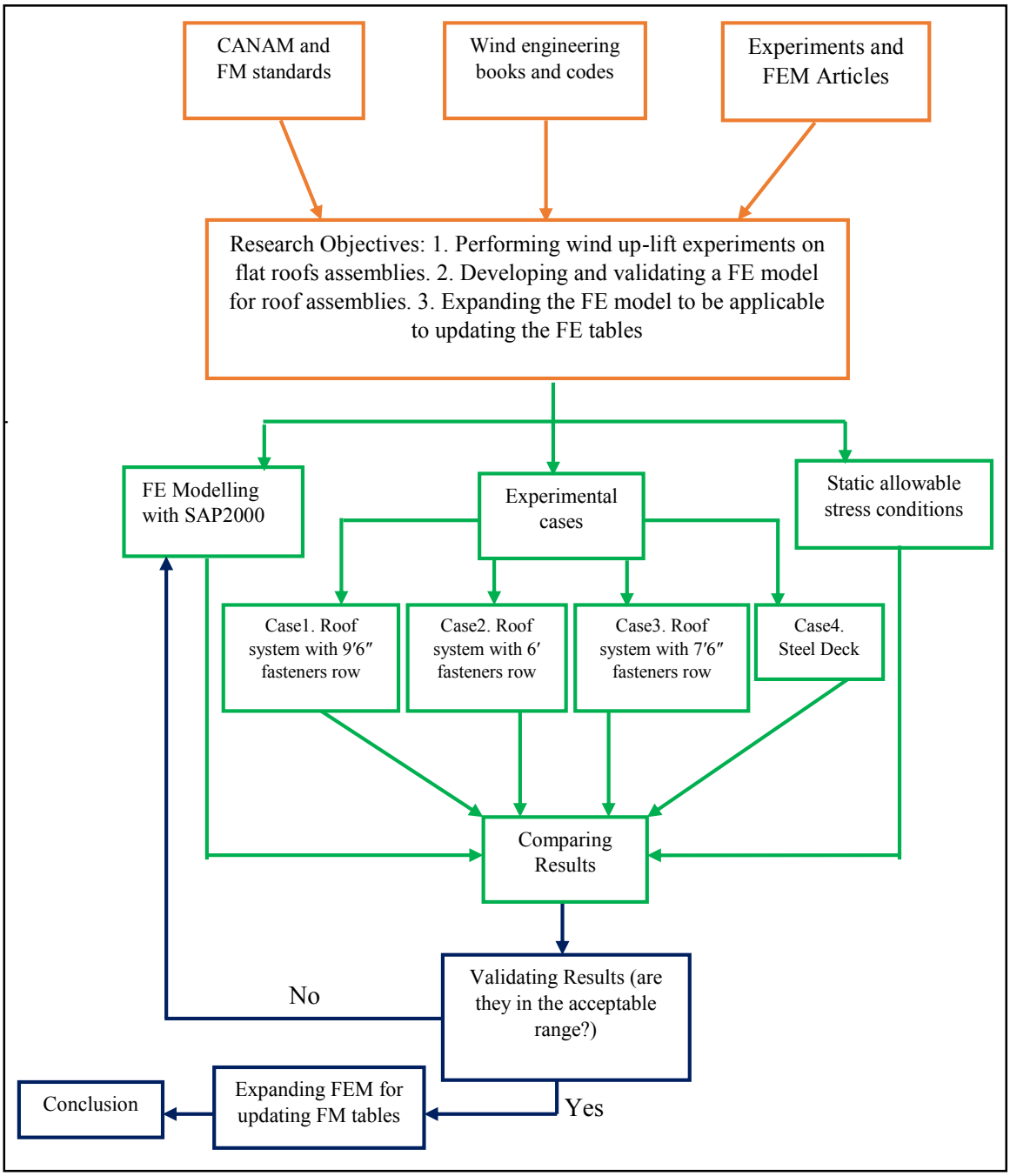

Figure 1.5 Research Methodology

1.5 **Thesis Layout**

The current research is comprised of six chapters as described below:

Chapter 1 provides introductory information about the main concept of the roofing systems' design process and discusses the research objectives in the light of the necessity of updating the FM design tables, which establishes the motivation of performing the current research.

Chapter 2 presents a literature review of previous research and related articles, standards and codes, which gives an overview of the research concepts besides the research design guidelines.

In Chapter 3, the experimental program is explained detailing the four different cases, which were performed at the National Research Council of Canada (NRC).

Chapter 4 defines the finite element modelling of the roofing assembly and the related modelling assumptions, such as the various loading cases and the method used to ensure precise FE model of the roofing assembly.

Chapter 5 is divided into two sub-chapters: i) Experimental results and ii) FEM results. Based on these results, the validation of the modelling is explained and the FEM is expanded to be applied for updating the FM tables.

Finally, in Chapter 6, the main conclusions of the current study are detailed, in addition to offering some recommendations for future research.

Chapter 2 Literature Review

2.1 Introduction

Wind damage on structures can become significant, especially for high- and medium-rise structures such as factories and shopping centres. The vulnerable components in these structures are mainly the top roofs, thus many roofing insurance companies raised concerns regarding the quantification and steps taken to avoid the occurrence of wind-induced damages. Therefore, comprehensive numerical and experimental studies regarding the performance of the roofing systems under extreme wind forces are constantly required, especially nowadays when the rate of occurrence and intensity of destructive winds has increased.

With technological development, the introduction of new construction methods was achieved, such as the Single-Ply Roof system (SPRs), which is installed on low-slope commercial and industrial buildings. However, it is known that SPR systems react differently to wind effects than conventional built-up roofs [4].

Each structural component of a building has a different response to wind-induced pressure. When the wind is passing around and over low-rise buildings exerts positive pressure on the windward wall and negative pressure (suctions) on the leeward sides and side walls, which are parallel to the flow direction [4]. In general, the roof of a building is under the suction effect and this force, which varies with time, is generated at any specific roof location. Each

roof component has a different behaviour when suction occurs, and this is highly dependent on the following parameters [2]:

- Wind speed
- Wind direction
- Turbulence intensity or gusts
- Building topography, geometry and architectural features

When the SPRs roofing systems were adopted, in order to ensure they are safe and perform well under static and dynamic wind-induced pressures, a standard testing methodology was developed by the National Research Council (NRC) and an industry-supported consortium team [10]. As presented in Figure 2.1, the membrane layers were attached to the structural roof deck by fasteners. The attachment locations were then overlapped with another membrane sheet and both sides of the sheets were seamed together. Wind-induced suction was experimentally applied and failure mechanisms such as lifting the membrane between the attachments and membrane stretching were discussed.

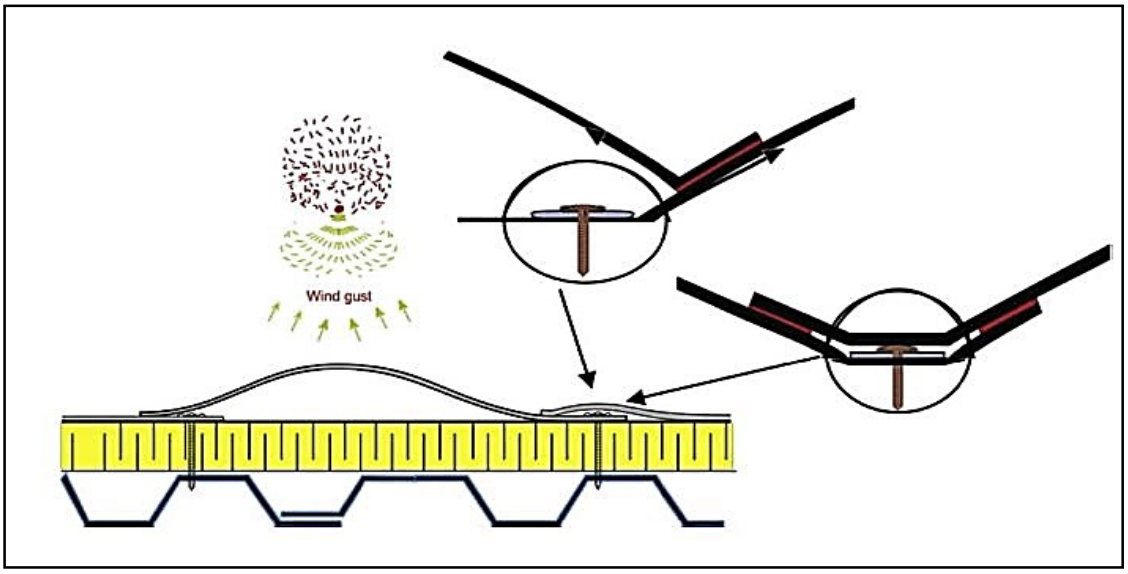

Figure 2.1 Wind effect on single-ply mechanically attached roof assemblies [2]

The mechanical properties of the membrane and the magnitude of the wind-induced pressure (suction) were analysed in order to determine the ratio of membrane stretching [4]. In the current performed study, a very similar experimental procedure was followed; however, the test concentrated on several types of failure encountered such as a rupture in the membrane or buckling of the steel deck.

2.2 **Single-ply Roof System**

The SPRI (Single-ply Roof Industry) definition states, "The class of commercial roofing membranes commonly described as 'single-ply' are flexible sheets of compounded synthetic materials that are manufactured in a factory to strict quality control requirements" [6].
Presently, the SPRI roofing system provides more strength, flexibility and durability compared to other types of roofing systems [6]. The main positive aspects of pre-fabricated sheets include the consistent quality of the products manufactured, the diversity of the attachment methods and their broader applicability. Based on SPRI division, there are three major categories of single-ply membranes: thermosets, thermoplastics and modified bitumen [6].

- *Thermoset membranes*: These types of membranes are made of rubber polymers. Another type of material can be used to produce thermoset membranes namely, the neoprene; however, this type of material is no longer widely accepted for roof membranes [11]. Thermoset membranes are one of the best acceptable roofing materials due to their durability against the potentially damaging effects of sunlight and some general chemicals that can be found on roofs [11]. Another material used in this type of membrane is the hepalon; although it is produced as a thermoplastic, it turns to a thermoset in time [11].

When two sheets of membranes are attached together at the seam location, heating them to the applied hepalon material will make the two membrane sheets be sealed together [11].

- *Thermoplastic membranes:* They are plastic polymers and the most common thermoplastic is the PVC (polyvinyl chloride) material, which has been made flexible by using some special ingredients (plasticizers) through the specific manufacturing procedure [11]. There are different types of products in the PVC category, each having its own characteristics [11]. This type of membrane can be attached in seams by heating two sides of the membranes or by chemical welding, thus they are as strong as the membrane itself or stronger. During the manufacturing process, a reinforcement layer (polyester or fiberglass) is used, thus its strength and dimensional stability are increased [11].

- *Modified bitumen membranes*: These types of membranes are produced as a corroboration of high-tech formulation and prefabrication advantages of single-ply products with some of the traditional installation techniques, which are used in built-up roofing systems [11]. For example, by using a specific type of asphalt, rubber or plastic ingredients, the flexibility of the membrane will be raised, and by combination of reinforcement its strength and stability will be increased [11]. During production, some modifiers may be used that regulate the method of sheet installation. For instance, based on the modifier type, in some cases hot asphalt is required. Two preliminary modifiers that are widely used are APP (atactic polypropylene) and SBS (styrene butadiene styrene) [12]. Some are mopped down using hot asphalt and others use torches to melt the asphalt so that it flows onto the layers. The seams are sealed by the same technique [12].

2.3 Types of SPR membrane attachments

Membrane attachments depend on different factors, but the most decisive parameter is the cost. However, it is not a proper decision if the attachment method is chosen only based on the cost, thus other parameters in the decision procedure include the following [12]:

- Building height
- Wind exposure
- Anticipated roof traffic
- Aesthetics

Apart from the above issues, another factor that has an effect on the selection of the type of attachment is the roof's structural system. For example, if the roof is flat and its structure (the deck) is capable of resisting the weight, a ballasted roof is almost always the best option [12]. But if it is a gable roof with a slope greater than 2″ to 12″, this type of membrane attachment is not appropriate [12]. The roof height is another issue that can determine some limitations in using the ballasted roof. The mechanical membrane attachment is the best option, if the structural part of the roof accepts fasteners efficiently, such as a steel or wood deck [12]. These systems can be designed to provide the necessary resistance to known wind forces and are not subject to slope limitations [12].

2.4 SPR Testing Methods

During the design process of the roof structural system, designers are recommended to use the national and regional building codes to calculate wind pressure for the geographic location of the building [13]. Moreover, and consequent to the verification of criteria fulfilment, the

proper roofing system and its connecting details such as fastener type, dimensions and application distance must be used for local wind conditions [13]. Therefore, before installing any of the SPR systems, the manufacturers should test samples according to the standards and codes to provide reliable information on the roof system to confirm it will be able to tolerate the design wind loads. The methods used for the certifying procedure are as follows [13]:

- *North American Test Methods*

The current certification standards in North America used to assess wind uplift ratings of SPR systems are those issued by Factory Mutual (FM) and some authorized laboratories [13]. However, these standards were developed for built-up roofing systems and do not simulate the dynamic wind conditions that generally cause mechanically fastened SPR roofs to fail [2].

- *European Test Methods*

Current European testing procedures simulate the actual wind conditions better than North American tests, thus they produce better measurements of the actual wind uplift resistance of roofs [13]. The current testing procedure uses pressure load cycles based on the meteorological data, in order to simulate dynamic wind loading and to account for size and edge effects. The procedure is very time consuming; for example, one cycle with 1415 gusts takes nearly three hours to complete, and it can take as long as 50 hours for a full investigation [10].

To have more efficient tests for mechanically fastened SPR systems, the Special Interest Group for Dynamic Evaluation of Roofing System (SIGDERS) introduced a new method to evaluate manufactured roof systems, but due to the dynamic focus of this method, it is ignored in this study [10].

2.5 **Attachment of Roofing Membranes to Steel Deck**

In 2007, the Canadian Sheet Steel Building Institute (CSSBI) conducted research regarding various types of roofing membrane attachments under the title of "feasibility of attaching roofing membranes to the steel deck in case of large spacing" [14]. It was considered that the roof system has incorporated wide membrane sheets that are attached to the steel deck. Therefore, the membrane itself has the performance characteristics to provide adequate tributary loading, meanwhile based on the existing design method, the steel deck is always under the effect of wind uplift uniform load. As noted in this research, "The large majority of the roof steel decks used for commercial buildings in North America is profiled with 38 mm (1 1/2″) flutes, with the structural supports usually spaced between 1.52 m (5′-0″) and 2.03 m (6′-8″)" [14]. Because of the large spacing between membrane attachment lines when the wind uplift force has been applied to the roof, point loads could be generated at the fastener connection points, which could exceed the capacity of the deck. But as per current design standards, this is acceptable if the same loading is applied uniformly to the entire steel deck. This represents a major discrepancy, and clarifying the real behaviour of the roofing systems under wind uplift forces is impetuously required. The same consideration also governs the FM design, and one of the objectives of the current study is comparing the results between the uniformly distributed loading system on the steel deck only and the same loading scenario when it is applied on a membrane with different assembly conditions. The assembly conditions, however, imply the conversion of uniformly distributed loading to the punctual loadings acting on the membrane and on the steel deck at the fastener locations.

The stability of the fasteners that are used to attach the membrane to the steel deck, as well as any fastened, welded or nailed attachment between the steel deck and the supports, can be calculated in regard to the CAN/CSA- CSA S136-07 North American Specification for the Design of Cold Formed Steel Structures Members Welding Requirements [14]. "These design values are based on the specified minimum mechanical properties (i.e. base steel thickness and yield strength) specified for the steel sheet roof deck, and should be lower than the strength determined by field testing. The use of field-test results for properties such as the pull-out strength of a screw into a steel deck needs to recognize that the properties of the steel deck can be higher than the minimum limits required by the steel specifications. Therefore, field-test results must be adjusted accordingly to account for the difference between the actual properties of the deck and the minimum properties of the steel according to the material specification used in design" [14].

The steel deck and its supports can have different structural responses to wind uplift pressure, varying with the fastener's line distance, along which the membrane is attached to the deck, and with the distance between fasteners as well. On the other hand, the structural members of the roof assembly behave differently when the membrane layers are adhered over its entire surface compared to the mechanical attachment system [2]. The fasteners will produce line loadings along the deck instead of a uniform load distributed on the entire deck surface. The line loads can be perpendicular or parallel to the deck flutes, which strictly depends on the position of the membrane [14]. The deck can register a different structural behaviour when different assembling conditions are influencing the loading for each scenario [14].

As shown in Figure 2.2, if the membrane seam is perpendicular to the flutes of the steel deck, there is a possibility of producing a bending moment in the deck that is 3.8 times bigger than

the moment that is produced by the equivalent uplift load when it is applied uniformly over the roof [14]. Moreover, in this condition, it is possible to produce an uplift load on the joists that is two times bigger than uplift load that produced by the equivalent uplift load applied uniformly over the surface of the roof [14].

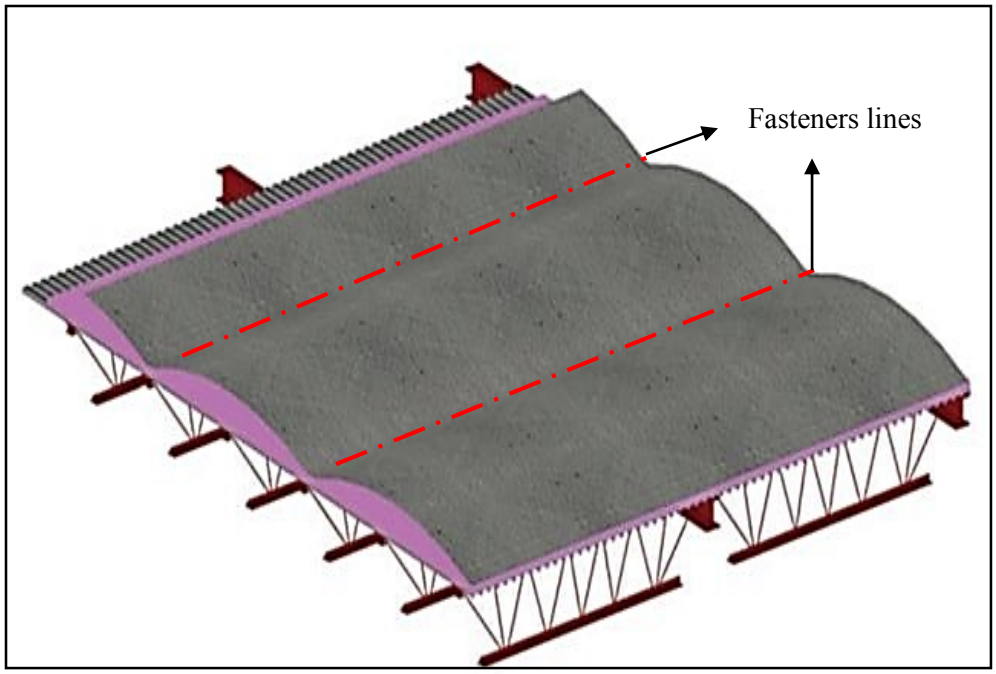

Figure 2.2 Roofing membrane seam perpendicular to deck span [14]

Nevertheless, if the roofing membrane is parallel to the flutes of the deck, as illustrated in Figure 2.3, it is possible to generate a bending moment, and shear forces in the steel deck can be up to 12 times bigger [14] than the conditions of the loading system applied uniformly to the entire roof. This response is significantly higher because the applied load cannot be upheld by the resistance of the entire width of the deck, but only those deck flutes adjacent to the applied line load [14].

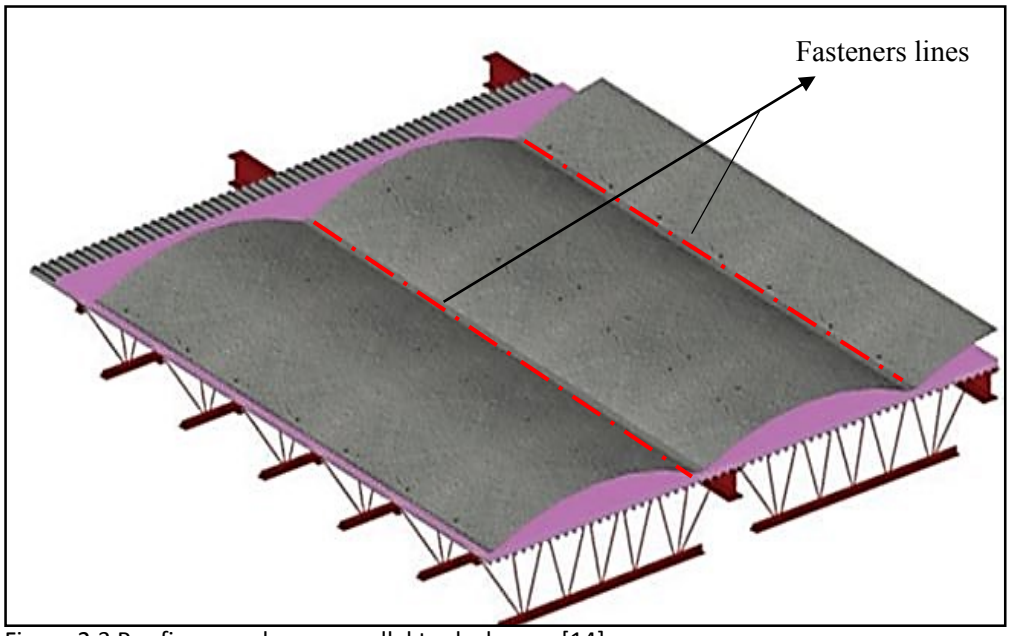

Figure 2.3 Roofing membrane parallel to deck span [14]

2.6 **SPRI's Calculation of Wind Uplift Pressure**

As stated in the newly released SPRI Technical Report [6], "Wind Design Standard provides general building design considerations as well as a methodology for selecting an appropriate roofing system assembly to meet the rooftop design wind uplift pressures that are calculated in accordance with the current version of the International Building Code (IBC). This Standard Practice is appropriate for non-ballasted Built-Up, Modified Bitumen, and Single-Ply roofing system assemblies installed over any type of roof deck" [6].

Based on ASCE 7-2005 standards for minimum design loads, the wind uplift load should be calculated for the entire field, perimeter and corners of the roof. Moreover, the Single-ply Roofing Industry (SPRI) Committee has convened that the tested uplift load capacity of a roofing system assembly shall be determined by testing in accordance with the FM 4450, FM 4470, UL 580, UL 187 AND CSA A 123, 21-10 [6]. The tested uplift load capacity values are

made available by the roofing system assembly suppliers through independent laboratory testing reports, evaluation reports and other publications [6].

Finding the proper safety factors is required based on the tested uplift load capacity; also it should be noted that the use of these factors is essential in order to determine the factored tested load capacity of the roofing system assembly [6]. Typically, in the initial testing technical reports, the safety factors are not considered as they simply identify the maximum tested uplift load capacity, which is the actual resistance capability of the particular roofing assembly tested [6]. In order to determine the factored tested load capacity (L_t), the tested uplift load capacity was divided by the assigned safety factor (Eq. 2.1). Based on designer determinations, the safety factors for roofing systems are between 1.0 and 2.0 [6].

Factored Tested Load Capacity in psf (L_t) = Tested Uplift Load Capacity / safety factor (2.1)

From evaluation reports, publications and manufacturers' websites, wind uplift resistance values can be obtained, and often include a safety factor, which means the listed wind-uplift resistance value is actually the factored tested load capacity (L_t). Therefore, no further factoring is necessary.

If the factored tested load capacity (L_t) is greater than or equal to the calculated wind uplift design load for the field area of a roofing system assembly, there is a possibility of using the given value for further design considerations [6].

However, if L_t is less than the calculated design wind uplift load for the field area, the roofing system assembly shall not be used on that particular building [6]. When L_t is greater than or equal to the field design pressure, the roofing system assembly, as tested, is suitable for use in

the field area of the roof [6]. In order to determine the appropriate assembly layout for the perimeter and corner areas of the roof, comparing the L_t to the calculated wind uplift design loads for the perimeter and corner areas is required [6]. When L_t meets or exceeds the calculated design load for either of these areas, the roofing system assembly, as tested, is suitable for use in those specific areas [6].

When L_t is less than the area design loads, one of the rational analysis methods should be used to increase the resistance of the roofing system assembly [6].

- *Adhered Membrane Roofing System Assemblies*

This analysis method can only be used when all of the following requirements are met [6]:

1. "The Tested Uplift Load Capacity (without consideration of any safety factor) must be greater than or equal to the calculated corner area wind uplift design load;

2. The adhered membrane roofing system assembly utilizes either mechanical fasteners or ribbons/beads of an adhesive for insulation attachment; and,

3. The Tested Uplift Load Capacity of the proposed adhered roofing system assembly was determined utilizing a test chamber of sufficient size to allow side-by-side positioning of a minimum of three full-size insulation/cover board/substrate boards/panels on the test frame" [6].

- *Adhered Membrane with Mechanically Attached Insulation*

Equation 2-2 is used to increase the number of fasteners per insulation layer (F_n) when the insulation is attached with mechanical fasteners [6]:

$$F_n = \frac{(F_t \times L_d)}{L_t} \quad (2\text{-}2)$$

where:

F_n is the number of fasteners per board needed to meet the calculated design load.

F_t is the number of fasteners per board used to achieve the tested load capacity.

L_d is the calculated design load for the perimeter or corner area of a roof, (psf).

L_t is the Factored Tested Load Capacity, (psf).

- *Adhered Membrane with Ribbon/Bead Adhesive Attached Insulation*

For insulation attached with ribbons/beads of an adhesive, the reduced ribbon/bead spacing (R_n) needed to meet the calculated design wind uplift load(s) shall be determined using the following equation [6]:

$$R_n = \frac{(R_t \times L_d)}{L_t} \quad (2\text{-}3)$$

where:

R_n is the ribbon/bead spacing needed to meet the calculated design load (inches).

R_t is the ribbon/bead spacing used to achieve the tested load capacity (inches).

L_d is the calculated design load for the perimeter or corner area of a roof (psf).

L_t is the factored tested load capacity (psf).

Therefore, when the insulation layers are attached by ribbons, the distance between them should be determined by the centre-to-centre distance of the top steel deck flutes, because they are attached on this part of the steel deck [6]. The rationalized ribbon/bead spacing shall be rounded down if it is necessary to coincide with a top flute spacing [6]. "The ribbon attachment of the insulation layer is not acceptable if the rationalized ribbon spacing is less than centre-to-centre of the steel deck top flutes; moreover, these equations shall not be used to rationalize backwards and reduce the number of fasteners or increase the spacing of ribbons of adhesive used in the field of the roof " [6].

- *Mechanically Fastened Membrane Roofing System Assemblies*

This method can be used only if the following issues can be met by the mechanically fastened membrane roofing system [6]:

Linearly-Attached

"The tested wind uplift load capacity of the proposed linearly-attached (rows) mechanically fastened roofing system assembly is determined utilizing a test chamber of sufficient size such that the tested row spacing is not exceed one half of the table length, and that one attachment row was centred along the length of the table. The minimum frame width shall be 8 feet" [6].

Spot-Attached

"The tested wind uplift load capacity of the proposed spot-attached mechanically fastened roofing system assembly is determined utilizing a test chamber of sufficient size to allow positioning of a minimum of nine attachment locations on the test frame. The minimum frame width shall be 8 feet" [6].

- Mechanically Fastened Membrane

By multiplying the number of fastener rows with the fastener spacing (along the row), the influence area per fastener (IA_t) can be calculated for this type of membrane attachment to the deck [6]. For spot-attached systems, by multiplying the distances between the attachment locations in each direction (2 ft x 2 ft, 2 ft x 3 ft, etc.), patches defining the influence area for each fastener can be calculated [6]. This value gives the number of square feet of membrane held in place by one fastener. The equation that determines the influence area is as follows [6]:

$$IA_n = \frac{(IA_t \times L_t)}{L_d} \tag{2-4}$$

where:

IA_n is the area of membrane needed to be held in place by one fastener, ft^2.

IA_t is the area of membrane held in place by one fastener for the tested assembly, ft^2.

L_d is the calculated design wind uplift load for the perimeter or corner area of a roof, psf.

Lt is the Factored Tested Load Capacity, psf.

By reducing the fastener row spacing or the spot attachment of the roofing system assembly, the square feet area of membrane held in place by each fastener will not exceed the IA_n value

[6]. For linearly-attached assemblies, the fastener spacing (along the row) shall be the same as was tested, and it should be considered that, for mechanically fastened membrane roofing system assemblies with linear (row) attachment, only the spacing between fastener rows shall be reduced to meet IA_n [6].

These methods are used for estimating the influence area for fasteners, but it cannot be applied for reducing the space between fasteners along the row and these calculations must be used to reduce fasteners' line spacing. On the other hand, these analysis methods cannot be used for increasing spaces between fasteners along the row, or even for increasing fasteners' line spacing [6].

2.7 **FM 4470 Standard and the FM Design Table**

The FM 4470 standard is used for single-ply, polymer-modified bitumen sheet, build-up roof (BUR) and liquid-applied roof assemblies evaluation regarding their behaviour under simulated wind uplift, fire from above and below the structural deck, corrosion of metal parts and optionally, puncture resistance and solar reflectance [9]. "When the roof assembly meets the FM requirements, it is qualified to be approved by the standard. The revised version of FM 4470 can be summarized as follows:

- Checking the steel deck and steel fasteners' stress calculations under wind uplift pressure to verify they are not overstressed;
- Some visible cracking and creasing of the insulation layer or cover board could be accepted if the load is less than the service load;

- For reroofing, when a rigid cover board is used to increase the stiffness of the current steel deck, the allowable bending stress shall be permitted to increase by 40%;
- Dynamic puncture resistance rating of roof covers as per ASTM D5635 has been added to FM 4470 (as an optional rating);
- Solar reflectance of roof surfaces rating as per ASTM C1549 has been added to FM 4470 (as an optional rating);
- Combustibility test requirements from below the roof deck may be met with either NFPA 276 or FM 4880;
- The susceptibility to heat damage test requirement has been added to FM4470; and,
- Corrosion resistance: a second test method is now offered" [9].

Table 2.1 shows part of the current FM table that recommends the allowable dimensions for the steel deck spans to be used for the roofing assembly and the fastener spacing, given the wind ratings. The example given in Table 2.1 is represented for a 33 ksi steel deck. As it can be seen, the table consists of different parameters: the wind rate, which shows the induced wind force on the roof; the fasteners' row spacing showing the distance between the fasteners along the deck span; and the gauge values referring to the thickness of the steel sheets. Additionally, the steel deck comes in various forms and dimensions; Figure 2.4 below represents the geometry of the CANAM steel sheet [15], which was also used in the current study.

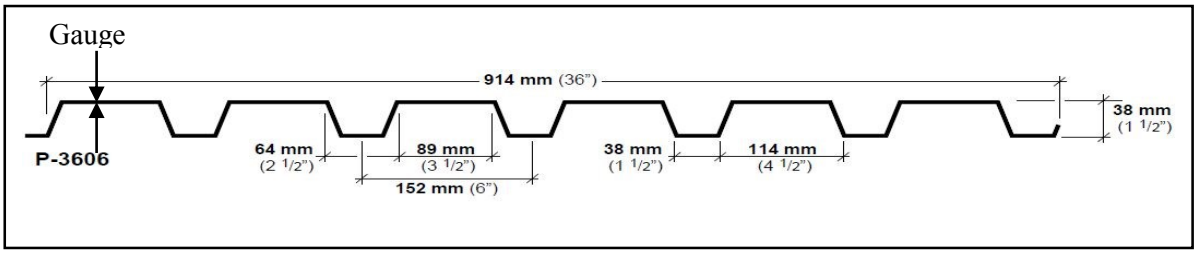

Figure 2.4 CANAM steel sheet [15]

By knowing the induced wind, the gauge of the steel sheet and the fastener spacing for the adequate span length can be obtained from Table 2.1.

Table 2.1 FM table [6]

Fastener Row Spacing (ft.)	Gauge	MAX DECK SPANS (FT) BY WIND RATING (PSF) / FASTENER SPACING, SHEET GAUGE FOR 33 Ksi																		
		330	315	300	285	270	255	240	225	210	195	180	165	150	135	120	105	90	75	60
3.5	18	4.5	5.5	5.5	5.5	5.5	5.5	6	6	6	6	6	6	6	6	6	6	6	6	6
	20	-	4	4	4.5	4.5	4.5	5	5.5	5.5	5.5	6	6	6	6	6	6	6	6	6
	22	-	-	-	-	-	4	4	4.5	4.5	4.5	5.5	5.5	5.5	6	6	6	6	6	6
4	18	4.5	4.5	5	5	5	6	6	6	6	6	6	6	6	6	6	6	6	6	6
	20	-	-	-	-	4	4.5	4.5	5	5	5.5	6	6	6	6	6	6	6	6	6
	22	-	-	-	-	-	-	-	-	4	4.5	5	5	6	6	6	6	6	6	6
4.5	18	-	4	4	4.5	5	5	5.5	6	6	6	6	6	6	6	6	6	6	6	6
	20	-	-	-	-	-	-	4	4	5	5	5.5	6	6	6	6	6	6	6	6
	22	-	-	-	-	-	-	-	-	-	-	4	4.5	5	5.5	6	6	6	6	6
5	18	-	-	-	4	4	4.5	5	5	5.5	6	6	6	6	6	6	6	6	6	6
	20									4	4.5	5	5.5	6	6	6	6	6	6	6
	22	-	-	-	-	-	-	-	-	-	-	-	4	4.5	5	6	6	6	6	6
5.5	18	-	-	-	-	-	-	4	4.5	5	5.5	6	6	6	6	6	6	6	6	6
	20	-	-	-	-	-	-	-	-	-	-	4	4.5	5	6	6	6	6	6	6
	22	-	-	-	-	-	-	-	-	-	-	-	-	-	4.5	5	6	6	6	6
6	18	-	-	-	-	-	-	-	-	4	5	5.5	6	6	6	6	6	6	6	6
	20	-	-	-	-	-	-	-	-	-	-	-	-	4.5	5.5	6	6	6	6	6
	22	-	-	-	-	-	-	-	-	-	-	-	-	-	-	4.5	5.5	6	6	6

Based on newly published FM reports [9], the current values for the deck span's allowable dimensions should be updated. Moreover, for the lower corner of Table 2.1, the fastener spacing and steel deck span dimensions were not released for higher wind ratings; therefore, expanded investigations are required for determining the new allowable values. The wind rating in Table 2.1 starts at 60 psf, but the experiment starts from 30 psf, thus updates of the table for lower wind pressure could also be pursued.

"In regard to the loading conditions, the fastener line distance (l) and the span length (L), considered for the design of the steel deck span, three cases were categorized:

- The roof system fastener row spacing (l) is less than ½ the distance of the steel deck span (L) under uniform loading conditions (Figure 2.5);

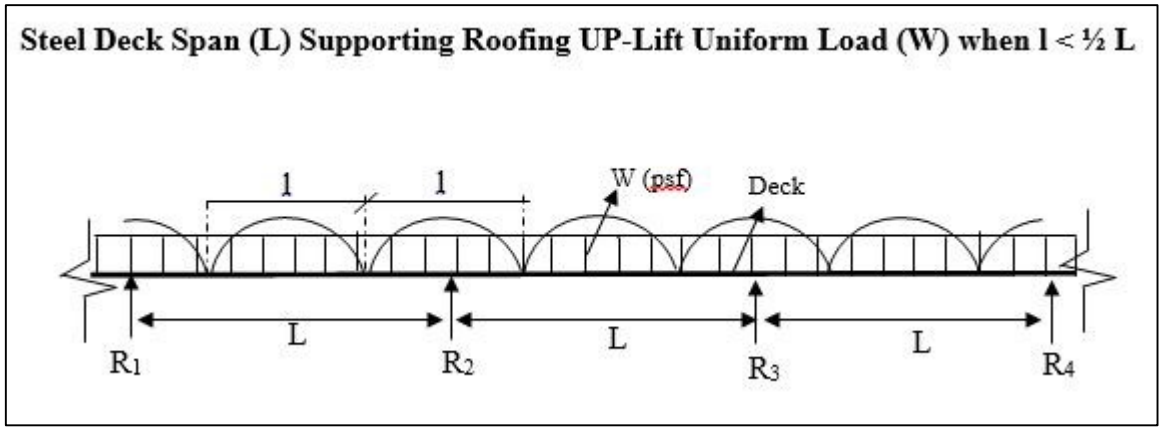

Figure 2.5 Steel deck span under uniform load [6]

- The roof system fastener row spacing (l) is equal to or greater than 1½ the distance of the steel deck span under point loading conditions (Figure 2.6);

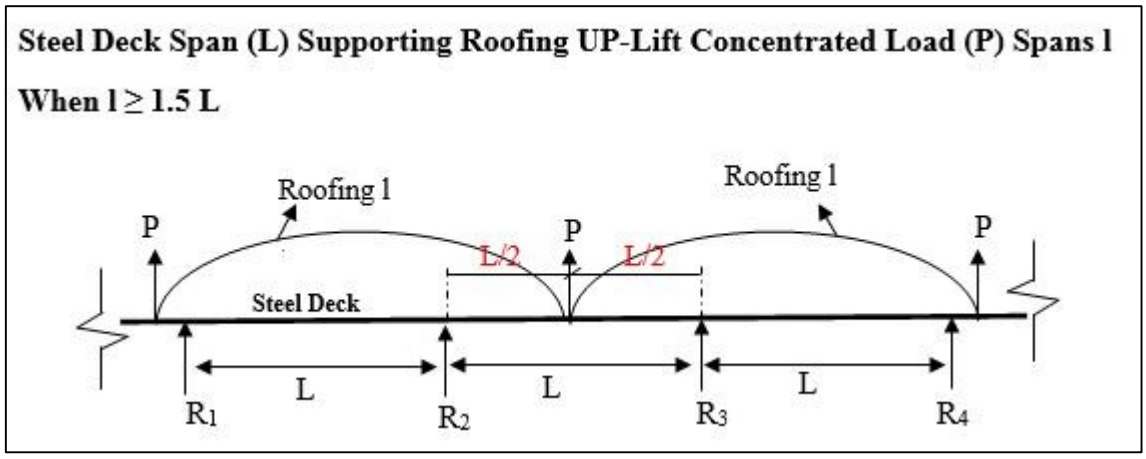

Figure 2.6 Roof span under point load [6]

- The roof system fastener row spacing (l) is equal to or greater than ½ and less than 1½ the distance of the steel deck span under point loading conditions (Figure 2.7)" [6].

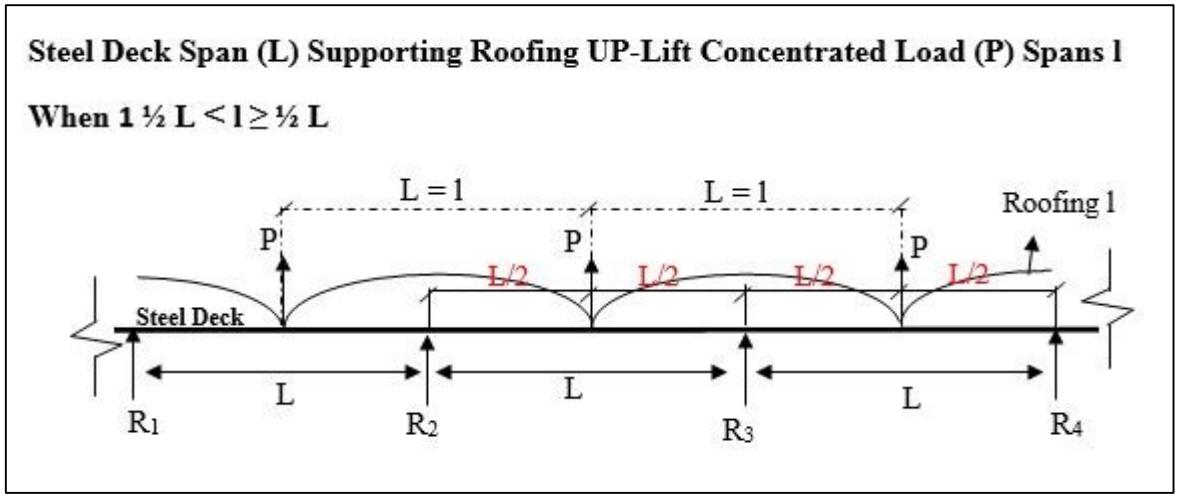

Figure 2.7 Roof span under point load [6]

Considering these loading conditions, only relatively small dimensions of the steel deck span are allowed to be installed as part of the SPR's roofing systems, and for high wind ratings the steel deck products are considerably reduced from the manufacturing and construction market [6].

2.8 **Roofing Assemblies Failure Mechanisms**

Most of the current roof damages are not caused by unsuitable wind uplift resistant components, but rather occur as a result of noncompliance issues with existing standards [16]. The failure occurrence in roofing systems (Figure 2.8) that are constructed in conformity with the FM guidelines is rare and the designer's specifications have an important role in this procedure. "Many current research studies have stated that the problems listed below have been the main reasons for recent roof failures:

- Installers do not always use the required number of roof fasteners, particularly at the perimeter, where the system attachment is most critical.

- The roof-edge details often failed to comply with the current ANSI/SPRI ES-1 compliant testing standard, and some edge protection features are missing.
- Rooftop equipment was not properly attached to equipment curbs, resulting in projectiles that caused membrane punctures. These mistakes often occur after the architect's plans are approved and equipment is installed by roofing non-professionals" [16].

The roofing systems manufacturers and designers must determine and verify their products in regard to the updated FM class 1-90 standard, thus delaying the certification-approval-installation process [16]. If designers follow the specifications stipulated in FM Class 1-90, the roof system can be easily insured by FM [16]. However, some professionals question the need for such a rigorous standard. "You are basically overdesigning with the FM 1-90, said an architect with almost 30 years of experience in roof design and installation. When 85% of the projects are not FM insured but still call for FM 1-90, there is a disconnection in the concept of the standard" [16].

By realising the new version of the FM standard, some parts of the roofing industry have increased their reliance to ASCE-7-2005 [16]. This has prompted FM to change some of the details in the Class I standard. Due to concerns expressed by a coalition of roofing industry trade groups, FM Global will now allow prescriptive enhancements where a Class 1-90 roof system is specified in a non-hurricane-prone area [16].

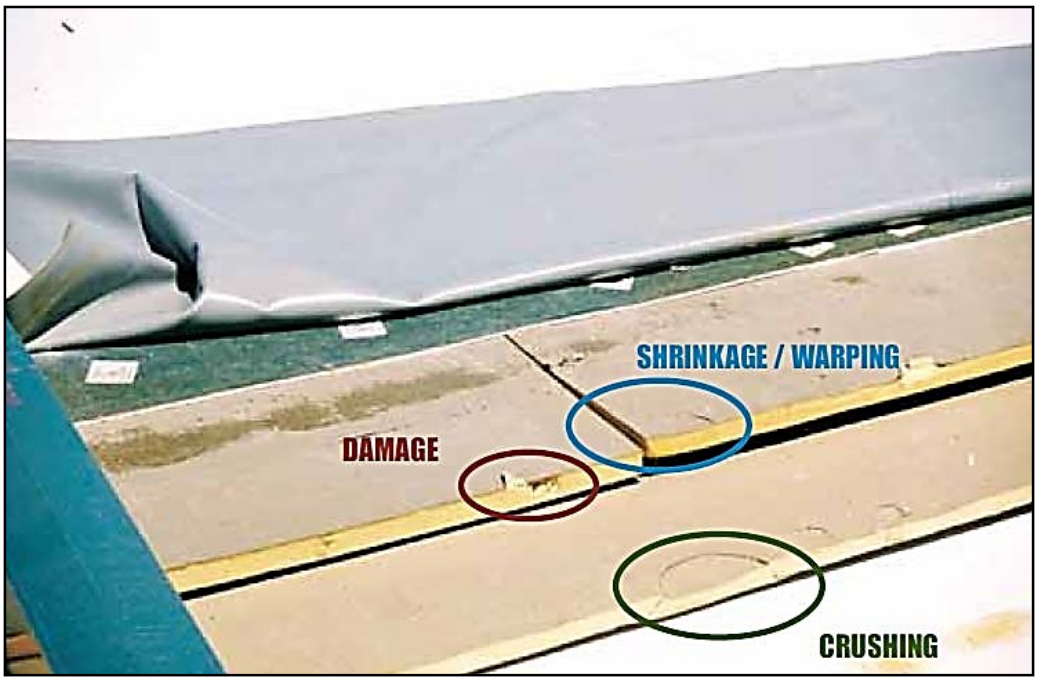

Figure 2.8 Damage to fragile insulation layer and evidence of cupping and bowing revealed after Hurricane Katrina. Photo courtesy of NOAA [16]

2.8.1 **Meeting FM's new requirements**

FM's wind uplift requirements are based on the American Society of Civil Engineers ASCE-7-2005 [10], and it recommends higher standards and safety factors than the code itself. Regarding the original ASCE-7-2005 standard [10], the FM recommendations provide several calculation procedures that influence the wind design process. All factors involved in the design process, such as building location, enclosure, height and ground roughness, are brought into the wind uplift load equation. "A common misconception in the design community is that 1-90 represents winds up to 90 mph. In fact, the standard requires that the roof system withstand 90 lbs per square foot (psf) of wind uplift tested pressure" [16].

As stated in the FM standard, 90 psf should be taken into account in high-wind areas for high-rise buildings, which make up a small part of the roof installations. Meanwhile, 1-90 is used

in more than 80% of roofing specifications, wherein 75 or 60 psf would be more adequate and more cost effective [9]. Currently, building design pressures up to 45 psf are using an FM safety factor of 2.00 and the FM standard requires that the roof assembly withstand the tested differential ultimate pressures [9].

Fixing percentages of fasteners for perimeters and corner areas of adhered roof systems was the simplest way to increase the spacing between the fasteners applied on the inside surface of the roof (also called the roof field), in the past, which is no longer accepted for the new revised version FM field of roof rating of 90 psf or higher; however, there are other methods of strengthening the edges and corners of roof systems, such as using a "peel stop" on roofing membranes [12].

Only a few of the specifications used for fully adhered roofing systems were approved in terms of the new accomplishments of the FM changes; therefore, many roof system manufacturers had to re-test their products in order to release them to the building industry [12]. In a recent study, Schneider stated, "one way to meet the new FM requirements, and increase the strength of the roofing assembly is to specify a 1/2″ pre-primed, moisture-resistant gypsum cover board fastened through the insulation to the roof deck" [16]. As the test has concluded, a three-ply BUR roof system with 1.5″ poly-iso insulation passed the 315 psf wind rating test, based on new revised FM requirements, which means it is 10 psf higher than the corner pressures required by FM 1-120 [1]. A number of membrane manufacturers have also tested various types of gypsum cover boards with their adhered membranes and have achieved a variety of responses for the high wind uplift results [1].

2.8.2 **FM 1-29 field of roof requirements**

For ratings below the 90 psf wind rating, the FM implementations have been revised gradually. Schneider has also mentioned, “The FM requirements below 90 psf have changed slightly. For FM fully adhered membranes with ratings of 75 psf or lower, finding the perimeter and corner fastening rates by multiplying the field fastening rate is still acceptable. However, the new 1-29 Loss Prevention Data Sheet requirements are more stringent. In the past, the increase in fastener count was 50 and 75% for the perimeter and corner areas, respectively, for adhered membranes. In 2006, these values were increased to 50 and 100%, respectively, with minimum fastening rates required unless testing showed the uplift pressures could be resisted with fewer fasteners” [16].

FM continues to work with the roofing industry. The new requirements may still increase the costs of many roof systems. If a project needs FM approval, the design and installment of the roof system should meet the requirements of the Approval Guide, RoofNav, Loss Prevention Data Sheets 1-28, 1-29 and 149, as well as wind design and perimeter flashing implementations [12]. In case of non-FM insured buildings, wind uplift requirements will be determined by a number of factors such as geographic area, exposure factors and the building design itself [16].

2.8.3 **Roof system performance**

To increase roof performance and to reduce the probability of roof failure in a reasonable way, the durability of the roof has to be ensured, which can be defined as a consolidation of roof

system strength and resistance. The current study is focused on the resistance of the roofing system, however, durability features are also presented for further clarifying of the interaction between the overall roofing system and the loads it has to withstand as per the FM standards [6]. The durability of a roof system can be increased if any type of cover-board such as wood fibre, plywood or gypsum is added to the roof by the designer [16]. The cover-board is quite thin (1/4″) and is installed between insulation and membrane [16]. There are different types of cover-board that may be chosen by designers as follows [16]:

- *Asphaltic board*
- *Plywood/OS*
- *Mineral fibre board*
- *Mineral fibre board*
- *Wood fibre board*
- *Perlite*
- *Cellulose-reinforced gypsum*
- *Paper-faced gypsum*
- *Glass-mat gypsum*

When the wind reaches the building, first uplift pressures tend to lift the membrane, and then the forces are continually transferred to the roof elements below the membranes, the insulation, fasteners, deck and structural components [16].

Although designers and builders have a common opinion to increase the strength of roofs without overdesigning them or following costly methods, the new FM fundamentals persisted

in recommending designing methodologies that increase the cost and complexity of the building compliant standards [16].

2.9 **Fasteners in Single-ply Roofing System**

The importance of fasteners in the roof industry was always debatable. Fasteners keep structures and their components stable under different forces such as wind uplift force. Although there are different types of fasteners based on their applications, the concept is the same for all types, which is the joining of pieces or multiple layers. Fasteners keep many roofs intact [12]. Most roofing fasteners are threaded but vary by type [12]. Presently, more and more threaded fasteners are being used in roofing applications. In 1973, Chicago Firm introduced threaded roofing fasteners to the roof industry, which attached different components of the roof by screws and plates that provided additional holding strength, especially for older systems [17]. This system has been widely accepted by the industry [17]. Before introducing this new method, spot-fastening with asphalt and cold-applied adhesive systems were used [17]. These methods of weak attachment decreased the risk of fire, but increased the potential for blow-off [17]. Factory mutual statistics have indicated that during the ten-year period from 1971–1980, there were 1,247 windstorm losses to steel-deck roofs, totalling $83.6 million [12, 17].

In 1983, FM accepted mechanical attachments for roof systems to prevent loss, and based on the data sheet 1-28, using screws and plates was the only recommended method for the attachment of a rigid insulation board to the metal deck [5]. “Recommendations suggested that some testing had been taken into account; therefore, FM developed an apparatus to test

mechanical fastening systems subject to simulated wind uplift loads. Two classifications of wind storm protections were set up: 1-60 and 1-90" [12].

There is a direct relation between roof damage and the strength of roof fasteners that connect different parts of the roof system and resist against the applied load to the roof. Each component of the mechanically attached roofing system such as deck, insulation and membrane experience some loads. Each component in the assembly plays an important role in keeping the entire mechanical fastening system secured. The fastener characteristics listed below can affect the fastening system's performance [5]:

- Drill point
- Threaded design
- Stress plate and fastener head
- Fastener back-out vs. pop up
- Corrosion
- Application guidelines

The most important part of a fastener is the drill point, which should be sharp. It is used to drill a pilot hole into a steel deck for threads to follow [18]. A threaded fastener that drills holes is called a self-drilling fastener. There are various types of self-drilling fasteners available based on their usage [18]. The self-drive fastener drills and taps the roof deck in one operation. The drilling time is a cost factor; therefore, an efficient way of drilling is a priority, which means choosing the correct tools to attach different layers to the deck [18]. A concentric drill point combined with an efficient thread design provides greater pull-out strength, higher

stripping torque and lower tapping torque [18]. Figure 2.9 [18] shows the drill point of a deck fastener.

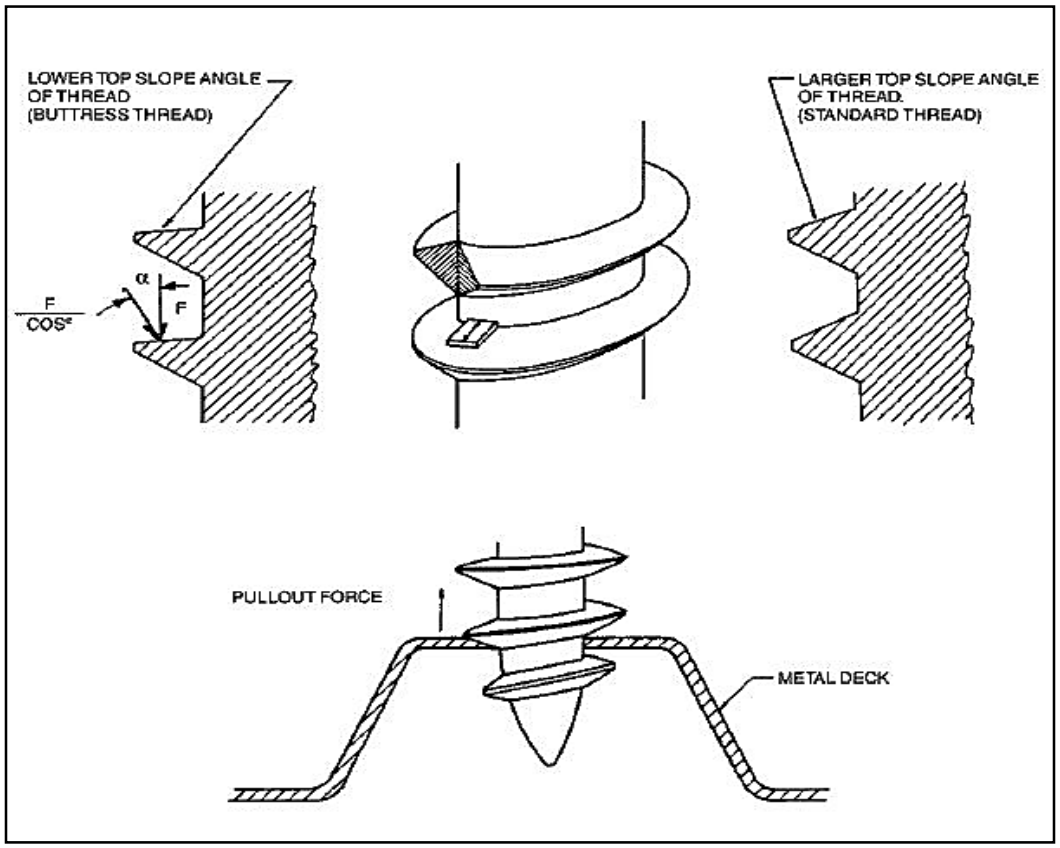

Figure 2.9 Lower top slope angle of buttress thread increase pull-out strength and resists fastener back-out [18]

Chapter 3 Experimental program

3.1 Introduction

To validate the FEM of the roofing system, which is proposed for expanding the FM tables, an experimental reference for comparison is needed. Therefore, several experimental cases were performed for comparing the force, moments and deflection results with the results obtained from the FEM and if these are found to be in agreement, within the acceptable 10% error range, the FEM can be validated. Otherwise, some modifications should be considered in the FEM, with the modified results compared to the experimental ones until an acceptable results are obtained. The experimental part of this research was carried out at the National Research Council of Canada (NRC) and consisted in performing tests on four full-scale samples of roofing assemblies as listed below and as explained in detail in the following sections:

- Roof assembly with 9′6″ membrane fasteners line distance
- Roof assembly with 6′ membrane fasteners line distance
- Roof assembly with 7′6″ membrane fasteners line distance
- Steel deck only

As shown in Figure 3.1, the test facilities comprised of the following main items:

- A 16″ by 32″ chamber with bottom frame
- A suction engine that can produce 500 psf wind pressure
- Custom joists, which are attached to the bottom frame by steel brackets
- CANAM steel sheets with 22 gauge (Figure 3.2)

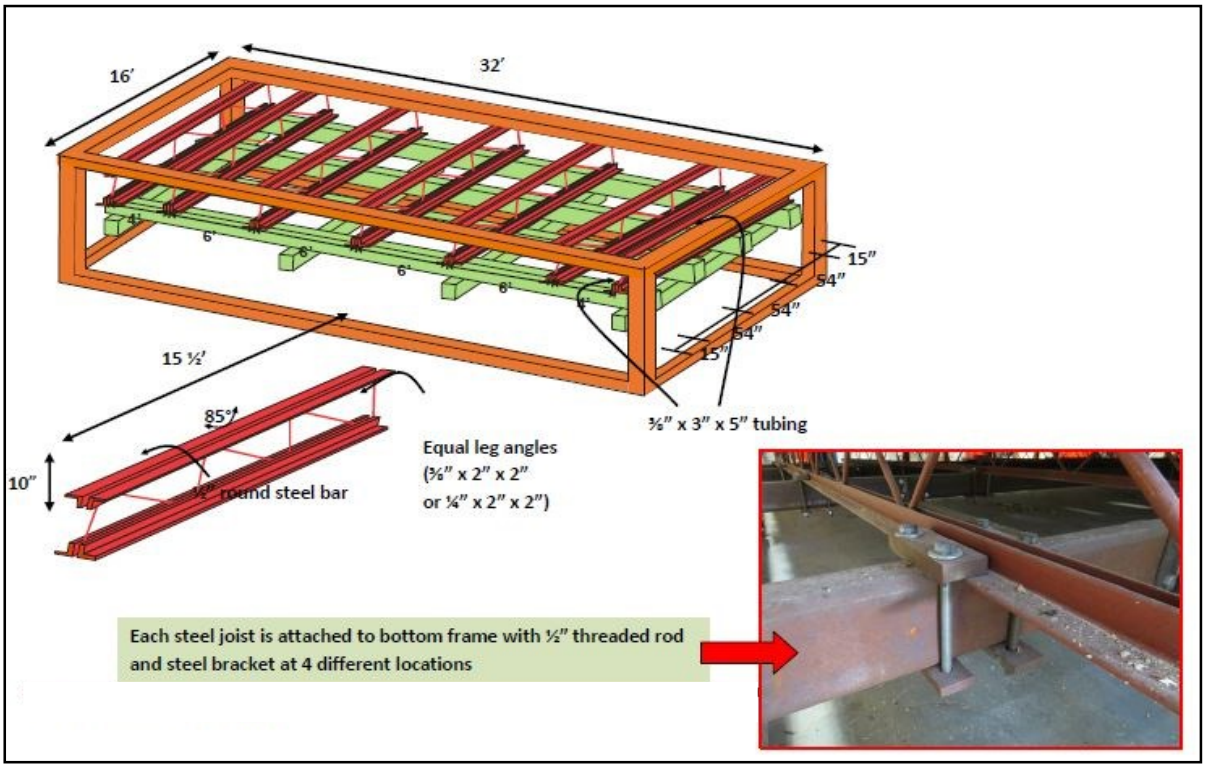

Figure 3.1 Experimental facilities

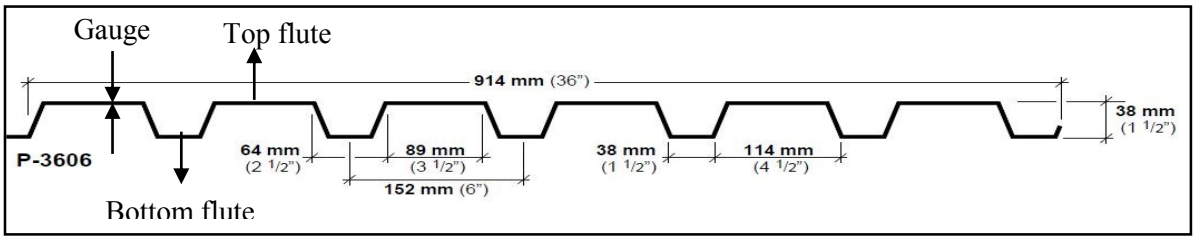

Figure 3.2 Geometry of CANAM steel sheet [15]

The chamber has a new suction engine that can apply up to 500 psf pressure on the tested samples. It has a 16′ width and 32′ length, and seven steel joists are used to provide an experimental sample of what will be constructed in reality. The length of joists is $15\frac{1}{2}$′, the height is 10″ and they are K-Series joists, which are used for small spans with low loading. The joist section is a 2″ x 2″ double angle with 0.5″ distance and 0.16″ thickness. The diagonal members are located at each 18″ and are inclined at 85 degrees.

3.2 Test Specimens

There are four experimental cases tested, for three of them the entire roof assembly was tested, with 6′, 7′6″ and 9′6″ membrane fasteners line distances and in one case only the steel deck was tested under the wind-induced forces, as detailed in Table 3.1. The 6′, 7′6″ and 9′6″ distances between the fasteners lines were selected because these represent the longest dimensions between the two consecutive loading lines; these would determine critical cases when converted from the uniform load to the line load and then would be transferred to the steel deck. Canadian General Tower Ltd., the industrial partner who also provided the 22 gauge steel deck specimens, was consulted when selecting these specific test cases. Also the SPRI's interest in validating and expanding the FEM for updating the lower corner of the FM table, which contains higher steel deck spans and bigger wind rating, was taken into consideration when choosing the three roof assembly test cases. The fourth case of steel deck only was selected for providing a bare roofing test case for validating the initial FEM for uniform load. The rest of three roofing assembly cases were used for validating the FEM for the point loading system obtained after conversion, as described in detail in Chapter 4. The tests were stopped if any failure could be observed under wind pressures; for instance, if the steel deck buckled or any of the fasteners were pulled out under the pressure. The entire roof system had to be reassembled with new materials for each experimental case and was subjected to several loading cycles. The first induced wind force was 30 psf, and this was increased by 15 psf for each cycle until failure occurred; on the occurrence of the mechanical failure the test was stopped. For example, the designated wind pressures for the first case were 30 psf, 45 psf, 60 psf, 75 psf and 90 psf, but due to the failure of the system, which occurred before reaching 90 psf, the test was interrupted. The loading pressure was applied for one

minute in each cycle, after which a few minutes were allowed, and without opening the chamber a new wind rate was simulated as part of the following loading cycle for the same experimental case. A procedure of eliminating the influence of the residual deformations was applied as will be explained later in this chapter.

Table 3.1 Experimental cases performed for the wind uplift loading tests

Case#	Explanation
1	Roof assembly with 9′6″ membrane fasteners line distance
2	Roof assembly with 6′ membrane fasteners line distance
3	Roof assembly with 7′6″ membrane fasteners line distance
4	Steel deck without any other layers on top

After reassembly of the roof for each case, and before the start of the test, the system was preloaded to simulate loads that have been applied to the system during the roof assembling, such as live load, to reduce errors and to achieve accurate results.

3.2.1 **Roof assembly with 9′6″ membrane fasteners line distance**

The objective of this case is to investigate the roof behaviour under a fastener line load.

The roof configuration for this case is as follows:

- Install a new set of roof deck (CANAM steel sheet, P-3606 series with 22 gauge)
- System detail: 45mil TPO membrane, 2″ insulation layer
- Fr (fastener row distance) = 9′6″ and Fs (deck fastener distance) = 6″
- Installation of all sensors and 6-component load cell
- Wind pressure up to 90 psf

Figures 3.3 and 3.4 provide illustrated procedures of assembling the roofing system used for testing. Initially, to ensure the fixed conditions at the steel deck, the CANAM steel sheets are

attached to the joists (Fig 3.3 a). After attaching the insulation pieces to the steel deck (Fig 3.3 b), the membrane layer is attached to the system using a fastener distance of 6 inches and the distance between the fastener rows of 9′6″ (Figs. 3.4, a and b).

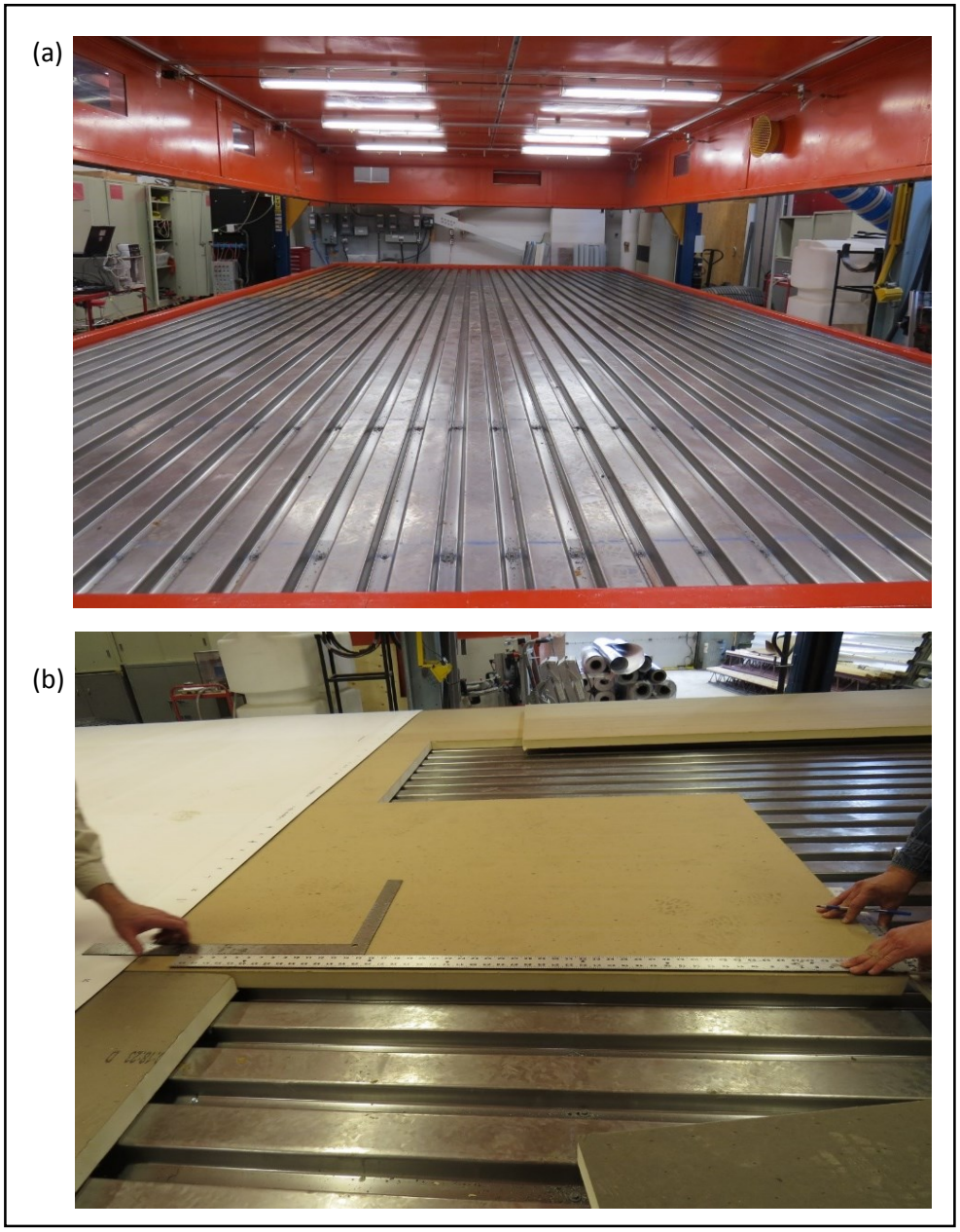

Figure 3.3 (a) Steel deck installation, (b) insulation layer setup

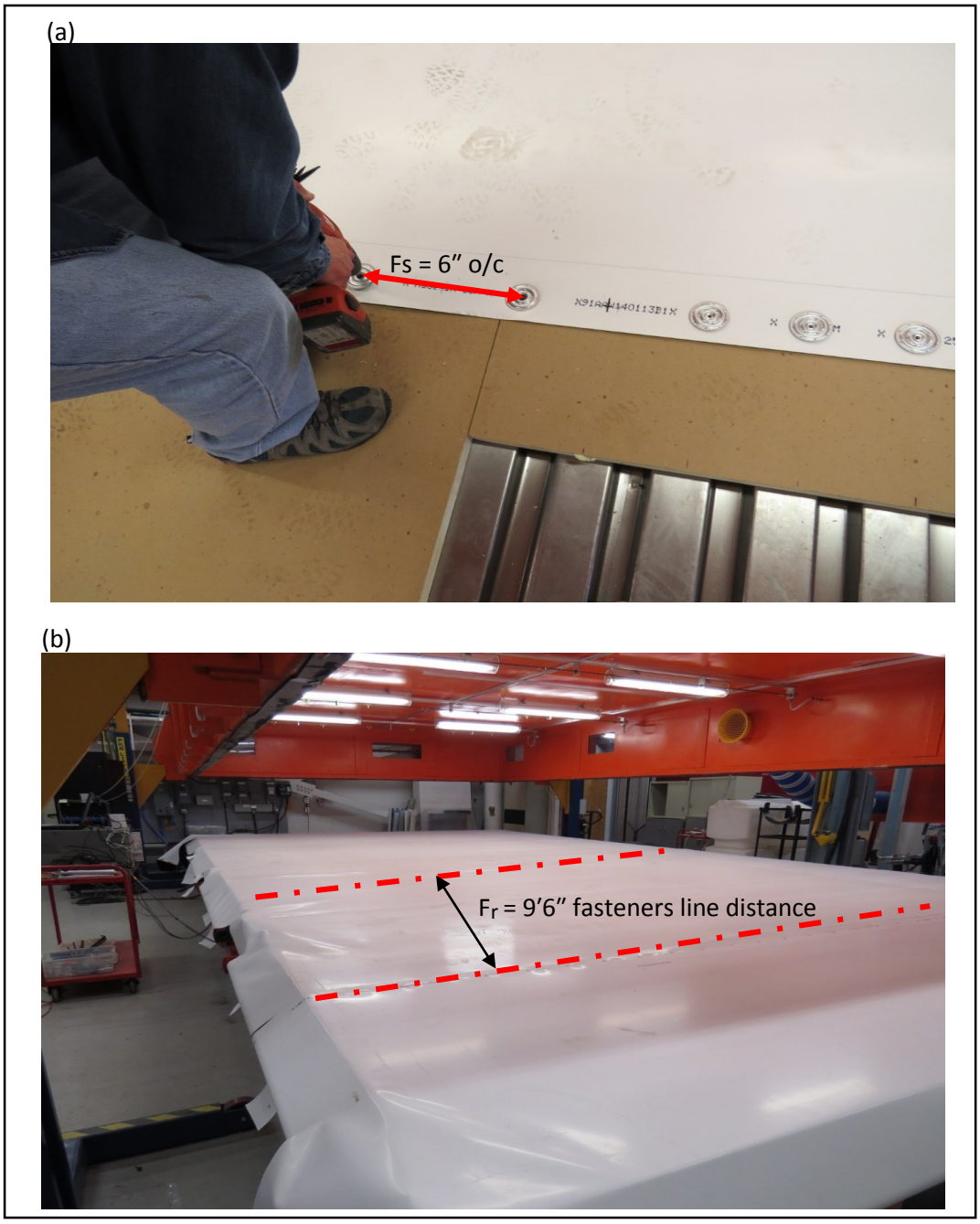

Figure 3.4 (a) Attaching membrane layer to steel deck, (b) Roof assembly

To attach two membrane sheets at the seam, a hot air machine is required. Thus, after attaching one strip of the membrane layer, the second membrane strip was brought and a Leister Hot Air machine was used for attaching the two strips, as shown in Figures 3.5 a) and b). Before adhering them to the main roofing system, a separate sample was adhered with the same

procedure, in order to find out the adequate working speed and applied temperature, which can provide a proper attachment.

After performing several trials of attachments, the speed and temperature of the machine were set at 6′/min and 1,014° F, respectively. If the two membrane sheets are correctly attached, when the samples are separated, the fabric of one part will remain on the other side, as shown in Figure 3.6.

(a)

(b)

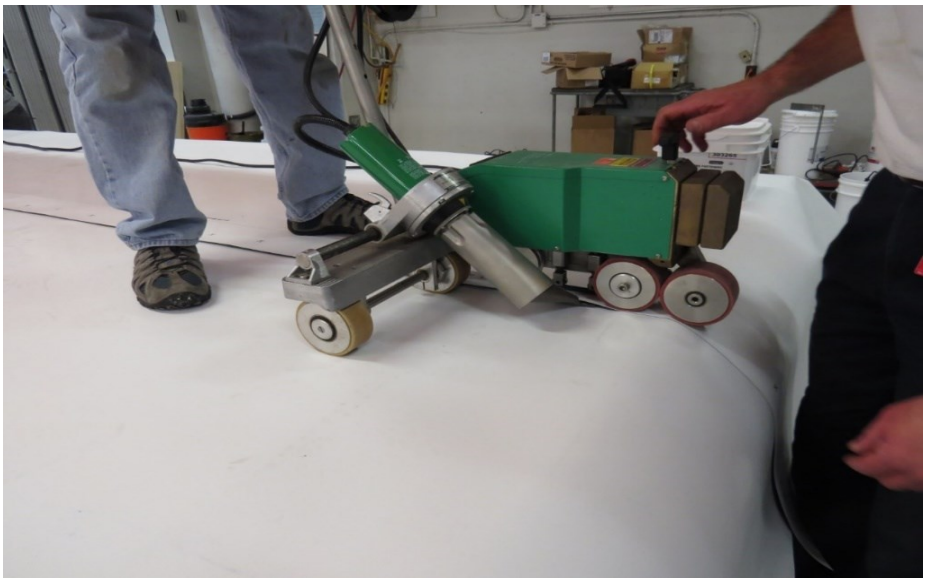

Figure 3.5 (a) Membrane seam, (b) adhering membrane seam by Leister hot air machine

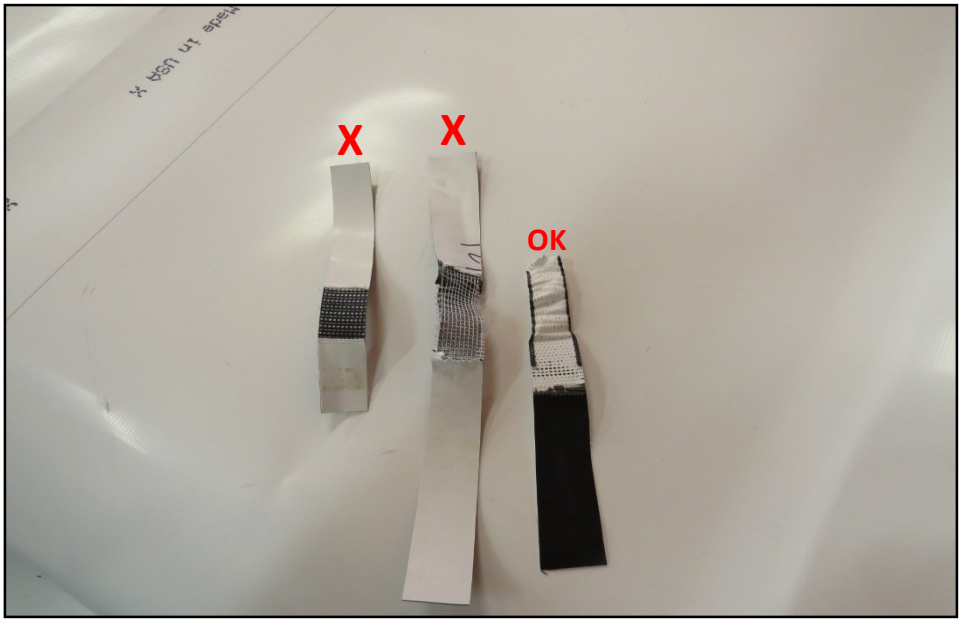

Figure 3.6 Adequate adhesive membranes

The line of membrane fasteners is located on the membrane sheets seam, and in this case the fasteners are covered by the other sheet, as illustrated in Figure 3.7.

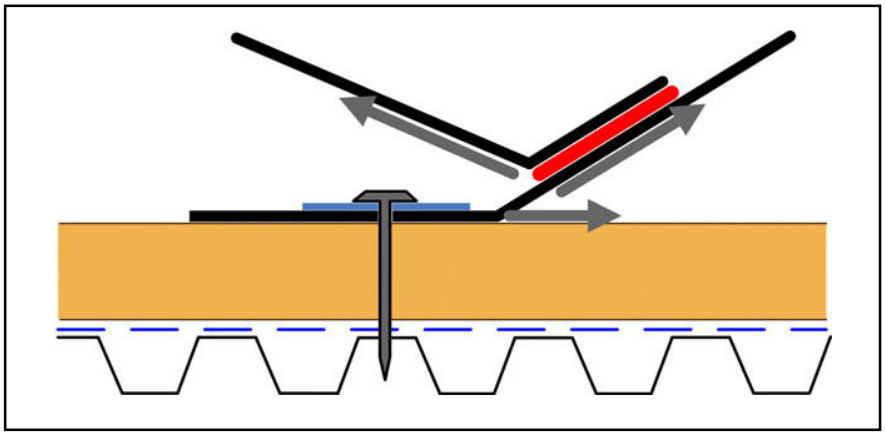
Figure 3.7 Schematic of covering fastener in overlapping membrane sheets [19]

As briefly mentioned at the beginning of this chapter, the designated wind loading pressures for this testing case were 30 psf to 90 psf, but when applying 80 psf the membrane ballooned

(Fig 3.8 a) and the failure occurred in the membrane layer as it is ruptured near the fastener's row (Fig 3.8 b and c).

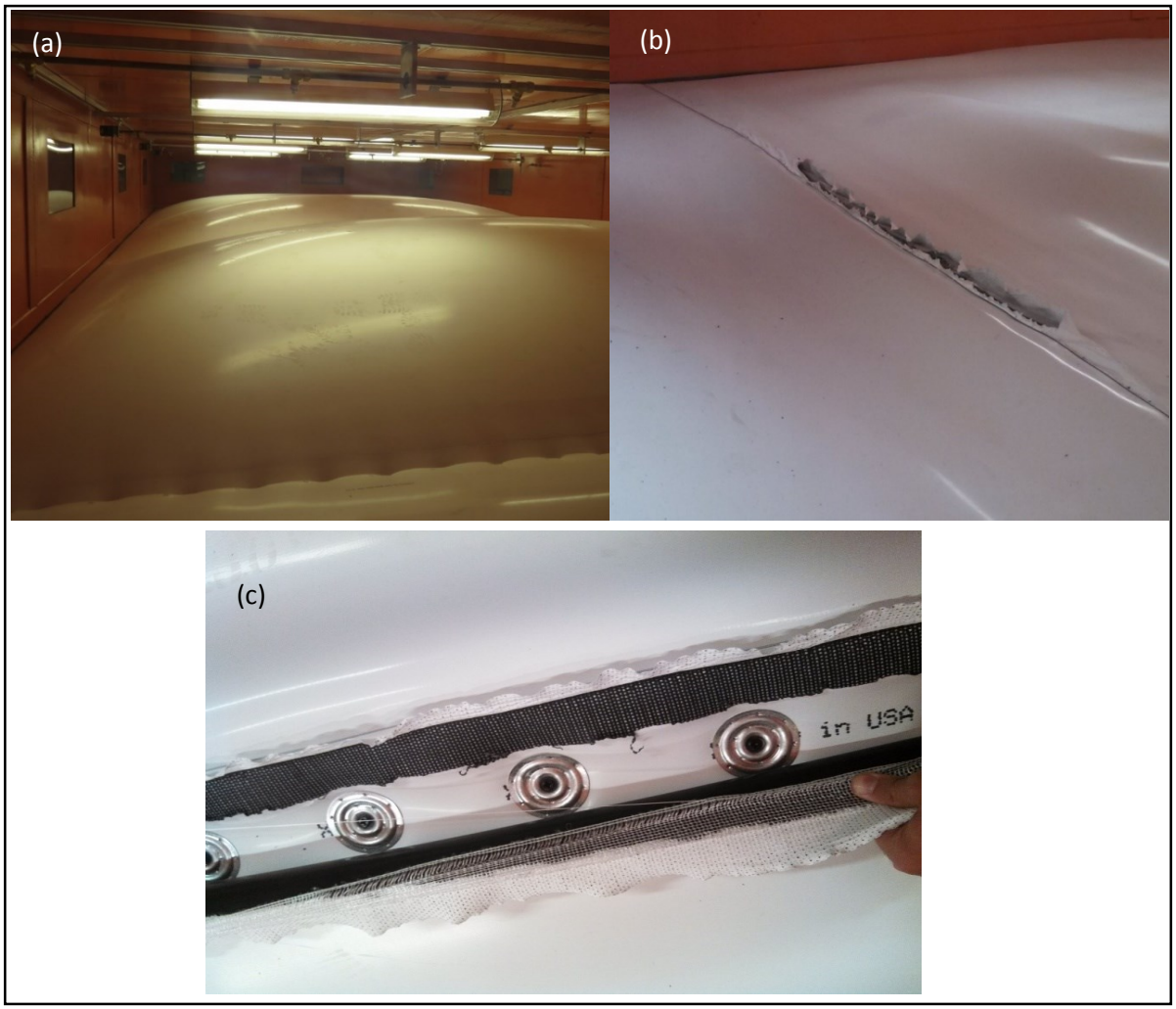

Figure 3.8 a) Roof assembly under pressure reaching 90 psf, (b) and (c) Membrane failure

3.2.2 **Roof assembly with 6′ membrane fasteners' line distance**

The objective of this case is to investigate the roof behaviour under the effect of a line load applied along the fastener line.

The roof configuration for this case is as follows:

- Remove the previously tested roof assembly

- Install a new set of roof deck (CANAM steel sheet, P-3606 series with 22 gauge)
- System detail: 45mil TPO membrane, 2″ Insulation layer
- Fr (fastener row distance) = 6′ and Fs (deck fastener distance) = 6″
- Install all displacement sensors and 6-load cell
- Simulate wind uplift pressures of up to 130 psf

In this case, the membrane fasteners were not covered at the attachment of the membranes, and the membrane seam was perpendicular to the joist as shown in Figure 3.9. The membrane seams used in case no.1 were parallel to the joists, therefore, the loading capacity was slightly lower than the loading capacity of the roof assembly tested in case no. 2.

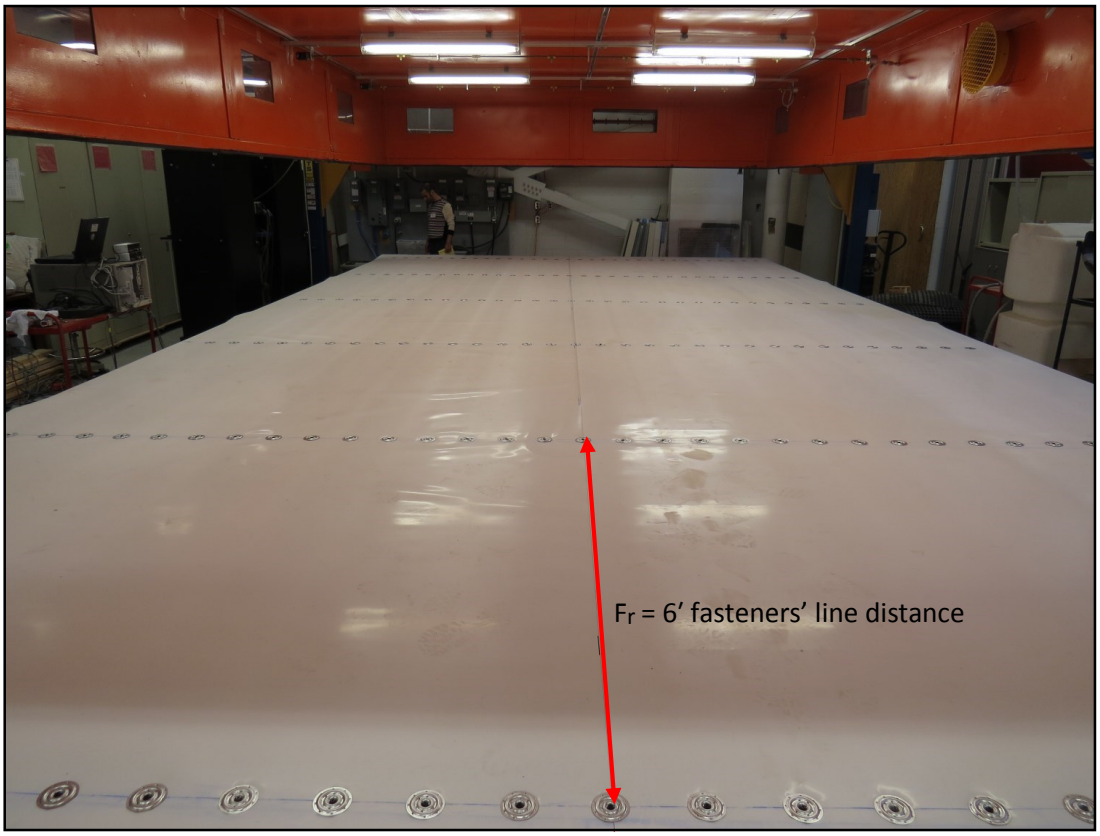

Figure 3.9 Roof assembly configuration for case no. 2

The procedure for running the test was the same as the one applied for the previous case. Picture (a) in Figure 3.10 shows the pressure on the fastener and its plate. The test was stopped when buckling could be observed in the steel deck and, as shown in Figure 3.10 b), the steel deck around the fasteners entered into the plastic range and registered permanent deformations.

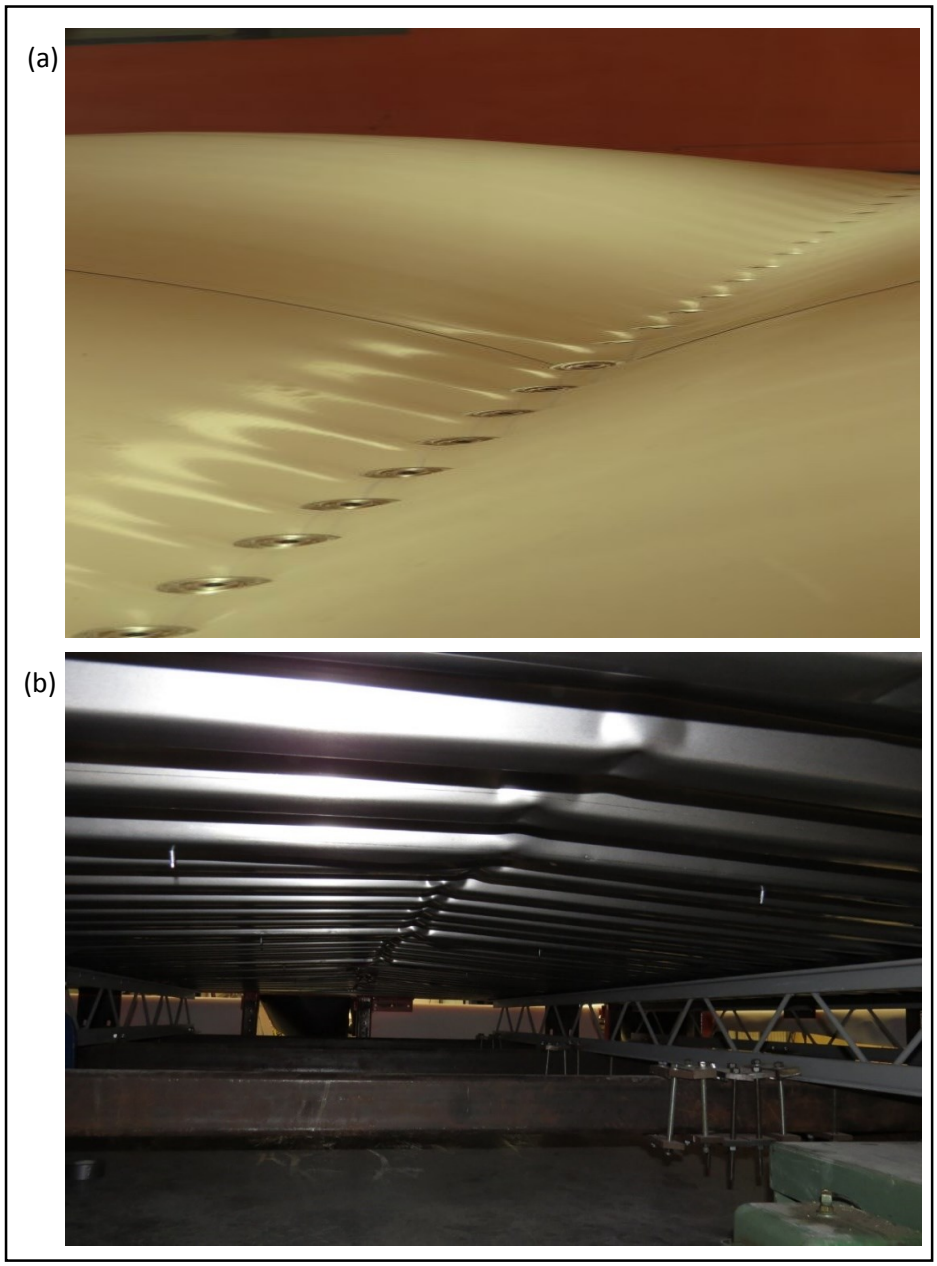

Figure 3.10 (a) Roof assembly under 130 psf pressure, (b) Buckling in mid-span of steel deck

3.2.3 **Roof assembly with 7′6″ membrane fasteners line distance**

Similar to the experimental case no.2, the objective of this case is to investigate the roof behaviour under the line load applied at the fastener row with 7′6″ distance.

The roof configuration for this case is similar to the case no.2, except for the geometry of the tested roofing assembly and the fastener row distance:

- Remove previously tested roof assembly
- Install a new set of roof deck (CANAM steel sheet, P-3606 series with 22 gauge)
- System detail: 45mil TPO membrane, 2″ Insulation layer

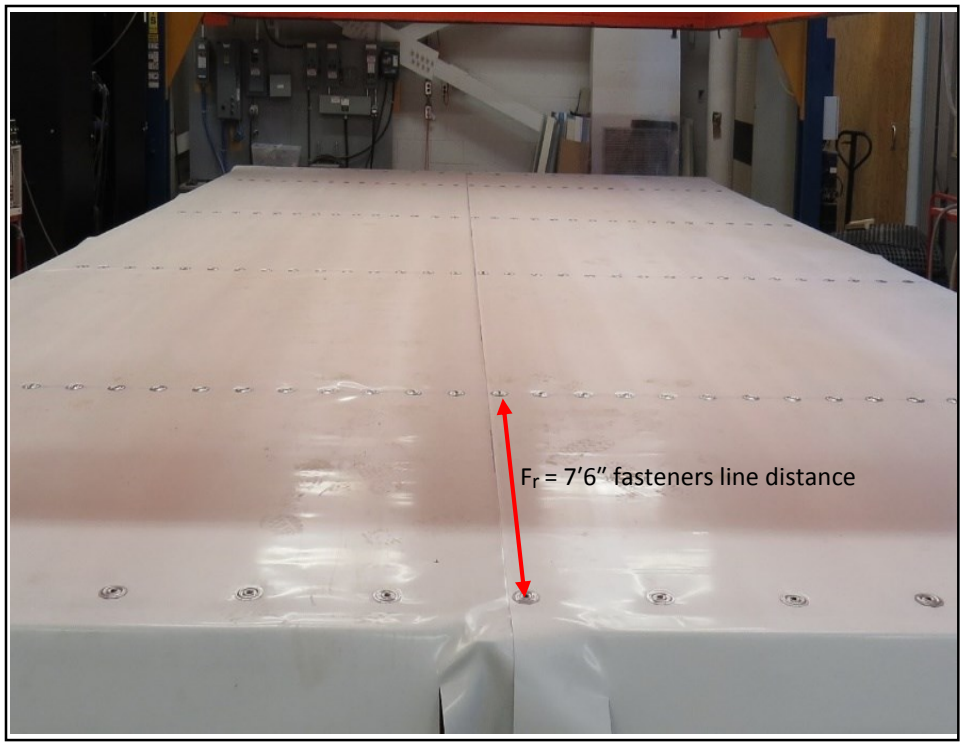

Figure 3.11 Roof assembly configuration for case no. 3

- Fr (fastener row distance) = 7′6″ and Fs (deck fastener distance) = 6″
- Install all sensors and 6-load cell
- Simulate wind pressures of up to 105 psf

Figure 3.11 shows the roof assembly configuration for the case no. 3. The assembly is the same as case no. 2, but the fastener line distance is different, which led to the application of wind uplift pressures in less number of cycles in comparison with test case no. 2.

Initially, it was estimated that the system can resist 105 psf wind uplift pressure, but due to buckling failure, which occurred in the steel deck under the effect of about 90 psf pressure, as it can be seen in Fig. 3.12, the test was stopped.

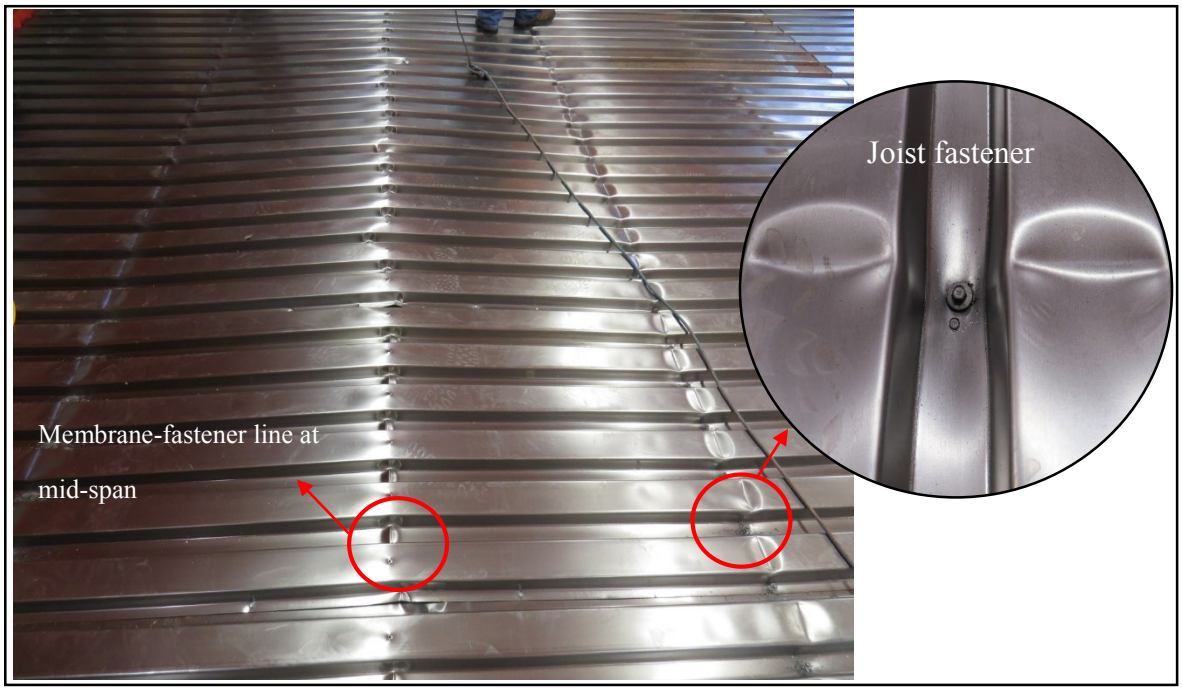

Figure 3.12 Buckled steel deck failure

By removing different parts of the tested roof, it became clear that failures occurred in the insulation boards and membrane layers as well. Figure 3.13 a) shows cracks in insulation boards and Fig. 3.13 b) shows wrinkling in the membrane layer. However, because the focus of the current study was the ultimate resistance of the roofing assembly, the failure modes of the steel deck were investigated.

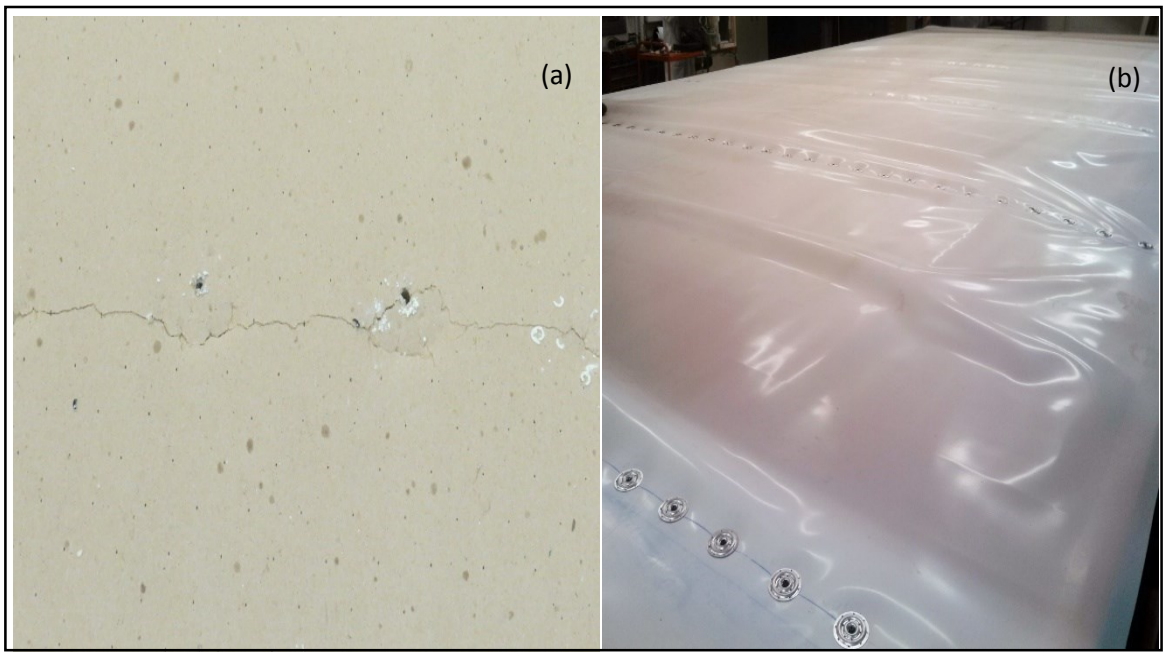

Figure 3.13 (a) Crack in insulation board under 90 psf, (b) membrane layers wrinkled under 90 psf

3.2.4 **Steel deck**

The objective of this case is to investigate the steel deck behaviour under the simulated uniform load.

The test configuration for this case is as follows:

- Remove previously tested roof assembly
- Install a new set of roof deck (CANAM steel sheet, P-3606 series with 22 gauge)
- Fs (deck fastener distance) = 6″
- Install all sensors and 6-load cell
- Simulate wind pressures of up to 180 psf

It was predicted that the steel deck could resist up to 180 psf, but at 135 psf buckling was observed at mid-span, so the test was stopped at this wind pressure. Figure 3.14 shows the assembled steel roof deck (case no. 4).

Figure 3.14 Steel deck roof test for case no.4

Figure 3.15 shows the buckled steel deck at 135 psf. As it can be seen in Fig. 3.15 a), plastic deformation was registered along the fasteners' line, however, the maximum deflection occurred between two fasteners' line spacing (Fig. 3.15 b), which was considered the dominant failure mode for test case no.4.

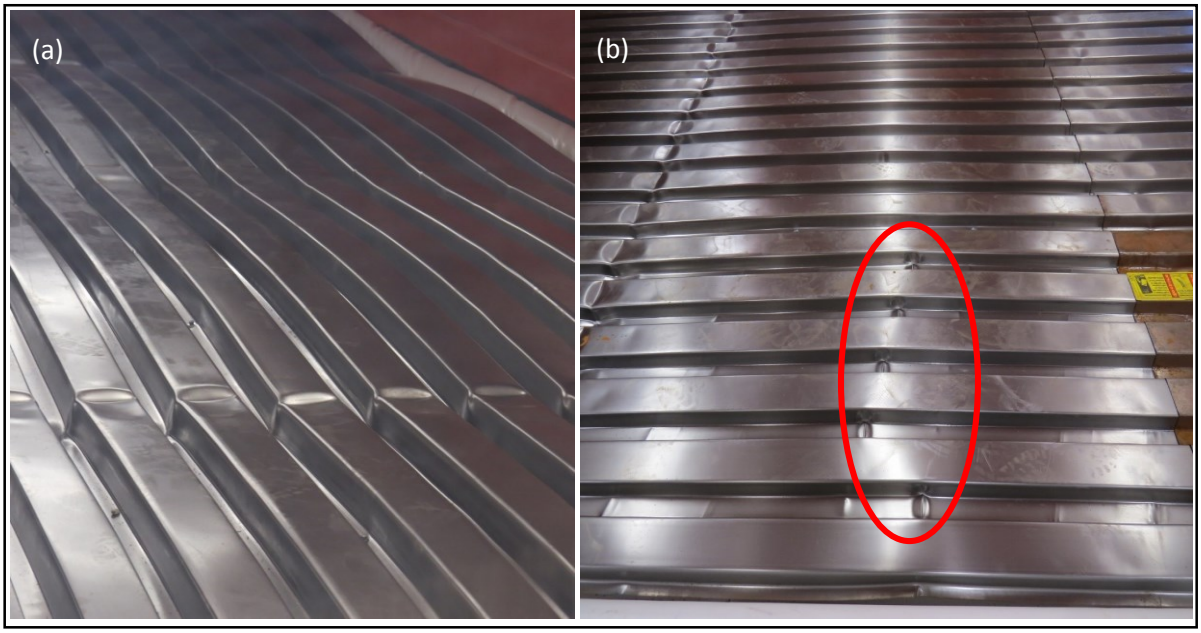

Figure 3.15 a) Steel deck failure (buckled), b) Detail of buckling failure between the fastener rows at 135 psf

3.3 **Fasteners Properties**

Different types of fasteners can be used in a roof system assembly, but they are divided into two main categories based on their attachment types [5]:

- Fasteners used for attaching the steel components to each other; e.g., attaching the steel deck to the joists.
- Fasteners used for attaching the non-steel components to the steel components, such as the membrane or insulation layers to the steel deck.

Based on steel deck and joist properties, as illustrated in Tables 3.2 and 3.3, the fastener model XLQ114B1224 (Fig. 3.16) of Simpson Strong-Tie company was used to attach the deck to the joists in the experiments.

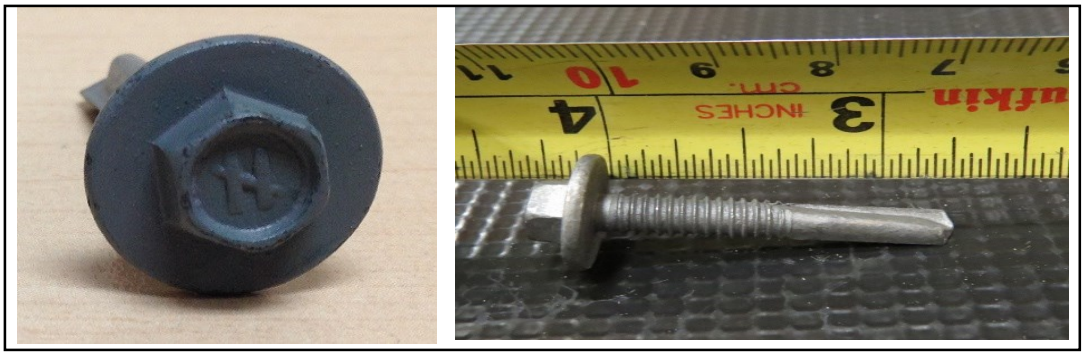

Figure 3.16 Steel deck fastener

Table 3.2 Steel deck properties [15]

Type	Nominal Thickness	Design Thickness	Overall Depth	Weight	Section Modulus		Moment of Inertia for Deflection
					M^+	M^-	
	mm (in.)	mm (in.)	mm (in.)	kg/m² (lb/ft²)	mm³ (in³)	mm³ (in³)	mm⁴ (in⁴)
22	0.76 (0.030)	0.762 (0.0300)	37.4 (1.47)	8.50 (1.74)	9 529 (0.1772)	10 081 (0.1875)	202 228 (0.1481)
20	0.91 (0.036)	0.909 (0.0358)	37.5 (1.48)	10.07 (2.06)	11 558 (0.2150)	12 005 (0.2233)	254 750 (0.1865)
18	1.21 (0.048)	1.217 (0.0479)	37.8 (1.49)	13.26 (2.72)	15 813 (0.2941)	15 994 (0.2975)	363 493 (0.2662)
16	1.52 (0.060)	1.511 (0.0595)	38.1 (1.50)	16.34 (3.35)	19 786 (0.3680)	19 786 (0.3680)	452 472 (0.3313)

• Effective properties are based on a unit width of 1 000 mm (S.I. units) or 12 in. (imperial units).
• Material according to ASTM A 653M SS Grade 230, yield strength of 230 MPa (33 ksi).

Table 3.3 Custom joist properties

Material	Module of Elasticity (kip/in^2)	F_y (ksi)	F_u (ksi)
Steel	29000	33	58

This type of fastener is a hand-drive screw and can be used for the following [5]:

• Steel decking to structural steel

• Steel stitching ("side-lap" stitching)

• Cold-formed steel framing

Some general features about this type of fastener are as follows [5]:

• 5/16" hex head

• Drill point

• Hand Drive

"These coated fasteners possess a level of corrosion resistance that makes them suitable for use in some exterior and corrosive environments and with some preservative-treated woods. For applications in higher-exposure applications, consider type-300 series stainless-steel fasteners for superior corrosion resistance" [5].

The Simpson Strong-Tie company could get the approval certificate from FM Approvals on 1/2912014, which means this type of fastener meets the approval requirements of FM Approvals for use as a component in Class 1-60, Class 1-75 and Class 1-90 wind uplift rated insulated steel deck roof constructions when installed as described in RoofNav [3]. Table 3.4 shows the usage of the fasteners for various wind class rates.

Table 3.4 Different spans and wind rates for steel deck fastener [19]

	Fastener O.C. Spacing, in.	Rating	Maximum Span															
			22 ga				20 ga				18 ga				16 ga			
			33 ksi		80 ksi		33 ksi		80 ksi		33 ksi		80 ksi		33 ksi		80 ksi	
			in	mm	in	mm	in	mm	in	mm	in	mm	in	mm	in	mm	in	mm
XLQ114B1224	6	60	338	8585	460	11684	411	10439	460	11684	460	11684	460	11684	460	11684	460	11684
		75	271	6883	368	9347	329	8357	368	9347	368	9347	368	9347	368	9347	368	9347
		90	225	5715	307	7798	274	6960	307	7798	307	7798	307	7798	307	7798	307	7798
	8	60	254	6452	345	8763	308	7823	345	8763	345	8763	345	8763	345	8763	345	8763
		75	203	5156	276	7010	246	6248	276	7010	276	7010	276	7010	276	7010	276	7010
		90	169	4293	230	5842	205	5207	230	5842	230	5842	230	5842	230	5842	230	5842
	12	60	169	4293	230	5842	205	5207	230	5842	230	5842	230	5842	230	5842	230	5842
		75	135	3429	184	4674	164	4166	184	4674	184	4674	184	4674	184	4674	184	4674
		90	112	2845	153	3886	137	3480	153	3886	153	3886	153	3886	153	3886	153	3886

It is not possible to use the same fastener to attach the non-steel components to the steel components; therefore, another type of fastener should be used to attach the membrane layer to the insulation and then to the steel deck of the roof system. In this experiment, the TRUFAST® #15 EHD roofing fastener is used. This type of fastener is used to attach roof components and wood substrates in the roof system. It is a #2 double flute self-drilling point and exclusive tapered entry thread design. Figure 3.17 shows the fastener's physical properties.

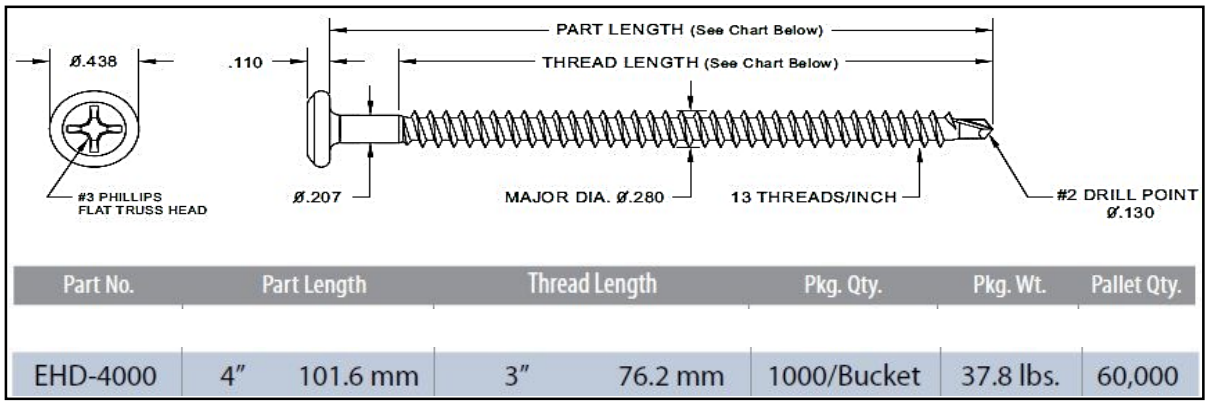

Part No.	Part Length		Thread Length		Pkg. Qty.	Pkg. Wt.	Pallet Qty.
EHD-4000	4″	101.6 mm	3″	76.2 mm	1000/Bucket	37.8 lbs.	60,000

Figure 3.17 Roof system fastener physical properties [19]

To install the fastener into the deck, a gun with 0-2500 rpm is required and the fastener must penetrate the steel deck at minimum of ¾ inch as measured from the underside of the deck to

the fastener tip. To prevent any damages to the membrane, it should be considered that the fasteners must be perpendicular to the deck and not to overdrive them. Table 3.5 shows the mechanical properties for this type of fastener.

Another fastener is used in the experiment to attach two steel sheets; this type of fastener is of the same model as the deck fastener but with different mechanical properties.

Table 3.5 Membrane fastener properties [19]

Property	Standard	Average Ultimate Value
Tensile Strength:	ASTM F606-10	4200 lbf.
Shear Strength:	NASM 1312-20	2400 lbf. (thread zone)
Corrosion Resistance:	FM 4470, DIN 50018	< 15% Red Rust after 30 cycles

Average Ultimate Pullout Values in Corrugated Steel Deck Substrates

Thickness	24 ga.	22 ga.			20 ga.			18 ga.			16 ga.		
Yield Strength	36.5 ksi	33.0 ksi	80.0 ksi	102.0 ksi	33.0 ksi	80.0 ksi	102.0 ksi	33.0 ksi	80.0 ksi	102.0 ksi	33.0 ksi	80.0 ksi	102.0 ksi
Pullout (lbf.)	390	465	695	805	605	855	970	925	1125	1215	1175	1370	1460

3.4 **Instrumentation and Data Collection**

This section comprises two parts: i) instrumentation for measuring the deflection; and ii) instrumentation used for measuring the forces. For the deflection measuring instrumentation, types of lasers and their locations are discussed after which the results from the laser's sensors are explained. In the second part, the compact 6-component force transducer (6-component load cell), its installation and converting its output signal to forces was described. The deflection results measured during the experiments at the mid-span and the forces measured by the 6-comnponent load cell were used for validating the FE model of the steel deck.

3.4.1 **Deflection-measuring instrumentation**

One of the important criteria in the recently published FM standard is the allowable deflection at the middle of the spans of the roof steel deck. Therefore, laser sensors have an important role to provide accurate measurements. In this research, three Keyence lasers are used at two different locations. After mounting the lasers, these are connected to the data logger and the main computers for data-acquisition purposes.

3.4.1.1 **Laser Sensors**

One of the two middle spans of the roof steel deck was instrumented by the aid of several laser sensors, to measure the deflection in three points of the tested specimens as follows:

- LKG-407 laser sensor was used at the middle of the joist
- Two LKG-507 laser sensors were used at ½ and ¼ length of the steel deck span

Figure 3.18 a) shows laser locations, installed between the axes E and F in the middle of the span. The Keyence lasers are very sensitive and accurate sensors. A total of three laser sensors were used, two of them at half and quarter span of the steel deck in the middle of the testing chamber, and one sensor was placed at the middle of the transversal joist, which supports the steel deck as shown in Figure 3.18 b).

All three lasers were installed underneath the deck, because installing them inside the pressurised chamber would not be doable; moreover, measuring the deflections of the steel deck and joists is the aim of the current project.

The data read by the lasers was transferred to a controller, and by connecting the controller to the NRC lab computer the final results were obtained.

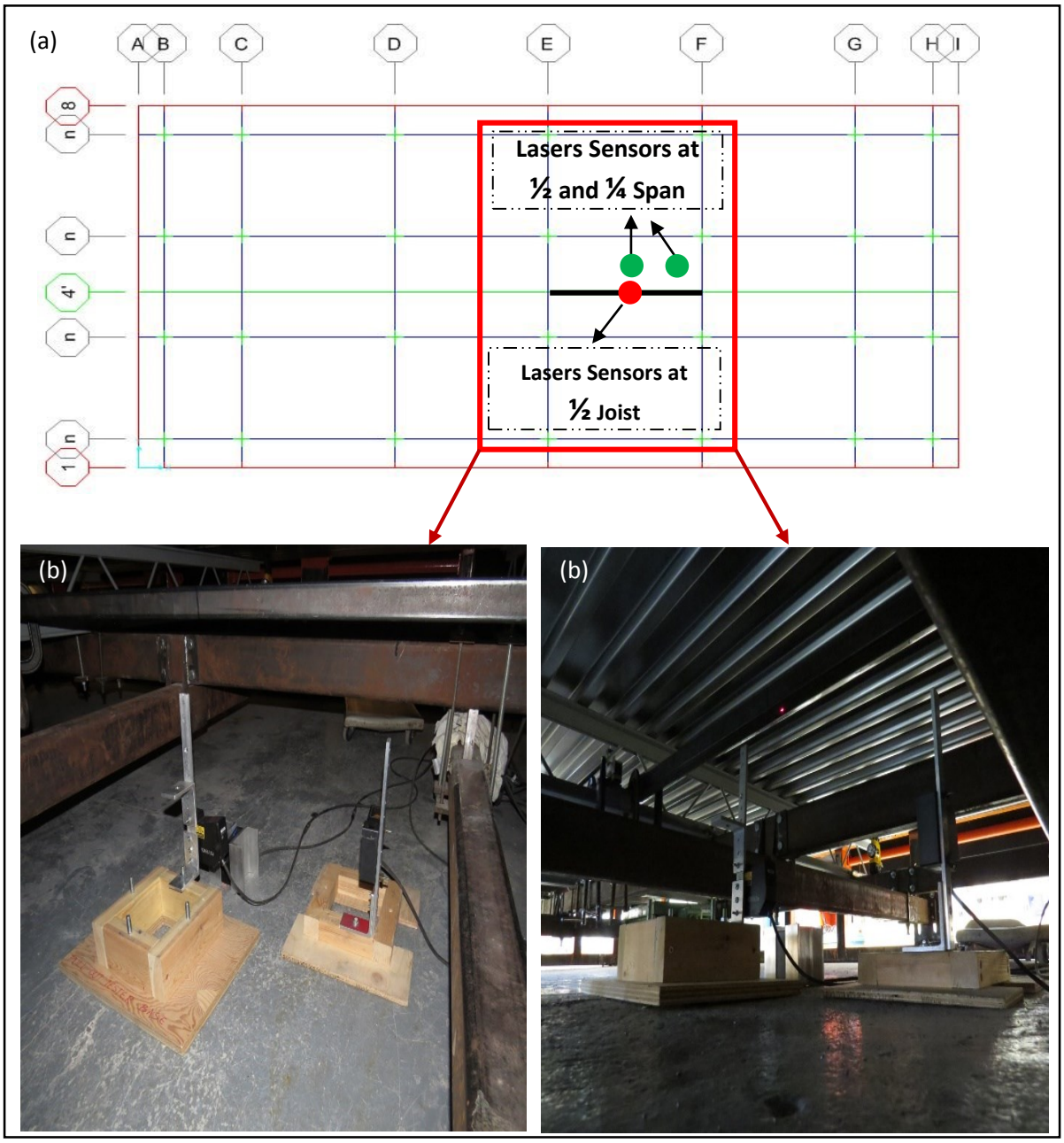

Figure 3.18 a) Schematic of the testing chamber and the laser locations, b) Installation detail of the lasers mounted underneath the steel deck and joists

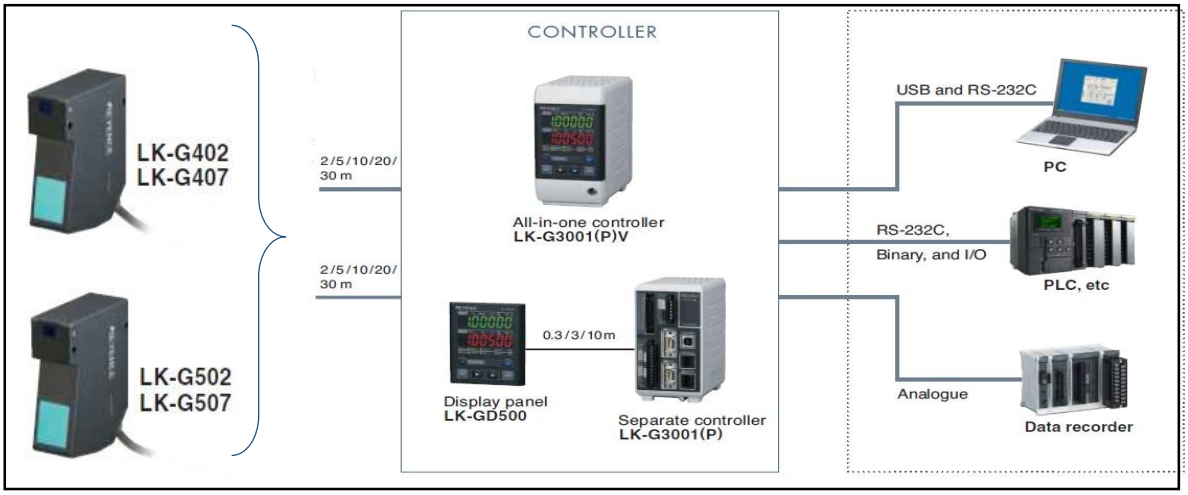

Figure 3.19 Laser output connection [20]

As shown in Figure 3.18, for joist deflection a strap was used, which is located in the middle of joists E and F. Then, one laser of LKG-407 series was placed in the middle of the strap. This model is used for measuring deflections at small distances of up to 500 mm, when compared to the LKG-507 model, which can measure signals up to 100 mm (Fig. 3.20).

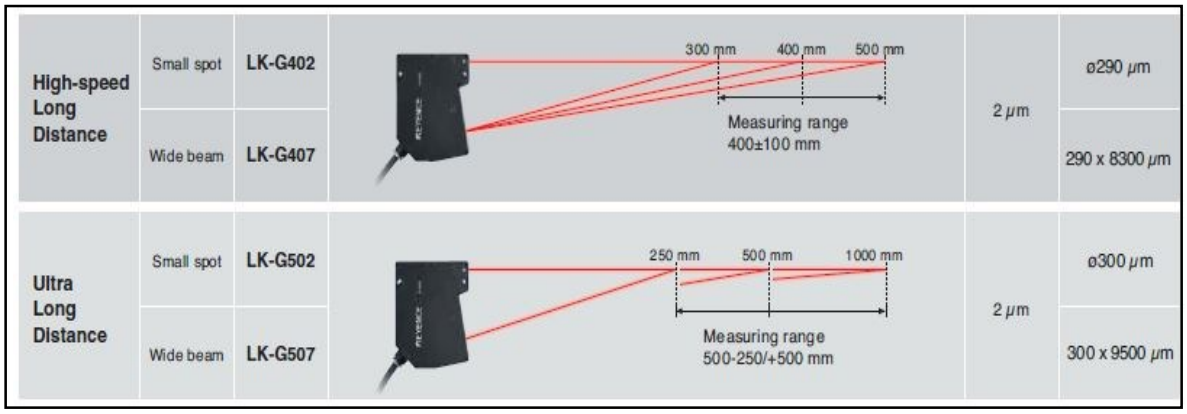

Figure 3.20 Keyence laser specifications [20]

The Keyence lasers have a new advanced technology for measurement as described in Figure 3.21. This technology has the following parts [20]:

- ABLE control technology

- Li-CCD, which reduces errors in pixel edges to improve accuracy
- HIGH-ACCURACY LENS UNIT, that reduces errors caused by irregular measurements
- DELTA CUT TECHNOLOGY, that accurately receipts the reflected laser beam from a long distance

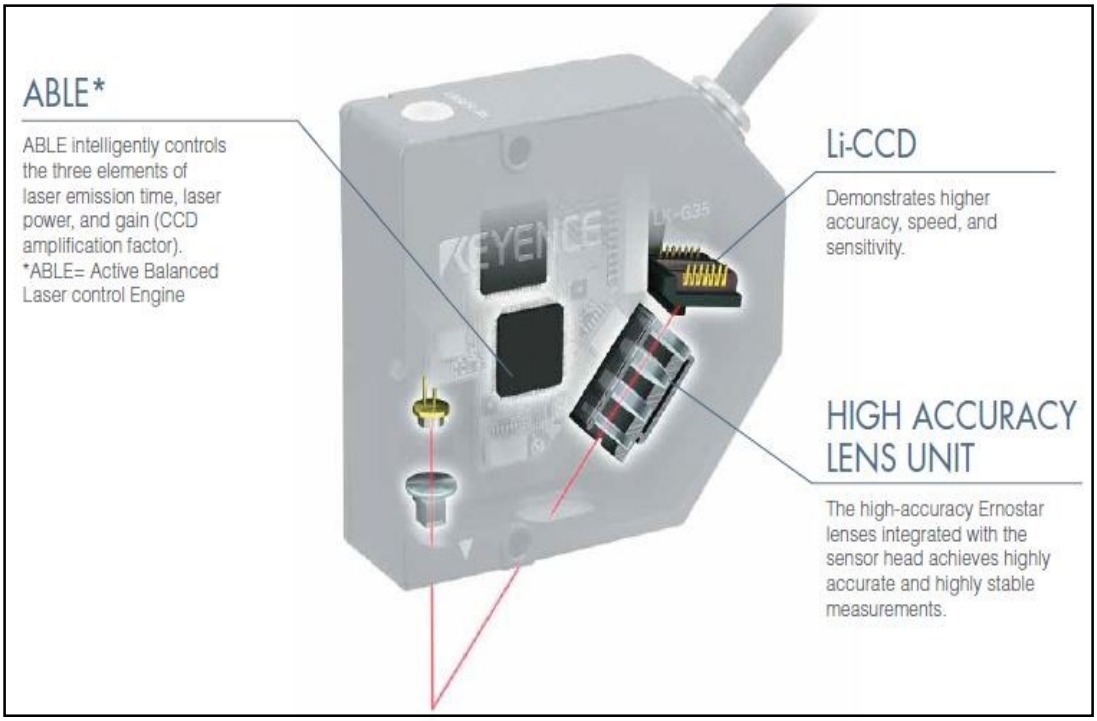

Figure 3.21 Advanced technology for high performance in Keyence lasers [20]

3.4.1.2 **Laser Data Interpretation**

The duration of the load cycles under the designated wind uplift pressure for all the tested cases had a continuous duration of one minute. In the calculation, to reduce the errors of the system that effected on the results, only the middle 30 seconds were considered, instead of the entire 60-second interval. Moreover, at the end of the one-minute period, before the roof

assembly was completely unloaded, the system applied more pressure than the initial designated wind pressure to prevent any damages to the suction engine of the fan.

For a better understanding of the deflection calculation procedure, the deflection variation with time registered for the second load cycle applied to the steel deck case, of 45 psf wind pressure was applied, is detailed in Figure 3.22 below.

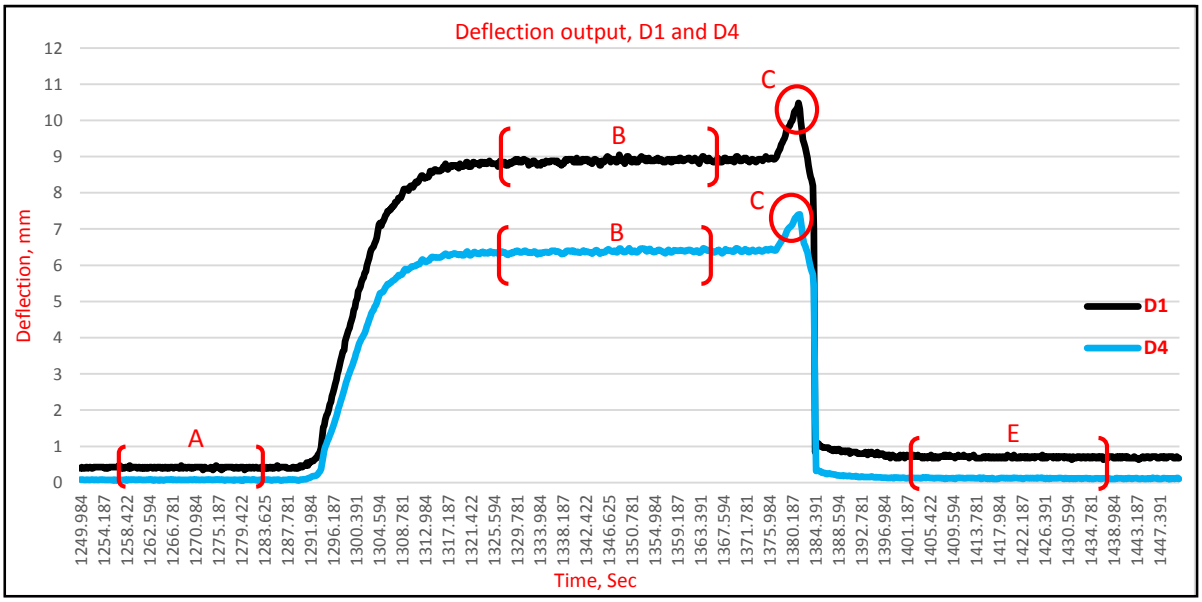

Figure 3.22 Steel deck deflection (D1, D4) procedure under 45psf

This graph (Fig. 3.22) represents the deflection registered for different parts of the tested sample, as described below:

- D_1 represents the steel deck deflection and D_4 represents the joist deflection.
- Part A is used to calculate the permanent residual deformation that remains after the previous loading cycle, and it should be subtracted from the main deflection of the current cycle (D_{1A}-D_{4A}). To estimate the A interval for measuring the residual deflection from the previous loading cycle, a time period of at least 60 seconds was considered before starting the new loading cycle.

- Similarly part B of the measured deflection is only the middle 30 seconds out of the entire loading time of 60 seconds.
- The spike represented by part C is the temporary deflection caused by a higher wind rate pressure encountered before stopping the test, due to the equipment operation stage.
- Part E is the permanent deformation remaining after the current cycle, which should be considered when determining the deflection for the next loading cycle.
- To calculate the deflection for one specific loading cycle, the three data columns recorded by the laser devices are needed: the time, D1 (the steel deck deflection) and D4 (the joist deflection). Table 3.6 shows an example of the laser output for the first seconds of the loading cycle as described above.

Table 3.6 Laser output data

Time	MKS	P2	P3	P4	P5	P6	P7	LFE	D1	D2	D3	D4	LFE-Flow
[s]	[psf]	[psf]	[psf]	[psf]	[psf]	[psf]	[psf]	[inch-wc]	[inch]	[inch]	[inch]	[inch]	[cfm]
Test	Started	At:	########	9:17:11									
0	-0.0045	0	0	0	0	0	0	0	0.0614	-0.0299	-0.013	-0.0063	0
0.234	-0.0045	0	0	0	0	0	0	-0.0025	0.0239	-0.0674	-0.013	-0.0063	-0.0002
0.422	-0.0045	0	0	0	0	0	0	-0.0025	0.1064	-0.0299	-0.013	-0.0063	-0.0002
0.641	-0.0045	0	0	0	0	0	0	-0.0025	0.0239	-0.0299	-0.058	-0.0183	-0.0002
0.828	0.0123	0	0	0	0	0	0	0	0.0614	-0.0299	-0.058	-0.0063	0
1.031	-0.0045	0	0	0	0	0	0	0	0.0239	-0.0299	-0.058	-0.0063	0
1.203	-0.0045	0	0	0	0	0	0	0	0.0239	-0.0299	-0.013	-0.0183	0
1.422	-0.0184	0	0	0	0	0	0	0	0.0239	-0.0674	-0.013	-0.0283	0
1.625	-0.0045	0	0	0	0	0	0	0	0.0614	-0.0299	-0.058	-0.0063	0
1.828	-0.0045	0	0	0	0	0	0	-0.0025	0.0239	-0.0299	-0.058	-0.0183	-0.0002
2	-0.0045	0	0	0	0	0	0	-0.0025	0.0239	-0.0299	-0.013	-0.0063	-0.0002
2.203	-0.0045	0	0	0	0	0	0	-0.0025	0.0614	-0.0674	-0.013	-0.0183	-0.0002
2.422	-0.0045	0	0	0	0	0	0	0	0.0239	-0.0674	0.0245	-0.0183	0

The net deflection for each loading cycle was calculated by subtracting the joist deflection from the steel deck span deflection. Then, the permanent deformation should be deducted to get the net deflection value. The calculation example for the net deflection of the steel deck (case no. 4) tested under the second loading cycle of 45 psf (as per Fig. 3.22), is provided below. In equation 3-1 to 3-4, D_n is the net deflection, D_c is the maximum cycle deflection

(the maximum deflection in the middle 30 seconds of the cycle) and D_p is the maximum permanent deformation. D_c is the difference between D_1 and D_4 in part B in Figure 3.22, and D_p is the difference between D_1 and D_4 in part A of the same figure.

$$D_n = D_c - D_p \quad (3\text{-}1)$$

$$D_c = (D_{1B}-D_{4B}) = 8.93 - 6.39 = 2.54 \text{ mm} \quad (3\text{-}2)$$

$$D_p = (D_{1A}-D_{4A}) = 0.7097 - 0.0697 = 0.64 \text{ mm} \quad (3\text{-}3)$$

$$D_n = 2.54 - 0.64 = 1.90 \text{ mm} \quad (3\text{-}4)$$

Therefore, the net deflection for this loading cycle was 1.9 mm and the same procedure was applied for all the rest of loading cycles to calculate the final deflection of the tested cases.

3.4.2 **Forces measuring instrumentation**

3.4.2.1 **Compact 6-component Force Transducer (6-component load cell)**

The 6-load cell is used in the current experiment to obtain a better understanding of the roof assembly behaviour under wind uplift pressure, especially at the attachment points between joist and steel deck sheets. By applying pressure on the roof, the induced force tends to uplift the roof, which causes the creation of resistance forces at the attachment points or on the deck fasteners. The 6-load cell is attached to the joist through a fastener that penetrates the steel deck and the joist, and connects directly into the 6-load cell (Figure 3.23). When pressure is applied based on the changes in the primary voltage, the forces and moments are calculated in the three main directions (X, Y, Z) [21]. Figure 3.23 shows different parts of the 6-load cell.

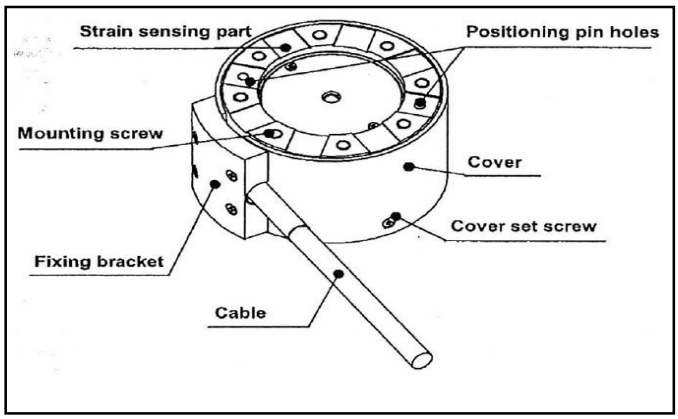

Figure 3.23 6-component load cell different parts [21]

Setting the axis direction is one of the most important points that should be taken into account during the installation of the 6-component load cell. By using the positioning pin holes as reference, the force direction can be determined. To do this, the 2-pin holes should be connected on one side of the 6-component load cell to provide the X-axis, and the fixing bracket side should be specified as the positive direction. Consequently, the side where the cover set screws are located becomes the negative direction [21]. Figures 3.24 a) and b) show the determination of the force direction. A custom solid base is made for the 6-load cell so this should be rigidly connected at its base, thus very stable.

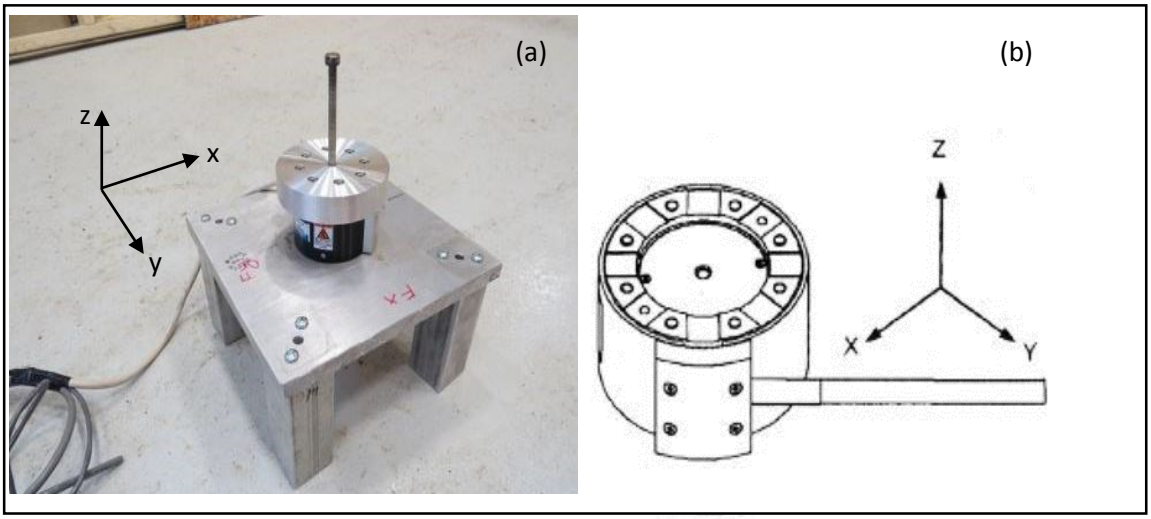

Figure 3.24 Determination of forces in the 6-component load cell: (a) experiment, (b) load cell manual [21]

In the experiment, the X axis is parallel to the length of the testing chamber, the Y axis is parallel to the width of the chamber and the Z direction is perpendicular to both axes X and Y. The 6-component load cell is very sensitive and is designed based on three reference axes coordinates. This means if the 6-component load cell is not perfectly aligned with the designated coordinate, the measured values may have a margin of error. For instance, if there is a 1-degree misalignment around the Z axis, the generated error is approximately 1.7% in the component forces F_X and F_Y Consequently, the 6-load cell must be installed in the proper position with much accuracy [21].

3.4.2.2 **Instrumentation Installation**

Due to sensitivity of the 6-component load cell before installing it to the system, the following should be noted [21]:

- The load exceeding more than the safe overload could lead to drastic damage of the 6-component load cell.
- It is really important that the contact surface of the target be as flat as possible. An uneven contact surface may affect the characteristics of the 6-component load cell. Therefore, to prevent this failure, it is recommended that the flat contact surface be adjusted to 0.01 mm or less, in the both inner and outer diameters (Figure 3.25).

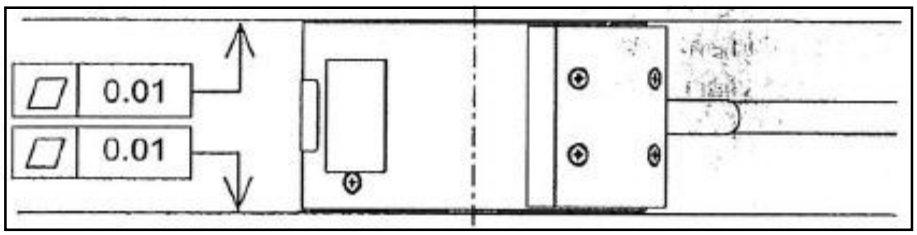

Figure 3.25 Mounting the 6-component load cell to surface of the target system [21]

- Because the materials of the target surface and the 6-component load cell are not the same, differences between the thermal expansions coefficients should be considered; therefore, the temperature was maintained constant at the time of installation and when the experiment was performed.

As shown in Figure 3.26, the 6-load cell was mounted on a steel flat plate with four stands to make installation on the joist possible. After choosing the right place for installation, the positioning pin holes were used to determine the force-detecting direction. Then, two parallel pins were installed on each side of the 6-component load cell and tightened with 8 hexagonal socket head bolts. As mentioned previously, the 6-component load cell should be connected to the joist to calculate the induced forces on the deck fasteners. To do this, one fastener needed to be replaced at the location of the 6-component load cell with a custom fastener as follows:

1. Remove a deck fastener and replace it with a load cell rod.

2. Drill a hole of $^{3}/_{8}''$ diameter, through the deck and steel joist.

3. Replace the deck fastener with a $^{1}/_{4}''$ fastener rod and insert the rod through the hole.

4. Attach the load cell to the fastener rod.

5. During alignment, the rod should move freely. Then, attach the load cell bracket to the bottom angles on the steel bars.

6. Regarding stability and rigidity of the 6-component load cell, a new bracket for its attachment was made as shown in Figure 3.26.

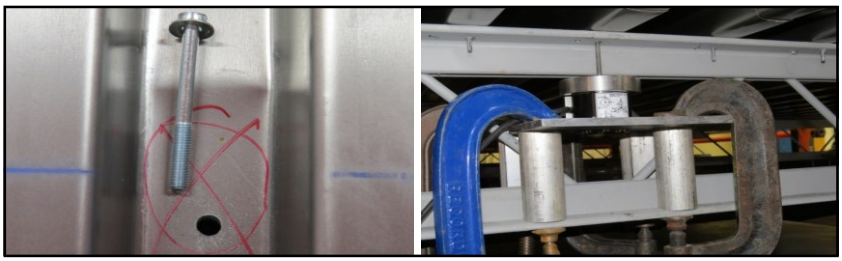

Figure 3.26 Installation of the 6-component load cell with the custom fastener

The 6-component load cell was attached on the joist in axis-E and axis-4′, as illustrated in Figure 3.27.

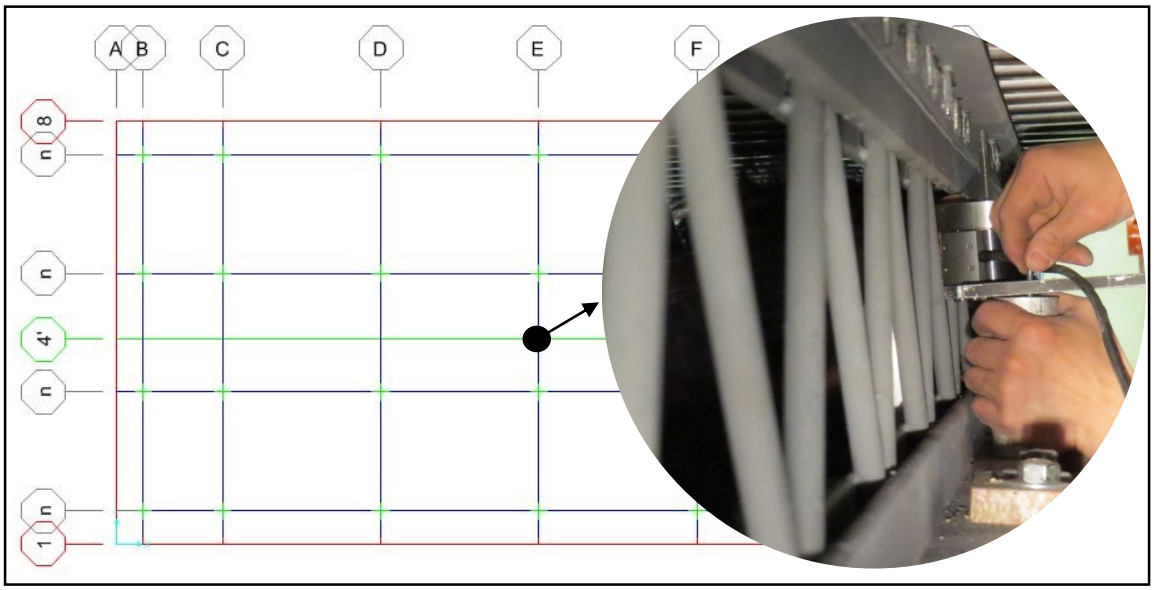

Figure 3.27 Location of the 6-component load cell

3.4.2.3 **Compact 6-component Transducer Force Output**

The outputs of the 6-component load cell comprise VFx to VFz and VMx to VMz, and are measured by taking special care of the excitation voltage, which means that by applying a designated pressure, the voltage increases, and based on interference correction the outputs are calculated. The final physical values (Fx to Fy and Mx to My) can be obtained by using the calculated outputs in a calibration constant matrix as shown in Figure 3.28.

$$\begin{pmatrix} FX \\ FY \\ FZ \\ MX \\ MY \\ MZ \end{pmatrix} = \begin{pmatrix} \text{Calibration} \\ \text{constant matrix} \\ 6 \times 6 \text{ matrix} \end{pmatrix} \begin{pmatrix} VFX \\ VFY \\ VFZ \\ VMX \\ VMY \\ VMZ \end{pmatrix}$$

Figure 3.28 Calibration matrix [21]

Figure 3.29 shows different models of 6-component load cell based on their load capacity. Therefore, in the calibration constant matrix, inputting the proper values based on the model used is required.

Model	Top: Rated capacity, Bottom: Rated output			Frequency response
	FX, FY, and FZ	MX and MY	MZ	
LFX-A-1KN	1 kN	40 N·m	25 N·m	500 Hz
	Approx. ±1500 mV (With output voltage at no load as reference)			
LFX-A-3KN	3 kN	100 N·m	50 N·m	500 Hz
	Approx. ±1500 mV (With output voltage at no load as reference)			

	aFx	aFy	aFz	aMx	aMy	aMz
Fx	1.9211	-0.0084	0.0122	-0.0112	0.6510	-0.0079
Fy	-0.0066	1.9217	-0.0084	-0.6767	-0.0376	-0.0028
Fz	0.0150	0.0051	2.0028	-0.0022	-0.0110	0.0022
Mx	0.0000	0.0074	0.0002	0.0640	-0.0002	-0.0002
My	-0.0075	-0.0001	-0.0001	0.0000	0.0641	0.0000
Mz	-0.0001	0.0004	0.0003	-0.0003	0.0005	0.0335

Figure 3.29 Calibration constant matrix for the selected model [21]

More details of the force calculation are presented in the results chapter. Figure 3.30 shows the force directions calculated by the 6-component load cell, when the bottom side is fixed.

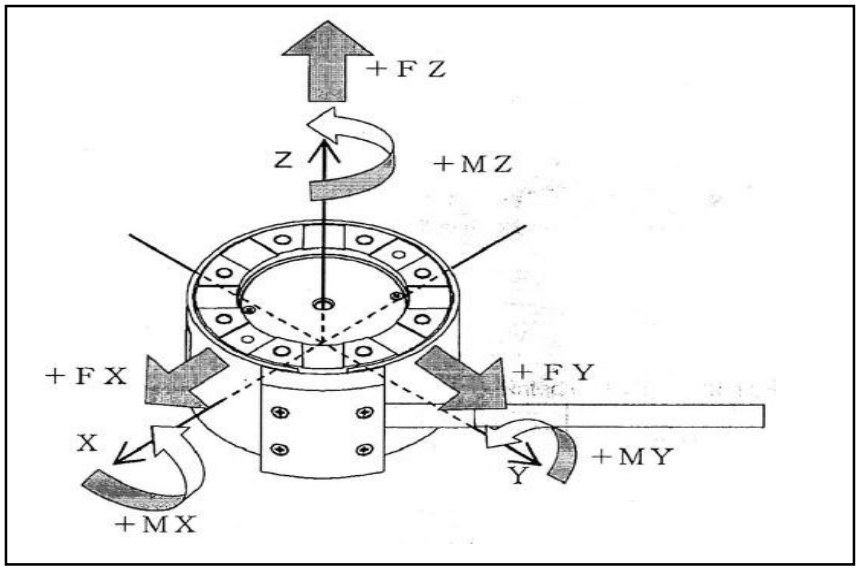

Figure 3.30 Loads and moments convention for the 6-componentload cell [21]

To use the 6-component load cell output, some modifications and conversions are needed. Therefore, an Excel file is used to convert the voltage from the data sheets to the real forces. Table 3.7 shows the 6-component load cell data report at the beginning of the loading cycle for Fz in the steel deck case. Only the values for the one-minute period when roof assembly was under the wind pressure were used.

Table 3.7 6-component load cell output report at the beginning of loading

6	Compone	Load	Cell	Calibratio	data	collected	on	21	Feb	2014		
Time	Fx	Fy	Fz	Mx	My	Mz	Fx2	Fy2	Fz2	Mx2	My2	Mz2
9:10:46	2528.32	2431.396	2467.407	2503.296	2500.366	2495.85	2490.967	2536.621	2456.421	2486.938	2484.741	2516.113
9:10:47	2528.931	2431.519	2466.309	2503.662	2501.099	2496.094	2490.601	2536.987	2455.811	2487.427	2484.741	2516.113
9:10:48	2529.053	2431.519	2466.675	2503.906	2501.221	2496.338	2491.211	2536.865	2456.055	2487.671	2484.741	2515.991
9:10:49	2529.053	2431.519	2466.675	2503.906	2501.221	2496.338	2491.821	2537.354	2345.093	2341.919	2323.73	2337.158
9:10:50	2529.053	2431.519	2466.675	2503.906	2501.221	2496.338	2491.943	2369.263	2293.823	2335.938	2484.375	2347.656
9:10:51	2528.687	2431.396	2307.861	2333.008	2324.341	2334.839	2491.211	2401.489	2375.854	2394.165	2484.009	2408.936
9:10:52	2528.687	2431.396	2467.529	2503.906	2500.732	2496.094	2490.356	2536.499	2457.397	2487.305	2484.863	2516.113
9:10:53	2528.442	2431.152	2467.651	2503.418	2500.488	2495.85	2490.723	2536.499	2457.153	2487.183	2484.741	2516.113
9:10:54	2528.442	2431.152	2467.651	2503.418	2500.488	2495.85	2491.089	2536.377	2456.421	2486.816	2484.619	2515.991

The important data columns used to calculate final forces are as follows (Table 3.7): Time, F_x, F_y, F_z, M_x, M_y and M_z. Each column shows different voltages based on different forces in three directions. These forces were applied to the custom fastener under the loaded cycle.

The Excel file consists of different parts as shown in Figure 3.31 that sampled for the steel deck case, under 60 psf wind pressure.

Wind pressure: applied wind pressure in each cycle of test

No load results (initial input): before starting the loaded cycle, the initial voltage was applied to the 6-component load cell. Therefore, when the cycle was started, voltage changes led to calculating the forces. Figure 3.32 shows how voltage was altered for Fz in the steel deck case.

As it can be seen, the voltage dropped sometimes because of measurement errors (part A). Thus, these drops in voltages should not be considered in the calculation of the initial average voltage.

								Calibration constant matrix (Type LFX-A-3kN, Product No. FM5650001					
									aFx	aFy	aFz	aMx	aMy	aMz
								Fx	1.9211	-0.0084	0.0122	-0.0112	0.6510	-0.0079
								Fy	-0.0066	1.9217	-0.0084	-0.6767	-0.0376	-0.0028
								Fz	0.0150	0.0051	2.0028	-0.0022	-0.0110	0.0022
								Mx	0.0000	0.0074	0.0002	0.0640	-0.0002	-0.0002
Wind pressure :	60 psf							My	-0.0075	-0.0001	-0.0001	0.0000	0.0641	0.0000
	2873 Pa							Mz	-0.0001	0.0004	0.0003	-0.0003	0.0005	0.0335
No load results (Voltage)								Second Load results (Engineering value)						
CH	Fx	Fy	Fz	Mx	My	Mz		Direction	Fx	Fy	Fz	Mx	My	Mz
Initial data	2521.118	2427.856	2675.486	2501.099	2485.352	2492.188		Unit	N	N	N	N・m	N・m	N・m
								Max.	50.08	15.82	683.84	5.36	5.58	2.07
L=	0.0635 m							Min.	-3.37	0.00	0.00	-10.85	-9.61	-5.20
								Unit	lb	lb	lb	lb.in	lb.in	lb.in
								Max.	11.25	3.56	153.67	47.45	49.40	18.34
								Min.	-0.76	0.00	0.00	-96.06	-85.06	-46.04
Load results (Voltage)								First Load results (Engineering value)						
CH	Fx	Fy	Fz	Mx	My	Mz		Direction	Fx	Fy	Fz	Mx	My	Mz
No	mV	mV	mV	mV	mV	mV		Unit	N	N	N	N・m	N・m	N・m
1	2509.888	2432.495	2970.215	2482.056	2432.983	2402.1		1			590.56	-1.09	-3.32	-2.95
2	2513.794	2427.246	2975.83	2486.572	2499.634	2486.816		2	-0.91	5.65	601.28	-0.87	0.93	-0.08
3	2514.038	2428.589	2973.267	2488.281	2501.831	2487.305		3	0.92	7.01	596.13	-0.75	1.07	-0.06
4	2512.817	2428.467	2967.529	2486.328	2500.488	2489.014		4	-2.36	8.20	584.65	-0.88	0.99	-0.01
5	2513.184	2428.955	2967.041	2485.962	2500.244	2488.037		5	-1.81	9.40	583.68	-0.90	0.97	-0.04
6	2512.939	2428.955	2963.989	2485.352	2500.732	2486.206		6	-1.98	9.83	577.55	-0.94	1.01	-0.10
7	2513.794	2428.467	2972.168	2486.694	2500.488	2487.671		7	-0.42	7.91	593.95	-0.86	0.98	-0.05
8	2514.16	2429.077	2969.482	2486.328	2502.319	2486.45		8	1.45	9.28	588.56	-0.88	1.10	-0.09
9	2514.16	2429.932	2969.482	2486.328	2373.169	2486.45		9		15.78	589.98	-0.84	-7.19	-0.15

Figure 3.31 Conversion Excel file

L (m) = It is the length of the custom fastener from its head until the point that attaches to the 6-load cell.

Load result (voltage): The voltages are recorded during the running one-minute test. After deduction of initial voltages (each force has its own initial voltage), they are inserted into the conversion matrix of the 6-component load cell as described in the last part.

Calibration Constant Matrix: Based on the 6-component load cell model, the appropriate calibration values are selected and inserted in the calculation of forces.

First load results (Engineering Value): These are the conversion values from the calibration matrix. As expected, for each recorded voltage in the load result part, there is a converted value in this table due to the SI – Imperial unit systems conversion.

It should be noted that, during running tests, some errors occur in the system as it can be seen in Figure 3.32 part B; therefore, these values must be deleted manually from the table in order to have an accurate result in the second load results.

Second Load Results (Engineering Value): This table is created based on the maximum and minimum values of each force column from the first load value table. It comprised two different units. The maximum values in this table must be considered.

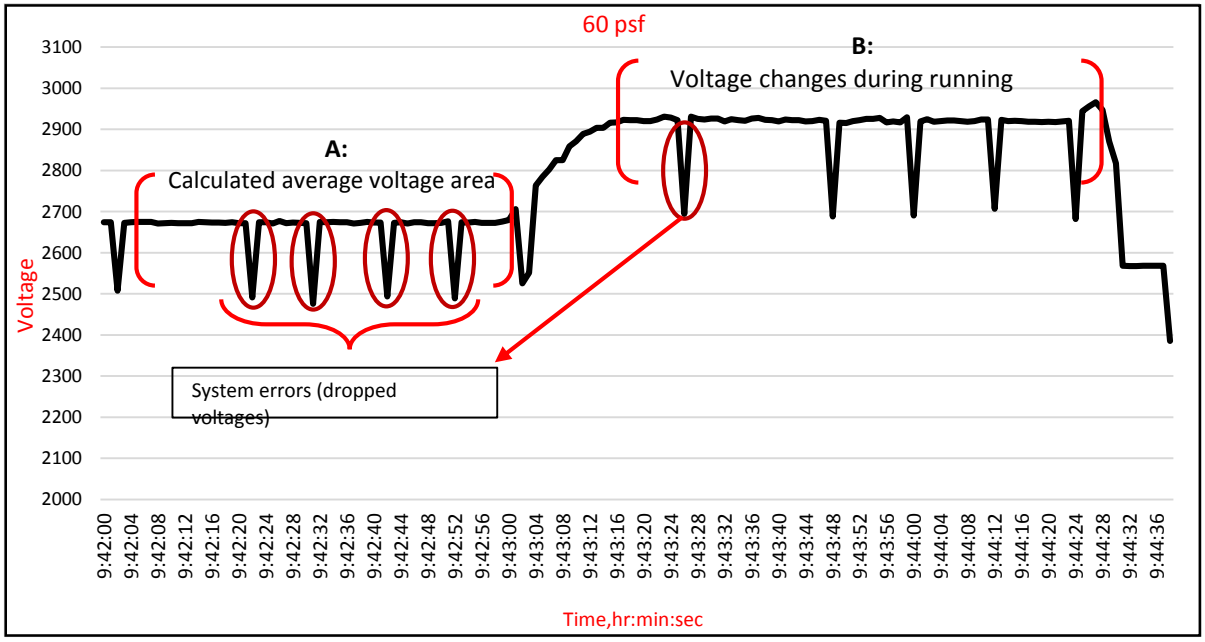

Figure 3.32 Calculation average voltage for F_z under 60 psf wind pressure in the steel deck case

To better visualize the results obtained by the 6-component load cell, the final forces recorded for the steel case under the second loading cycle are shown in Figure 3.33. These are provided for exemplification purposes; however, complete discussions and explanations about the

forces registered for the entire experiment are presented in the results Chapter 5.

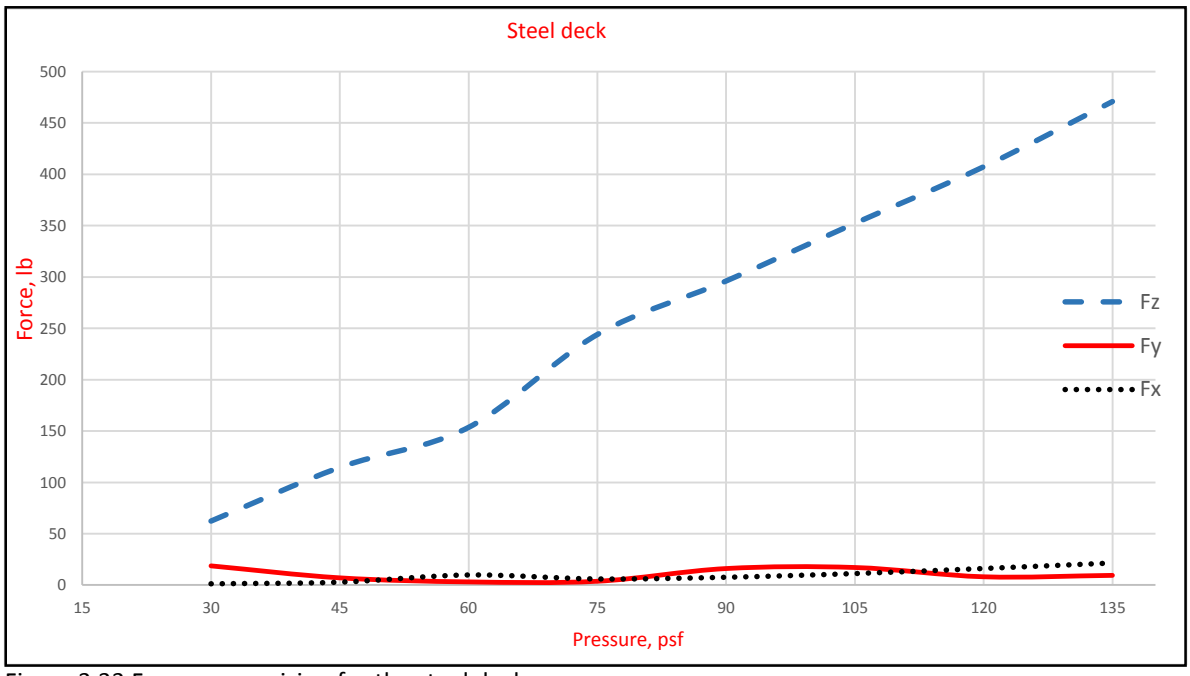

Figure 3.33 Force comparision for the steel deck case

Chapter 4 **Finite Element Modelling**

4.1 **Introduction**

To update the FM design tables, an extensive number of experiments is required; however, with the aid of a properly calibrated Finite Element Model, which can take into account the wind uplift pressure conditions, re-calculating most of the wind rating cases presented in the FM design tables is achievable. In the current study, the commercial finite element software SAP2000 was used to simulate the experimental conditions and to achieve an accurate numerical model to be used for extending the FM design tables. Appendix A includes a sample of the output data provided by the software analysis upon performing each simulation case. The actual model is comprised of different structural elements: two types of beams used for simulating the adequate support for holding the joists, on top of which the steel deck is located, the shell element representing the steel deck and the trusses accounting for the actual joists used in the experiment. Therefore, the numerical model used in this study provided the major structural elements used in the experiment, and also represent the actual roof assembly though they omit inessential details that can increase the analysis effort. An accurate geometry of the fasteners, for example, not only expands the analysis but also may cause some errors in final results. Thus, some minor details such as geometry type of the fasteners or of the steel deck sheet profiles were approximated with equivalent simplified elements with similar properties. The shell elements used in the current model had sharing nodes in most parts of the steel deck and also contained some disconnected nodes, predefined in SAP, for showing two different steel sheets. To represent the joists with diagonal elements, continuous frames were used as the second type of truss elements. The FEM was created based on the dimensions and

configuration of the experimental chamber at NRC, as described in Chapter 3. Figure 4.1 shows the layout and different parts of the chamber and joists that were used for the current experiments. Accounting for the same structural components, the bottom of Figure 4.1 shows the truss elements used to create the FEM. As it can be seen, two clips on each side of the joists were used at four points to attach them to the beams. The restrained type of boundary condition was chosen in the SAP to model fixed supports corresponding to this type of connection.

Figure 4.1 Geometry of the actual experimental sample in SAP2000

4.2 **Elements**

Different structural analysis software are used to represent the FEM, and based on the type of analysis and the results sought, the proper finite element software is chosen. Therefore, each software provides different types of elements that can be used to simplify and adequately represent a structural system, with the aim of replicating the structural behaviour of the real sample of the same structure.

In SAP2000, in reference to our study, two different types of elements are used:

- ✓ Shell elements, for representing the roof assembly layers such as steel deck, insulation and membrane; therefore, based on their structural behaviour, proper shell type element was used (Figure 4.2).
- ✓ Frame elements that were used for the joists and truss element was used for fasteners

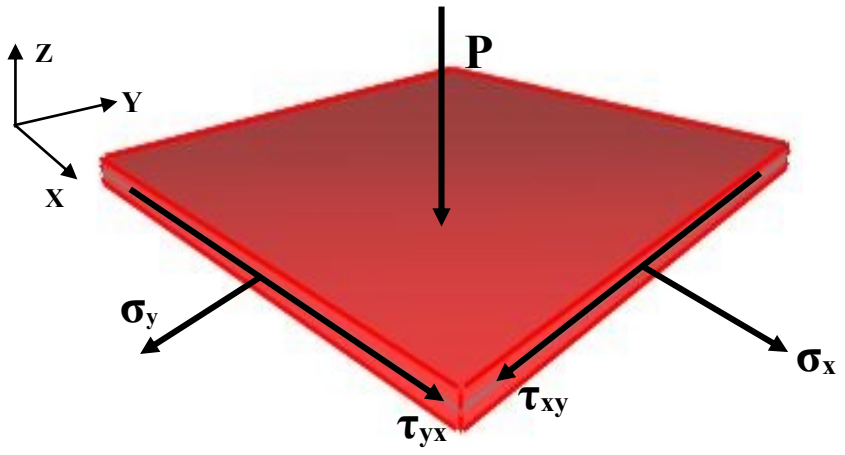

Figure 4.2 Internal stresses of shell element

The SAP2000 structural software has three types predefined for the basic elements for section-area modeling procedures [22]:

1. *Shell:* This element has three translational and three rotational degrees of freedom. It also supports forces and moments.
2. *Plane:* This is a two-dimensional solid element with three translational degrees of freedom that support forces but not moment (stress or strain).
3. *Asolid (axisymmetric solid):* This element is used for symmetrical elements with a translational degree of freedom and as a plane it is capable of forces only.

The shell elements were chosen to represent these three section area elements in SAP2000, based on the different types of section area properties and dimensions, and based on the overall behaviour of the roofing system, which consists of the steel deck, insulation layer and membrane [22]. The shell elements are comprised of four-node rectangular shapes, with six degrees of freedom for each node. As shown in Figure 4.3, shell elements are used for modelling the structural components that have a significantly large longitudinal dimension in comparison to their thickness dimension [22].

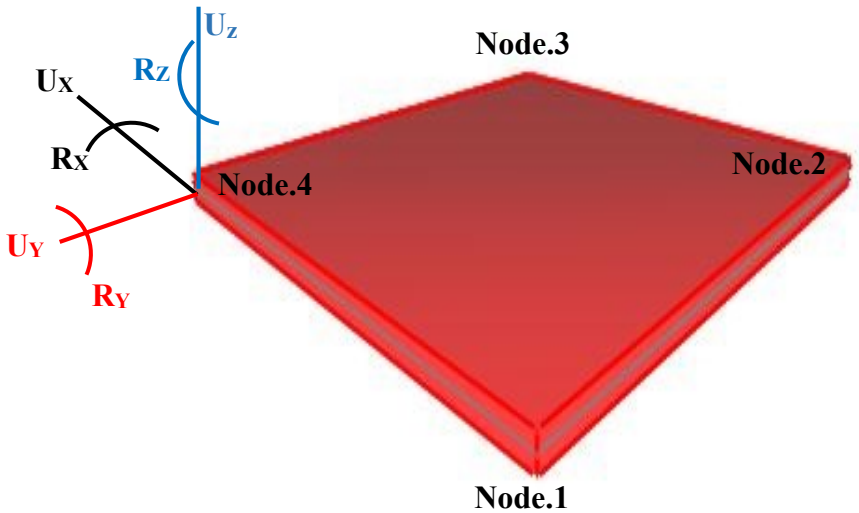

Figure 4.3 Six degree of freedom for each node for shell element in SAP2000

The focus of this study is to determine the behaviour of the steel deck under wind-induced pressures; therefore, a proper shell section type must be chosen. In SAP2000, various types of shell sections are described based on the element behaviour [22]. In the experiments, roof system test samples consisted of three main layers that are attached together with fasteners. However, it is not suitable to consider it as shell-layered elements, because the roofing system tested was mechanically fastened and no adhesive was used between the layers, thus the layers were just placed on top of each other, without further conditions at the interface, while for a structural shell-layered element, there must be an interaction between the elements of the layered system [22]. Therefore in SAP2000, the plate element was chosen instead of the shell-layered element. Based on the plate element description provided by the software [22, 23] and considering the parameters of interest in this research, which are bending moments and transverse forces, shell-plate elements were chosen [23]:

- Shell-plate elements

– It must have the pure plate behaviour

– It supports only the bending moments and the transverse forces

– It follows thick and thin plate formulation

– It must have a linear and homogeneous material

After choosing the appropriate modelling element, the correct values for the thickness of the plate need to be inputted to have an accurate analysis and response. In SAP2000, shell-plate-thin and shell-plate-thick elements represent whether transverse shearing deformation is considered in elements' behaviour or not. To do this, the software considers two different thickness formulations [22, 23]:

- Mindlin/Reissner formulation for thick plate, which calculates the effects of transverse deformation
- Kirchhoff formulation for thin plate, which neglects the transverse shear deformation

If the thickness of the element is greater than 1/10 to 1/15 of the span length, the shear deformation should be included in the analysis and can become an important factor for the points where bending-stress are very high, such as near sudden changes in thickness or at the supports or near holes [23]. When the shear deformation is not considered in the analysis, the thick-plate formulation is more accurate than the thin-plate formulation [23]. The thick-plate formulation considers more stiffness for elements and is sensitive to mesh distortion [22, 23].

Normally, it is recommended to choose the thick-plate option in SAP unless the curvature meshing system is used, or the shear deformations are too small and can be neglected; if fitting a theoretical thin-plate solution is the priority of the analysis, other options should be considered [22]. It should be noted that the thickness formulation affects the plate-bending behaviour and there is no effect on the membrane behaviour.

In this research, the shear deformations were ignored due to the high length of the entire model when compared to its thickness. Moreover, because the direction of the induced forces is along the vertical (the z axis), it was considered there is no major shear deformation along the other two directions. Therefore, the shell-thin-plate element was chosen.

“Three different layers with homogenous material properties were used. Each homogenous section has two different thicknesses as described below:

- Membrane thickness is used for the calculation of
  - Complete shell membrane stiffness and pure membrane sections
  - The element volume for the element self-weight and mass calculations
- Bending thickness is used for the calculation of
  - Complete shell plate-bending and transverse-shearing stiffness and pure-plate sections" [22].

These double thickness parameters are actually very similar and are needed to input membrane thickness. However, in some cases, the membrane or the plate element stiffness should be changed artificially based on the modelling requirements [22]. To do this, a different value of membrane thickness must be included for the bending thickness. In this study, it was considered the same value for both thicknesses [22].

For modelling joists and fasteners, different frame elements were used and were categorized based on their mechanical properties. For the fasteners used to connect the steel deck to the joists, a simplified model was used instead of a fully detailed model of the fastener. Thus the head of the fasteners and their threading were not included in the FE model due to their complicated geometry. However, by using the boundary conditions provided by SAP2000, the fastener was modelled as a truss element with a fixed support for the joist-deck fastener, and as a truss element with restraining support on top for membrane-deck fasteners. Figure 4.4 shows a standard truss element with axial load in Z direction.

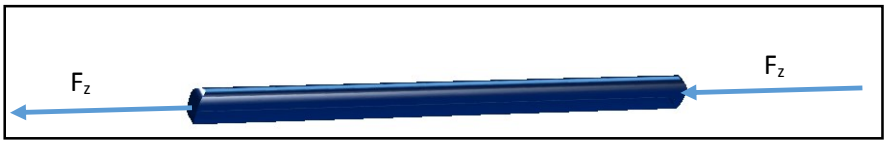

Figure 4.4 Axial load in Z direction along the truss element

4.3 **Boundary Conditions**

The focus of this study is the steel deck behaviour under wind uplift pressure, which depends very much on the type of connections used in the experiment; therefore, for modeling the experimental conditions, choosing the right boundary conditions in modelling the connections is very important for achieving an accurate result.

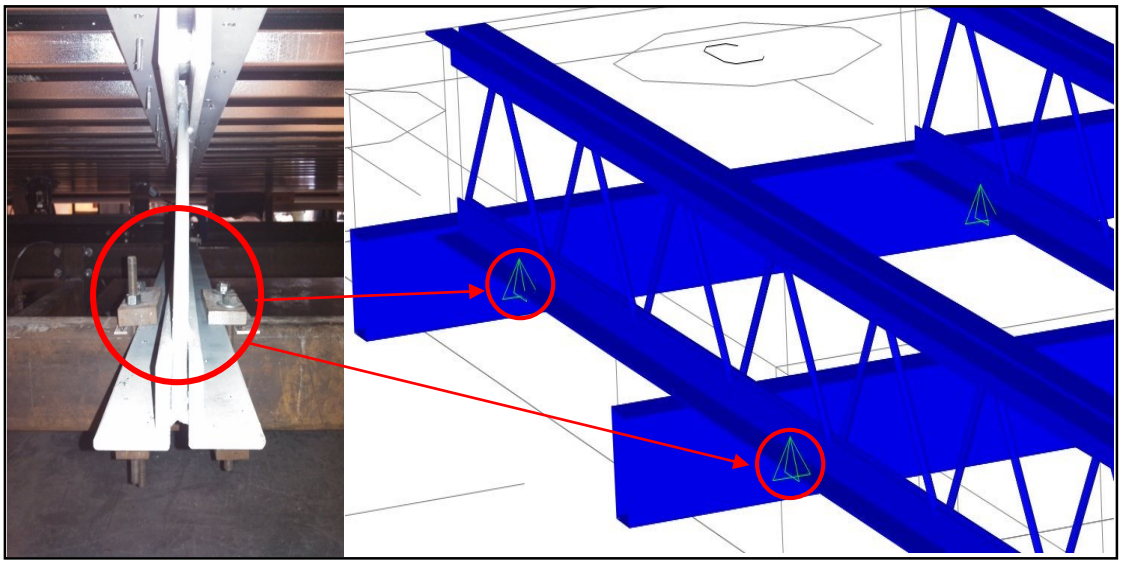

Figure 4.5 Boundary condition for joist attachment in the modelling

The joists were attached by four frames to the body of the chamber. This connection was made by steel clamps as shown in Figure 4.5. For modeling in SAP2000 the lock up the clamps provided in this connection, simply support condition (known as restrained boundary condition in SAP2000) was considered for each connection point along the joists.

Another boundary condition was considered for the fasteners' connection. For joist-deck fasteners, simple support conditions have been chosen at the connection point based on the experiments performed as part of this research, and based on the FM recommendations of considering the fastener connection as simply support when determining the allowable

deflections and moments. In addition, there is no any fix condition at the end of fasteners. Moreover a very small distance between the steel deck and joists was assumed, for avoiding the direct interaction between the joist element and the shell element, which would be incorrect considering the experimental conditions employed, and to provide the space for the fastener truss model. Thus the connection between the steel deck and the joist would rely entirely on the fasteners, as also used in the experimental setup, and also the fastener's resistance can be considered in the SAP2000 structural analysis. Figure 4.6 shows the modelling of the fasteners in SAP2000 and the fasteners' experimental application.

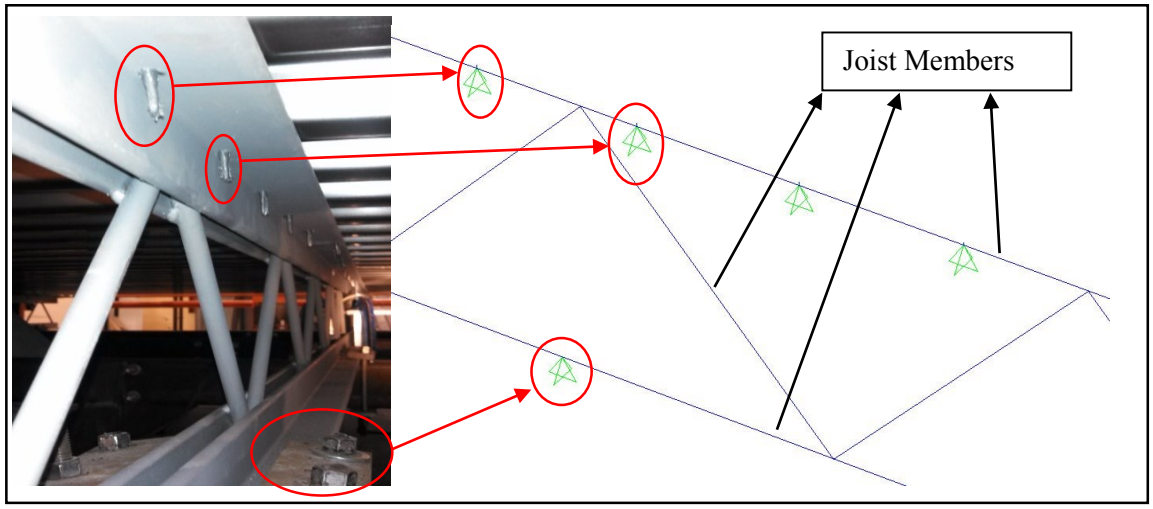

Figure 4.6 Fasteners simulation in SAP2000

In this study, apart from computational effort reduction, certain simplifications have been done for the structural members' geometries. For example, to represent the CANAM steel deck sheet, which has a trapezoidal profile, this was replaced with a plate with equivalent thickness, which provided the same moment of inertia as the CANAM steel deck. To do this, a simple calculation was performed. The moment of inertia for gauge 22 CANAM steel deck is 0.1481 in^4 and the nominal thickness is 0.03 in, therefore these dimensions were used in the moment of inertia formula:

$$I = \frac{b\,h^3}{12} \tag{4-1}$$

b = length of member

h = thickness of member

Because the moment of inertia in the CANAM catalogue is based on 12 inches, b and h should be in inches; to calculate h for the equivalent plate, it is needed to use the same value of the moment of inertia of the steel deck:

$$0.1481 = \frac{12\,h^3}{12} \tag{4-2}$$

$$h = 0.5291 \text{ in} \tag{4-3}$$

By inputting the calculated value for plate thickness in the membrane thickness and bending thickness, the replacement of steel sheets by plates is possible. Figure 4.7 shows how the CANAM sheets were modelled in SAP based on the described method.

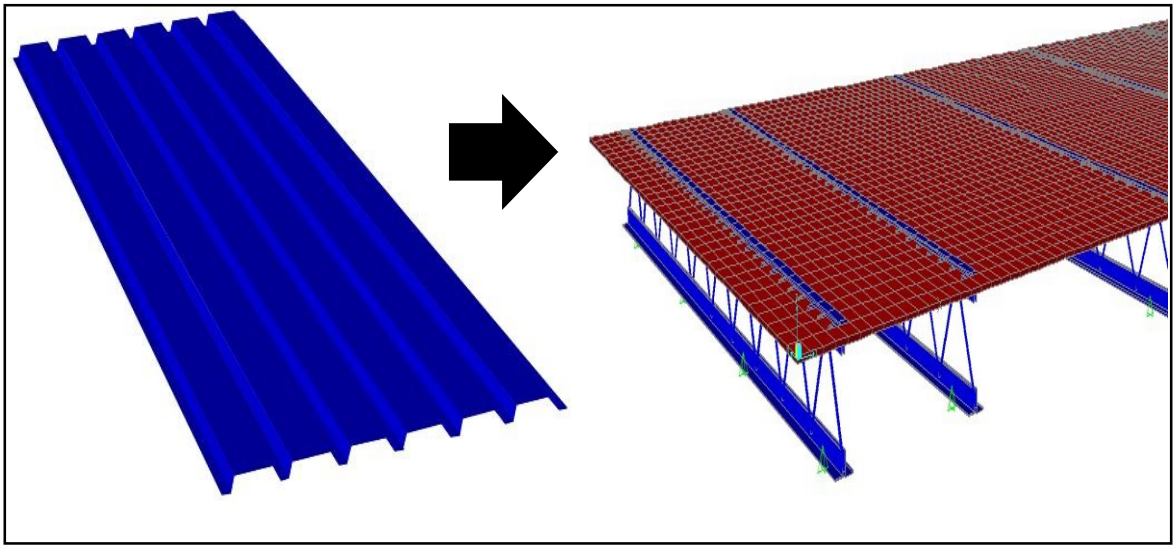

Figure 4.7 Steel deck conversion to plate element

As shown in Figure 4.8, in the experiment, two adjacent steel deck sheets are connected every 2 feet by fasteners, along an overlapping line. To model this assembly in SAP2000,

disconnecting the nodes of the shell-plate at the points of connection (at fasteners) between the two sheets is required. When two shell-plate elements are used in SAP2000 with an overlapping region, the nodes in the overlapping elements, with the same location, are merged automatically by the SAP2000 software into one single node; to properly replicate the experimental conditions, the overlapping nodes of the two steel deck sheets models were first disconnected at the connecting points, then by manually connecting the appropriate plate-shell element with the corresponding nodes, the 2′ distance used in the attachment region can be admitted by the SAP2000 software.

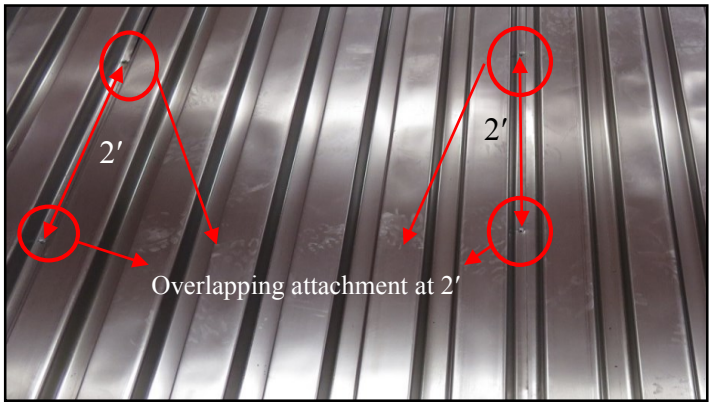

Figure 4.8 Connecting two steel sheets

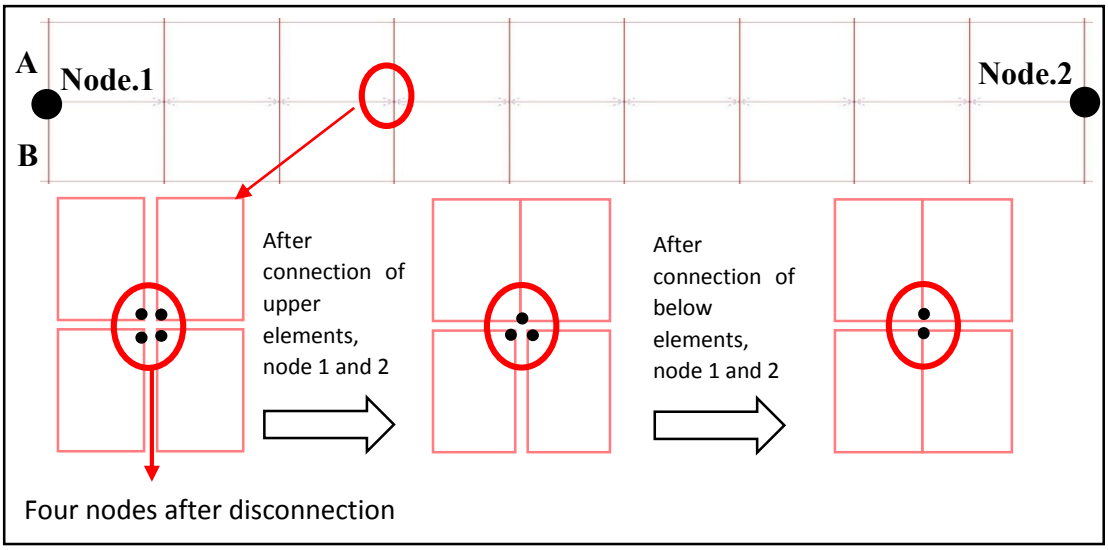

Figure 4.9 Connecting procedure of two steel sheets in SAP2000

As shown in Figure 4.9, nodes 1 and 2 are connecting points (fasteners). The inner nodes between them are selected excluding nodes 1 and 2, then the selected nodes were disconnected and divided into four nodes. By selecting nodes 1, 2 and the upper shell elements (A) between these nodes, and by connecting them, the inner four nodes are reduced to three nodes. The same procedure was performed for the lower shell elements (B), in regard to nodes 1 and 2, thus reducing again the number of the nodes to only two nodes; therefore, after this procedure, SAP2000 considered the shell elements connect at nodes 1 and 2, and no other attachment between these two nodes.

For modelling membrane-deck fasteners in SAP2000, frame elements were considered without any additional constraint connection, because the interaction between fasteners and layers provided an accurate behaviour of elements. In addition, because the stiffness between fasteners and layers was not as joists and fasteners, only the resistance in the X and Y directions were considered for the membrane-deck fasteners. Figure 4.10 shows how fasteners were modelled in SAP2000.

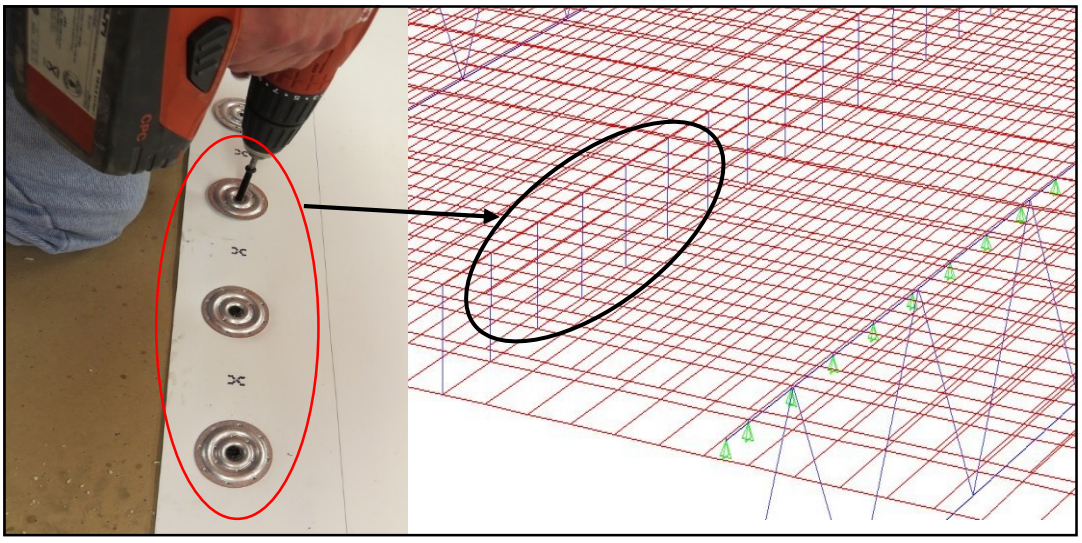

Figure 4.10 Membrane-deck fastener modelling in SAP2000

4.4 **Mesh Sensitivity**

There are two different types of loading used in the experiment: a) uniform load on the steel deck and b) point load on the roof assembly, which is applied at fastener points along the membrane-deck fasteners line. For data comparison between the Finite Element Modelling and the experiments, deck analysis data at mid-span and exactly at the location of the fastener, which was connected to the 6-component load cell, is required. Therefore, shell elements with the dimensions of 1.5″ x 1.5″ in the X and Y directions were considered. The shell elements of 3″ by 6″ dimensions in the X and Y directions, respectively, were considered as well. As it can be seen in Figure 4.11 the analysing time is almost half of the first mesh sizing. Both had the same analysing results; for example, Figure 4.12 shows the result of Fz for the steel deck case. Because the result of this research should be released in a specific time to update the FM table in a short period as requested, a second mesh sizing was considered. Moreover, the analysing information must be considered for a specific point (6-component load cell). Figure 4.13 shows two different types of meshing in SAP2000.

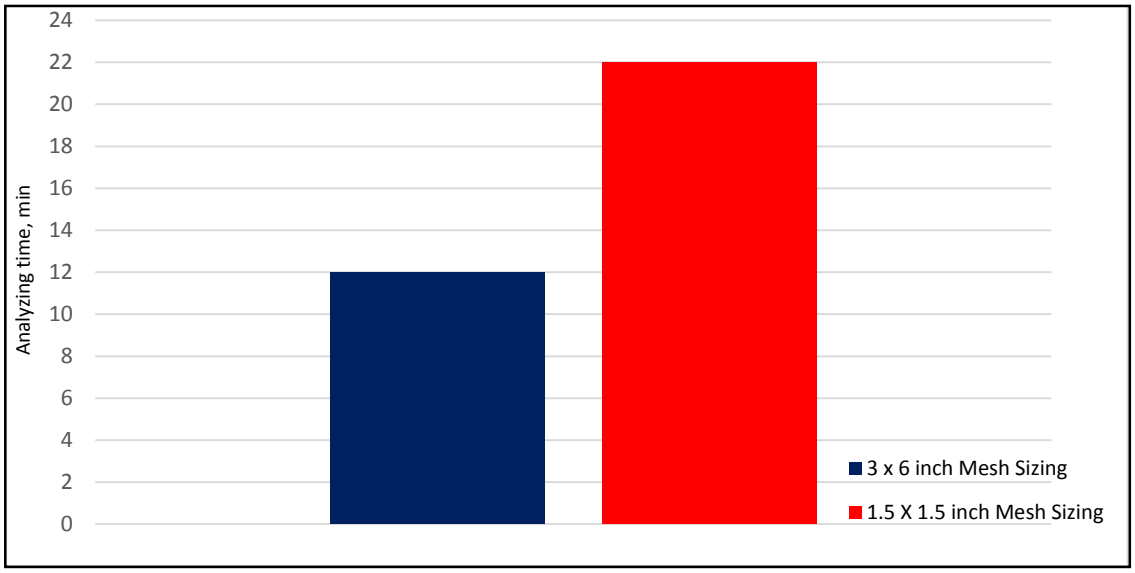

Figure 4.11 Analyzing time comparison between two different mesh sizings

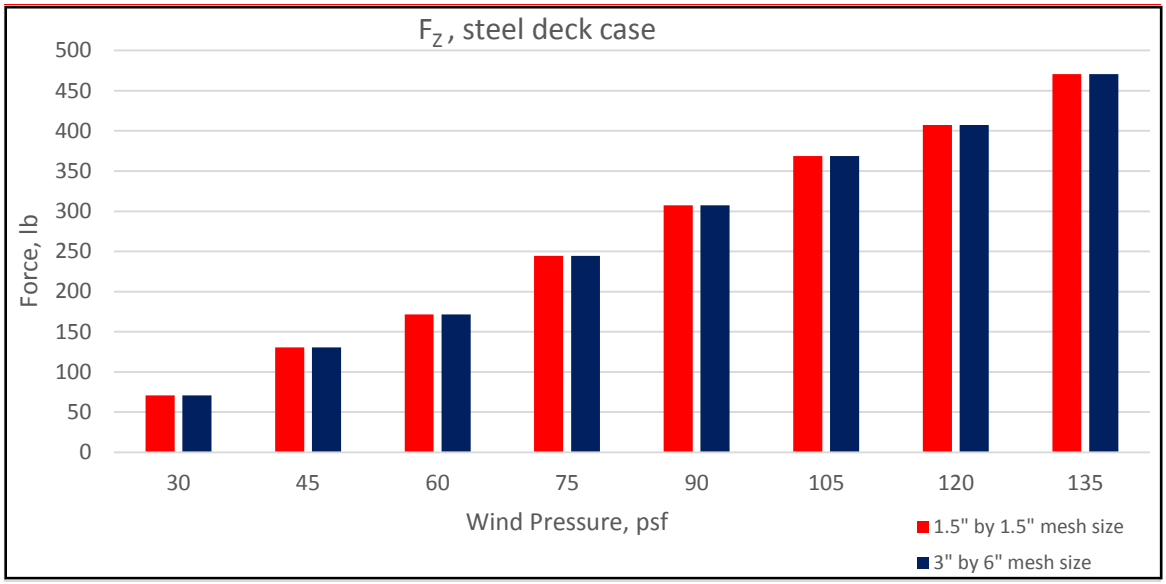

Figure 4.12 Comparison of F_z for two different mesh sizes

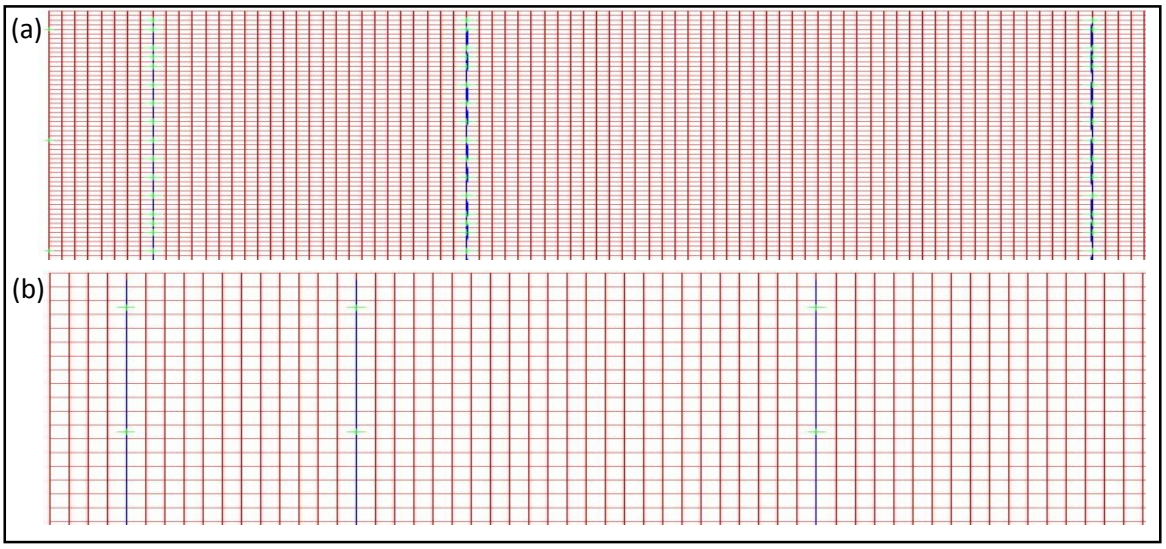

Figure 4.13 Mesh comparison: a) 1.5 x 1.5 inches, b) 3 x 6 inches

The line load distance is a multiple of three, so the shell dimension should be the same to have a line of nodes in the location of point loads, which was applied in each 6 inches along the line. Figure 4.14 shows the location of the two points where obtaining the deflection and moment responses is very important in the output of the FEM, because these can be directly compared with the responses measured during the experiments at these points.

The node between axes E - 4′ is for the 6-component load cell location and the node between axes E′- 4′ is for the laser location.

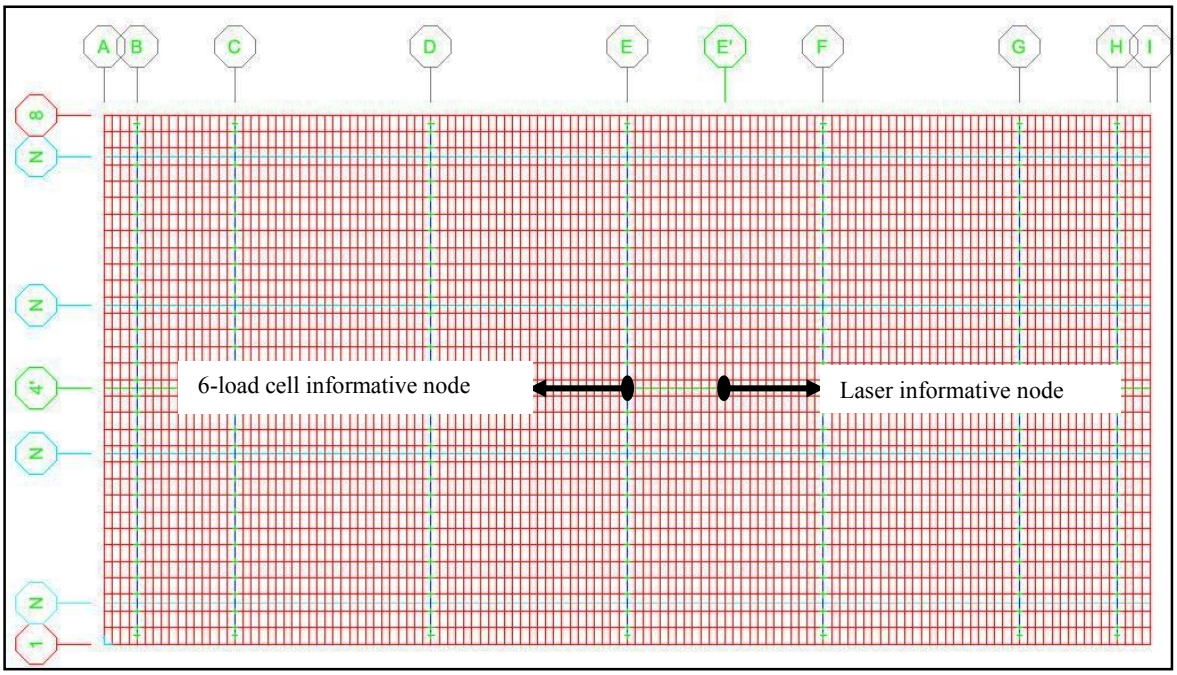

Figure 4.14 Informative node locations

4.5 **Mechanical Properties of Materials**

In this study, CANAM steel sheets, model P-3606 with 22 gauge of the CANAM steel sheets were used. F_y was 33 ksi based on ASTM A 653M for the deck; therefore, in the FE modelling the same value or specification as mentioned in the CANAM catalogue is selected.

In the experiments, custom K-series joists were used with properties as per ASTM A370, and for diagonal members of joists (bars), ASTM A36 standards were followed. Fasteners were ordered from Simpson Strong-Tie Company and were manufactured as per the ASTM C1513 standard, which covers self-drilling screws to attach cold-formed steel members. Table 4.1 shows the most relevant mechanical properties that are employed in the FE modelling for the steel members.

Table 4.1 Mechanical properties of steel elements

Member Type	Standard	Modulus of Elasticity- E (ksi)	F_y (ksi)	F_u (ksi)	F_{ye} (ksi)	F_{ue} (ksi)
Joist Steel	ASTM A370	29000	33	58	36.3	63.8
Joist Bars	ASTM A36	29000	33	45	36.3	50.8
Steel Sheet	ASTM A 653M	29500	24	45	-	-
Fasteners	ASTM C1513	29000	33	45	36.3	50.8

The type of membrane layer in the experiment was 45mil TPO, which is Thermoplastic PolyOlefin, and the main material in this type of roof membrane is Polyethylene (PE). Polyethylene accepts a wide range of colours, and can be transparent, translucent, textured or metal coated. Therefore, it is widely used in the construction industry [11].

In the experiment, 2″ thick insulation boards were used. The main and important material in the insulation layer is Polystyrene (PS), which comes in three types: a) as the simple material (general PS); b) as the high-impact variant, blended with polybutadiene; and c) as polystyrene foam, the most familiar and cheapest of all polymer foams [11]. PS can be foamed to a very low density, and these foams have low thermal conduction. Therefore, they are the most proper material for in-house insulation [11]. Table 4.2 shows the mechanical properties for insulation layer.

Table 4.2 Mechanical properties for insulation and membrane layers

Member type	Weight per unit volume (lb/ft^3)	Modulus of Elasticity- E (ksi)	Poisson's ratio U
Insulation layer (PS)	64.98	174	0.39
Membrane layer (PE)	58.62	90.07	0.42

4.6 **Loading Types**

Although only uniform loading was applied in the experimental tests, in the modelling, the uniform wind uplift pressure was considered only for the steel deck case, and the point loading system was used when the roof assembly was under wind pressure. This study has been done to validate a proper model to modify FM design tables. The FM table has been produced based on static analysis of structures; therefore, the static concept governs in this study as well. The membrane layer was attached by membrane-deck fasteners in each 6″ on the basis of the FM design, these connection points are considered as the location of the point load. Thus, for roof assembly cases in SAP2000, the uniform load was converted into the point load based on the tributary area of each point and the distance of membrane-deck fastener lines. The loading type is described completely in chapter 5.

- *Uniform load:* Figure 4.15 shows wind-induced pressure on the steel deck in SAP2000 for 135 psf.

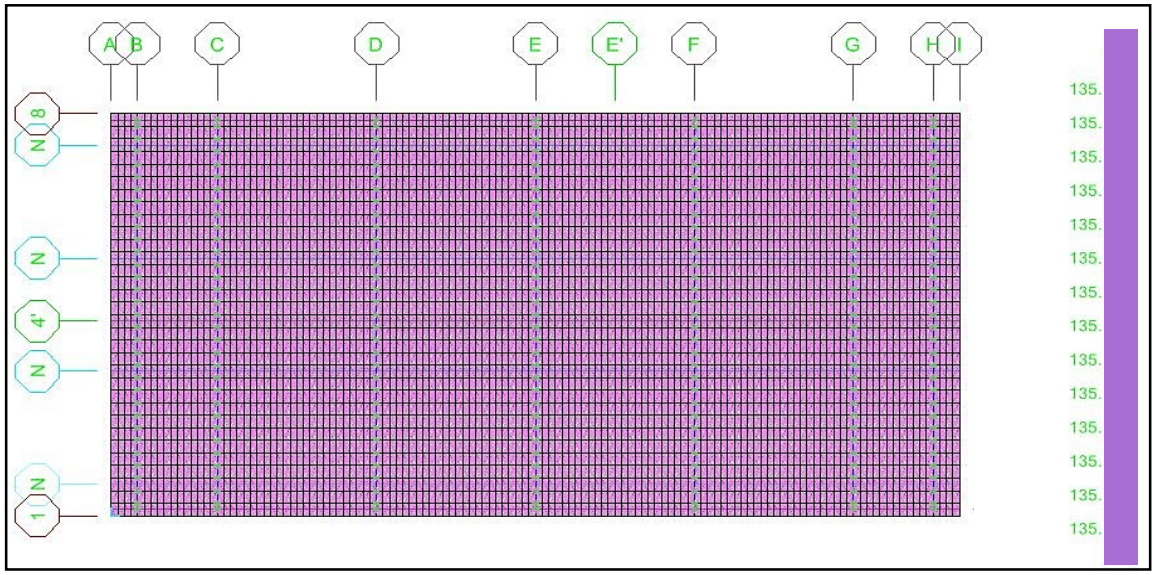

Figure 4.15 Steel deck uniform loading (135 psf)

- *Point load:* In the experiment, the wind uplift pressure was applied on the roof assembly for three cases. Table 4.3 shows applied wind pressure for these three cases.

Table 4.3 Applied uniform load on roof assembly cases

membrane-deck fastener line distance in x direction	applied wind pressure (psf)							
	30	45	60	75	90	105	120	135
9′6″	x	x	x	x				
6′	x	x	x	x	x	x	x	
7′6″	x	x	x	x	x			

In the experiment, all the distances were measured starting from a reference line. The axis-E′ in Figure 4.15 is the reference line, which is exactly at the middle of span E-F (228 inches in x direction from local axis in SAP2000). Figure 4.16 shows an overview of the point loading type of 9′6″ membrane-deck fasteners' line distance.

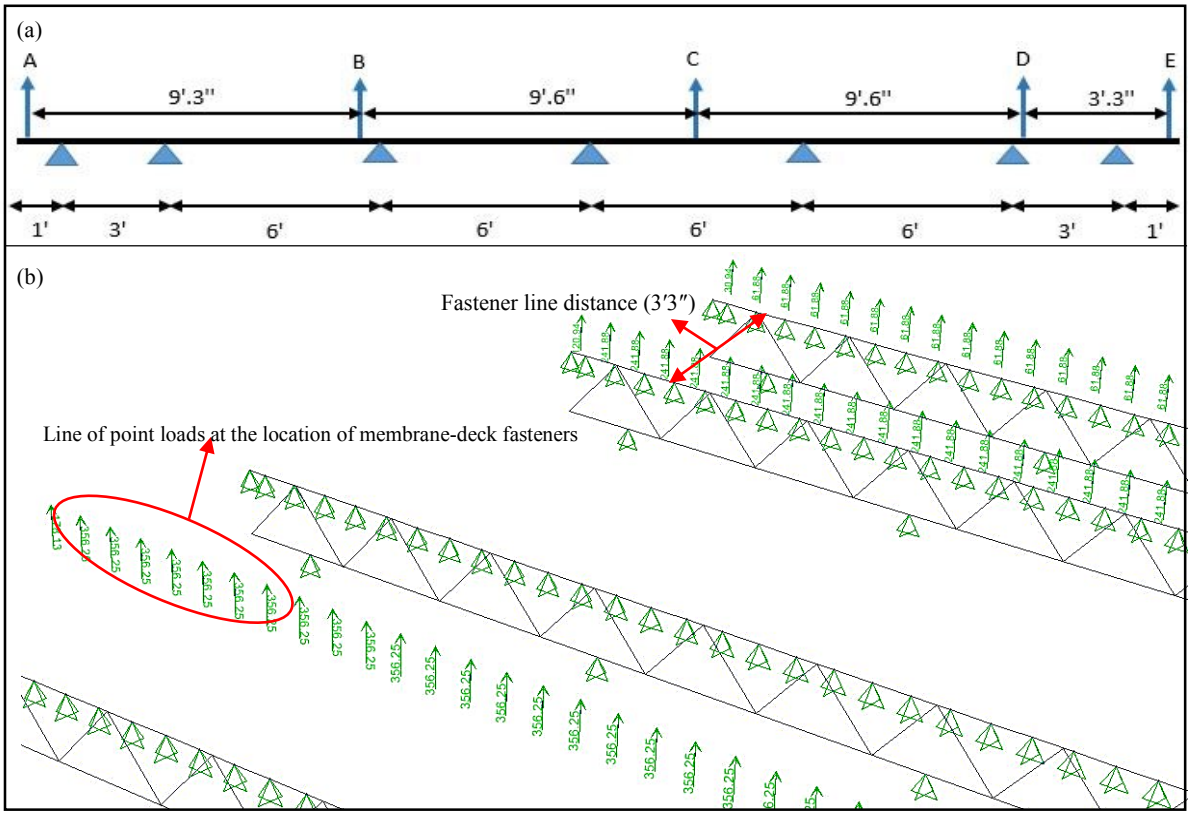

Figure 4.16 a) Point loading scheme for 9′6″ fasteners' line distance, b) Applying point load in SAP2000

Apart from the loading system based on the FM table, another loading type was considered in SAP2000 to check whether the scenario of converting the uniform load to point loads at the location of the membrane-deck fasteners is correct or not. To do this, the uniform load was converted to a distributed load along the fasteners' line. However, in SAP2000 it is not possible to apply a line of distributed load on shell elements; therefore, two load modeling options were considered to achieve the same uniform load to point loads conversion:

a) The value of the load distributed along the line was divided by the distance between fasteners (6″in this case) to calculate the point load applied at these nodes.
b) By dividing shell elements that were located on both sides of the fasteners' line into smaller elements, then by applying the uniform load only on the smaller shell elements, the distributed line load was simulated in the location of the fasteners. Although this procedure seems to be an acceptable modelling assumption for this type of loading, this method needed too much calculated effort, thus another solution is considered for the distributed line load system.

To obtain an accurate result for the load distributed along the fastener line, it was decided to apply the distributed line load on a horizontal frame element that was modelled along the fasteners line (Figure 4.17). Thus, the membrane strip considered, located on the fasteners' line, has common nodes with the frame and shell elements, automatically assign by SAP2000. On the other hand, because of the thickness of the membrane strip material, the stiffness of this frame could be ignored, and there is no effect on the accuracy of the results, thus this assumption resembling a tape with point loadings applied at the common nodes.

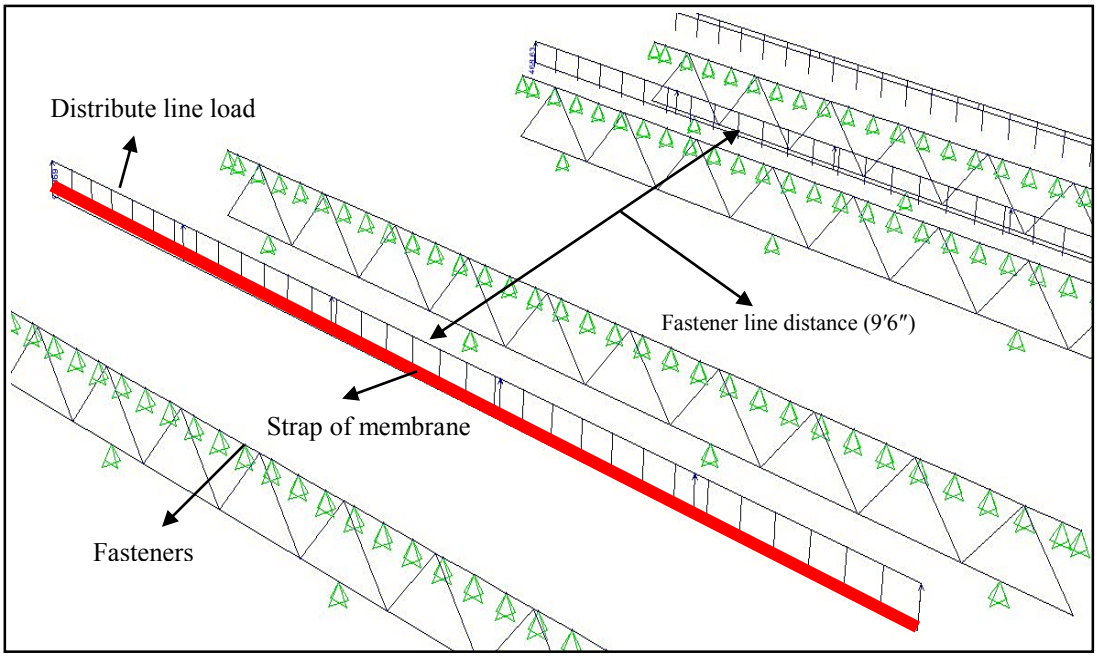

Figure 4.17 Distributed line load on membrane frame at the location of the fasteners in SAP2000

It should be explained here that calculating the uniform load into the point load at the connection points is needed. To do this, the tributary area for each membrane-deck fastener should be calculated. The distance between fasteners (x) in each line is 6″, therefore,

$$x = 0.5\ ft \tag{4-4}$$

$$y = Fastener\ line\ distance\ (ft) \tag{4-5}$$

This value should be divided by two because based on the loading calculation, half of each area should be considered when determining the tributary area for a structural component.

$$N = x\ \times (y/2) \quad (ft^2) \tag{4-6}$$

N is the tributary area for each fastener, and by multiplying the wind rate to this value, the point load can be calculated. It should be noticed that the tributary area for the first and last

fastener in each row is half of the middle fasteners because it is 3″ instead of 6″. For example, Figure 4.18 shows schematic data for 9′6″ fastener line spacing for 30 psf.

$$N = x \times (y/2) \tag{4-7}$$

$$N = 0.5' \times (9.25'/2) = 2.3125\ ft^2 \tag{4-8}$$

$$F = 2.3125 \times 30 = 69.375\ lb \tag{4-9}$$

F is the point load that should be applied at the location of fasteners in the modelling, which, for this example, is 69.375 lb, and for the first and end fasteners in each row is 34.6875 lb.

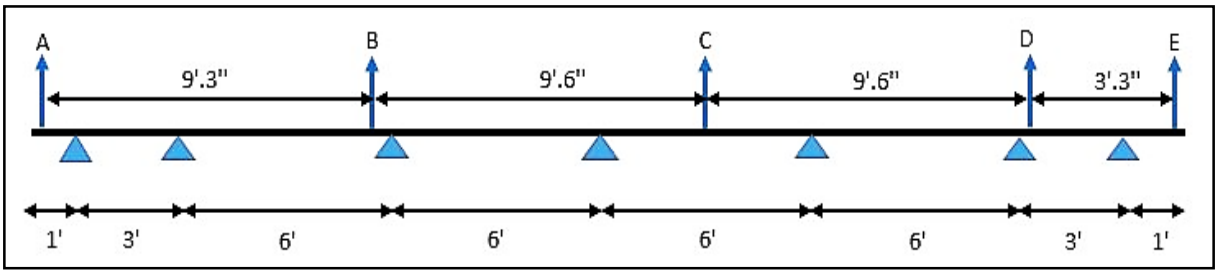

Figure 4.18 Point load scheme for roof assembly (9′6″ fastener line distance)

4.7 Type of Analysis

After choosing the proper load types, it is important to define the load pattern in SAP2000. Point load (pl) and uniform load (ul) were specified in the system with wind type subdivision. But without determining load cases, running the model is impossible because load patterns do not create any response, such as stress or deflections, thus load cases should be defined to consider how loads are to be applied to the structure and how the structure behaves regarding applied loads.

After describing the loading systems, the appropriate load case type should be chosen. In SAP2000, there are different types of analysis, but because one of the objectives of this research is updating the FM table which was created based on the static analysis, the same method of analysis is considered in the modelling.

There are linear and nonlinear types of analysis in SAP2000, but in this research, the linear behaviour of structures was contemplated because of small deflections in the steel deck and based on the following explanations. In addition, the test was stopped during the experiment when the nonlinear behaviour of the roof assembly could be observed. "The characteristics of linear analysis are as follows:

- Structural properties and materials are considered linear during analysis.
- Initial condition is linear, which means the analysis starts from zero stress even it uses stiffness from nonlinear analysis.
- Structural response is linear; for example, all displacements, reactions and stresses are linearly dependent on magnitude of applied loads.
- The deformations are small: [12].

The linear behaviour of structures can be calculated upon the linear static analysis in SAP2000 based on the below linear equation [12]:

$$K \times u = r \tag{4-10}$$

Where K is the stiffness matrix, r is the vector of applied loads and u is the vector of resulting displacements [12]. The last step of FEM is running the software based on all the previous

definitions and explanations in this chapter. When the analysis was run, all objects in the model were converted to finite elements. Then, based on load cases and analysis type, the behaviour of the roof assembly under the wind uplift pressure was calculated and the results of the modelling were received. This procedure was repeated for all four cases. The same method of analysing was used in the FM table under various wind rating to update and develop the table.

Chapter 5 Results

This chapter comprises three main parts. First, the results from the experiments are discussed. The second part contains the detailed results from the FEM. Finally, the comparison between the two sets of results is presented.

5.1 Experimental Results

In this section, the outcomes of the experiments performed on the four different roofing systems are described. The experimental results are based on the deflections at different locations of laser sensors and the 6-component load cell which characterizes all forces for one deck-joist fastener system. Among the forces, the vertical force F_z and the bending moment $M_{y,}$ are more significant for this study than other force and moment components, because the FM design table is established based on the allowable criteria for these moments and forces.

5.1.1 **Steel deck**

For the steel deck itself, it was desired to run the experiment up to 180 psf wind rate, but due to some observed failures such as buckling of the steel deck, the test was stopped at 135 psf.

- *Deflection*

Net deflection is one of the important parameters to update the FM table. As a brief explanation, the deflection registered for each loading cycle is computed by subtracting the deflection of joists from the steel sheet deflection in order to isolate the steel deck response. The same procedure should be followed to calculate the permanent deflection. Afterwards, by deducting the permanent deformation from the cycle deflection, the net deflection will be

computed. Table 5.1 shows the deflection results for this case. Complete details and an example of such calculation are provided in section 3.4.1.2. (Fig. 3.22).

Table 5.1 Experimental deflection for steel deck case

Wind Rating (psf)	Span deflection, D1-D4 (in)	Permanent deformation, D1-D4 (in)	Net deflection, (in)
30	0.058	0.015	0.043
45	0.1	0.025	0.75
60	0.145	0.041	0.104
75	0.193	0.057	0.136
90	0.250	0.079	0.17
105	0.305	0.109	0.196
120	0.370	0.145	0.225
135	0.434	0.177	0.257

- *Forces*

All the results in this section are obtained from the output of the 6-component load cell, and the force and moments were calculated and calibrated as detailed in section 3.4.2. Table 5.2 shows the axial forces in three directions at the same location of the specific deck-joist fastener instrumented.

Table 5.2 Forces for steel deck case

Wind Rating (psf)	Fx (lb)	Fy (lb)	Fz (lb)	Mx (lb.in)	My (lb.in)	Mz (lb.in)
30	1.30	18.68	70.97	1.585903	8.138	0.995
45	2.87	7.05	130.42	0.369939	8.069	0.765
60	9.91	3.13	171.67	0	10.33	0.132
75	6.02	3.75	244.34	0	18.16	0.707
90	7.69	16.10	307.49	0	26.85	0.176
105	11.30	17.11	368.67	0	37.23	0.313
120	16.25	8.09	407.40	0	51.91	0.378
135	21.61	9.47	470.88	0	68.655	0.824

Figure 5.1 shows a comparison between the axial forces. As it can be seen, the vertically applied force in the Z direction is the dominant force representing the reaction to wind uplift pressure. Compared with the vertical force, the longitudinal and transversal forces developed

in the plane of the steel deck are very small. Figure 5.2 shows the moments for the three directions, and except for M_y, which increases by raising the wind force, M_x and M_y are almost zero.

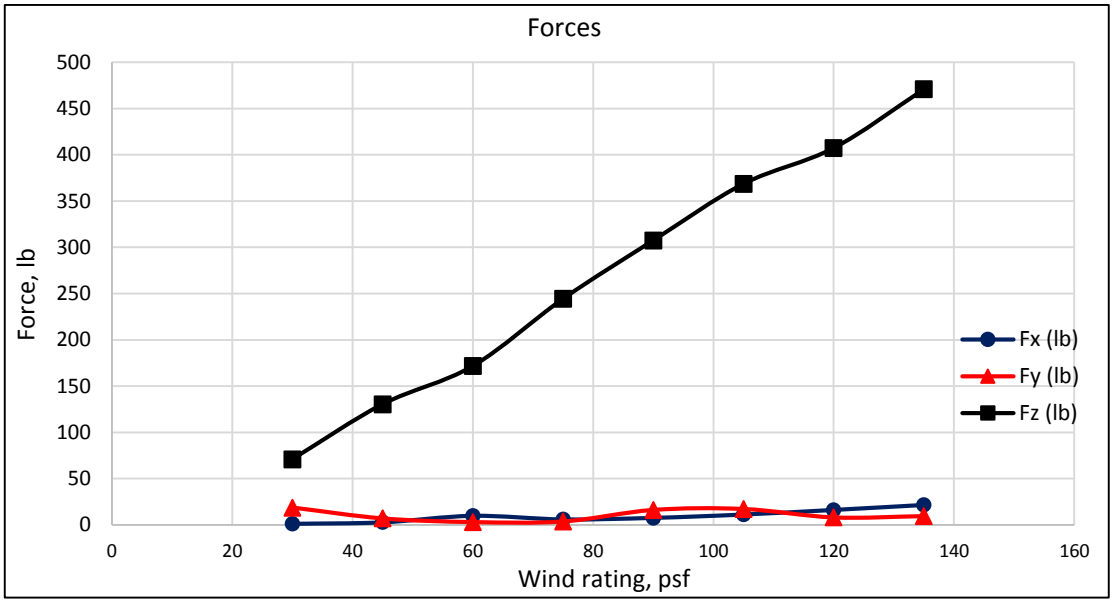

Figure 5.1 Force comparison for the steel deck case

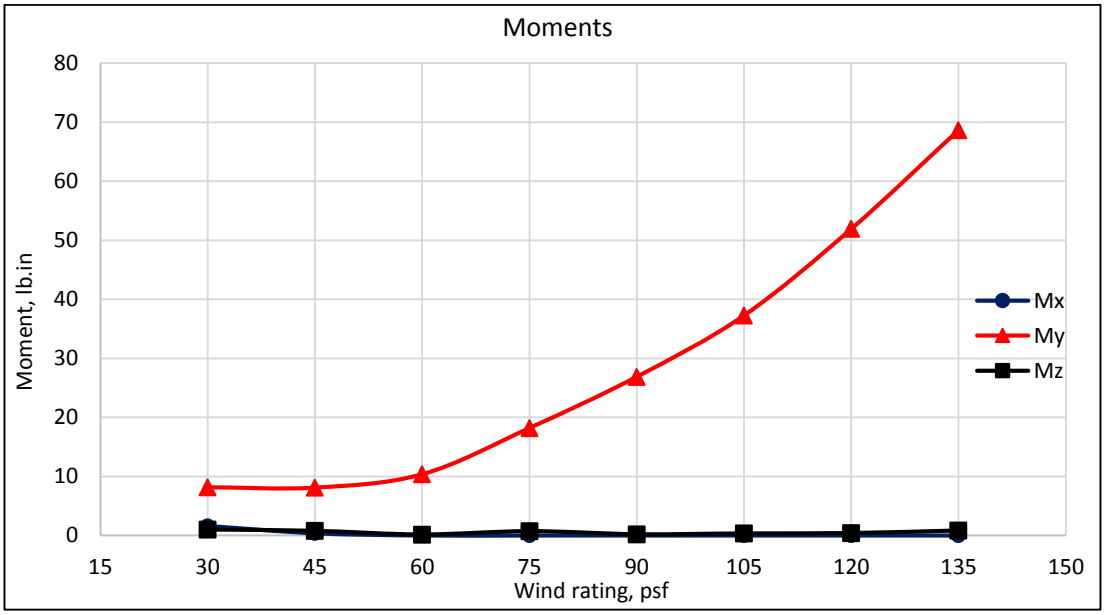

Figure 5.2 Moment comparison for the steel deck case

5.1.2 **Roof assembly (9′6″ membrane fasteners' line distance)**

For this case, it was predicted to run the test until 90 psf wind pressure, but when the roof was at 80 psf, the steel deck buckled and the test was stopped.

- *Deflection*

The same procedure as the steel deck case should be followed for this case. Table 5.3 shows deflection information for this case.

Table 5.3 Roof assembly deflection for 9′6″ membrane fastener line distance

Wind Rating (psf)	Span deflection, D1-D4 (in)	Permanent deformation, D1-D4 (in)	Net deflection, (in)
30	0.236	0.001	0.235
45	0.341	0.001	0.339
60	0.505	0.001	0.504
75	0.778	0.001	0.777

- *Forces*

Figure 5.3 provides illustrated information about force comparison. It is clear that by increasing the wind force, F_z increases as well, meanwhile, the other forces remain stable. Table 5.4 shows the experimental results for the case of 9′6″ membrane fastener line distance.

Table 5.4 Roof assembly forces for 9′6″ membrane fastener line distance

Wind Rating (psf)	Fx (lb)	Fy (lb)	Fz (lb)	Mx (lb.in)	My (lb.in)	Mz (lb.in)
30	0.60	17.28	92.33	2.51	2.67	0.78
45	1.24	17.59	177.89	3.44	3.91	0.78
60	2.08	18.74	222.94	3.31	4.54	1.40
75	0.69	24.40	255.73	1.32	0	0.84

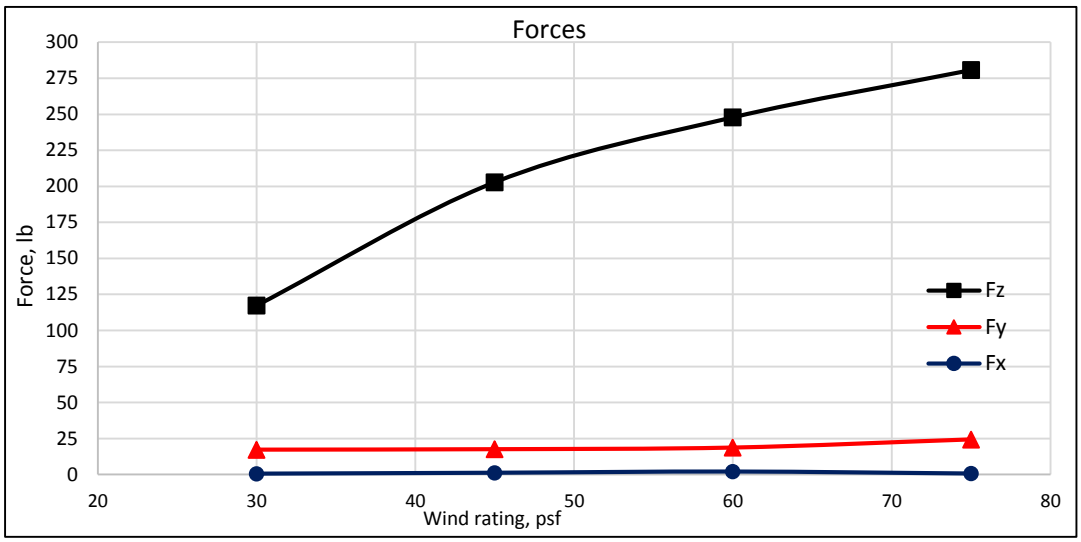

Figure 5.3 Force comparison for 9’6” membrane fastener line distance

As it can be seen from Figure 5.4, there is a sudden drop at 75 psf, which means there is a failure in the roof assembly.

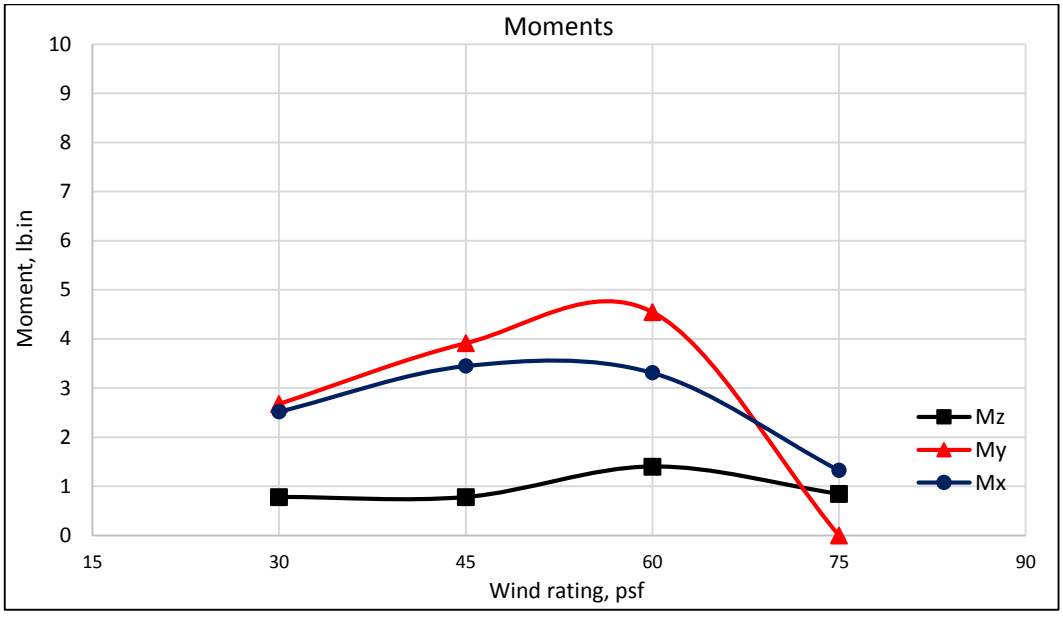

Figure 5.4 Moment comparison for 9’6” membrane fastener line distance

5.1.3 **Roof assembly (6′ membrane fasteners' line distance)**

In this case it was predicted to apply a wind pressure up to 120 psf. In this wind rate, deck deformed which was completely visible as it was shown in chapter 3.

- *Deflection*

Table 5.5 shows different deflections for each cycle in the case.

Table 5.5 Roof assembly deflection for 6′ membrane fasteners line distance

Wind Rating (psf)	Span deflection, D1-D4 (in)	Permanent deformation, D1-D4 (in)	Net deflection, (in)
30	0.123	0.019	0.104
45	0.192	0.048	0.144
60	0.275	0.070	0.205
75	0.366	0.111	0.255
90	0.495	0.155	0.34
105	0.713	0.263	0.45
120	1.105	0.505	0.6

- *Forces*

It would be appear from Figure 5.5 that vertical forces F_z increased by applying higher pressure, meanwhile for the other directions, the 6-component load cell recorded smaller forces therefore forces F_x and F_y did not reach critical values during the test. Table 5.6 shows forces and moments for roof assembly with 6 feet fastener line spacing.

Table 5.6 Roof assembly Forces for 6′ membrane fasteners line distance

Wind Rating (psf)	Fx (lb)	Fy (lb)	Fz (lb)	Mx (lb.in)	My (lb.in)	Mz (lb.in)
30	3.75	1.69	101.74	0.83	11.85	1.27
45	6.25	15.87	230.02	0.00	17.46	0.23
60	8.57	20.10	289.04	0.00	23.90	1.49
75	12.60	23.16	374.96	0.06	33.07	0.13
90	17.95	18.74	459.21	0.83	43.01	0.20
105	25.84	17.31	544.94	4.47	57.89	0.67
120	37.99	12.63	612.29	14.84	82.47	0.62

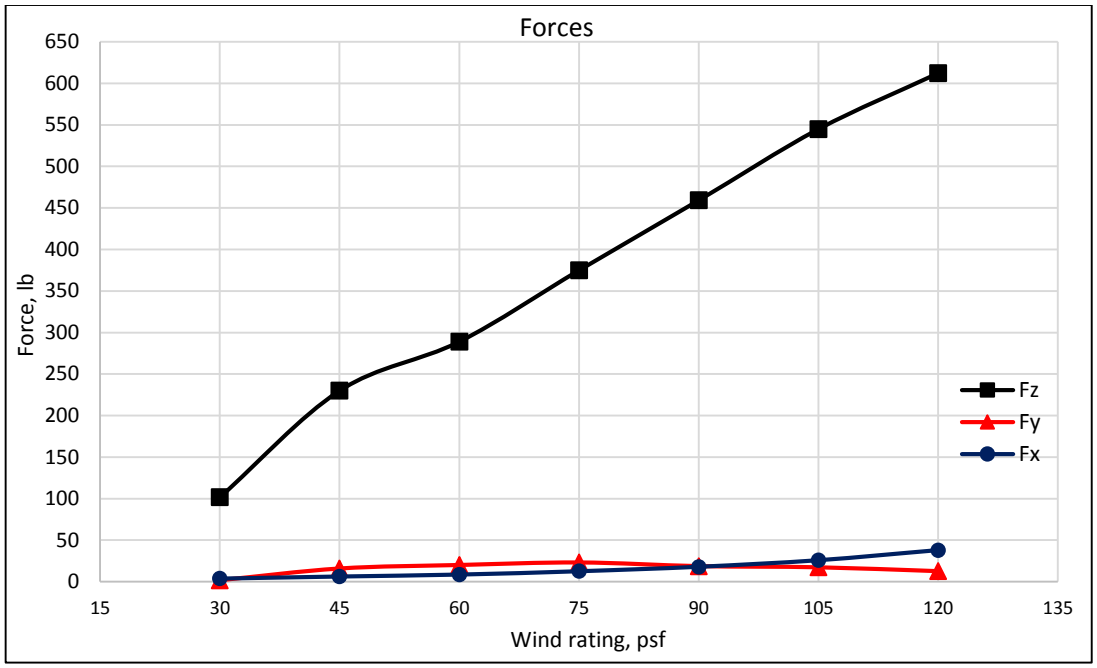

Figure 5.5 Forces comparison for 6' membrane fasteners line distance

In Figure 5.6, M_y goes up when wind force increases but the others are almost zero except for M_x at 120 psf which shows the roof assembly did not have a linear behaviour.

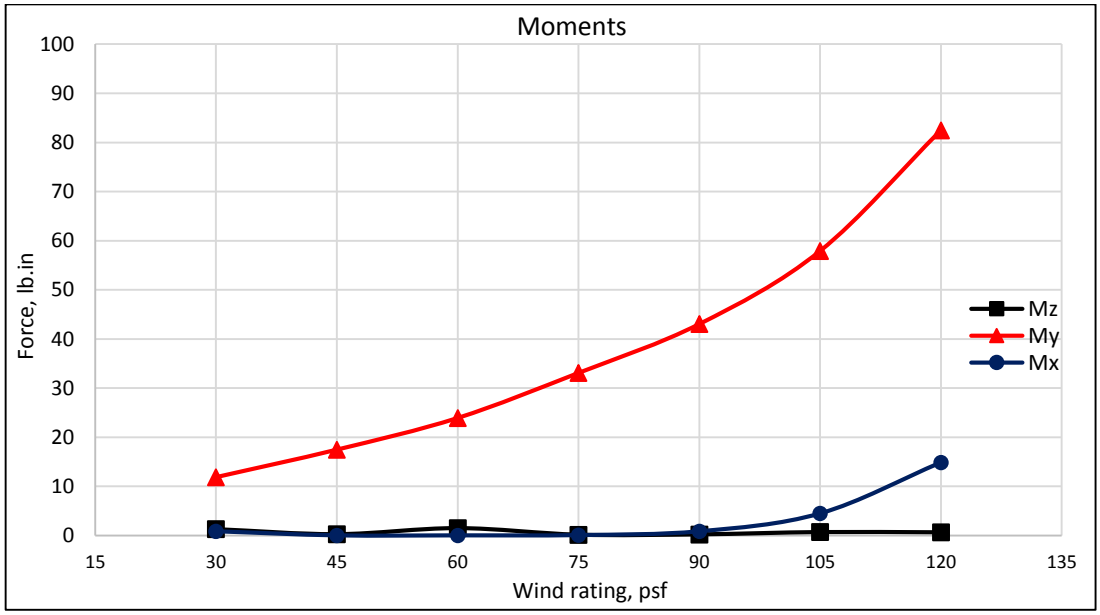

Figure 5.6 Moment's comparison for 6' membrane fasteners line distance

5.1.4 **Roof Assembly (7′6″ membrane fasteners' line distance)**

As in previous cases, the results for the last test configuration are divided into deflection and forces. It was scheduled to apply the wind pressure up to 120 psf but due to the buckled steel deck, the test was stopped after 90 psf.

- *Deflection*

Table 5.7 provides the output results from deflection lasers.

Table 5.7 Roof assembly deflection for 7′6″ membrane fasteners' line distance

Wind Rating (psf)	Span deflection, D1-D4 (in)	Permanent deformation, D1-D4 (in)	Net deflection, (in)
30	0.137	0.008	0.129
45	0.227	0.029	0.198
60	0.355	0.068	0.287
75	0.525	0.129	0.396
90	1.081	0.260	0.821

- *Forces*

As Table 5.8 shows the vertical forces F_z registered dominant values, when compared with the other forces. M_y increased gradually, from pressures 45 psf to 75 psf, but it remained constant for the last tested pressure of 90 psf. Even if lower than the M_y, the moment in regard to the z axis, M_z, had a similar evolution, increasing gradually from 30 psf until 90 psf, however the M_x moment decreased after 45 psf reaching the value of 0 lb.in at 75 psf and 90 psf. Figure 5.7 provides a comparison between three forces, and as it shows, F_y and F_x remain zero, meanwhile, F_z increases.

Table 5.8 Forces for 7′6″ membrane fasteners' line distance

Wind Rating (psf)	Fx (lb)	Fy (lb)	Fz (lb)	Mx (lb.in)	My (lb.in)	Mz (lb.in)
30	0.00	1.52	153.35	0.76	1.95	0.24
45	3.48	0.84	280.55	1.63	3.05	0.85
60	0.27	1.86	362.77	0.75	5.53	1.77
75	1.19	3.29	436.33	0.00	6.72	2.27
90	2.78	4.44	511.59	0.00	6.78	4.68

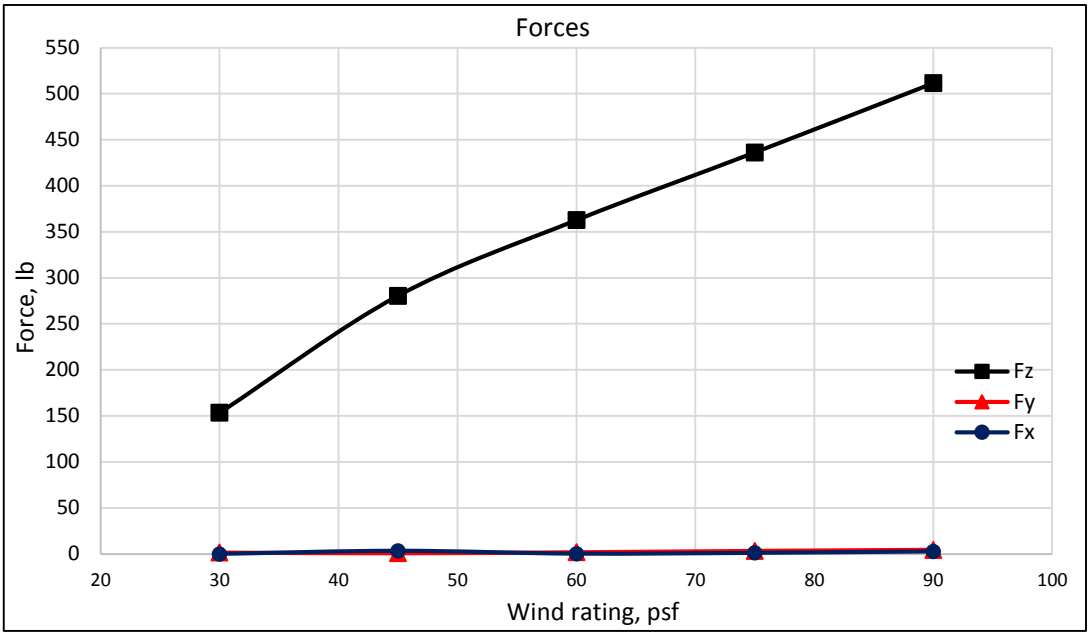

Figure 5.7 Forces comparison for 7'6" membrane fasteners' line distance

Figure 5.8 has provided the results for moments, and by way of contrast among them except M_x, others have almost the same behaviour, especially in the lower wind pressure. Meanwhile, for the higher pressure, the situation is different and M_x tends to be zero in the positive direction and M_y remains almost stable. M_z, as it can be seen, increases gradually.

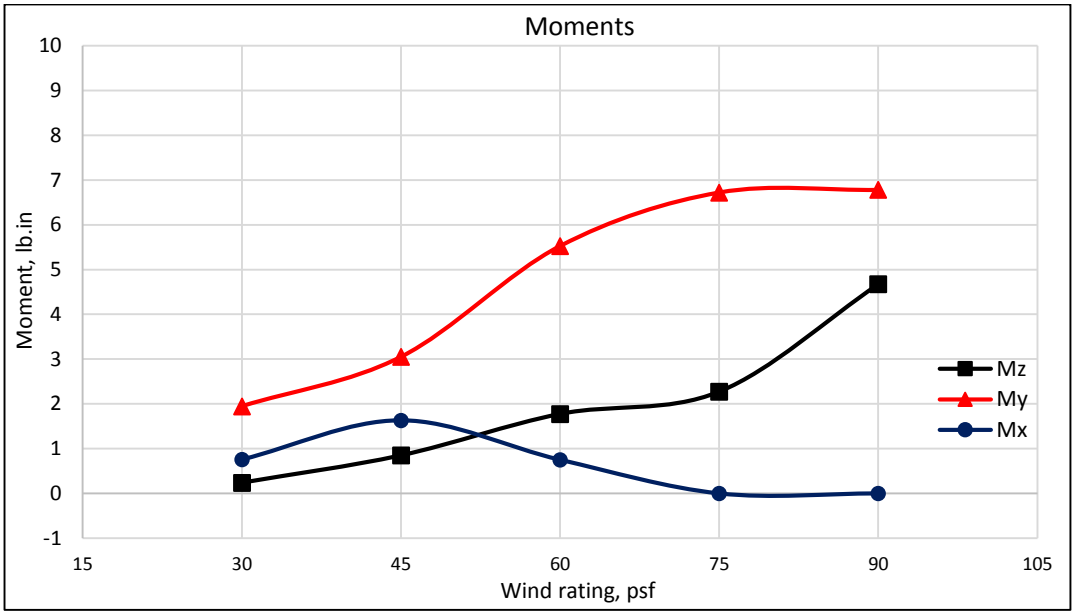

Figure 5.8 Moment comparison for 7'6" membrane fasteners' line distance

5.2 FEM Results

This part consists of three main subdivisions. First, the result for the steel deck (without the membrane layer) will be explained. Then based on SPRI design criteria, the applied wind pressure was converted to the point load for roof assembly cases (steel deck with membrane layer). Moreover, as described in Chapter 4, it was considered to have a line of distributed load on the location of the membrane-deck fastener. At the end, the results of point load and distributed load will be compared to figure out which analysis can meet the requirements.

5.2.1 FEM results for steel deck (without membrane layer)

The same procedure as the previous step should be followed here. F_z and M_y are important values for comparison, and based on defined boundary conditions, the outputs of the SAP2000 are limited to the force in Z direction and M_y at the specific location (6-component load cell). Table 5.9 shows the results for the steel deck modelling.

Table 5.9 FEM results for steel deck

Wind Rating (psf)	Net deflection, (in)	Fz (lb)	My (lb.in)
30	0.037	90.96	7.36
45	0.07	137.23	9.435
60	0.105	183.61	12.24
75	0.135	229.51	18.9
90	0.16	275.41	29.96
105	0.189	321.32	37.5
120	0.216	367	45.76
135	0.242	413.12	54.74

For a better visual, Figure 5.9 has provided a graphic scheme of roof assembly under the wind pressure of 135 psf.

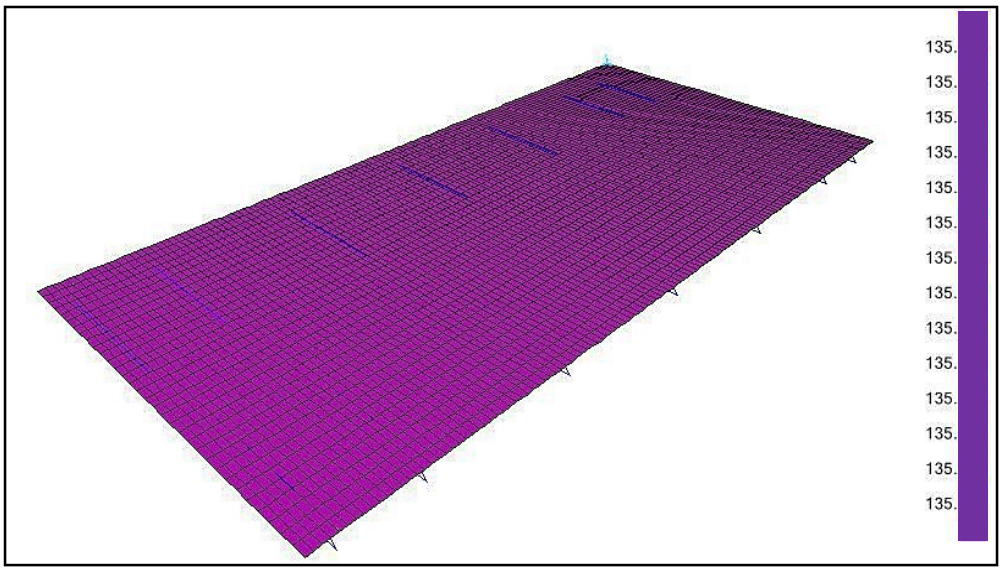

Figure 5.9 Applied uniform load for the steel deck, wind rating 135 psf

Figure 5.10 shows a graphic deflection of the steel deck elements under 135 psf in inches at the location of the lasers. Figure 5.11 shows the moment for the same cycle in the steel deck case at the specific location of the 6-component load cell.

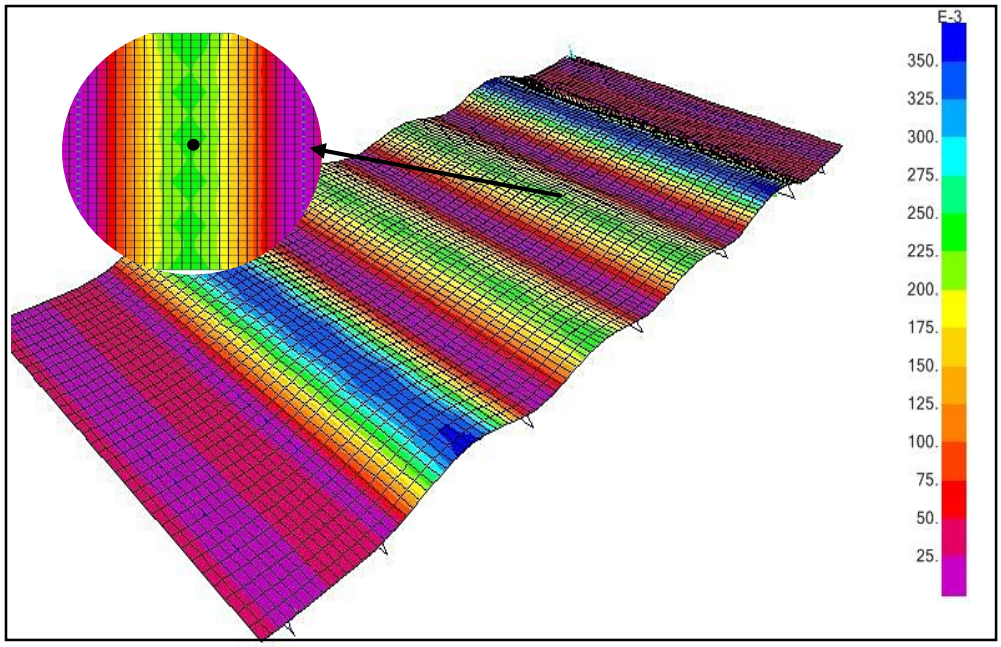

Figure 5.10 Steel deck deflection (in) under wind pressure 135 psf

To better comprehend the behaviour of the steel deck, a shape factor of 20 was used to exaggerate the deformed shape of the roof. In appendix B, the whole figures of the cycle's case (moments and deflection) will be illustrated.

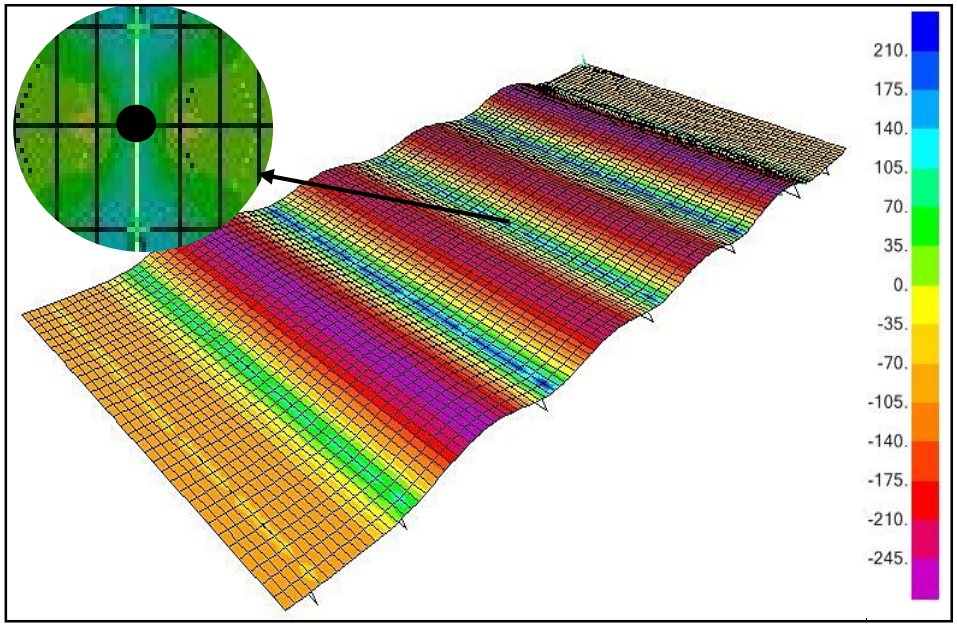

Figure 5.11 Steel deck moment (lb-in) under wind rating 135 psf

5.2.2 **FEM results for roof assembly (9′6″ fastener line distance, PL)**

Table 5.10 shows the results for 9′6″ fastener line spacing. As it can be seen, deflection, force and moment for the 75 psf wind pressure are three times bigger than 30 psf.

Table 5.10 FEM results for roof assembly (9′6″ fastener line distance)

Wind Rating (psf)	Net deflection, (in)	Fz (lb)	My (lb.in)
30	0.243	78.04	1.92
45	0.36	117.20	2.99
60	0.51	155.17	3.78
75	0.75	192.63	5.60

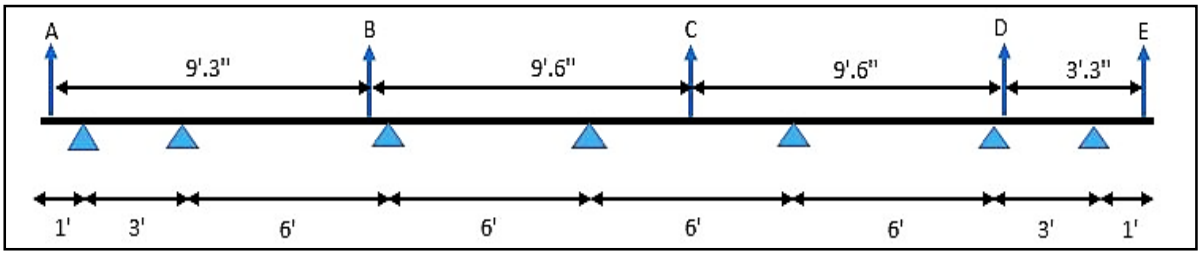

Figure 5.12 Point load scheme for roof assembly (9'6" fastener line distance)

Table 5.11 shows the point load calculation for this case that should be applied in the modelling. The calculation of the values in the table is explained in chapter 4 (loading). In this table, P.L is the point load of each row, which can be found from Figure 5.12. M stands for the load at the middle fasteners, and F/E stands for the load at the first or end fastener in each row.

Table 5.11 Point load calculation

Fasteners' line distance (ft)	Load (psf)	P.L.A (lb)		P.L.B (lb)		P.L.C (lb)		P.L.D (lb)		P.L.E (lb)	
		M	F/E	M	F/E	M	F/E	M	F/E	M	F/E
9.5	30	69.4	34.7	140.6	70.3	142.5	71.3	96.8	48.4	24.4	12.2
9.5	45	104.1	52.0	210.9	105.5	213.8	106.9	145.1	72.6	37.1	18.6
9.5	60	138.8	69.4	281.3	140.6	285.0	142.5	193.5	96.8	49.5	24.8
9.5	75	173.4	86.7	351.6	175.8	356.3	178.1	241.9	120.9	61.9	30.9

Figure 5.13 and 5.14 show the deflection and moment, respectively. Steel deck behaviour is the main object of this study; therefore, any results for the membrane layers or insulation are ignored. As shown in the figures, the biggest deflection and moment occurred at span E-F.

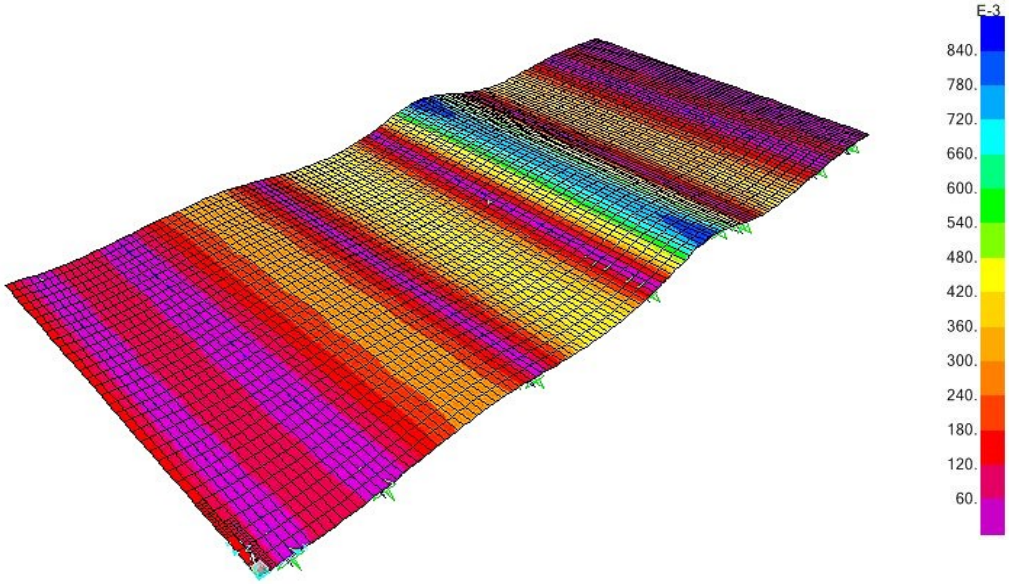

Figure 5.13 Steel deck deflection (in), 75 psf point load (9’6” fastener line distance)

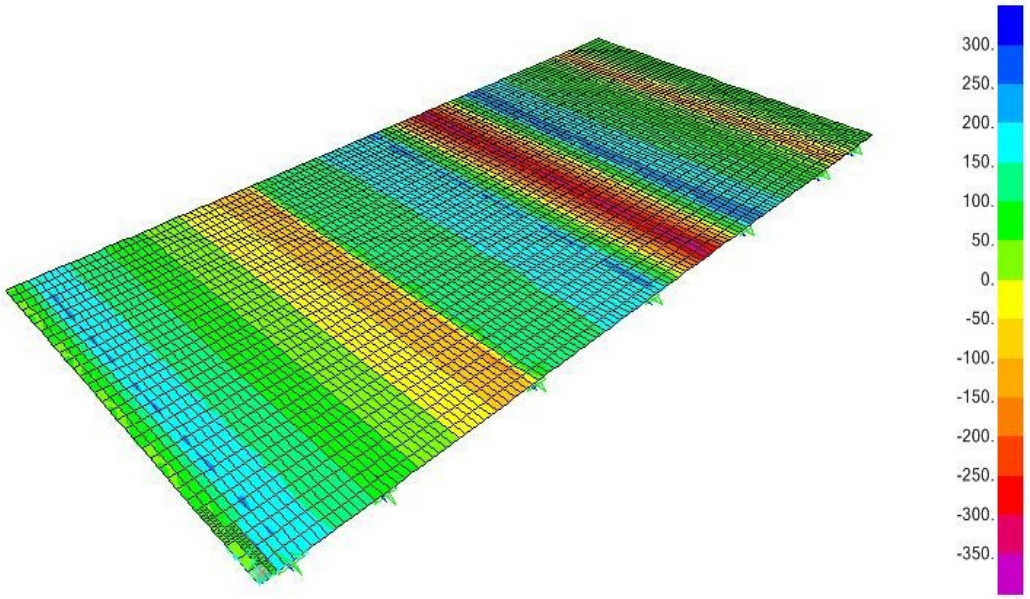

Figure 5.14 Moment for steel deck (lb-in), 75 psf point load (9’6” fastener line distance)

5.2.3 **FEM results for roof assembly (6′ fastener line distance, PL)**

Table 5.12 shows the values for the modelling of this case.

Table 5.12 FEM result for roof assembly (6′ fastener line distance)

Wind Rating (psf)	Net deflection, (in)	Fz (lb)	My (lb.in)
30	0.075	104.70	12.18
45	0.119	158.32	15.75
60	0.19	212.64	19.58
75	0.25	267.70	25.08
90	0.34	324.78	33.12
105	0.423	381.52	44.72
120	0.57	443.73	64.79

The procedure for the point load is the same as previous modelling, which means the tributary area for each fastener should be calculated by multiplying wind pressure to obtain the point load. Table 5.13 shows the point load calculation, and Figure 5.15 has provided a schematic picture of point loads.

Table 5.13 Point load calculation for roof assembly (6′ fastener line distance)

Fasteners' row distance (ft)	Load (psf)	L.L.A (lb)		L.L.B (lb)		L.L.C (lb)		L.L.D (lb)		L.L.E (lb)		L.L.F (lb)	
		M	F/E	M	F/E	M	F/E	M	F/E	M	F/E	M	F/E
6	30	45	22.5	90	45	90	45	90	45	90	45	45	22.5
6	45	67.5	33.75	135	67.5	135	67.5	135	67.5	135	67.5	67.5	33.75
6	60	90	45	180	90	180	90	180	90	180	90	90	45
6	75	112.5	56.25	225	112.5	225	112.5	225	112.5	225	112.5	112.5	56.25
6	90	135	67.5	270	135	270	135	270	135	270	135	135	67.5
6	105	157.5	78.75	315	157.5	315	157.5	315	157.5	315	157.5	157.5	78.75
6	120	180	90	360	180	360	180	360	180	360	180	180	90

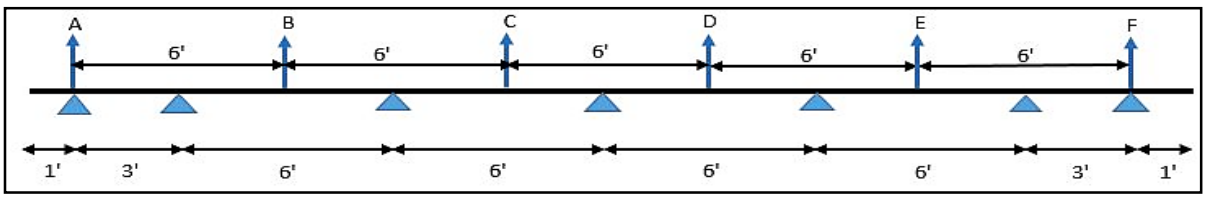

Figure 5.15 Point load scheme for roof assembly (6′ fastener line distance)

Figures 5.16 and 5.17 show deflection and moment analysis, respectively, for the wind pressure 120 psf. As it can be seen from the figures, the roof assembly has a symmetric behaviour when the fastener line spacing is 6′.

Figure 5.16 Deflection of roof assembly (in), 120 psf point load (6′ fastener line distance)

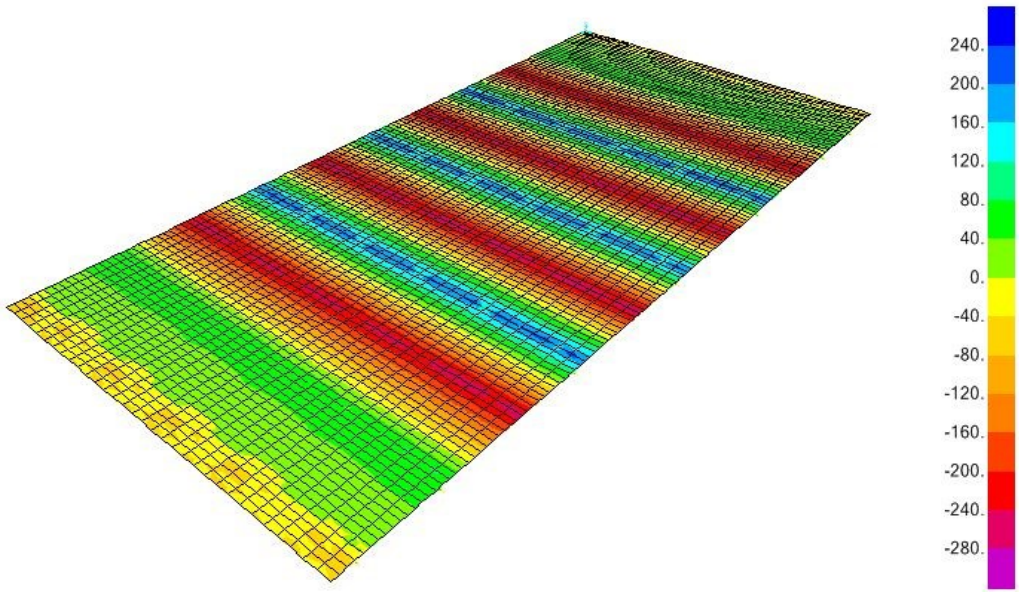

Figure 5.17 Moment of roof assembly (lb-in), 120 psf point load (6′ fastener line distance)

5.2.4 **FEM results for roof assembly (7′6″ fastener line distance, PL)**

Similar to the loading modelling assumptions used in the previous case (6′ fastener line distance, PL), calculating the point loads for the fasteners was required. Table 5.14 shows computed values for point loads. Figure 5.18 provides a drawing of the loading.

Table 5.14 Point load calculation for roof assembly (7′6″ fastener line distance)

Fasteners' row distance (ft)	Load (psf)	L.L.A (lb)		L.L.B (lb)		L.L.C (lb)		L.L.D (lb)		L.L.E (lb)		L.L.F (lb)	
		M	F/E	M	F/E	M	F/E	M	F/E	M	F/E	M	F/E
7.5	30	28.7	14.4	85.0	42.5	112.5	56.3	112.5	56.3	96.2	48.1	40.0	20.0
7.5	45	43.1	21.5	127.5	63.7	168.8	84.4	168.8	84.4	144.3	72.2	60.0	30.0
7.5	60	57.5	28.7	170.0	85.0	225.0	112.5	225.0	112.5	192.5	96.2	80.0	40.0
7.5	75	71.8	35.9	212.4	106.2	281.3	140.6	281.3	140.6	240.6	120.3	99.9	50.0
7.5	90	86.2	43.1	254.9	127.5	337.5	168.8	337.5	168.8	288.7	144.3	119.9	60.0

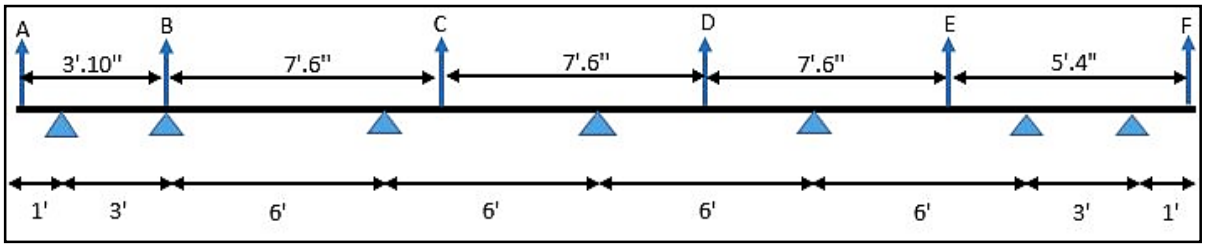

Figure 5.18 Point load scheme for roof assembly (7′6″ fastener line distance)

Table 5.15 shows the FEM results for this case. Figures 5.19 and 5.20 represent the deck deflection and moment, respectively, for induced wind pressure (90psf) that is applied on the membrane layer. It should be mentioned that a specific factor of 20 was used in the software output to obtain a clearer vision.

Table 5.15 FEM results for roof assembly (7′6″ fastener line distance)

Wind Rating (psf)	Net deflection, (in)	Fz (lb)	My (lb.in)
30	0.12	102.67	1.60
45	0.22	154.58	2.48
60	0.29	206.00	4.00
75	0.39	259.00	4.95
90	0.64	314.30	5.92

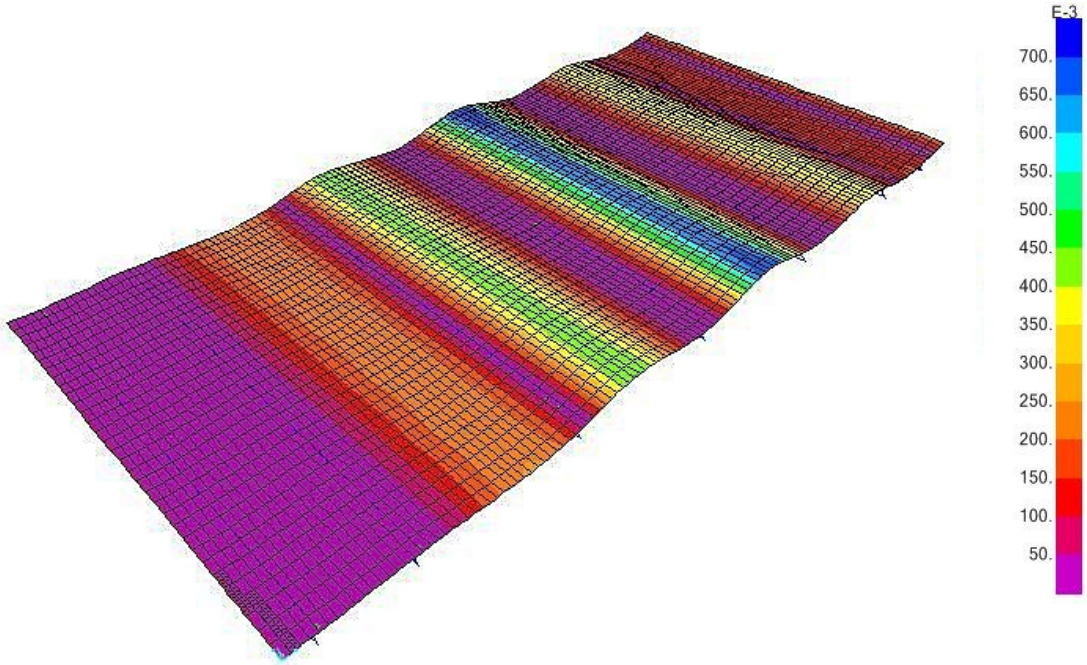

Figure 5.19 Deflection for roof assembly (in) under 90 psf point load (7’6” fastener line distance)

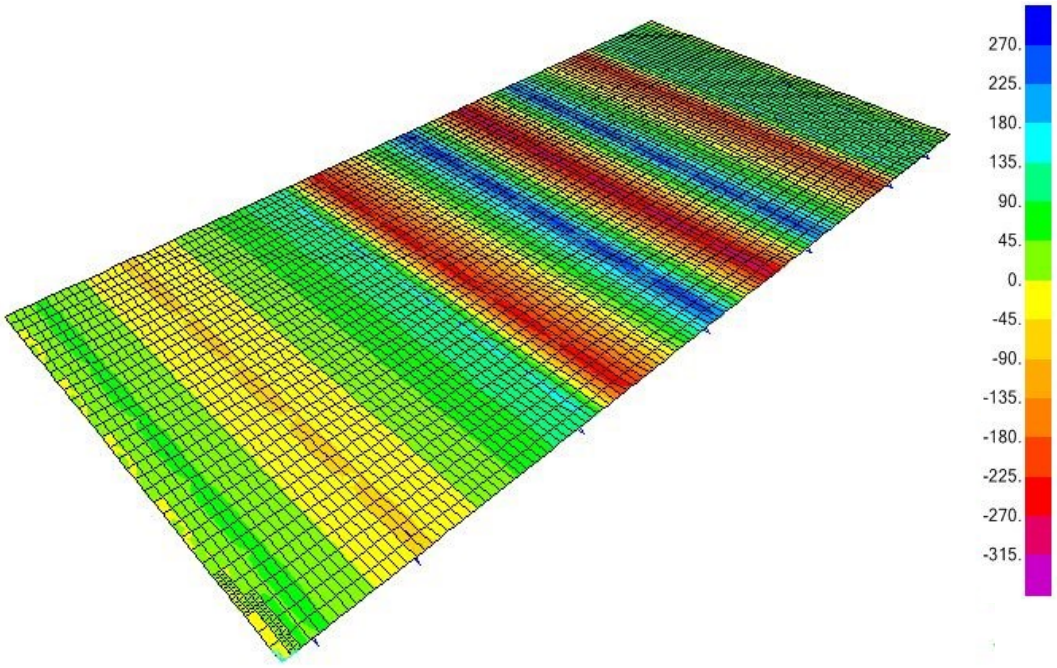

Figure 5.20 Moment for roof assembly (lb-in) under 90 psf point load (7’6” fastener line distance)

5.2.5 **FEM results for roof assembly (9′6″ fastener line distance, DL)**

The FM table is calculated based on the static equations for the two-dimensional beam analysis. To calculate the deflection and the moment, it is assumed that the wind pressure should be converted to point load at the connections between joists and deck (fasteners). However another assumption was used in this case and instead of point load, distributed load (DL) along the fasteners' line was applied. As a brief remark, it was assumed that there is a membrane strip along the fasteners line, so that the nodes were common to the membrane strip, the fasteners and the steel deck, and the distributed load was applied to this membrane strip. Due to the thickness of this strap, and non-structural behaviour, there is no additional stiffness effect for the overall FEM.

For modeling the load in this case, the uniform load acting on the fasteners was converted to the distributed load acting on the strip, by multiplying the wind pressure by half of the fastener line distance. In this way, the distributed load along the fasteners line can be estimated.

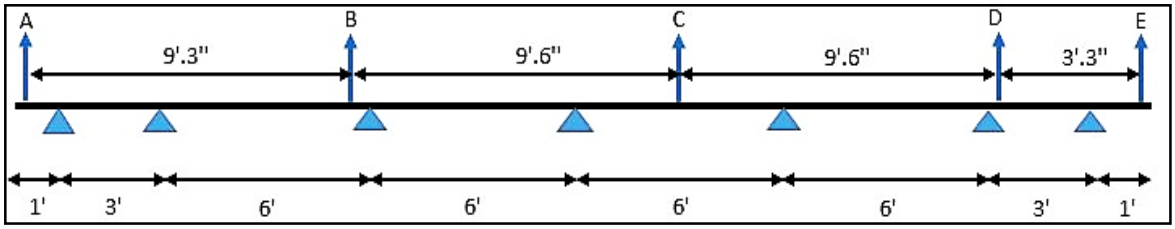

Figure 5.21 Fasteners' line distance

As it can be seen from Figure 5.21, for calculating the distributed load along the line A, it is required to multiply wind load (lb/ft^2) with half of the distance of fastener line to obtain the equivalent wind pressure in lb/ft. Table 5.16 shows the summarized calculation of the distributed load for this case. In this table, D.L means distributed load for the defined fasteners' lines (A, B, C, D and E).

Table 5.16 Calculation of distributed load for 9'6" fastener line distance

Fasteners' row distance (ft)	Load (psf)	D.L.A (lb/ft)	D.L.B (lb/ft)	D.L.C (lb/ft)	D.L.D (lb/ft)	D.L.E (lb/ft)
9.5	30	138.75	281.25	285	191.25	48.75
9.5	45	208.125	421.875	427.5	286.875	73.125
9.5	60	277.5	562.5	570	382.5	97.5
9.5	75	346.875	703.125	712.5	478.125	121.875

After loading the model for these wind pressures, Table 5.17 can be obtained. The noticeable point is that almost all values have increased significantly compared to the point load modelling. This means that distributed loads applied more pressure to the system, which are higher than real pressure. Figure 5.22 shows how distributed loads were applied to the roof assembly.

Table 5.17 FEM results for 9'6" fastener line distance (DL)

Wind Rating (psf)	Net deflection, (in)	Fz (lb)	My (lb.in)
30	0.345	434.59	8.46
45	0.485	472.46	10.27
60	0.608	500.82	11.18
75	0.894	545.77	13.20

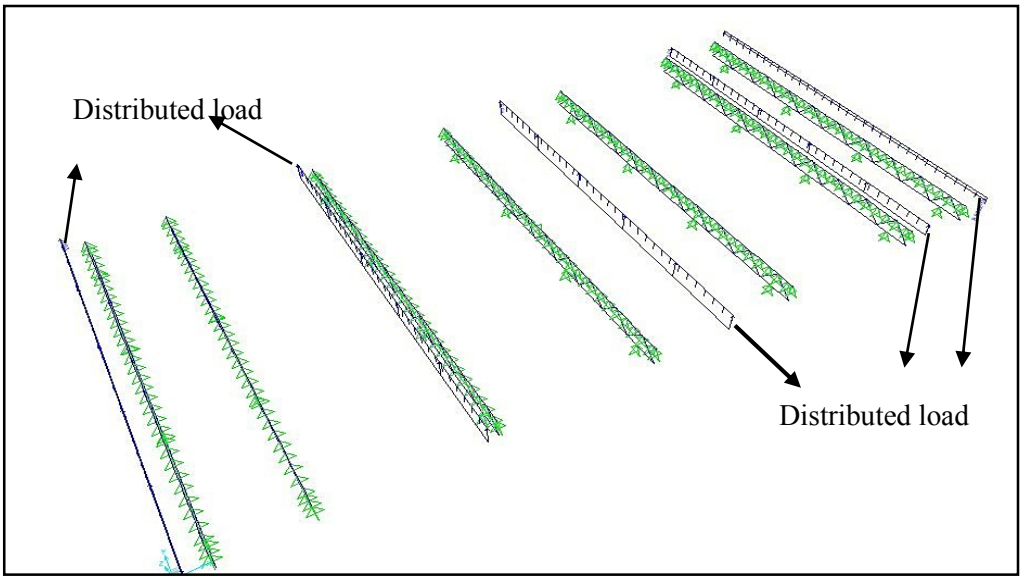

Figure 5.22 Distributed loading for 9'6" fastener line distance

Figure 5.23 shows deflection (inch) based on the loading method that was applied to the roof system. The deflection at span E-F is higher than other spans. The same result was obtained when it comes to moment as Figure 5.24 shows.

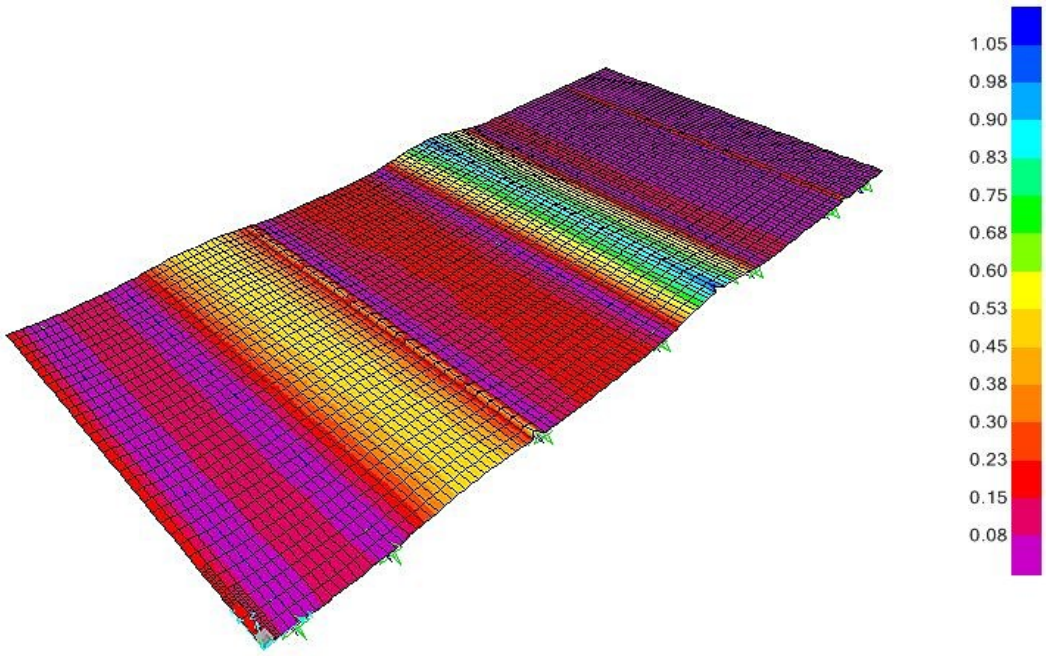

Figure 5.23 Deck deflection (in) under distributed load for 9’6” fastener line distance (75 psf)

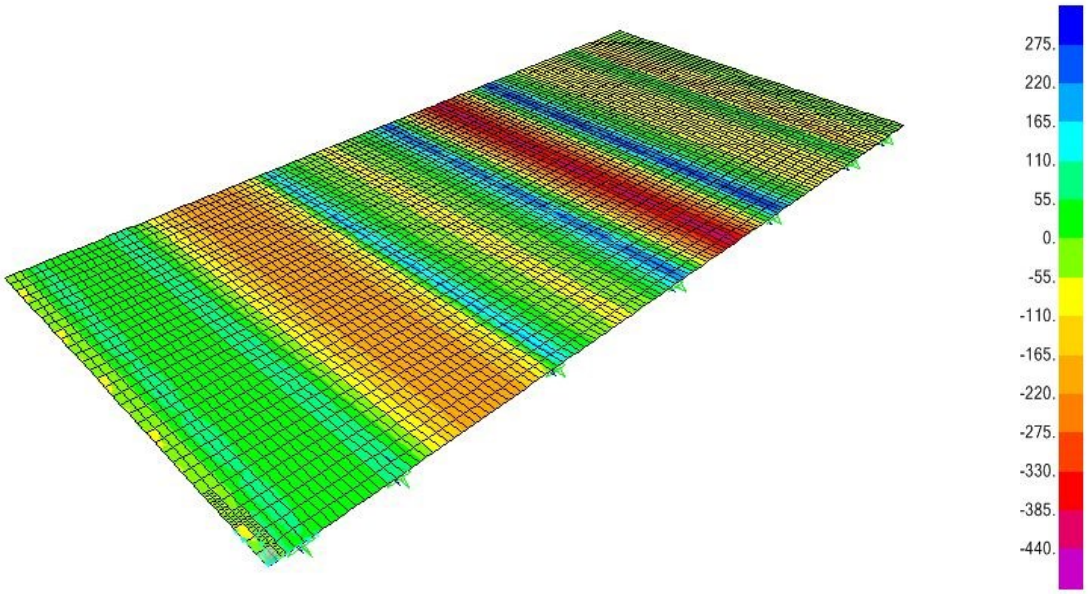

Figure 5.24 Deck moment (lb-in) under distributed load for 9’6” fastener line distance (75psf)

5.2.6 **FEM results for roof assembly (6′ fastener line distance, DL)**

The procedure, as in previous modelling, should be followed for this case as well. Table 5.18 shows the calculation of the distributed load.

Table 5.18 Calculation of distributed load for 6′ fastener line distance

Fasteners' row distance (ft)	Load (psf)	D.L.A (lb/ft)	D.L.B (lb/ft)	D.L.C (lb/ft)	D.L.D (lb/ft)	D.L.E (lb/ft)	D.L.F (lb/ft)
6	30	90	180	180	180	180	90
6	45	135	270	270	270	270	135
6	60	180	360	360	360	360	180
6	75	225	450	450	450	450	225
6	90	270	540	540	540	540	270
6	105	315	630	630	630	630	315
6	120	360	720	720	720	720	360

Table 5.19 presents the FEM results for this case. By way of comparison with the same case in point load modelling, no significant shift was observed in the results except for the small changes in deflection specifically for higher pressures. Due to symmetric loading acting on the roof assembly, the distributed line load and the point load show the same results. The small distance (6″) between two fasteners in one line can be another reason for having the same results for both loading systems.

Table 5.19 FEM results for 6′ fastener line distance (DL)

Wind Rating (psf)	Net deflection, (in)	Fz (lb)	My (lb.in)
30	0.076	104.70	12.18
45	0.12	158.32	15.75
60	0.19	212.64	19.58
75	0.256	267.70	25.08
90	0.346	324.78	33.120
105	0.425	381.52	44.720
120	0.539	441.00	64.790

Figure 5.25 shows deflection for the roof assembly. The laser recorded 5.39 (in) as the mid-span deflection. As it can be seen from Figure 5.26, the 6-component load cell calculated 64.8 (lb-in) for moment under the wind rate of 120 psf.

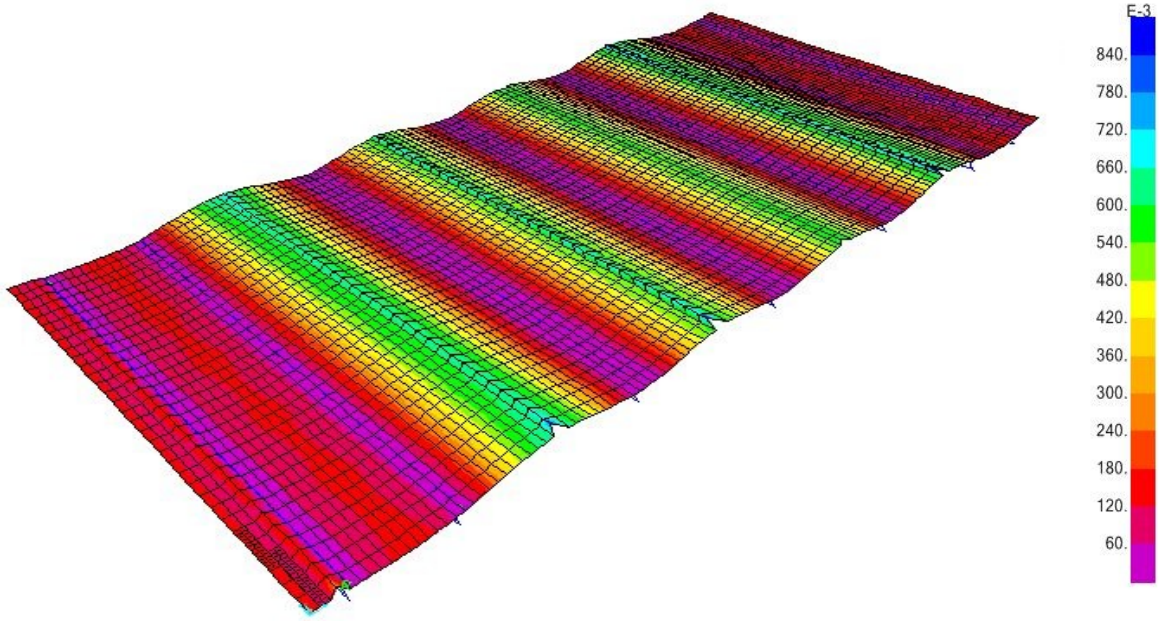

Figure 5.25 Deck deflection (in) under distributed load for 6′ fastener line distance (120 psf)

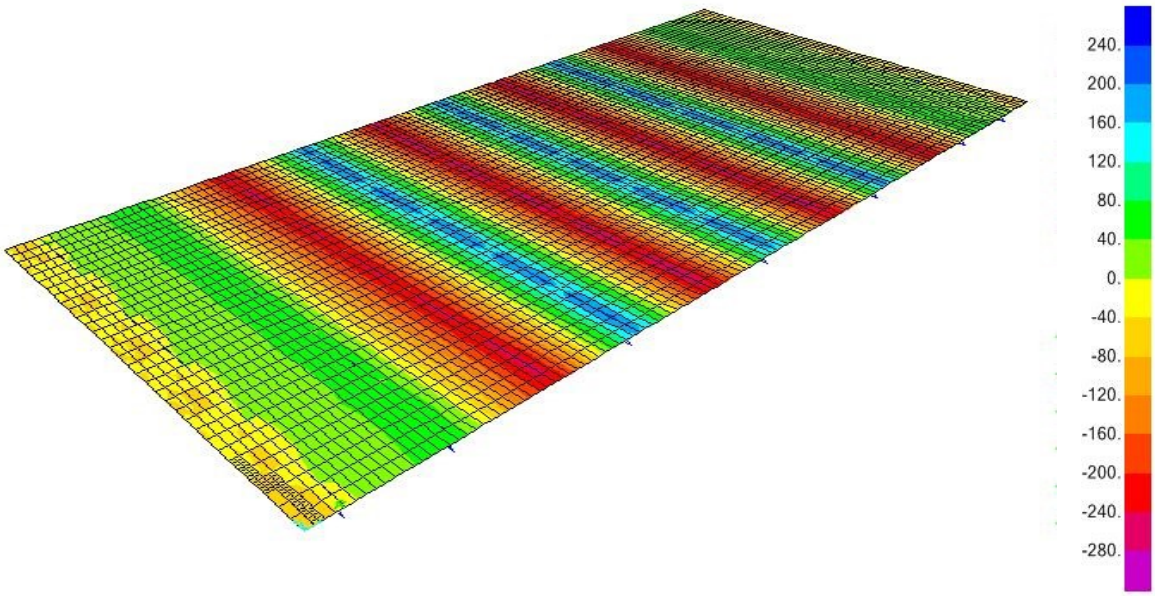

Figure 5.26 Deck moment (lb-in) under distributed load for 6′ fastener line distance (120 psf)

5.2.7 **FEM results for roof assembly (7′6″ fastener line distance, DL)**

Table 5.20 shows the converted uniform loads to distributed loads for this case.

Table 5.20 Distributed load calculation for 7′6″ fastener line distance

Fasteners' row distance (ft)	Load (psf)	D.L.A (lb/ft)	D.L.B (lb/ft)	D.L.C (lb/ft)	D.L.D (lb/ft)	D.L.E (lb/ft)	D.L.F (lb/ft)
7.5	30	57.45	169.95	225	225	192.45	79.95
7.5	45	86.175	254.925	337.5	337.5	288.675	119.925
7.5	60	114.9	339.9	450	450	384.9	159.9
7.5	75	143.625	424.875	562.5	562.5	481.125	199.875
7.5	90	172.35	509.85	675	675	577.35	239.85

Figure 5.27 shows the roof deflection under wind pressure of 90 psf. The span instrumented by lasers shows the bigger deflection compared to others.

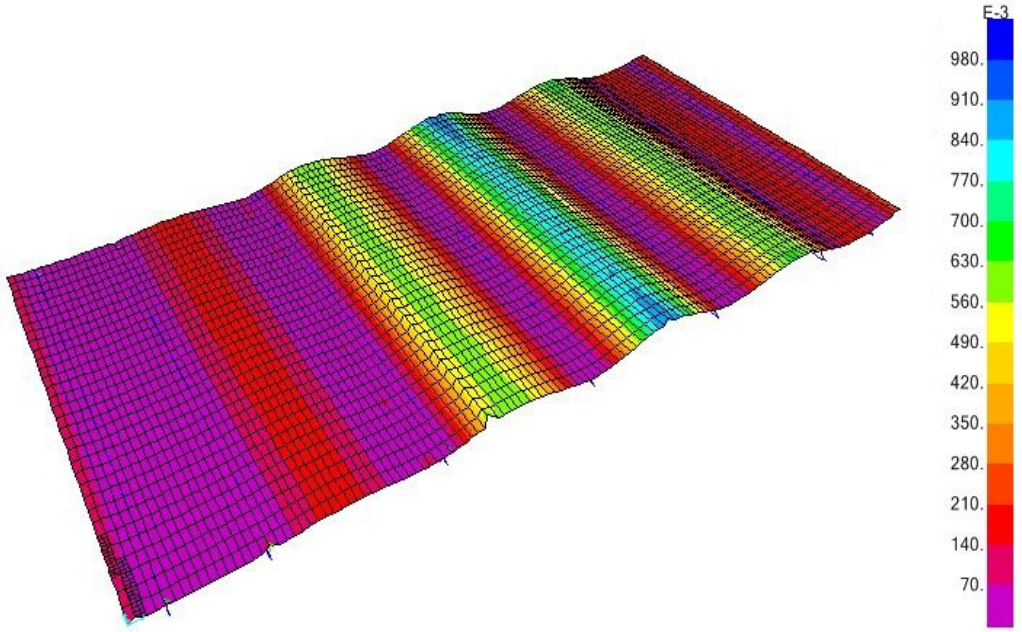

Figure 5.27 Deck deflection (in) under distributed load for 7′6″ fastener line distance (90 psf)

As it can be found from Table 5.21, the FEM results for the DL pattern were significantly higher than the 7′6″ roof assembly under the point loading (PL) system presented in section 5.2.4. This change occurred due to an asymmetric loading. Moreover, when the results are compared to experimental outcomes for the same case of 7′6″ roof assembly, it can be noticed that the deflection and moment values are very different, thus it can be concluded that the distributed loading (DL) system modelling is not representing the experiment assembly with accuracy. Figure 5.28 shows the FE moment results for the for 7′6″ roof assembly under DL loading pattern.

Table 5.21 FEM distributed results for 7′6″ fastener line distance

Wind Rating (psf)	Net deflection, (in)	Fz (lb)	My (lb.in)
30	0.262	469.10	5.43
45	0.36	522.14	7.32
60	0.46	575	8.32
75	0.575	628	9.48
90	0.84	685.0	11.32

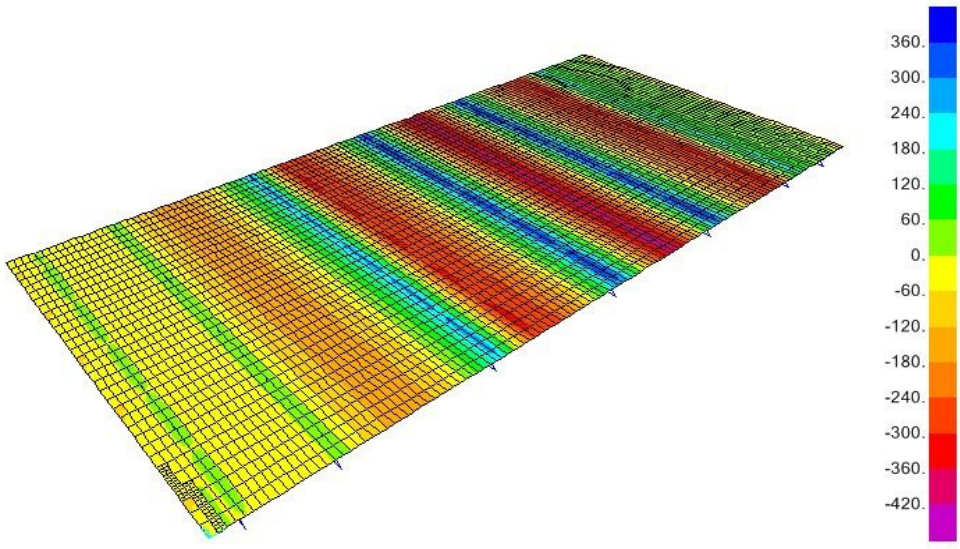

Figure 5.28 Deck moment (lb-in) under distributed load for 7′6″ fastener line distance (90 psf)

5.3 Comparison between experimental results and FEM

In this section, the results are discussed to determine whether the FEM modelling could be validated based on the comparison of experimental results, or if some modifications in modelling assumptions are needed to obtain accurate results. It was mentioned previously that this study follows the static analysis, which is used to publish the FM table. Therefore, any dynamic analysis was ignored in the modelling and the linear behaviour was followed. This part consists of two comparisons: the FEM results for the steel deck and roof assembly with point load assumptions are compared, then in the second section the FEM results of distributed loading will be compared with experimental outputs.

5.3.1 Experimental and FEM comparison (roof assembly with PL assumption)

Table 5.22 shows the deflection comparison between different cases. Moreover, Figure 5.29 provides the representation of the deflection results comparison as a ratio of the FEM results to experimental results.

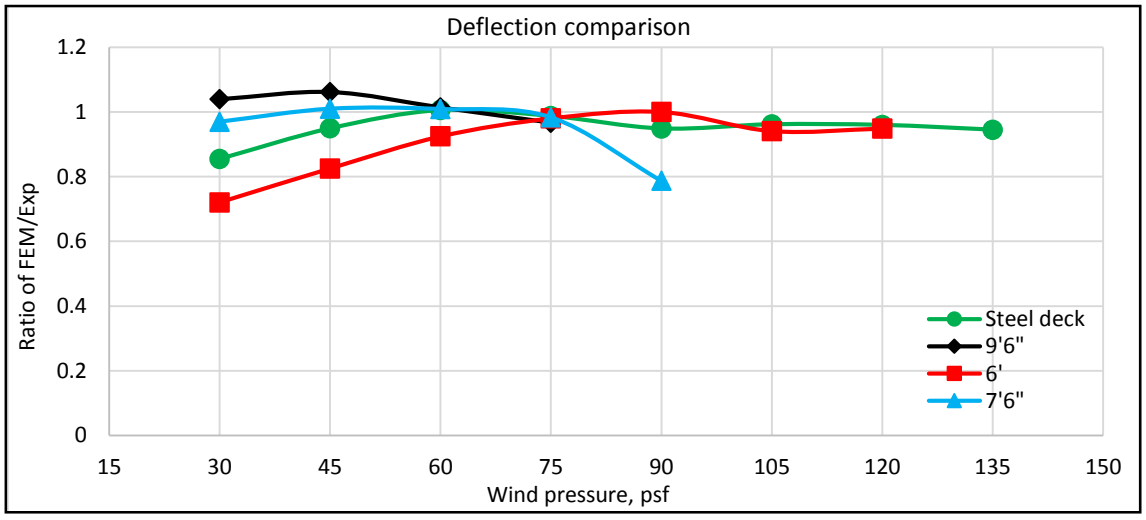

Figure 5.29 Deflection comparison for the ratio of FEM/Exp (roof assembly with PL in FEM)

Table 5.22 Deflections comparison (roof assembly with PL in FEM)

Experimental deflection (in)				
Wind rate (psf)	Steel Deck	9′6″ fastener line distance	6′ fastener line distance	7′6″ fastener line distance
30	0.043	0.235	0.104	0.129
45	0.075	0.339	0.144	0.198
60	0.104	0.504	0.205	0.287
75	0.136	0.777	0.255	0.396
90	0.17	-	0.34	0.821
105	0.196	-	0.45	-
120	0.225	-	0.6	-
135	0.257	-	-	-
FEM deflection (in)				
Wind rate (psf)	Steel Deck	9′6″ fastener line distance	6′ fastener line distance	7′6″ fastener line distance
30	0.037	0.243	0.075	0.125
45	0.07	0.36	0.119	0.2
60	0.105	0.51	0.19	0.289
75	0.135	0.75	0.25	0.389
90	0.16	-	0.34	0.645
105	0.189	-	0.423	-
120	0.216	-	0.57	-
135	0.242	-	-	-
Comparison results (ratio of FEM / Exp)				
Wind rate (psf)	Steel Deck	9′6″ fastener line distance	6′ fastener line distance	7′6″ fastener line distance
30	0.85	1.04	0.72	0.97
45	0.95	1.06	0.82	1.01
60	1	1.01	0.92	1.01
75	0.99	0.97	0.98	0.98
90	0.95	-	1	0.79
105	0.96	-	0.94	-
120	0.96	-	0.95	-
135	0.94	-	-	-

As it can be seen from Figure 5.29, except for the first loading cycle, all others are in an acceptable range, because the ratio FEM to experimental results is lower than 1.0, and the best matches occur between 60 psf and 90 psf. There are discrepancies between the FEM and experiments results for roof assembly with 6′ fasteners' line spacing, at 30 psf and 45 psf.

However this difference is less than 0.5″. Also there is a sudden drop in the deflection curve for 7′6″ fasteners' line spacing case at 90 psf, and it can be explained by the fact that the steel deck might have had nonlinear behaviour under this high pressure, meanwhile in the FE modelling only the linear behaviour was considered.

Table 5.23 Forces comparison (roof assembly with PL in FEM)

Experimental Force, Fz (lb)				
Wind rate (psf)	Steel Deck	9′6″ fastener line distance	6′ fastener line distance	7′6″ fastener line distance
30	70.97	92.33	101.74	153.37
45	130.42	177.89	230.02	280.57
60	171.67	222.94	289.04	362.79
75	244.34	255.73	374.96	436.35
90	307.49	-	459.21	511.61
105	368.67	-	544.94	-
120	407.40	-	612.29	-
135	470.88	-	-	-
FEM Force, Fz (lb)				
Wind rate (psf)	Steel Deck	9′6″ fastener line distance	6′ fastener line distance	7′6″ fastener line distance
30	90.96	78.04	104.70	102.67
45	137.23	117.20	158.32	154.58
60	183.61	155.17	212.64	206.00
75	229.51	192.63	267.70	259.00
90	275.41	-	324.78	314.30
105	321.32	-	381.52	-
120	367.00	-	443.73	-
135	413.12	-	-	-
Comparison results (ratio of FEM / Exp)				
Wind rate (psf)	Steel Deck	9′6″ fastener line distance	6′ fastener line distance	7′6″ fastener line distance
30	1.28	0.85	1.03	0.67
45	1.05	0.66	0.69	0.55
60	1.07	0.7	0.74	0.57
75	0.94	0.75	0.71	0.59
90	0.9	-	0.71	0.61
105	0.87	-	0.7	-
120	0.9	-	0.72	-
135	0.88	-	-	-

Table 5.23 shows the comparison between the FE results under PL loading pattern and the experimental forces, for all the investigated roof assemblies. Except for the steel deck case,

where the FE and experiment results show good agreement, for the other cases there is a significant discrepancy, as the values of the forces measured in the experiments and determined from the FE analysis with PL loading pattern modelling had considerable differences. Figure 5.30 provides graphic comparison of the ratio of the FEM and experiment forces. Based on these discrepancies, it can be mentioned that for the steel deck case, converting the uniformly distributed load into point loads is not an accurate assumption for representing the experimental conditions, and instead better results agreement could be obtained if the loads would be applied as a uniformly distributed force on the surface of the entire steel deck for the FEM or analysis calculation. Such loading case was not considered in this research, because the current investigation aims at clarifying the differences and similarities between the experimental results, the FEM results with PL modeling assumption and the FEM results with DL modeling assumption for roof assemblies with different fasteners lines distances; thus the DL loading assumption considers the loading distributed along the fasteners line, as detailed in the previous section.

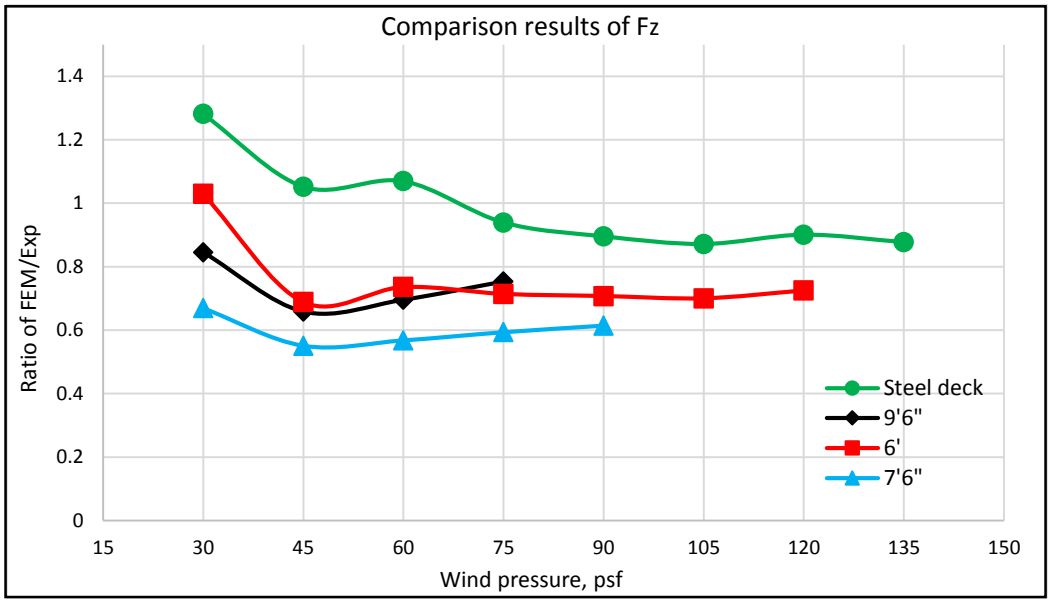

Figure 5.30 Force comparison for the ratio of FEM/Exp (roof assembly with PL in FEM)

Also from Figure 5.30 it can be noticed that for higher wind pressures the differences between FEM and experiments tend to increase especially for 9′6″ and 7′6″ roof assemblies. Moreover, the 6′ roof assembly has very similar evolution with the 9′6″ roof assembly case and both show good agreement between the experiments and FEM results.

Table 5.24 shows the results for bending moments at the specific location of the fastener, which is attached to the 6-components load cell in the experiments.

Table 5.24 Moments comparison (roof assembly with PL in FEM)

Experimental bending, My (lb.in)				
Wind rate (psf)	Steel Deck	9′6″ fastener line distance	6′ fastener line distance	7′6″ fastener line distance
30	8.14	2.68	11.85	1.95
45	8.07	3.91	17.46	3.05
60	10.33	4.55	23.90	5.53
75	18.17	0.00	33.07	6.72
90	26.85	-	43.01	6.78
105	37.24	-	57.89	-
120	51.91	-	82.47	-
135	68.66	-	-	-
FEM bending, My (lb.in)				
Wind rate (psf)	Steel Deck	9′6″ fastener line distance	6′ fastener line distance	7′6″ fastener line distance
30	7.36	1.92	12.18	1.60
45	9.44	2.99	15.75	2.48
60	12.24	3.78	19.58	4.00
75	18.90	5.60	25.08	4.95
90	29.96	-	33.12	5.92
105	37.50	-	44.72	-
120	45.76	-	64.79	-
135	54.74	-	-	-
Comparison results (ratio of FEM / Exp)				
Wind rate (psf)	Steel Deck	9′6″ fastener line distance	6′ fastener line distance	7′6″ fastener line distance
30	0.9	0.72	1.03	0.82
45	1.17	0.76	0.9	0.81
60	1.18	0.83	0.82	0.72
75	1.04	-	0.76	0.74
90	1.12	-	0.77	0.87
105	1.01	-	0.77	-
120	0.88	-	0.79	-
135	0.8	-	-	-

The most effective moment on deflection under wind pressure in Z direction is M_y, therefore, only this value for bending in the y direction is compared. Moreover, bending in other directions is almost zero thus they can be ignored. Figure 5.31 has provided some schematic data regarding the ratio of FEM results and experimental results.

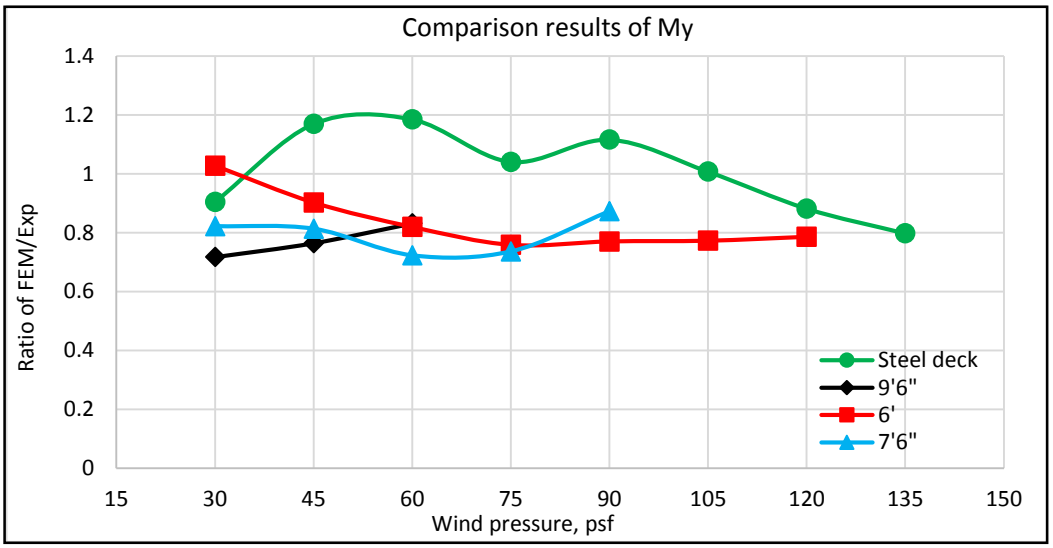

Figure 5.31 Moment comparison for the ratio of FEM/Exp (roof assembly with PL in FEM)

As it can be concluded from Figure 5.31, the moment results ratio for the steel deck case increased initially, but decreased at 75 psf, followed by another increase at 90 psf and again decreasing until 135 psf; this means for some wind rating cases the moments in FEM are bigger than experimental values. A different evolution was noticed for the cases of 9′6″ and 7′6″ roof assembly, which showed more consistency of the moment results ratios, without sudden variations, which means that by applying wind rating pressure as a PL loading pattern, the FEM is more efficient for replicating the experimental conditions. For the 6′ roof assembly, after the moments registered a dropping for lower wind force, their values tend to remain constant for the higher pressure, which means there is a constant ratio for both FEM and experimental moments results.

5.3.2 Experimental and FEM comparison (roof assembly with DL assumption)

The FM table was developed based on static analysis, which used linear formulation for determining the allowable moments and deflections. Therefore, when developing the FEM of the roofing assemblies, for verifying the deflection and moments obtained under the wind rating loading conditions, as specified by the FM table and as applied in the experiments, first the uniformly distributed load for the entire surface of the tested sample was converted to point loads (PL) applied at the location of the fasteners. The results obtained from the FE analysis for the PL loading system were shown in the section 5.3.1, but because discrepancies were noticed for some of the cases investigated, an additional assumption was taken into account, and instead of converting the uniformly distributed wind pressure to point loads (PL) applied at the attachment points between the deck and supports, the uniformly distributed load was converted to a line load, distributed along the line of the fasteners (DL). This loading system is considered as the second assumption and the results obtained from the FE analysis under this loading condition is presented in the current section. Figure 5.32 shows the ratio of deflections between the FEM and experimental cases performed.

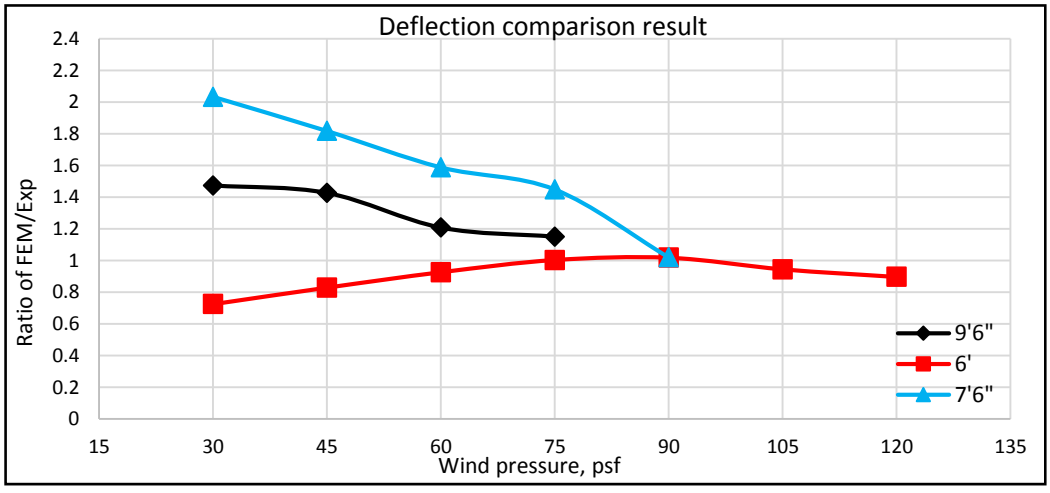

Figure 5.32 Deflection comparison for the ratio of FEM/Exp (roof assembly with DL in FEM)

Table 5.25 provides experimental and FEM deflection results under the DL loading pattern condition. Except for the roof assembly with 6′ fastener line distance that shows the same ratio of differences as the PL assumption, the others show a decreased ratio for higher pressure.

Table 5.25 Deflections comparison (roof assembly with DL in FEM)

Experimental deflection (in)			
Wind rate (psf)	9′6″ fastener line distance	6′ fastener line distance	7′6″ fastener line distance
30	0.234	0.104	0.129
45	0.34	0.144	0.198
60	0.504	0.206	0.287
75	0.777	0.256	0.396
90	-	0.341	0.821
105	-	0.45	-
120	-	0.602	-
FEM deflection (in)			
Wind rate (psf)	9′6″ fastener line distance	6′ fastener line distance	7′6″ fastener line distance
30	0.345	0.076	0.263
45	0.484	0.12	0.36
60	0.609	0.191	0.456
75	0.894	0.256	0.574
90	-	0.346	0.837
105	-	0.425	-
120	-	0.539	-
Comparison results (ratio of FEM / Exp)			
Wind rate (psf)	9′6″ fastener line distance	6′ fastener line distance	7′6″ fastener line distance
30	1.47	0.72	2.03
45	1.43	0.83	1.82
60	1.21	0.93	1.59
75	1.15	1.00	1.45
90	-	1.02	1.02
105	-	0.94	-
120	-	0.90	-

It was noted that the deflection increased gradually from the 6’ to 7’6” and 9’ roofing assemblies, especially for the lower wind rate pressure of 30 psf; meanwhile, for higher pressure, changes are significant. When compared with the deflections obtained under the PL loading conditions, the evolution of the deflections seems to have change significantly when

the wind pressure was applied as a distributed line load (DL). As it can be seen from Figure 5.32, the FEM to experiment deflection ratios for 7′6″ and 9′6″ roofing assemblies are 2 and 1.5, respectively. This means the deflection results from the FEM with DL loading pattern assumption are higher than experimentally obtained deflections.

Figure 5.33 shows a comparison for the FEM to experimental results ratios for the three roofing assembly cases analysed under a distributed loading (DL) system.

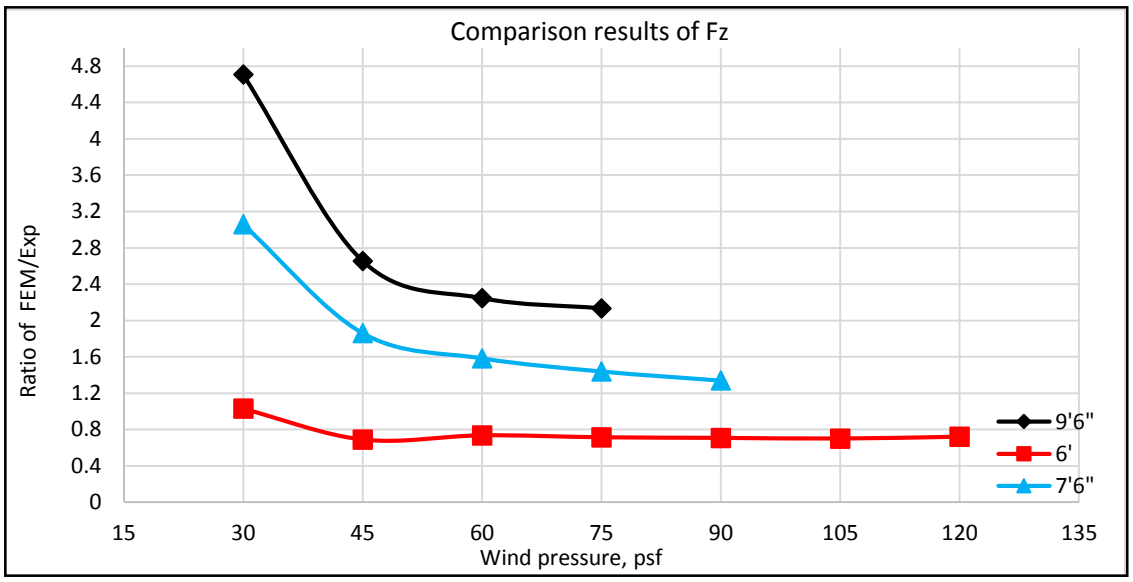

Figure 5.33 Force comparison for the ratio of FEM/Exp (roof assembly with DL in FEM)

As it can be noticed from Figure 5.33, the ratios of the FEM obtained vertical forces and the experimentally measured vertical forces have very similar evolution for the three roofing assemblies 6′, 7’6” and 9′. In spite of the very high ratios registered for lower wind rating pressures of 30 psf, a decreasing trendy was noticed for higher wind rating pressures, reaching a constant evolution, especially for the 6′ roofing assembly, for wind pressures between 60 psf and 120 psf. Therefore the FEM results and the experiment results had a very good agreement for each loading cycle applied for the roof assembly with 6′ fasteners’ line distance which had an almost constant ratio, slightly lower than 0.8 for higher wind rating pressures.

Table 5.26 provides the detailed vertical force results for the FEM with DL loading assumption and for the experimental cases investigated.

Table 5.26 Forces comparison (roof assembly with DL in FEM)

Experimental Force, Fz (lb)			
Wind rate (psf)	9′6″ fastener line distance	6′ fastener line distance	7′6″ fastener line distance
30	92.33	101.74	153.37
45	177.89	230.02	280.57
60	222.94	289.04	362.79
75	255.73	374.96	436.35
90	-	459.21	511.61
105	-	544.94	-
120	-	612.29	-
FEM Force, Fz (lb)			
Wind rate (psf)	9′6″ fastener line distance	6′ fastener line distance	7′6″ fastener line distance
30	434.59	104.70	469.10
45	472.46	158.32	522.14
60	500.82	212.64	574.70
75	545.77	267.70	628.00
90	-	324.78	685.00
105	-	381.52	-
120	-	441.00	-
Comparison results (ratio of FEM / Exp)			
Wind rate (psf)	9′6″ fastener line distance	6′ fastener line distance	7′6″ fastener line distance
30	4.71	1.03	3.06
45	2.66	0.69	1.86
60	2.25	0.74	1.58
75	2.13	0.71	1.44
90	-	0.71	1.34
105	-	0.7	-
120	-	0.72	-

The moment results comparison between the FEM and the experimental outputs considering the distributed line (DL) loading assumption is also presented as a final step in evaluating the discrepancies and agreements between the two loading systems (PL and DL) and the experimental loading conditions.

Table 5.27 provides the values of moment used for the comparison of the experimental outputs and the FEM results. Moreover, the ratio between results shows how much higher or lower the FEM moments are in regard to the experimentally obtained moments.

Table 5.27 Moments comparison (roof assembly with DL in FEM)

Experimental bending, My (lb.in)			
Wind rate (psf)	9′6″ fastener line distance	6′ fastener line distance	7′6″ fastener line distance
30	2.68	11.85	1.95
45	3.91	17.46	3.05
60	4.55	23.90	5.53
75	0.00	33.07	6.72
90	-	43.01	6.78
105	-	57.89	-
120	-	82.47	-
FEM bending, My (lb.in)			
Wind rate (psf)	9′6″ fastener line distance	6′ fastener line distance	7′6″ fastener line distance
30	8.46	12.18	5.43
45	10.27	15.75	7.32
60	11.18	19.58	8.32
75	13.20	25.08	9.48
90	-	33.12	11.32
105	-	44.72	-
120	-	64.79	-
Comparison results (ratio of FEM / Exp)			
Wind rate (psf)	9′6″ fastener line distance	6′ fastener line distance	7′6″ fastener line distance
30	3.16	1.03	2.79
45	2.63	0.9	2.4
60	2.46	0.82	1.51
75		0.76	1.41
90	-	0.77	1.67
105	-	0.77	-
120	-	0.79	-

As it can be seen from Figure 5.34, the ratio for 6′ roof assembly is approximately the same especially for the higher wind rating pressures; meanwhile, the other results tend to decrease, which means that the differences between the FEM results and experimental outputs reduce for higher pressure.

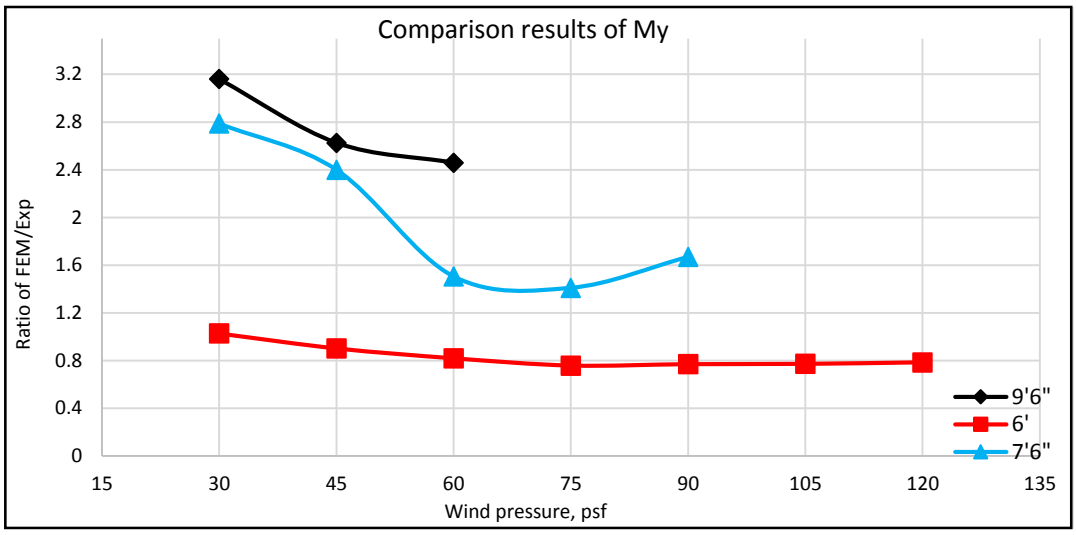

Figure 5.34 Moment comparison for the ratio of FEM/Exp (roof assembly with DL in FEM)

5.3.3 **FEM validation and extension for application to FM tables**

The deflections, moments and forces results comparison for the PL loading assumption, presented in Figures 5.29 to 5.31 above showed that most of the FEM to experiment results ratios are lower than 1.0, as expected; for the DL loading pattern the Figures 5.32 to 5.34 showed that except for the case of 6' roof assembly, for all the other cases the deflections, moments and forces obtained from the FEM were higher than those measured in the experiments. Overall the deflections, forces and moments obtained from the FEM and from the experiment proved to be in good agreement except for some roofing assemblies cases where differences were noticed as discussed below. For the point loading (PL) system, the deflection comparison showed differences between the FEM and experiments were in the acceptable range of 10%. By considering F_Z forces comparison, except for the case of 7′6″ fastener line spacing, which showed that the experimental results are higher than the FEM results, the others cases did not encounter major differences between the FEM results obtained under PL loading conditions and the experimental results; the FEM developed for the steel

deck case showed that the Fz forces were about 12% to 10.3% higher than the experimental results for lower wind rating pressures (30 psf to 60 psf) while for higher wind rating pressures the experimental results were slightly higher. Also the M_y moments results indicated that, except for the case of steel deck, the experimental results were slightly higher than the FEM results for the PL loading pattern, but for higher wind rating pressures the moment registered for 6' roof assembly case remained constant, while other cases increased, which means that with the increase of the wind pressure applied in the experiments and just before roofing assembly failure occurred, the experimentally measured moments decreased; this might be caused by the non-linear behaviour of the roofing assembly tested, which was not accounted for in the FEM developed. However, even if only the linear behaviour was modeled, overall the FEM results showed good agreement with the experimental results, the differences being lower than 10%. Only the steel deck case showed differences of up to 16%. For the second loading assumption, when the distributed loading (DL) system was modeled along the fasteners' lines for the roof assembly cases 9′6″, 6′ and 7′6″ fasteners line spacing, it could be noticed that the deflection, moments and forces results were higher than 10%, therefore were not in the acceptable range, except for the case of 6′ fasteners line spacing. For this case, for most of the wind rating pressures, the FEM to experiment results comparison ratio was between 0.8 and 1.0, which means there is a good agreement between the FEM model deflections, forces and moments and those measured in the experiment. The discrepancy between the FEM and the experiments results was higher for the other cases. These results discrepancies showed that the FEM of the roofing assemblies with DL loading model do not reflect entirely the experimental conditions for the wind uplift applied on the roofing assemblies tested; these experiments were better simulated by the PL loading system in the

FEM. Thus it can be concluded that the FE model with PL loading pattern developed for the investigated roof assemblies is validated with the experimental results. The validated FE model with the PL loading system was further extended in the current research and was applied for other steel deck span dimensions stipulated in the current FM table, because the results from the FEM with PL loading showed a better agreement when compared with the experimental results. Thus the FEM was extend by including additional dimensions for the steel deck span length of 3.5′, 5′ and 5.5′ and fasteners spacing of 3.5′, 4′, 4.5′, 5′ and 5.5′ . Table 5.28 shows the current FM table used for the design recommendations of the roof assemblies; one of the cases considered in the experimental part of this study was the 6′ fasteners line distance with the 6′ span, as indicated by the red oval in Table 5.28.

Table 5.28 FM table design [21], red oval shows experimental cases

Fastener Row Spacing (ft.)	MAX DECK SPANS (FT.) BY WIND RATING/FASTENER SPACING, SHEET GAUGE for 33 ksi																		
	Gauge	330	315	300	285	270	255	240	225	210	195	180	165	150	135	120	105	90	75	60
3.5	18	4.5	5.5	5.5	5.5	5.5	5.5	6	6	6	6	6	6	6	6	6	6	6	6	6
	20	-	4	4	4.5	4.5	4.5	5	5.5	5.5	5.5	6	6	6	6	6	6	6	6	6
	22	-	-	-	-	-	4	4	4.5	4.5	4.5	5.5	5.5	5.5	6	6	6	6	6	6
4	18	4.5	4.5	5	5	5	6	6	6	6	6	6	6	6	6	6	6	6	6	6
	20	-	-	-	-	4	4.5	4.5	5	5	5.5	6	6	6	6	6	6	6	6	6
	22	-	-	-	-	-	-	-	-	4	4.5	5	5	6	6	6	6	6	6	6
4.5	18	-	4	4	4.5	5	5	5.5	6	6	6	6	6	6	6	6	6	6	6	6
	20	-	-	-	-	-	-	4	4	5	5	5.5	6	6	6	6	6	6	6	6
	22	-	-	-	-	-	-	-	-	-	-	4	4.5	5	5.5	6	6	6	6	6
5	18	-	-	-	4	4	4.5	5	5	5.5	6	6	6	6	6	6	6	6	6	6
	20									4	4.5	5	5.5	6	6	6	6	6	6	6
	22	-	-	-	-	-	-	-	-	-	-	-	4	4.5	5	6	6	6	6	6
5.5	18	-	-	-	-	-	-	4	4.5	5	5.5	6	6	6	6	6	6	6	6	6
	20	-	-	-	-	-	-	-	-	-	-	4	4.5	5	6	6	6	6	6	6
	22	-	-	-	-	-	-	-	-	-	-	-	-	-	4.5	5	6	6	6	6
6	18	-	-	-	-	-	-	-	-	4	5	5.5	6	6	6	6	6	6	6	6
	20	-	-	-	-	-	-	-	-	-	-	-	-	4.5	5.5	6	6	6	6	6
	22	-	-	-	-	-	-	-	-	-	-	-	-	-	-	4.5	5.5	6	6	6
6.5	18	-	-	-	-	-	-	-	-	-	4	4.5	5.5	6	6	6	6	6	6	6
	20	-	-	-	-	-	-	-	-	-	-	-	-	-	4.5	5.5	6	6	6	6
	22	-	-	-	-	-	-	-	-	-	-	-	-	-	-	-	4.5	5.5	6	6

The FM design table (Table 5.28) recommends the use of 4.5′ and 5.5′ span lengths, for 120 psf and 105 psf wind ratings, respectively, but to provide extended cases for FM table, 6′ span length was also tested in the experiment for the same wind ratings of 105 psf and 120 psf. The experimental results for this case showed that the 6′ span length can successfully pass the wind

up-lift test for wind ratings up to 120 psf and can be considered within the acceptable limits based on the SPRI's allowable values of 0.33″ for deflection, and allowable values of 6072 lb.in and 6006 lb.in for negative and positive moments respectively [6].

The current FM table is calculated based on the uniform wind pressure on the steel deck converted to concentrated point loads at the fasteners lines [6], therefore, the FEM model developed, which showed good agreement with the experimental results, could be used for updating the FM table. For estimating the applicability of the developed FEM model for the recommendations provided by the FM table, the same cases were analysed by employing the proposed FEM; however when the deflections and moments' results obtained from the FEM were smaller than the allowable values, a bigger dimension of the steel deck span length was employed in the FE model and again the deflections and moments were verified against the allowable values. Thus some of the cases in the current FM table were considered too conservative and were proposed for an increase of the span dimension as indicated below. The FE analysis performed was similar with the FEM simulation with PL loading system explained in the sections above; therefore this procedure was not detailed in the current chapter, but all the steps were included in Appendix B. The summary of these results are presented in Table 5.29, which shows the updated version of the current FM table for 22 gauge and 33 ksi steel deck.

As it can be seen from the updated FM table (Table 5.29), for small fasteners' line distance, the span length is extended completely for 3.5′, 4′ and 4.5′ cases. By increasing the fasteners line distance, the span length and the wind rating decrease, therefore there is no recommended value provided for some of the cases which employ very high values for the three mentioned parameters. For example, for a 5′ fastener line distance, there is no value recommended for the

span length if the wind rate of 315 psf was applied, because the deflections and/or moments allowable limits were not met when the FEM was utilised. Similarly for the 6′ fastener line distance, there is an updated value of 4.5′ span length for 210 psf, but for higher wind ratings the allowable limits for moments and deflections were not met; the current FM table recommends a limit of 4.5′ span length for 120 psf for 22 gauge and no recommendations are provided for higher wind ratings (Table 5.28). Moreover, if the 4.5′ fastener line distance is compared with 5′ at 165 psf wind rate in the Table 5.28, it can be noticed that the span lengths are 4.5′ and 4′, respectively are recommended, which means the span is reduced by 0.5′.

Table 5.29 Updated FM table based on the validated the FEM

Fastener Row Spacing (ft)	Gauge	MAX DECK SPANS (FT) BY WIND RATING (PSF) / FASTENER SPACING, SHEET GAUGE FOR 33 Ksi																		
		330	315	300	285	270	255	240	225	210	195	180	165	150	135	120	105	90	75	60
3.5	18	.	.	.	.	.	.	.	.	.	.	.	.	.	.	.	.	.	.	.
	20	.	.	.	.	.	.	.	.	.	.	.	.	.	.	.	.	.	.	.
	22	5	5	5	5	5	5	5.5	6	6	6	6	6	6	6	6	6	6	6	6
4	18	.	.	.	.	.	.	.	.	.	.	.	.	.	.	.	.	.	.	.
	20	-	-	-	-	.	.	.	.	.	.	.	.	.	.	.	.	.	.	.
	22	4.5	4.5	5	5	5	5	5	5	5.5	6	6	6	6	6	6	6	6	6	6
4.5	18	.	.	.	.	.	.	.	.	.	.	.	.	.	.	.	.	.	.	.
	20	-	-	-	-	-	-	.	.	.	.	.	.	.	.	.	.	.	.	.
	22	4	4	4	4.5	4.5	5	5	5	5	5.5	5.5	6	6	6	6	6	6	6	6
5	18	.	.	.	.	.	.	.	.	.	.	.	.	.	.	.	.	.	.	.
	20								.	.	.	.	.	.	.	.	.	.	.	.
	22	.	.	4	4	4	4.5	4.5	5	5	5	5	5.5	6	6	6	6	6	6	6
5.5	18	-	-	-	-	-	-	-	-	-	-	-	-	-	-	-	-	-	-	.
	20	-	-	-	-	-	-	-	-	-	-	-	-	-	-	-	-	-	-	-
	22	-	-	-	-	-	4	4.5	4.5	5	5	5	5	5.5	6	6	6	6	6	6
6	18	-	-	-	-	-	-	-	-	-	-	-	-	-	-	-	-	-	-	.
	20	-	-	-	-	-	-	-	-	-	-	-	-	-	-	-	-	-	-	.
	22	.	.	.	.	.	.	.	.	4.5	4.5	5	5	5	5.5	6	6	6	6	6

The updated values in Table 5.29 were obtained by comparing the FEM results with the allowable values determined as per the formulations recommended by SPRI. A numerical example which shows the steps of calculation of allowable values is shown below.

In order to convert the uniform load to the point load the following steps are performed:

a) Calculation of the tributary area:

For the case of 6′ the fastener line distance the tributary area is (Fig. 5.35):

$$A = X * Y \tag{5-1}$$

$$A = 6' * 0.5' = 3' \tag{5-2}$$

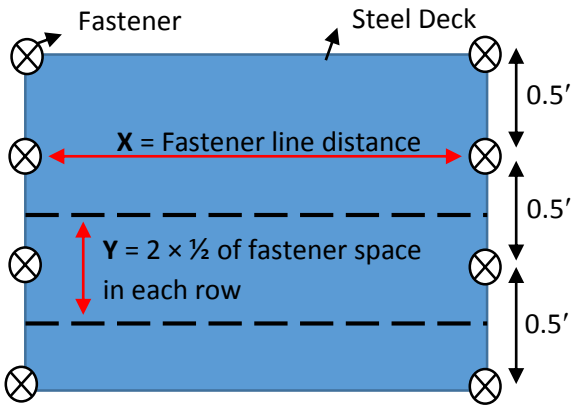

Figure 5.35 Tributary area for 6′ the fastener line case

b) Multiplying wind rate by tributary area, for the wind rate is 60 psf, a point load is obtained as follows:

W = 60 psf

$$P = W \times A \tag{5-3}$$

$$P = 60\ (lb/ft^2) \times 3\ (ft^2) = 180\ \text{lb} \tag{5-4}$$

For the FM table development, the results of the FEM for the deflections and moments must be compared with the allowable values, which were determined based on the SPRI and CSSBI [6] recommendations.

- **Allowable Deflection**

The allowable deflection is calculated based on the CSSBI formula considering the following procedure:

For a single span [24]:

$$\Delta = \frac{5\,W\,L^4}{384\,E\,I} \tag{5-5}$$

For two equal spans [24]:

Δ = 0.42 times single span value

For three or more equal spans [24]:

Δ = 0.53 times single span value

Where,

Δ = deflection, in

W = maximum uniform load, psf

L = span length, in

E = modulus of elasticity of steel, ksi

I = Moment of inertia of the steel roof deck with top flange of the deck in compression, in^4

For example, for 6′ span length with the wind rating of 90 psf, the allowable deflection Δ is 0.33 inch.

For each case presented in the Table 5.29, the FEM deflection must be compared with the allowable deflection. Table 5.30 shows the deflection results for the three steel deck spans

AB, BC and CD and the comparison with the allowable deflection determined based on the Eq. 5.5 for cases of 3.5 to 6 fastener line distances and wind ratings up to 255 psf. If the FEM deflection is smaller than the allowable value, the result is considered as acceptable (green box), otherwise it is not accepted (yellow box).

Table 5.30 Comparison of FEM and allowable deflection

22 Gauge												
Fastener row(ft)	Load (psf)	$D_{allowable(in)}$	Span Length (ft)	SAP Deflection								
				A-B(in)		Da / Ds	B-C(in)		Da / Ds	C-D(in)		Da / Ds
3.5	225	0.83	6	0.68	ok	1.224763	0.06	ok	13.88065	0.74	ok	1.125458
3.5	240	0.89	6	0.73	ok	1.216933	0.06	ok	14.80602	0.8	ok	1.110452
4	195	0.72	6	0.66	ok	1.093627	0.01	ok	72.17937	0.66	ok	1.093627
4	210	0.78	6	0.72	ok	1.079606	0.02	ok	38.86581	0.72	ok	1.079606
4.5	165	0.61	6	0.6	ok	1.017914	-0.02	ok	30.53742	0.56	ok	1.090622
4.5	180	0.67	6	0.65	ok	1.025032	-0.03	ok	22.20904	0.6	ok	1.110452
5	150	0.56	6	0.55	ok	1.009502	0.09	ok	6.169177	0.23	ok	2.414026
5	165	0.61	6	0.6	ok	1.017914	0.1	ok	6.107485	0.26	ok	2.349033
5.5	135	0.50	6	0.5	ok	1	0.09	ok	5.552259	0.49	ok	1.019803
5.5	150	0.56	6	0.63	no	0.881311	0.01	ok	55.52259	0.55	ok	1.009502
6	90	0.33	6	0.33	ok	1	0.12	ok	2.77613	0.33	ok	1
3.5	240	0.63	5.5	0.52	ok	1.206236	0.06	ok	10.45404	0.47	ok	1.334558
3.5	255	0.67	5.5	0.58	ok	1.149043	0.06	ok	11.10742	0.5	ok	1.33289
4	210	0.55	5.5	0.54	ok	1.018519	-0.025	ok	22	0.55	ok	1
4	225	0.59	5.5	0.55	ok	1.069163	-0.03	ok	19.60133	0.6	no	0.980066
4.5	195	0.51	5.5	0.5	ok	1.019269	0.05	ok	10.19269	0.27	ok	1.887535
5	165	0.43	5.5	0.42	ok	1.026736	0.08	ok	5.390365	0.42	ok	1.026736
5.5	150	0.40	5.5	0.39	ok	1.025641	0.1	ok	4	0.38	ok	1.052632

- **Allowable Moment**

The moment M_y has the highest impact on the steel deck, as the experimental results showed; therefore, the allowable negative moment at mid-span and the positive moment at supports were compared with the moment results obtained from the FEM.

To determine the allowable moment, the formulas below should be used (CSSBI) [9]:

$$M_{allowable} = F_y \times S \quad (5\text{-}6)$$

The F_y is design yield stress and S is steel deck section modulus

Positive bending, $M_{allowable} = 33000 lb/in^2 \times 0.182 in^3 = 6006$ lb.in (5-7)

Negative bending, $M_{allowable} = 33000$ lb/in^2 $\times$ 0.184 in^3 = 6072 lb.in (5-8)

For the moments' comparison, the middle part of six inches is considered for the mid-span moments. Table 5.31 shows the results comparison between FEM moment results and allowable moment values.

Table 5.31 Comparison of FEM and allowable negative moment

22 Gauge												
Fastener row(ft)	Midspan(-)											
	M_{FM} (lb.in)	Load (lb/ft^2)	span(ft)	A-B M_{sap} (lb.in)		MF / MS	B-C M_{sap} (lb.in)		MF / MS	C-D M_{sap} (lb.in)		MF / MS
3.5	-6072	225	6	-6071.4	ok	1.0001	-914	ok	6.643326	-3113.4	ok	1.95028
3.5	-6072	240	6	-6488	no	0.93588	-975	ok	6.227692	-3321	ok	1.82836
4	-6072	195	6	-5970	ok	1.01709	-252.2	ok	24.07613	-5166.11	ok	1.17535
4	-6072	210	6	-6428.2	no	0.94459	-234.2	ok	25.92656	-4797.1	ok	1.26576
4.5	-6072	165	6	-5717.3	ok	1.06204	-208.8	ok	29.08046	-2296.8	ok	2.64368
4.5	-6072	180	6	-6237	no	0.97354	-227.8	ok	26.65496	-2505.5	ok	2.42347
5	-6072	150	6	-5677.14	ok	1.06955	-1000	ok	6.072	-937.8	ok	6.47473
5	-6072	165	6	-6245	no	0.9723	-1100.3	ok	5.518495	-1031.5	ok	5.88657
5.5	-6072	135	6	-5738.24	ok	1.05816	-1627.5	ok	3.730876	-2585	ok	2.34894
5.5	-6072	150	6	-6376	no	0.95232	-1808.3	ok	3.35785	-2872.2	ok	2.11406
6	-6072	150	6	-5670	ok	1.0709	-3240	ok	1.874074	-5670	ok	1.0709
6	-6072	165	6	-6237	no	0.97354	-3564.1	ok	1.703656	-6237	no	0.97354
3.5	-6072	240	5.5	-5847.8	ok	1.03834	-493.8	ok	12.29648	-3351.26	ok	1.81186
3.5	-6072	255	5.5	-6213.3	no	0.97726	-524.6	ok	11.57453	-3560.8	ok	1.70523
4	-6072	210	5.5	-5929	ok	1.02412	-125.5	ok	48.38247	-2918	ok	2.08088
4	-6072	225	5.5	-6352	no	0.95592	-134.5	ok	45.14498	-3126.5	ok	1.94211
4.5	-6072	195	5.5	-6070	ok	1.00033	-868.4	ok	6.99217	-1218.7	ok	4.98236
5	-6072	165	5.5	-5831	ok	1.04133	-1579.5	ok	3.844255	-2459.3	ok	2.469
5.5	-6072	150	5.5	-4746	ok	1.27939	-2721.8	ok	2.230877	-4746	ok	1.27939
6	-6072	135	5.5	-5882.3	ok	1.03225	-1761.5	ok	3.447062	-2500	ok	2.4288

Similarly, Table 5.32 shows the positive moment comparison between FEM moment results and allowable moment values. The A M_{sap} and D M_{sap} columns which are the first and last spans of the FEM have no value due to the principle of equilibrium which means that the summation of all the forces (applied forces and the reaction of supports) is equal to zero.

Based on the moment diagram and the loading patterns the moments in the first and last supports are zero. In the appendix, the moment diagrams and numerical calculations show how the moments in the first and last spans are zero.

Table 5.32 Comparison of FEM and allowable positive moment

22 Gauge													
Fastener row(ft)	Support (+)												
	M_{FM} (lb.in)	A M_{sap} (lb.in)		MF / Ms	B M_{sap} (lb.in)		MF / Ms	C M_{sap} (lb.in)		MF / Ms	D M_{sap} (lb.in)		MF / Ms
3.5	6006	0	ok	-	4399	ok	1.36531	5585.8	ok	1.07523	0	ok	-
3.5	6006	0	ok	-	4692.12	ok	1.28002	5958.2	ok	1.00802	0	ok	-
4	6006	0	ok	-	4445.8	ok	1.35094	4445.8	ok	1.35094	0	ok	-
4	6006	0	ok	-	4787.8	ok	1.25444	4787.8	ok	1.25444	0	ok	-
4.5	6006	0	ok	-	4176	ok	1.43822	2090	ok	2.87368	0	ok	-
4.5	6006	0	ok	-	4555.5	ok	1.31841	2279	ok	2.63537	0	ok	-
5	6006	0	ok	-	4375	ok	1.3728	2625	ok	2.288	0	ok	-
5	6006	0	ok	-	4812.3	ok	1.24805	2887.3	ok	2.08014	0	ok	-
5.5	6006	0	ok	-	4142.5	ok	1.44985	3740.2	ok	1.6058	0	ok	-
5.5	6006	0	ok	-	4603	ok	1.3048	4155.8	ok	1.44521	0	ok	-
6	6006	0	ok	-	4860	ok	1.2358	4860	ok	1.2358	0	ok	-
6	6006	0	ok	-	5346	ok	1.12346	5346	ok	1.12346	0	ok	-
3.5	6006	0	ok	-	4476.7	ok	1.34161	4652.4	ok	1.29095	0	ok	-
3.5	6006	0	ok	-	4756.5	ok	1.26269	4943.2	ok	1.215	0	ok	-
4	6006	0	ok	-	4343.6	ok	1.38272	2997.5	ok	2.00367	0	ok	-
4	6006	0	ok	-	4654	ok	1.2905	3211.57	ok	1.87011	0	ok	-
4.5	6006	0	ok	-	4668.2	ok	1.28658	2838.5	ok	2.11591	0	ok	-
5	6006	0	ok	-	4250.7	ok	1.41294	3754.5	ok	1.59968	0	ok	-
5.5	6006	0	ok	-	4099	ok	1.46524	4095	ok	1.46667	0	ok	-
6	6006	0	ok	-	3920	ok	1.53214	3514.3	ok	1.70902	0	ok	-

By comparing Tables 5.30 to 5.32 it can be noticed that some of the cases such as 5.5′ span length with 4′ fastener row distance under 225 psf wind pressure or 6′ span length with 4.5′ fastener row distance under 180 psf wind pressure, had deflections lower than the allowable deflection condition, however for these cases the moments were higher than the allowable (negative) moment values; therefore these cases were not included in the updated FM table proposed in Table 5.29.

Overall, following the same FE analysis as described at the beginning of Chapter 5, more cases for the steel deck span dimensions recommendations were formulated for higher wind ratings; the lower corner of the FM table however, could not be entirely populated with steel deck span dimensions, because no experiments were performed for these critical cases with very high wind ratings and bigger span dimensions, and for which, the FEM would not be validated; considering the results obtained for the investigated cases, linear material behavior assumption might not lead to the deflection and moments' results the experiments might report. Therefore a new experimental program, with a FEM development and validation step and FE analysis specifically for these critical cases is required for proposing the steel deck dimensions for the lower corner of the FM table.

Chapter 6 Conclusions

In this chapter, concluding remarks were made regarding the research objectives stated at beginning of the current research project and the research targets which were put forward for further recommended research. The main objectives of the current research project were as follows:

- To develop and validate the finite element model for the roof assembly, with the results obtained from the experimental cases.
- To evaluate the static wind uplift force on the flat roof using the finite element model under point load and distributed load assumptions.
- To provide an application of the validated FEM for updating the conservative FM design tables, based on the allowable stresses and deflections.

To achieve these goals, a FEM was developed, representing the roof assembly and the loading conditions used in the experiments which were conducted as per the recommendations of the current FM design table. One of the roofing assembly cases tested as part of this study had dimensions of 6′ for the steel deck span with 6′ fastener line distance, and this case was used to validate the FEM developed; two loading patterns were analysed and as shown in Chapter 5, the FEM with PL loading assumption had deflections, moments and forces results within an acceptable 10% difference from the experimentally measured deflections, moments and forces, for most of the roofing assemblies cases and wind ratings investigated; therefore the FEM with PL loading assumption was employed for providing an application for other steel deck span dimensions and fasteners spacing, which could serve for updating the FM table.

The data necessary for updating the FM table, included the following: i) positive moment verification at supports, ii) negative moment verification at mid-spans and iii) deflection verification at mid-spans of the steel deck. The FEM deflections moments and forces results obtained for the roofing assemblies under the distributed line (DL) load, were not in good agreement with the experimental results, thus it could be concluded that, the DL assumption could not be used to simulate the experimental conditions for the wind uplift on roofing systems. The FEM developed with point load (PL) model however, provided results which were consistent with the deflections and moments measured during the experiments. Moreover, as shown in Table 5.29, the case of 6′ steel deck span can be used for investigating more wind rating pressures when comparison with the current FM table is conducted. By applying the PL-FEM model for the fasteners distances and steel deck span dimensions stipulated in the FM tables, it was noticed that for more than 100 cases the deflections and moments obtained were below the allowable limits for the given wind ratings; thus bigger values for the wind ratings were applied, and the new cases of steel deck span dimensions and fasteners distance which were still within the allowable deflection and moments, were reported in Table 5.29. This table can be useful when a future update of the FM table will be considered, because it contains new steel deck span cases and wind ratings, for which the allowable deflections and moments verifications were performed. For instance, if the 22 gauge steel deck of 6′ span with fastener line spacing of 3.5′ is considered the current FM table wind rating pressures of up to 90 psf can be applied, while in the FEM model used for proposing the updated FM table, this steel deck case proved to have results within the acceptable limits when wind ratings of up to 120 psf were applied.

Finally, after each case was individually simulated and the results were compared with the SPRI's allowable values, it was determined that the current FM table contains conservative values for some of the steel deck span dimensions; for a better representation, the structural design principle based on which the values in the FM design table are determined should consider the three-dimensional aspect of the roofing assembly, especially when converting the uniformly distributed loading to the point loading.

When the experiments were performed, it was noticed that the vertical force F_z was higher when compared to the force on the other two directions, therefore the effect of this vertical force F_z should be also considered when the wind uplift pressure is investigated. However, there were some discrepancies between the FE model results and the measurements registered by the 6-component load cell, during certain experimental cases, which might be caused by one of the following reasons:

- The outputs of experiments were based on the uniform loading system, but in the FEM, except for the steel deck, the uniform loads were converted to point loads, which was applied to the specific locations (fasteners) to follow the FM and SPRI's assumptions [17].
- The 6-components load cell is one of the most sensitive measuring devices, and it was the first time this instrument has been used for wind uplift tests conducted on roofing assemblies. Moreover, a custom-made fastener was attached to a 6-component load cell, and the static loading cycles were run continuously, which leads to movement and probably loosening of the fastener at the joist or at the connection with the 6-component load cell. Therefore whenever the fastener moves from the positive direction to a negative direction

on one of the three axes, the 6-components load cell interpreted this as a significant pressure, and the recorded data suddenly increased or dropped, which must be an error.

Based on the above issues, some errors have been observed especially for the F_z data in the measurements outputs that should be corrected manually by deleting the incorrect record in the first load result section of the Excel file (it is described in section 3.4.2.3).

The second objective of this research was developing a FEM which can replicate the experimental conditions used when testing of different roofing assemblies was conducted for static wind uplift pressure. Therefore, as part of a preliminary study, the 2D-FE modelling was developed for roofing assemblies, and the results were compared with SPRI formulations for allowable deflections and moments. After confirming the basic concept of the FE modelling developed for the general case of three 6′ span with 3′ steel sheets' width, the 2D model was expanded and modified to reflect the current experimental configuration.

With respect to the third objective, different roofing assemblies configurations were considered for the FE modelling step (Figure 1.5 in section 1.4) of this research, but when the results were compared (Figure 1.5 in section 1.4), some obvious differences were noticed. Thus, by considering additional roofing assemblies configurations for the FEM, the preliminary 2D and 3D models provided important information regarding the results accuracy of the basic modeling assumptions used in this study.

It can be stated that for the steel deck the FEM results obtained under the PL loading assumption were accurate. For the roof assembly configurations, the PL-FEM results were within the acceptable limits of 10% for moment and deflection, when compared with the experimentally determined deflections and moments, which are considered as the most

important results in this study; however regarding the forces results obtained from the FEM developed, for some loading scenarios these did not show good agreement with the forces recorded during the experiments; this might be caused by the measurements taken by the 6-components loading cell connection to the fastener, as mentioned above. The forces results obtained from the PL-FE model for the 6′ roof assembly has better agreement with the forces measured during the experiments, than the forces results obtained for the other two configurations of 7′6″ and 9′6″ roofing assemblies.

For the future work the following recommendations are made:

- This study tries to investigate the behaviour of the roofing assembly steel deck under wind uplift pressures, but due to time and instrumentation limitations, the reaction and the behaviour of the fasteners, especially the deck joist-fasteners effect, was not considered, which has an important effect on the overall deck behaviour. Therefore the steel deck joist-fasteners should be specifically modeled in a future study.
- The current research considered the static effect of the wind uplift pressure applied for the roofing assemblies investigated and a linear behaviour of the structural elements composing the FEM was assumed. However many of the failures of the steel deck observed during the experiments, were caused by nonlinear behaviour, when the test had to be stopped. Thus, considering the dynamic analysis, and also studying the non-linear behaviour of the roofing assembly under high wind rating pressures, can be an interesting topic for future research.
- In this study, the 6-component load cell sensor was attached to the fastener connecting the joist and the steel deck, due to the experiment configuration limitations; measuring the loading on the steel deck itself is recommended for future studies; a different type of load sensor which could be attached to the deck would provide better outputs. In addition the

static tests loading is performed by applying a constant pressure for a specific interval of time, then the loading is stopped and the test is ran for the next wind rate tested; this loading procedure should be repeated using a more stable sensor, because the very high sensitivity of the measuring device can lead to the occurrence of errors.

References

1. Liu. H, Wind Engineering (1991), A hand book for structural engineering, University of Missouri, Columbia.

2. Baskaran, A., Molleti, S., and Roodvoets, D. (2007) "Understanding flat roofs under Hurricane Charely from field to practice." Journal of ASTM International, v. 4, no. 10.

3. CBC News, "Power returning to Toronto in the wake of a storm" http://www.cbc.ca/news/canada/toronto, (November 15, 2012).

4. Baskaran. A, (2003) Dynamic Wind Testing of Commercial Roofing Systems, National Research Council, Ontario, Canada.

5. Sachs. P (1978), Wind of Forces in Engineering, 2nd Edition, Pergamon Press publisher.

6. SPRI's group (October, 2013) code revision.

7. SPRI standards and Technical Reports, http://www.spri.org/perspective/ (2014).

8. American Society of Civil Engineers (2005), Standard ASCE 7-2005, Minimum Design Loads for Buildings and Other Structures.

9. Changes to FM Approval Standard 4470 (March 2013), 28th RCI International convention and trade show.

10. Baskaran. A, Chen, Y (1998). "Wind Load Cycle Development for Evaluating Mechanically Attached Single-Ply Roofs," Journal of Wind Engineering and Industrial Aerodynamics, Vol. 77–78.

11. ProcessUniverse Producers.Co (2010), material definition, mechanical properties manual.

12. Factory Mutual Research (April 1986), Approval Standard: Class I Roof Covers (4470).

13. Schneider. R (June 2008), Wind uplift solution, RCI Incorporated, RCI journals (Interface).

14. Canadian sheet steel building institute (2008), Fact sheet 23.

15. CANAM group (2012), CANAM joists and steel deck catalog.

16. Schneider. R (June 2008), Wind uplift solution.

17. National Research Council of Canada (2005), National Building Code of Canada NBCC, Ottawa, Ontario, Canada.

18. S. Riaz A. Hodder (2000) Performance of fastener, ITW Buildex.

19. Simpson Strongtie.Co, Strong-Drive XL Large-Head Metal Screw, Steel deck fastnere http://www.strongtie.com/webapps/fastenerfinder/index.aspx?modelno=XL&type=Collated%20Screw%20(Quik%20Drive) (2014).

20. Keyence Company (2014), KL-G Laser catalog.

21. Kyowa Electronic instruments Co (2014), 6-component force transducer with manual instruction.

22. CSI Company (2014), CSI Analysis Reference Manual.

23. Torabi. A (2012), SAP2000, 3rd edition, Tehran University publication.

24. CSA Group (2007), CAN/CSA- CSA S136-07 North American Specification for the Design.

25. Y.Chen, A.Baskaran, W,Lei (1998), Wind load resistance of modified bituminous roofing system, Construction and Building Materials 12(8):471-480.

Appendix A

In this section, a summarized report of SAP2000 output is provided. This report is for the steel deck case under 135 psf wind force.

```
B E G I N   A N A L Y S I S

RUNNING ANALYSIS AS A SEPARATE PROCESS
USING THE ADVANCED SOLVER (PROVIDES LIMITED INSTABILITY INFORMATION)

NUMBER OF JOINTS                          =        5306
   WITH RESTRAINTS                        =         259
NUMBER OF FRAME/CABLE/TENDON ELEMENTS     =         763
NUMBER OF SHELL ELEMENTS                  =        4145
NUMBER OF LOAD PATTERNS                   =           3
NUMBER OF ACCELERATION LOADS              =           6
NUMBER OF LOAD CASES                      =           1

E L E M E N T   F O R M A T I O N


L I N E A R   E Q U A T I O N   S O L U T I O N

FORMING STIFFNESS AT ZERO (UNSTRESSED) INITIAL CONDITIONS

TOTAL NUMBER OF EQUILIBRIUM EQUATIONS     =       31056
NUMBER OF NON-ZERO STIFFNESS TERMS        =      749919

* * * W A R N I N G * * *
THE STRUCTURE IS UNSTABLE OR ILL-CONDITIONED !!
CHECK THE STRUCTURE CAREFULLY FOR:
- INADEQUATE SUPPORT CONDITIONS, OR
- ONE OR MORE INTERNAL MECHANISMS, OR
- ZERO OR NEGATIVE STIFFNESS PROPERTIES, OR
- EXTREMELY LARGE STIFFNESS PROPERTIES, OR
- BUCKLING DUE TO P-DELTA OR GEOMETRIC NONLINEARITY, OR
- A FREQUENCY SHIFT (IF ANY) ONTO A NATURAL FREQUENCY

TO OBTAIN FURTHER INFORMATION:
- USE THE STANDARD SOLVER, OR
- RUN AN EIGEN ANALYSIS USING AUTO FREQUENCY SHIFTING (WITH
  ADDITIONAL MASS IF NEEDED) AND INVESTIGATE THE MODE SHAPES

NUMBER OF EIGENVALUES BELOW SHIFT         =           0

L I N E A R   S T A T I C   C A S E S

USING STIFFNESS AT ZERO (UNSTRESSED) INITIAL CONDITIONS

TOTAL NUMBER OF CASES TO SOLVE            =           1
NUMBER OF CASES TO SOLVE PER BLOCK        =           1

LINEAR STATIC CASES TO BE SOLVED:

CASE: UL

A N A L Y S I S   C O M P L E T E
```

Appendix B

This section consists of different figures of FEM. At first, the figures of the steel deck under the uniform load and point loading system are shown, then distributed loading is illustrated.

Point load:

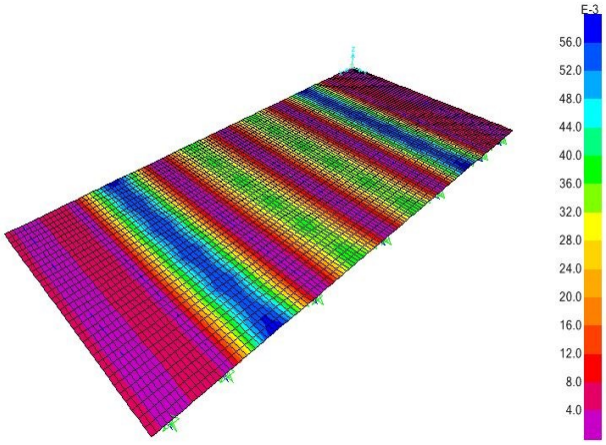

Steel deck deflection (in), 30 psf uniform load

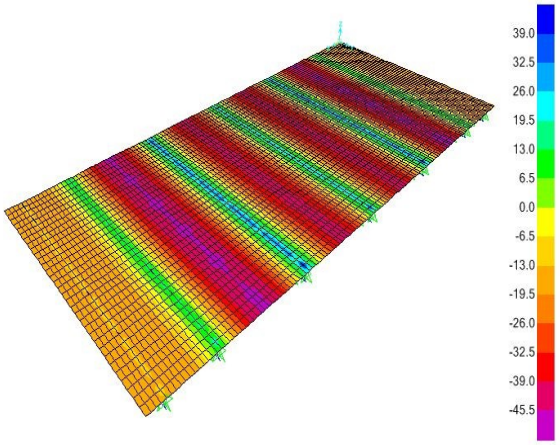

Steel deck moment (lb-in), 30 psf uniform load

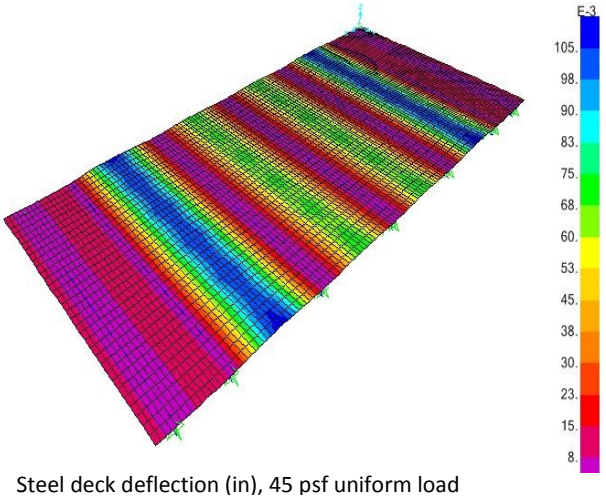

Steel deck deflection (in), 45 psf uniform load

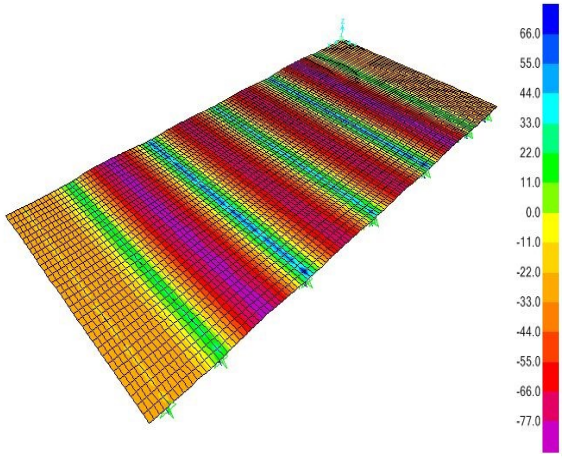

Steel deck moment (lb-in), 45 psf uniform load

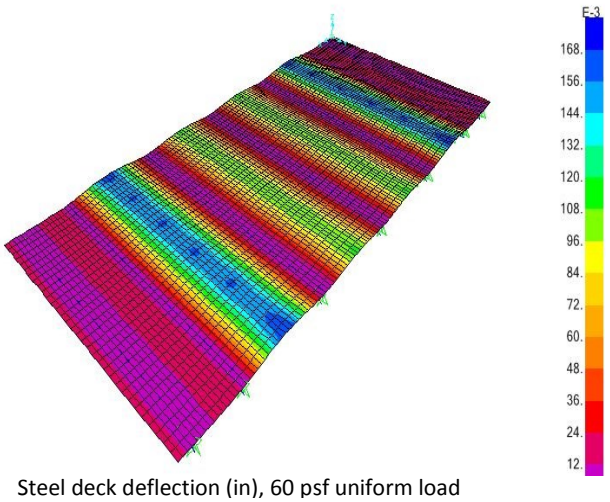

Steel deck deflection (in), 60 psf uniform load

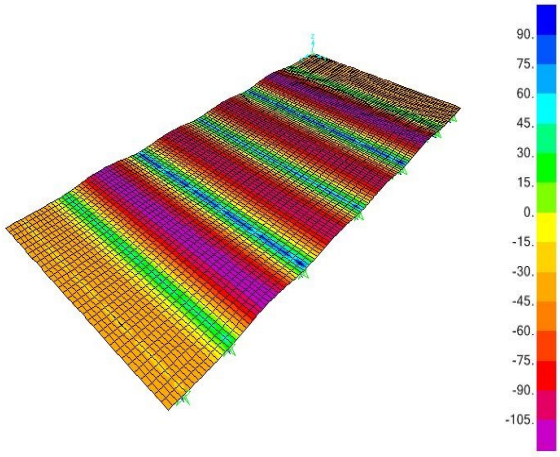

Steel deck moment (lb-in), 60 psf uniform load

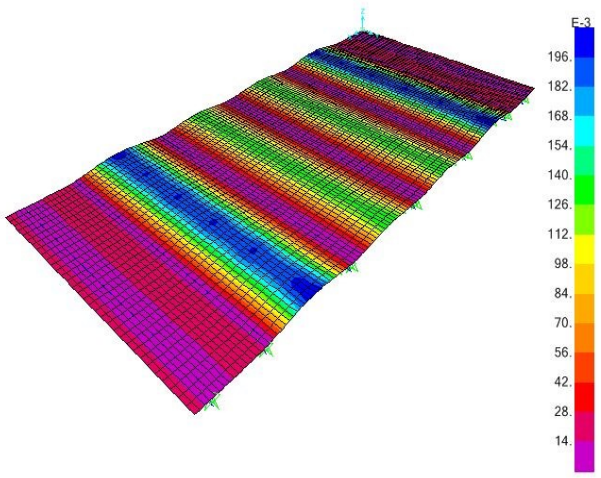

Steel deck deflection (in), 75 psf uniform load

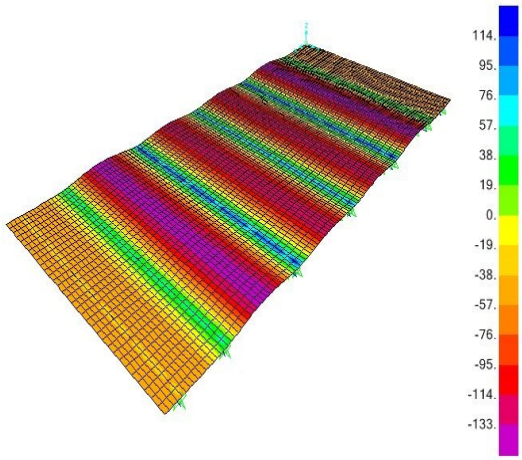

Steel deck moment (lb-in), 75 psf uniform load

Steel deck deflection (in), 90 psf uniform load

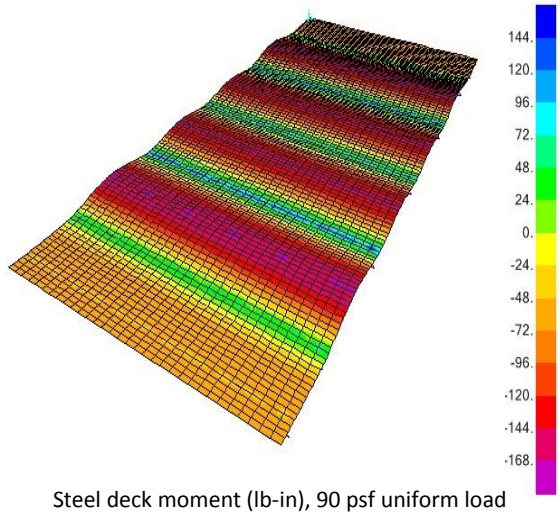

Steel deck moment (lb-in), 90 psf uniform load

Steel deck deflection (in), 105 psf uniform

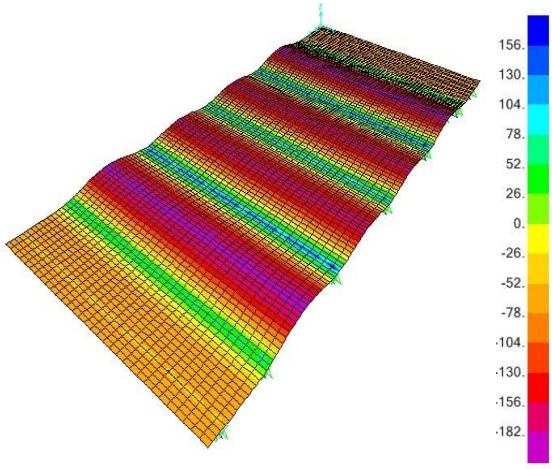

Steel deck moment (lb-in), 105 psf uniform load

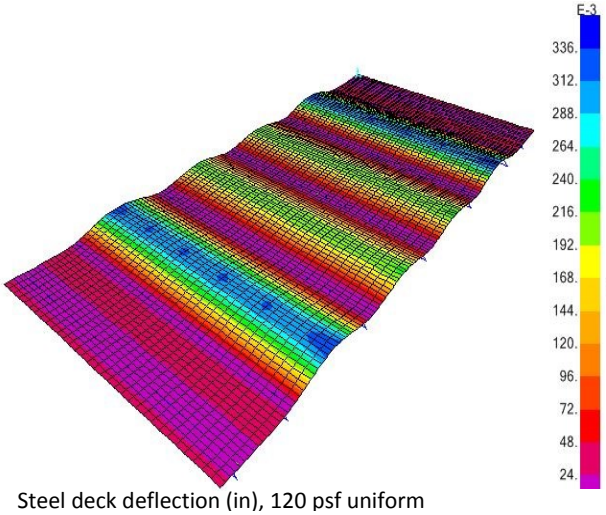

Steel deck deflection (in), 120 psf uniform

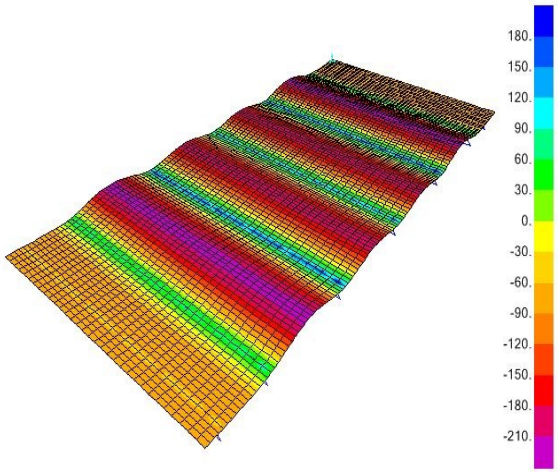

Steel deck moment (lb-in), 120 psf uniform load

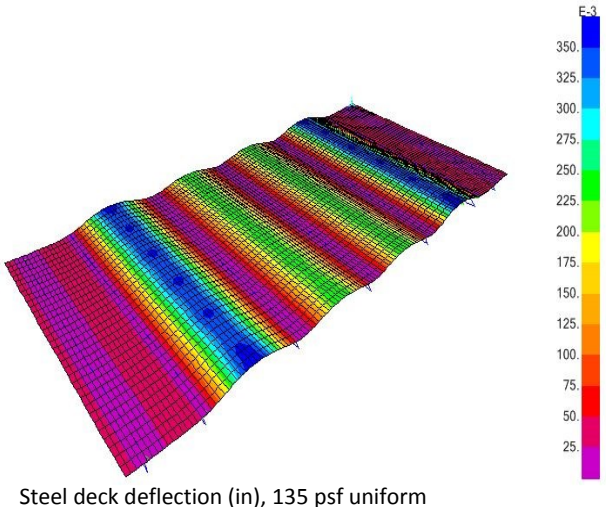

Steel deck deflection (in), 135 psf uniform

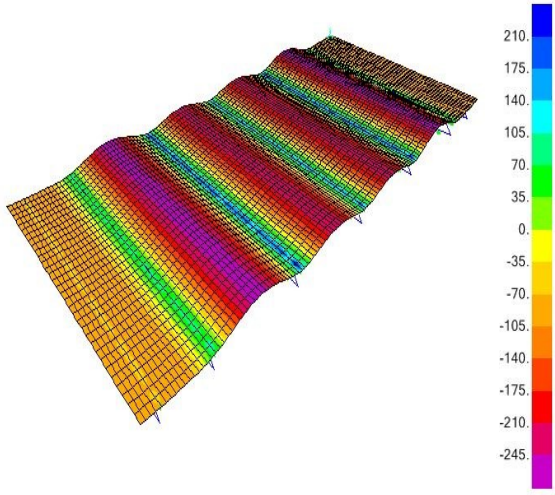

Steel deck moment (lb-in), 135 psf uniform load

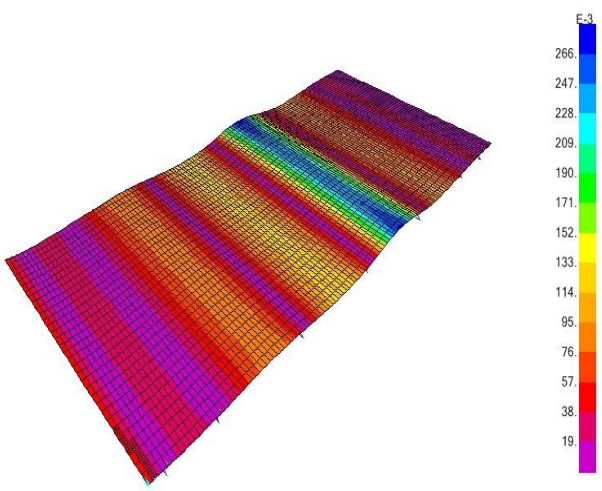

Roof assembly 9’6”, deflection (in), 30 psf point load

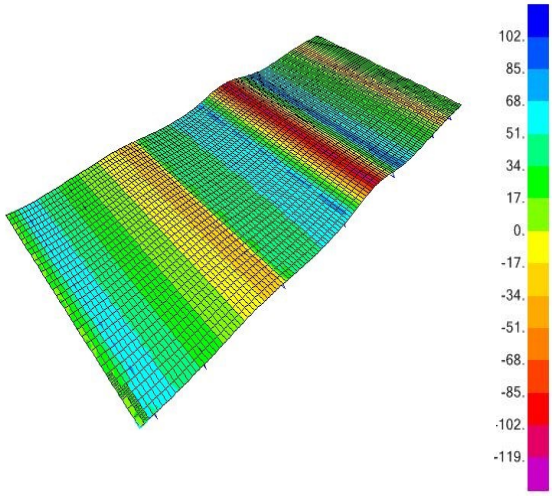

Roof assembly 9’6”, moment (lb-in), 30 psf point load

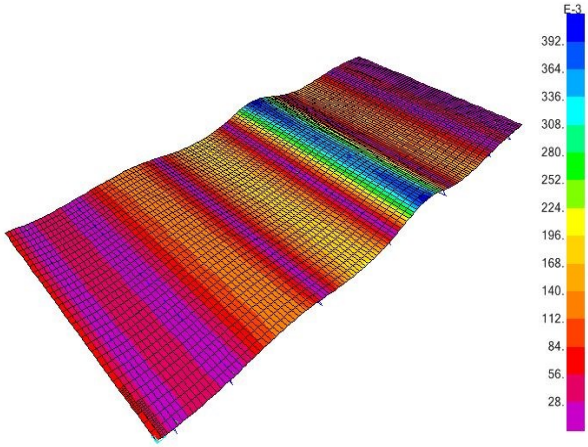

Roof assembly 9’6”, deflection (in), 45 psf point load

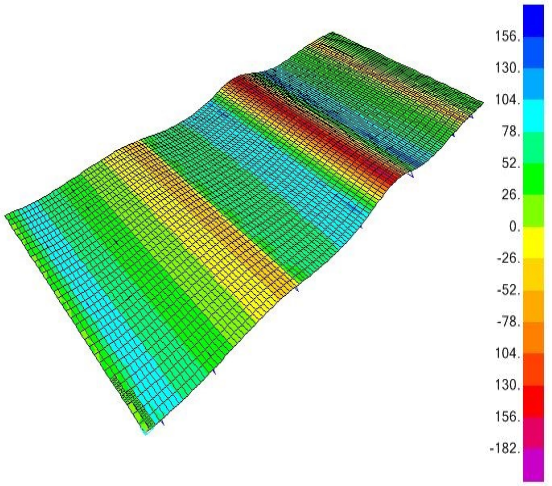

Roof assembly 9’6”, moment (lb-in), 45 psf point load

Roof assembly 9’6”, deflection (in), 60 psf point load

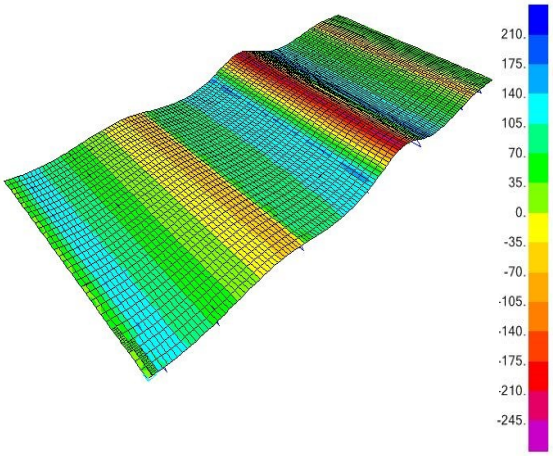

Roof assembly 9’6”, moment (lb-in), 60 psf point load

Roof assembly 9’6”, deflection (in), 75 psf point load

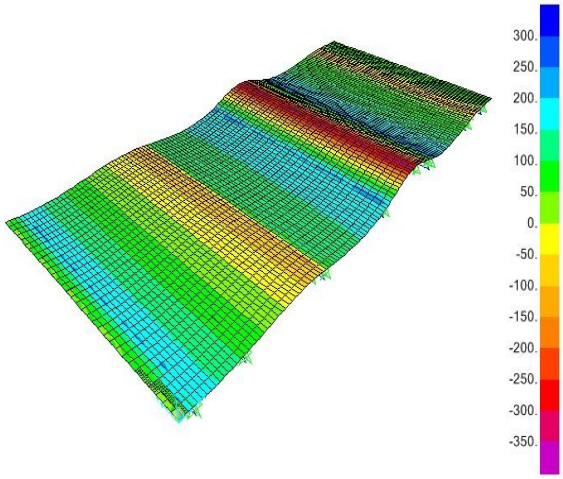

Roof assembly 9’6”, moment (lb-in), 75 psf point load

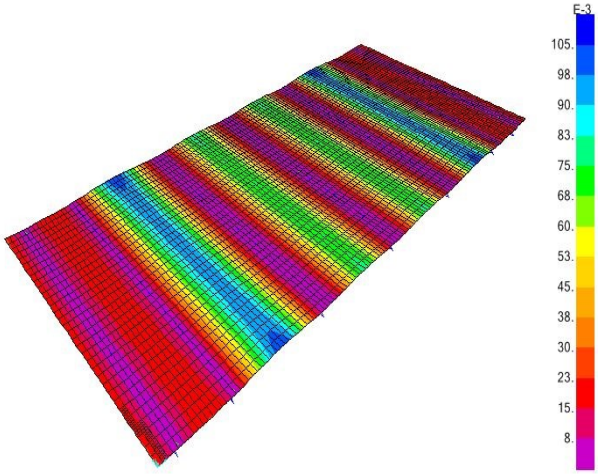

Roof assembly 6’, deflection (in), 30 psf point load uniform

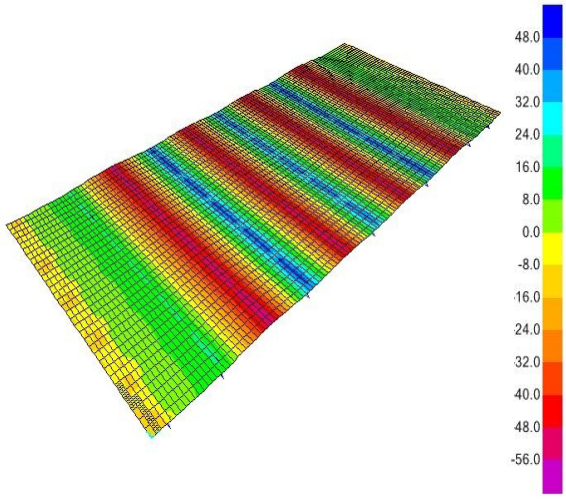

Roof assembly 6’, moment (lb-in), 30 psf point load

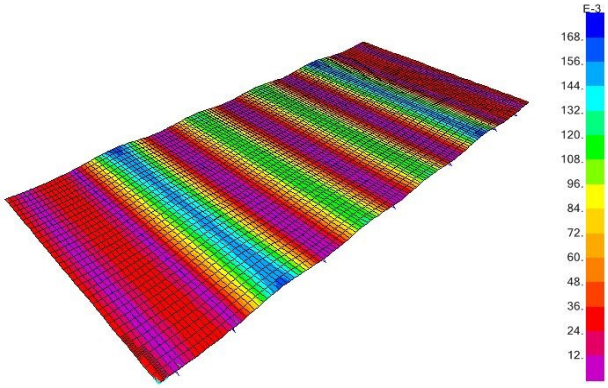

Roof assembly 6’, deflection (in), 45 psf point load uniform

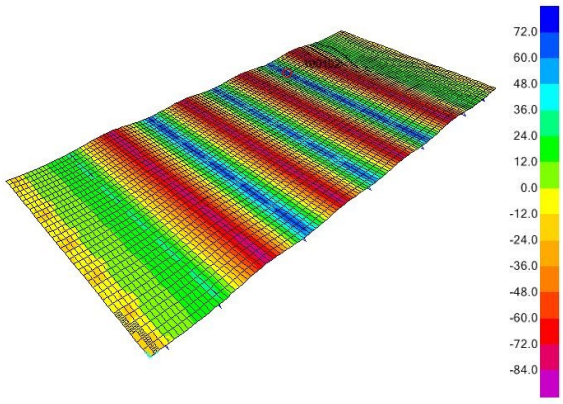

Roof assembly 6’, moment (lb-in), 45 psf point load

Roof assembly 6', deflection (in), 60 psf point load uniform

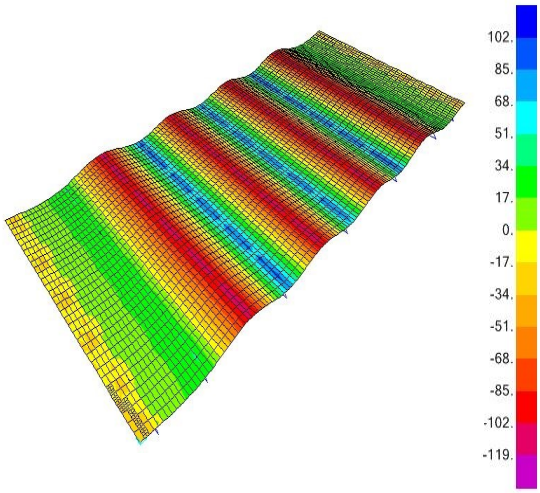

Roof assembly 6', moment (lb-in), 60psf point load

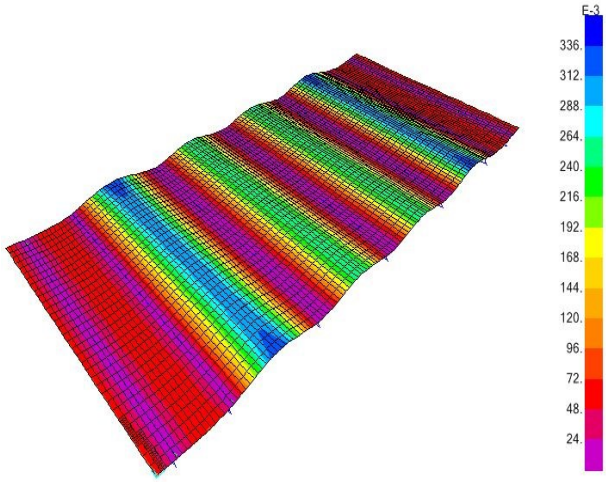

Roof assembly 6', deflection (in), 75 psf point load uniform

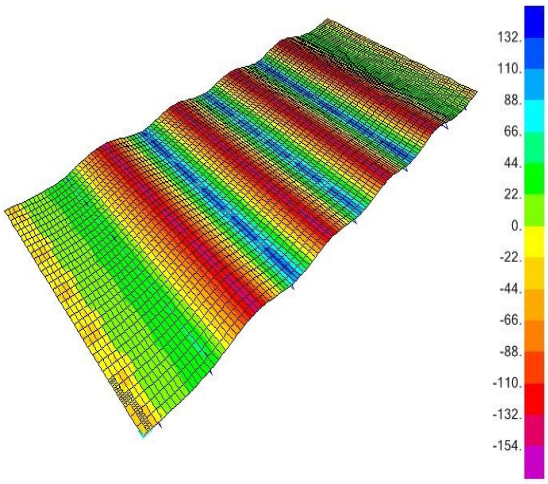

Roof assembly 6', moment (lb-in), 75 psf point load

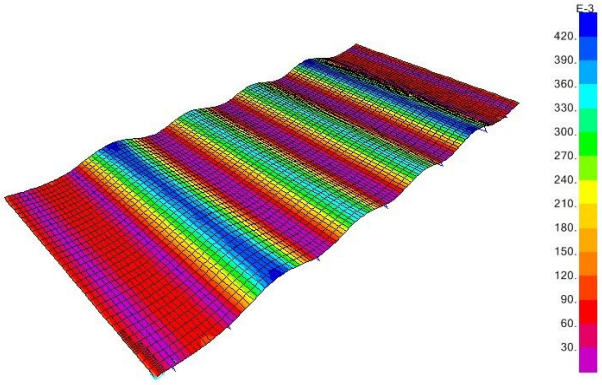

Roof assembly 6', deflection (in), 90 psf point load uniform

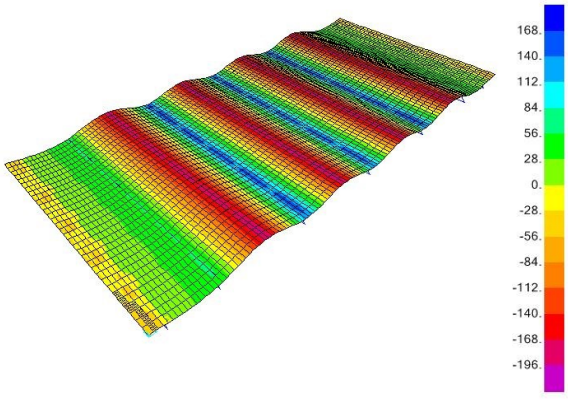

Roof assembly 6', moment (lb-in), 90 psf point load

Roof assembly 6’, deflection (in), 105 psf point load

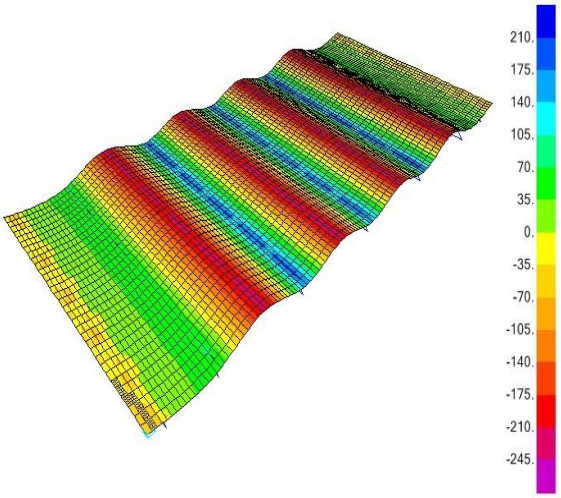

Roof assembly 6’, moment (lb-in), 105 psf point load

Roof assembly 6’, deflection (in), 120 psf point load

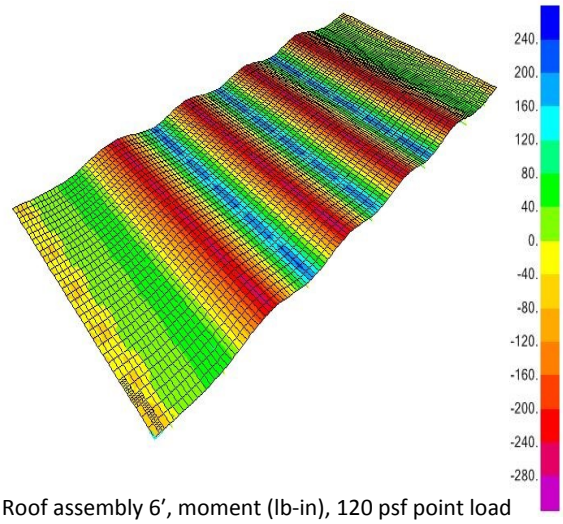

Roof assembly 6’, moment (lb-in), 120 psf point load

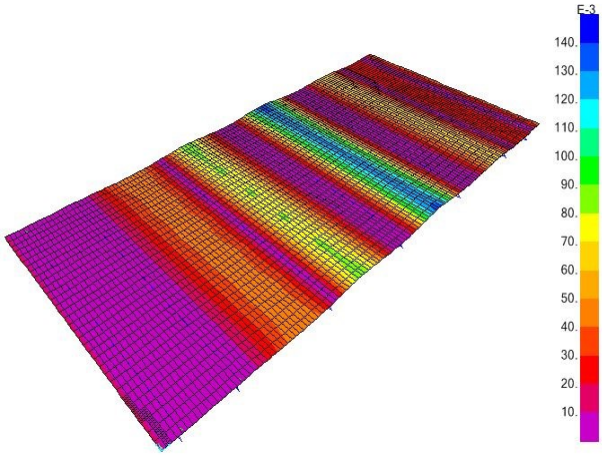

Roof assembly 7’6”, deflection (in), 30 psf point load

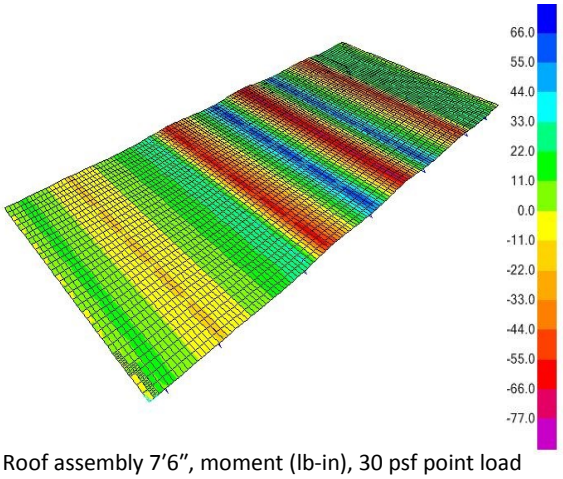

Roof assembly 7’6”, moment (lb-in), 30 psf point load

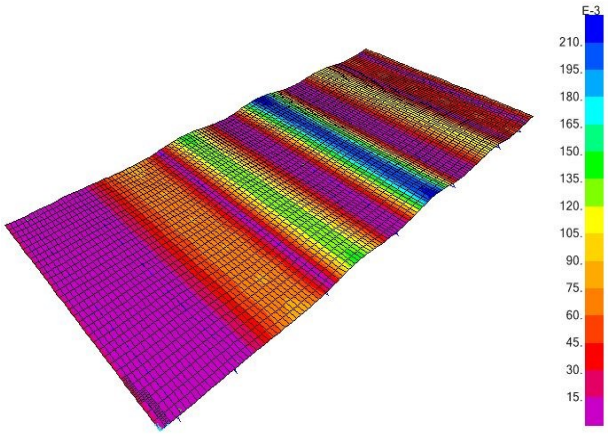

Roof assembly 7’6”, deflection (in), 45 psf point load

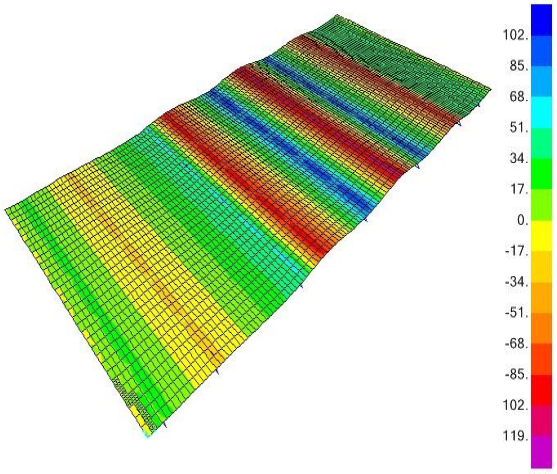

Roof assembly 7’6”, moment (lb-in), 45 psf point load

Roof assembly 7’6”, deflection (in), 60 psf point load

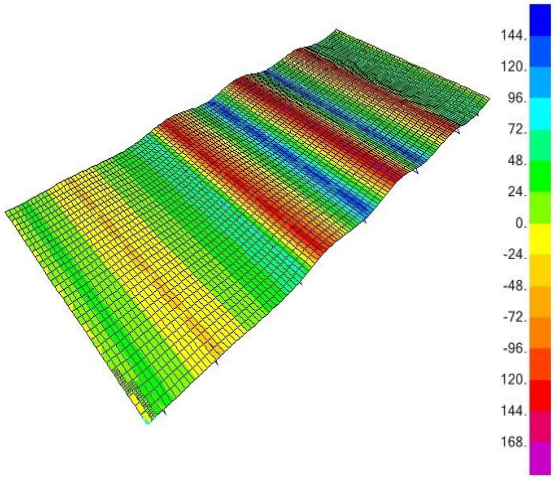

Roof assembly 7’6”, moment (lb-in), 60 psf point load

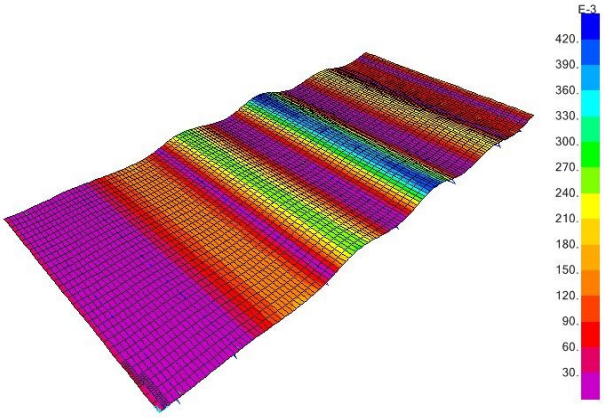

Roof assembly 7’6”, deflection (in), 75 psf point load

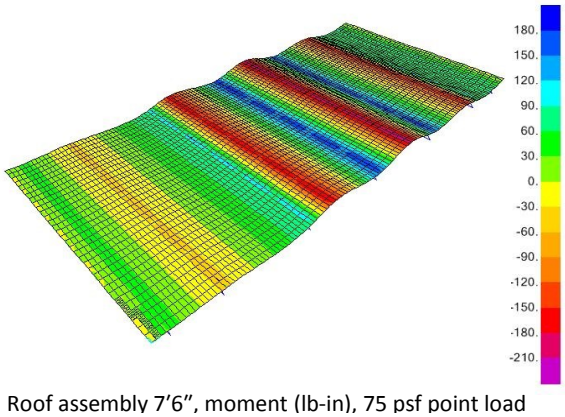

Roof assembly 7’6”, moment (lb-in), 75 psf point load

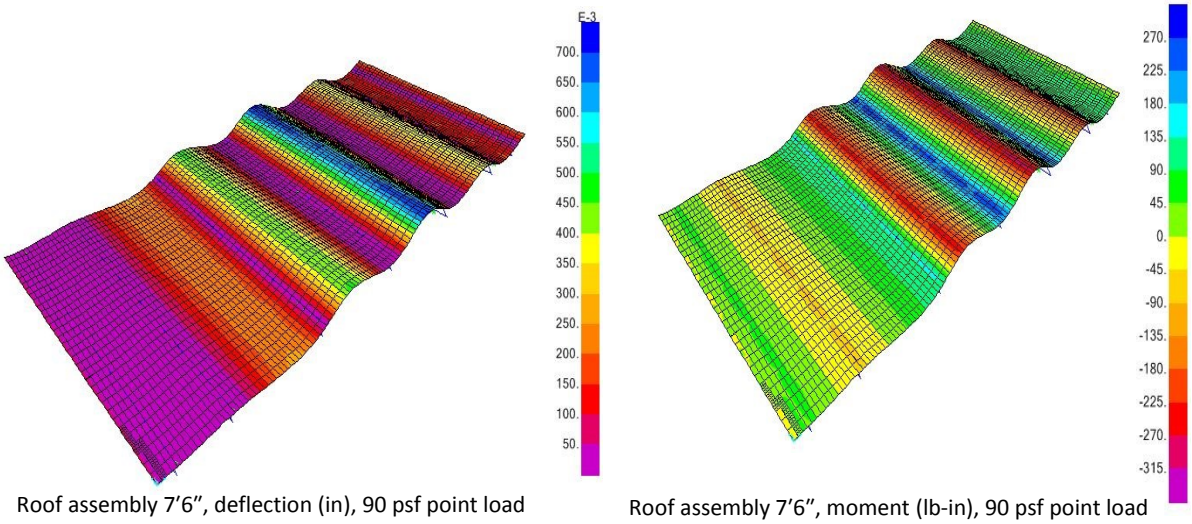

Roof assembly 7’6”, deflection (in), 90 psf point load

Roof assembly 7’6”, moment (lb-in), 90 psf point load

In this section, figures for the distributed loading system are shown.

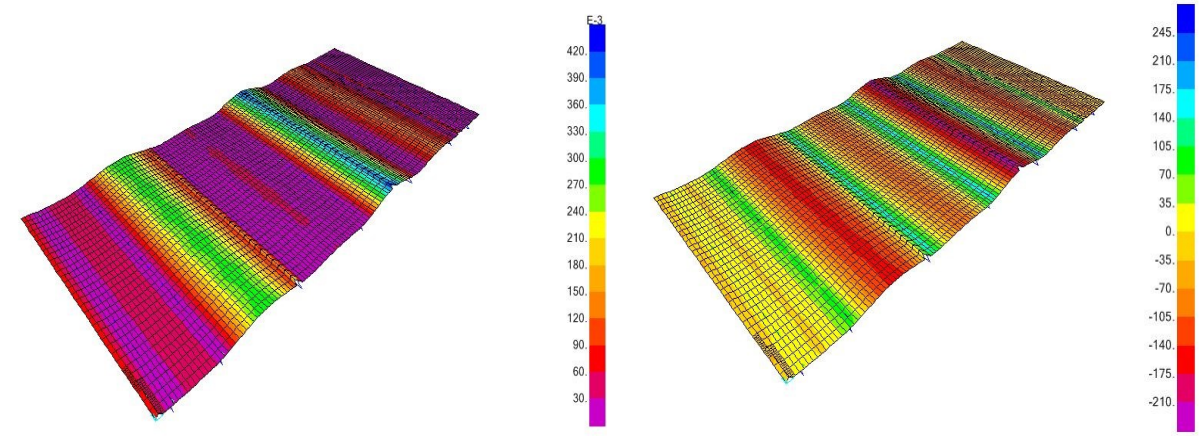

Roof assembly 9’6”, deflection (in), 30 psf distributed load

Roof assembly 9’6”, moment (lb-in), 30 psf distributed load

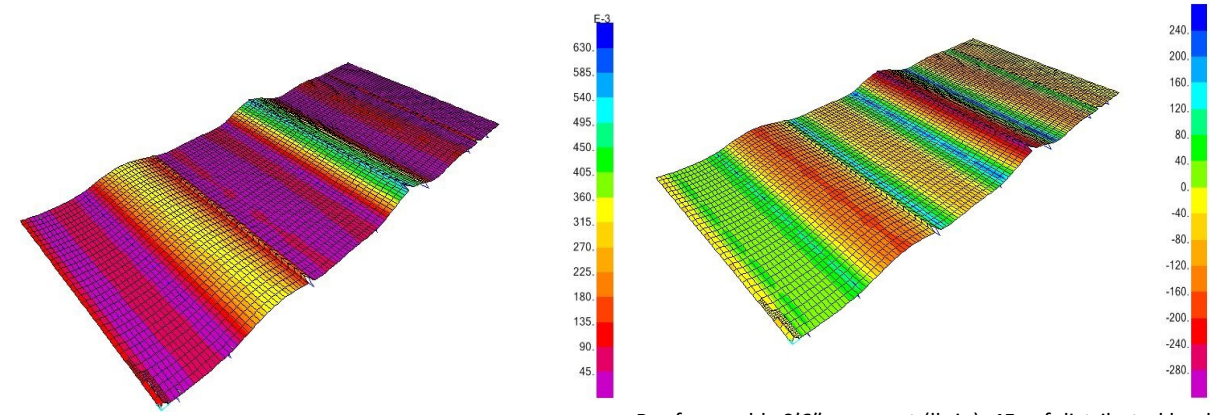

Roof assembly 9’6”, deflection (in), 45 psf distributed load

Roof assembly 9’6”, moment (lb-in), 45 psf distributed load

Roof assembly 9’6”, deflection (in), 60 psf distributed load

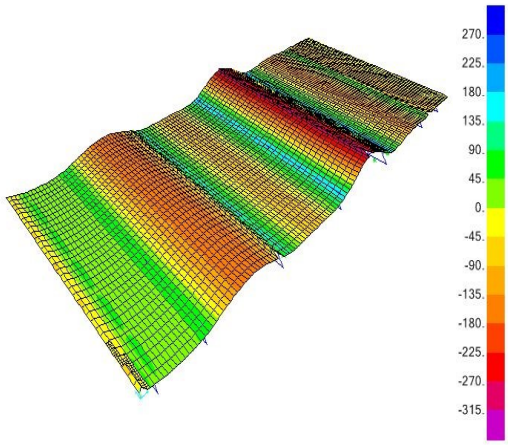

Roof assembly 9’6”, moment (lb-in), 60 psf distributed load

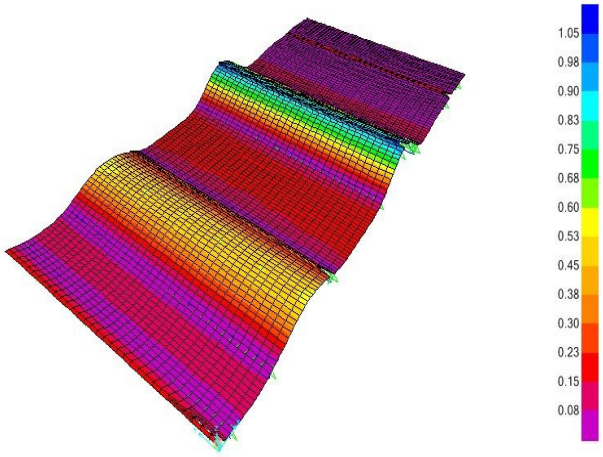

Roof assembly 9’6”, deflection (in), 75 psf distributed load

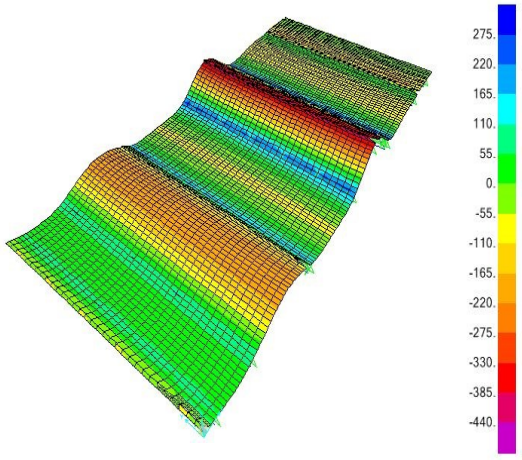

Roof assembly 9’6”, moment (lb-in), 75 psf distributed load

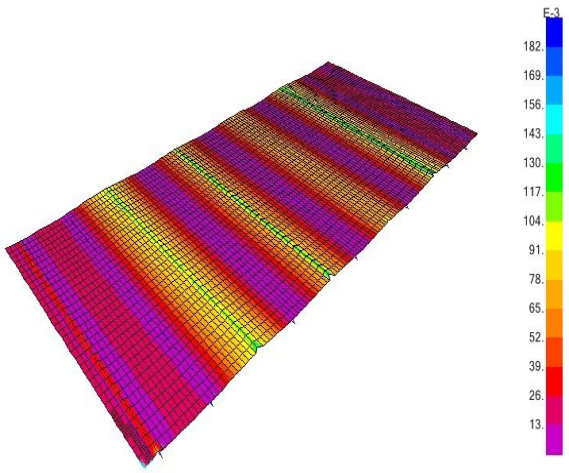

Roof assembly 6’, deflection (in), 30 psf distributed load

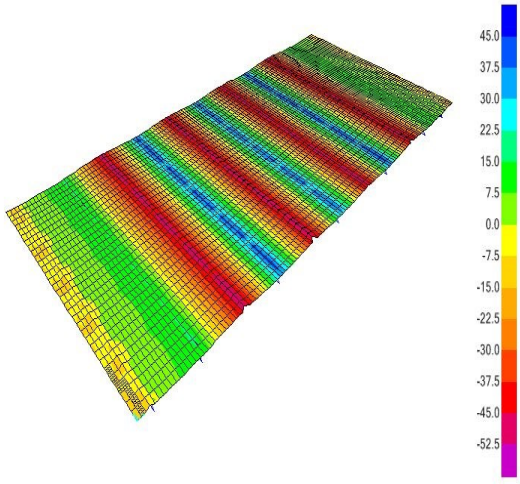

Roof assembly 6’, moment (lb-in), 30 psf distributed load

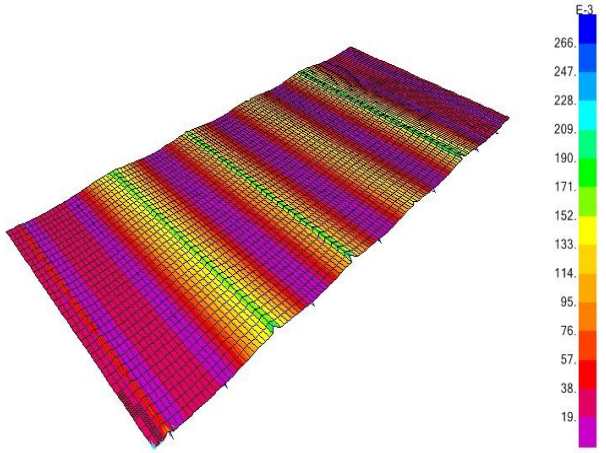

Roof assembly 6', deflection (in), 45 psf distributed load

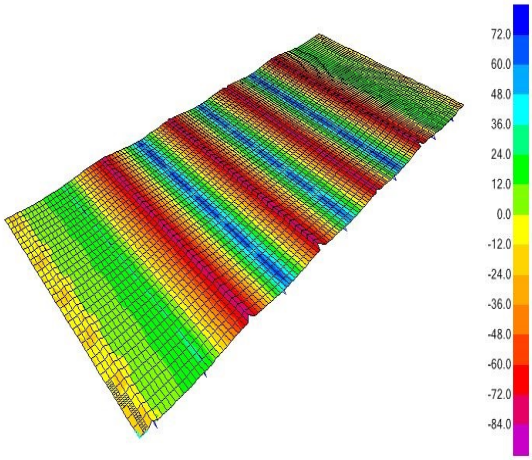

Roof assembly 6', moment (lb-in), 45 psf distributed load

Roof assembly 6', deflection (in), 60 psf distributed load

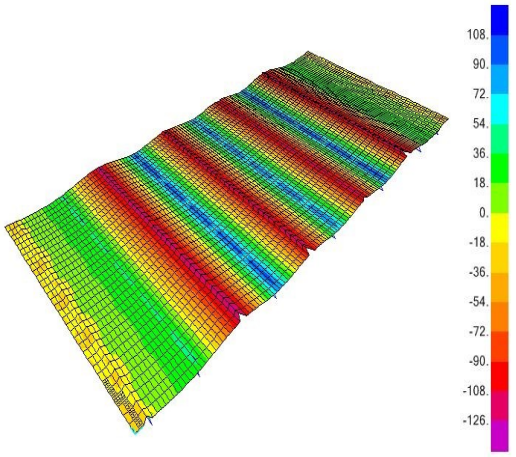

Roof assembly 6', moment (lb-in), 60 psf distributed load

Roof assembly 6', deflection (in), 75 psf distributed load

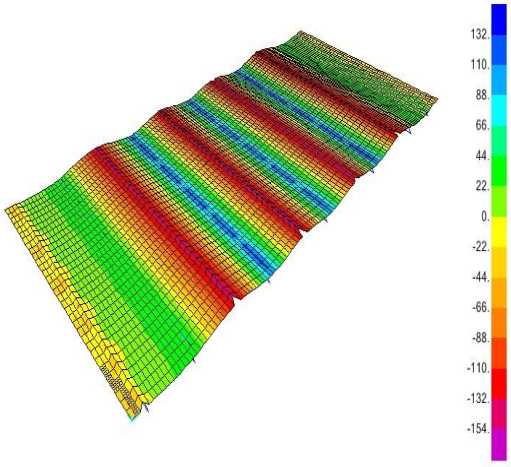

Roof assembly 6', moment (lb-in), 75 psf distributed load

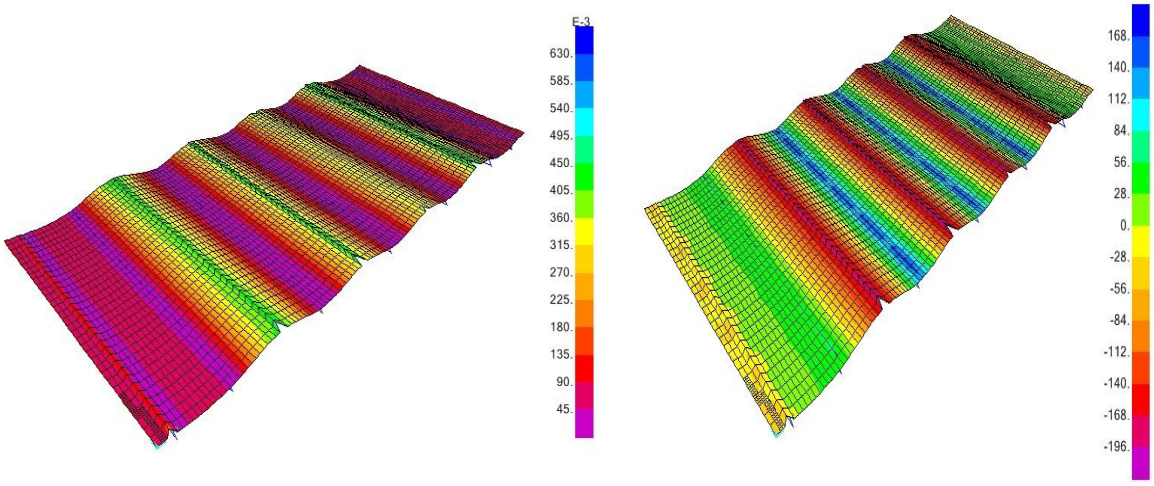

Roof assembly 6', deflection (in), 90 psf distributed load

Roof assembly 6', moment (lb-in), 90 psf distributed load

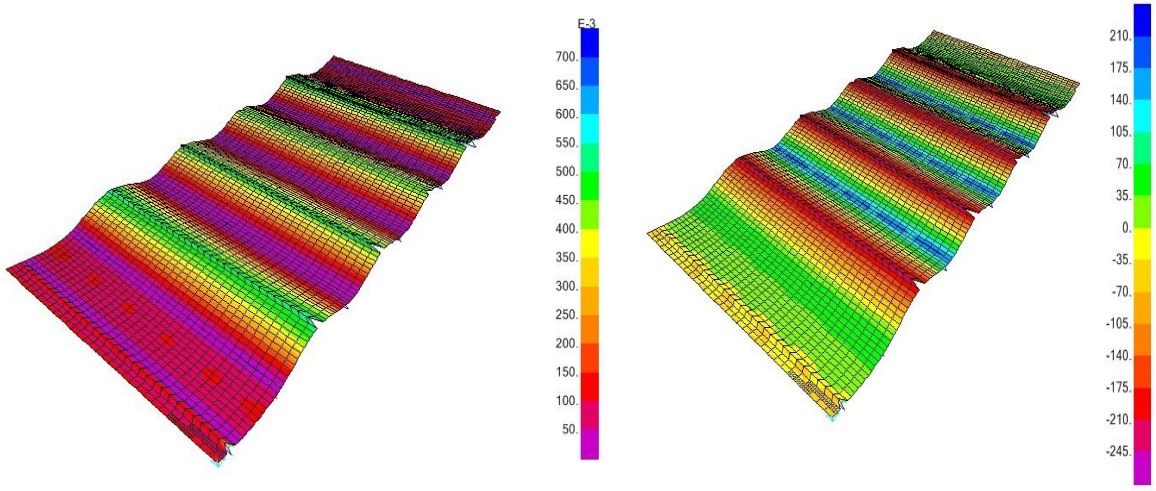

Roof assembly 6', deflection (in), 105 psf distributed load

Roof assembly 6', moment (lb-in), 105 psf distributed load

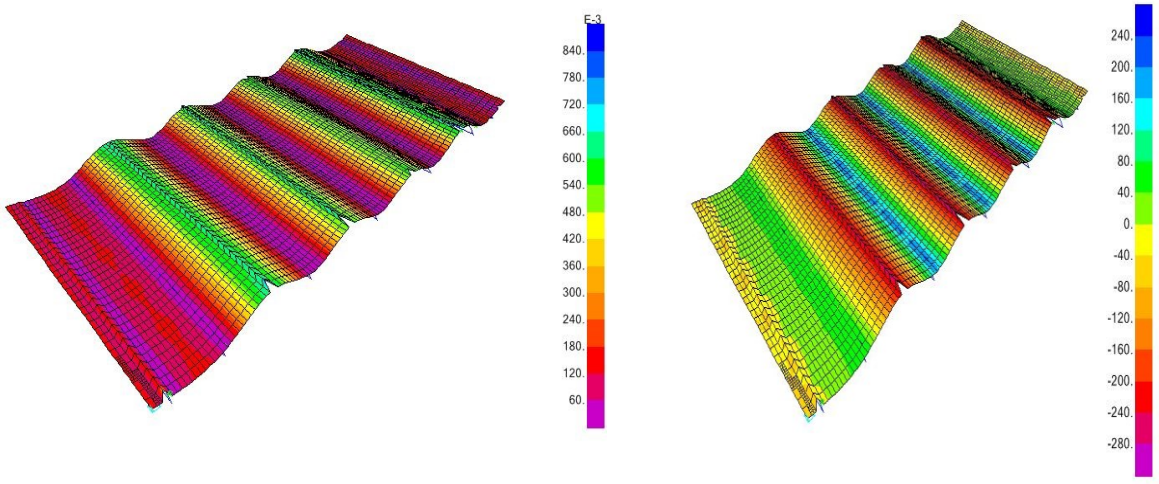

Roof assembly 6', deflection (in), 120 psf distributed load

Roof assembly 6', moment (lb-in), 120 psf distributed load

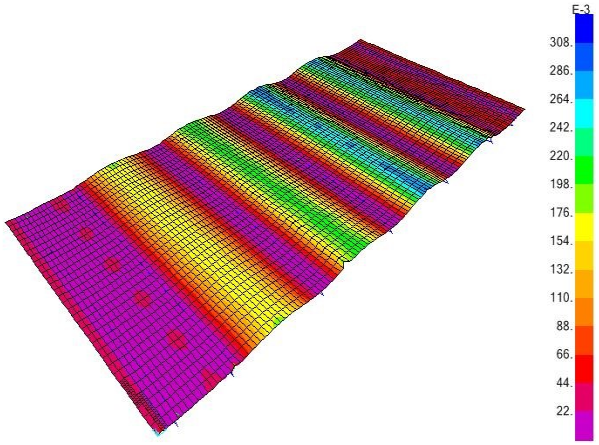

Roof assembly 7’6”, deflection (in), 30 psf distributed load

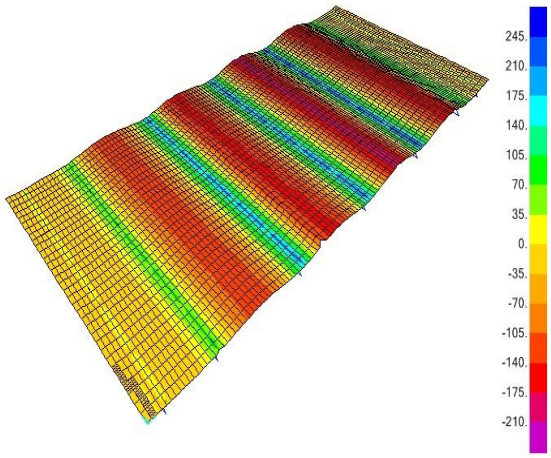

Roof assembly 7’6”, moment (lb-in), 30 psf distributed load

Roof assembly 7’6”, deflection (in), 45 psf distributed load

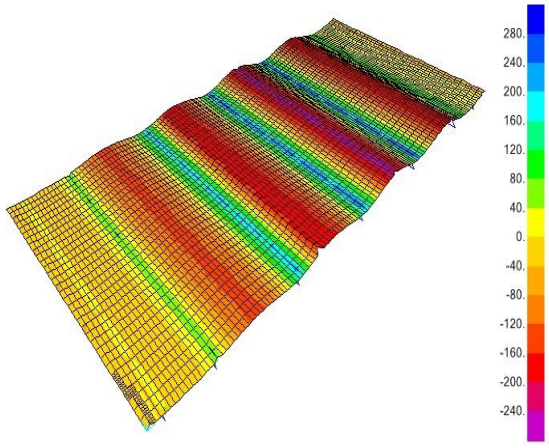

Roof assembly 7’6”, moment (lb-in), 45 psf distributed load

Roof assembly 7’6”, deflection (in), 60 psf distributed load

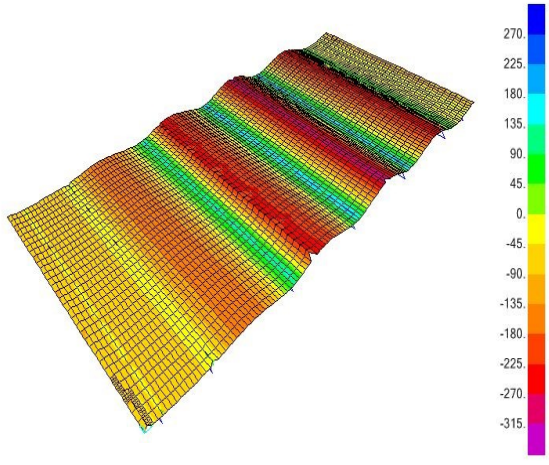

Roof assembly 7’6”, moment (lb-in), 60 psf distributed load

Roof assembly 7’6”, deflection (in), 75 psf distributed load

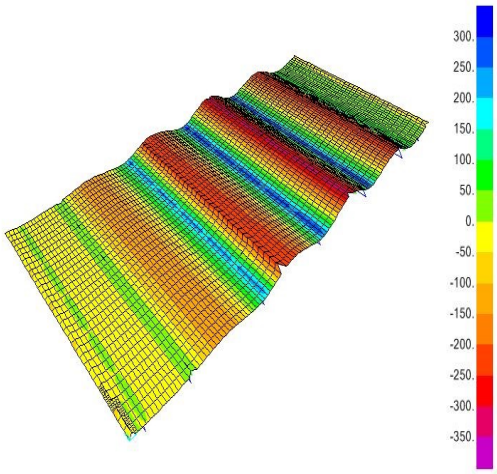

Roof assembly 7’6”, moment (lb-in), 75 psf distributed load

Roof assembly 7’6”, deflection (in), 90 psf distributed

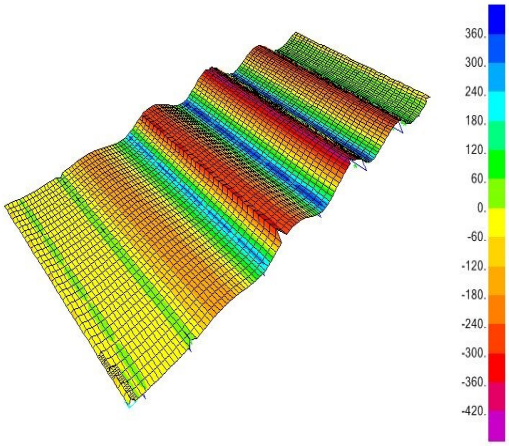

Roof assembly 7’6”, moment (lb-in), 90 psf distributed load

Converting uniform load to point load:

Converting uniform load, which applied to the membrane layer, to point load and applying the point load on the roof assembly is a fundamental issue in this research. Finding tributary area to convert uniform load is the first step. Then by multiplying it by wind pressure, point load can be computed. The point loads are parallel to the steel deck fastener as it is shown in figure A.

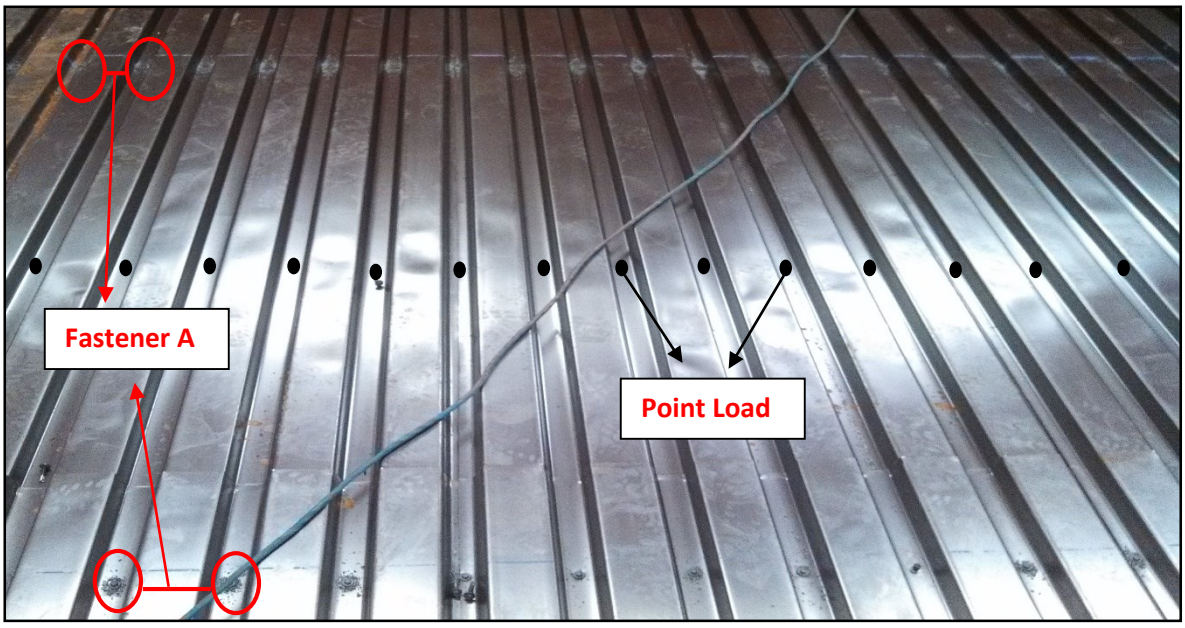

Figure A. Fasteners A attach steel deck to the joists and they modeled as supports in FEM and the point load are the location that point loads are applied.

The distance between two fasteners or two point loads is 6″ and the distance between two lines of point load is defined based on FM table. Therefore the tributary area is a rectangular as below:

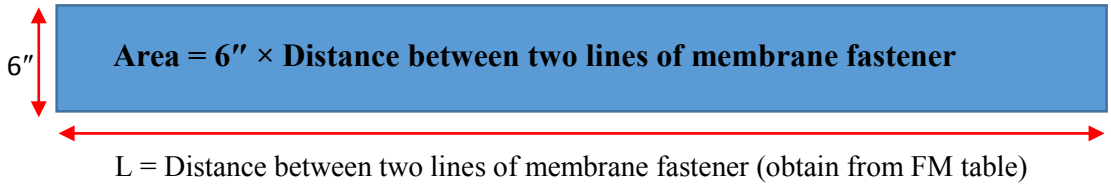

So the area is calculated and by considering the wind pressure, point load can be calculated.

For example:

W = 90 psf , L = 6′ , P = ?

Area = 6′ × 0.5′ = 3′ ft2 P = 90 × 3′ = 270 lb

A) Behaviour of Three equal span under the same point load

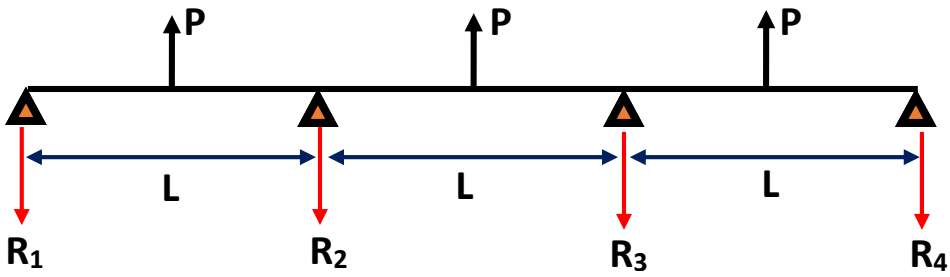

Figure B. 3-equal span with point load

As it can be seen from the figure B, there are three equal spans with the same point load pattern. The reaction of restraints can be calculated as:

$$R_1 = R_4 = 0.35 \times P$$

$$R_2 = R_3 = 1.15 \times P$$

The moment at the middle of spans for the first and third spans are equal and can be computed as below:

$$M_1 = M_3 = 0.175 \times PL$$

The moment at the middle of second span is equal to:

$$M_2 = 0.1 \times PL$$

Also the moment at support 2 and 3 can be calculated as below:

$$M_{S2} = M_{S3} = 0.15 \times PL$$

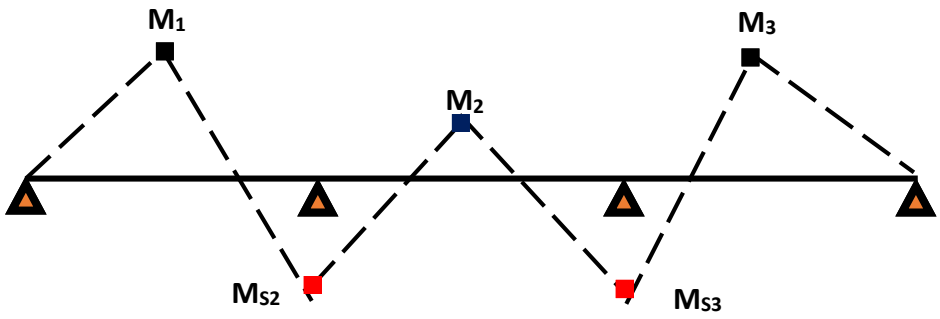

Figure C. Moment diagram

As it can be seen from the above figure C, the first and second spans behaviour as the same meanwhile the middle span have a different reaction compared to other two spans.

Figures D and E show how loading patterns are applied to the roof system.

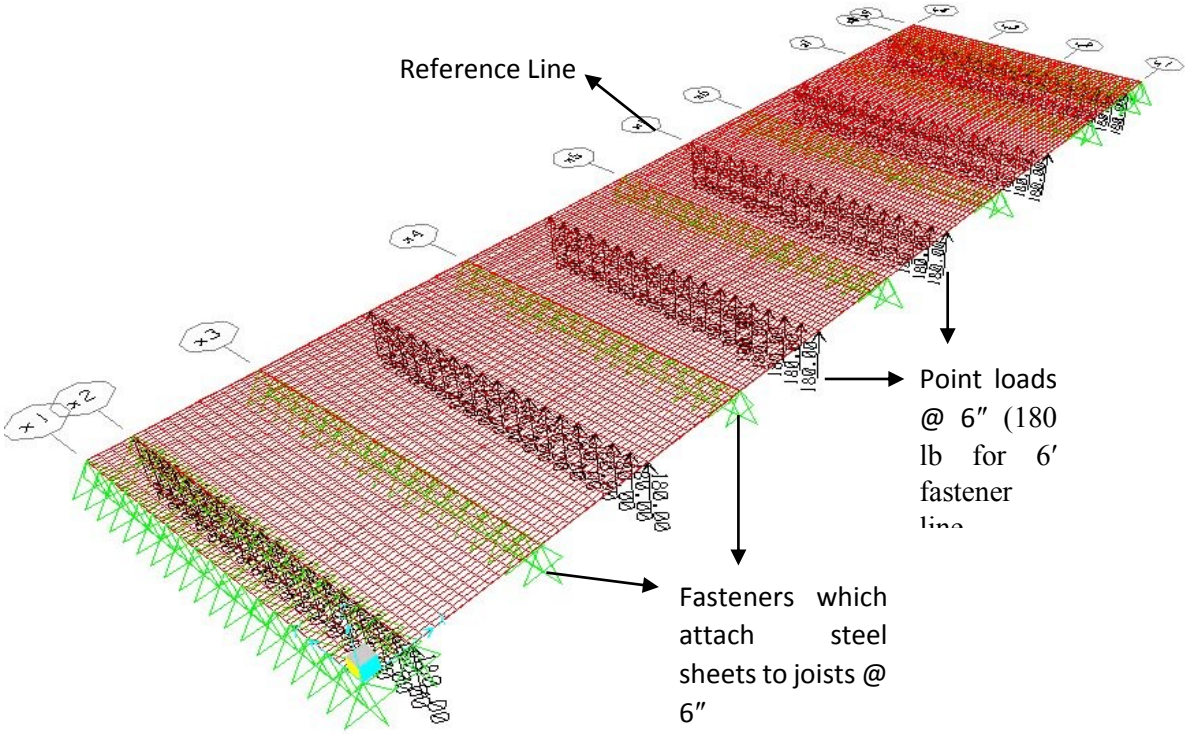

Figure D. point load pattern for 180 psf with 6′ fastener line distance

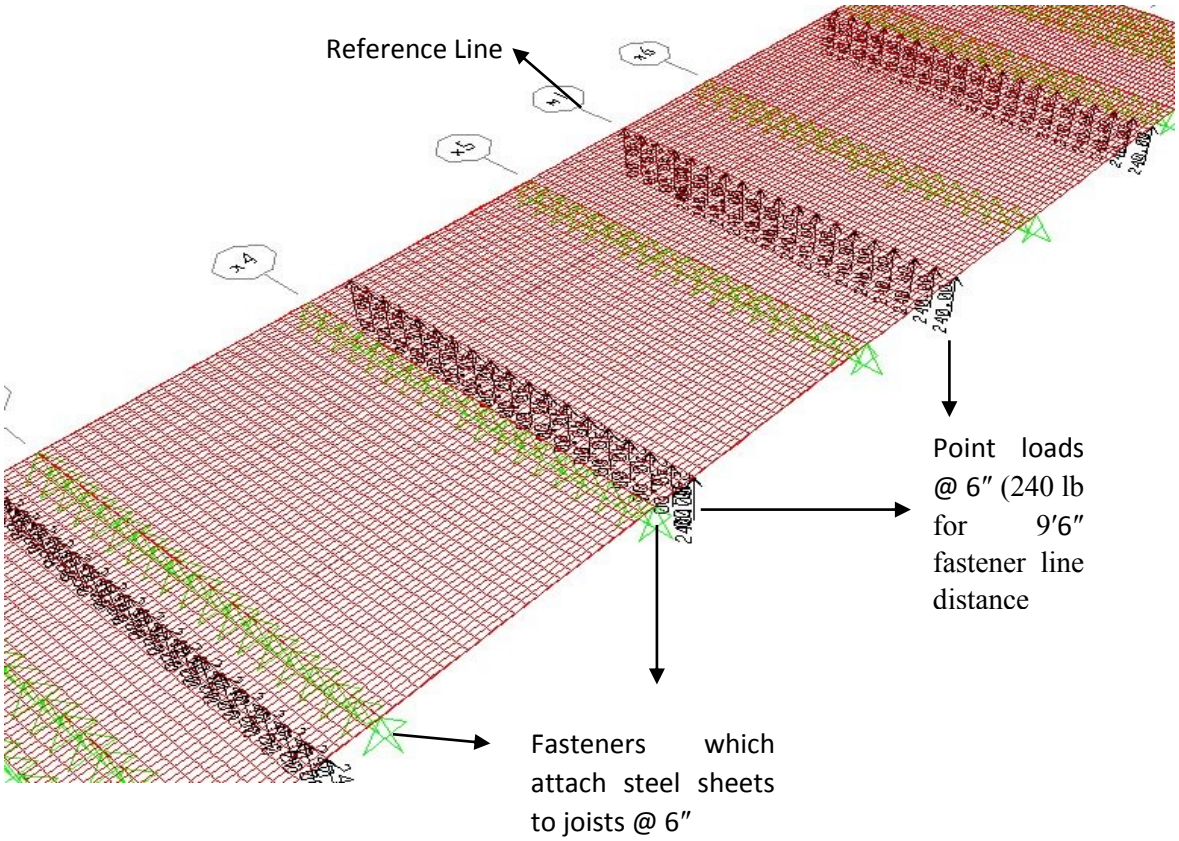

Figure E. point load pattern for 240 psf with 9′6″ fastener line distance